ΧΑΡΟΚΟΠΕΙΟ ΠΑΝΕΠΙΣΤΗΜΙΟ
HAROKOPIO UNIVERSITY

SCHOOL OF HEALTH SCIENCE & EDUCATION

DEPARTMENT OF NUTRITION AND DIETETICS

Doctoral dissertation

Functional analysis of genes involved in cardiovascular disease

Panagiota Giardoglou,

Biologist, M.Sc

This research is co-financed by Greece and the European Union (European Social Fund- ESF) through the Operational Programme «Human Resources Development, Education and Lifelong Learning» in the context of the project "Strengthening Human Resources Research Potential via Doctorate Research" (MIS-5000432), implemented by the State Scholarships Foundation (IKY)

Ευρωπαϊκή Ένωση
European Social Fund

Operational Programme
Human Resources Development, Education and Lifelong Learning
Co-financed by Greece and the European Union

ΕΣΠΑ 2014-2020
ανάπτυξη - εργασία - αλληλεγγύη

This research is conducted in:

Biomedical Research Foundation, Academy of Athens

ACADEMY OF ATHENS
BRFAA

Athens, 2022

ΧΑΡΟΚΟΠΕΙΟ ΠΑΝΕΠΙΣΤΗΜΙΟ
HAROKOPIO UNIVERSITY

ΣΧΟΛΗ ΕΠΙΣΤΗΜΩΝ ΥΓΕΙΑΣ ΚΑΙ ΑΓΩΓΗΣ

ΤΜΗΜΑ ΕΠΙΣΤΗΜΗΣ ΔΙΑΙΤΟΛΟΓΙΑΣ-ΔΙΑΤΡΟΦΗΣ

Διδακτορική διατριβή

Λειτουργική Μελέτη της Βιολογίας της Καρδιαγγειακής Νόσου

Γιαρδόγλου Παναγιώτα,

Βιολόγος, M.Sc

Το έργο συγχρηματοδοτείται από την Ελλάδα και την Ευρωπαϊκή Ένωση (Ευρωπαϊκό Κοινωνικό Ταμείο) μέσω του Επιχειρησιακού Προγράμματος «Ανάπτυξη Ανθρώπινου Δυναμικού, Εκπαίδευση και Διά Βίου Μάθηση», στο πλαίσιο της Πράξης «Ενίσχυση του ανθρώπινου ερευνητικού δυναμικού μέσω της υλοποίησης διδακτορικής έρευνας» (MIS-5000432), που υλοποιεί το Ίδρυμα Κρατικών Υποτροφιών (ΙΚΥ)

Ευρωπαϊκή Ένωση
Ευρωπαϊκό Κοινωνικό Ταμείο

Επιχειρησιακό Πρόγραμμα
Ανάπτυξη Ανθρώπινου Δυναμικού,
Εκπαίδευση και Διά Βίου Μάθηση
Με τη συγχρηματοδότηση της Ελλάδας και της Ευρωπαϊκής Ένωσης

ΕΣΠΑ 2014-2020
ανάπτυξη - εργασία - αλληλεγγύη

Τόπος διεξαγωγής έρευνας

Ίδρυμα Ιατροβιολογικών Ερευνών της Ακαδημίας Αθηνών

ΑΚΑΔΗΜΙΑ ΑΘΗΝΩΝ
ΙΙΒΕΑΑ

Αθήνα, 2022

ΧΑΡΟΚΟΠΕΙΟ ΠΑΝΕΠΙΣΤΗΜΙΟ
HAROKOPIO UNIVERSITY

This Doctoral Dissertation was examined by the following committee:

George Dedoussis (Supervisor), Professor of Molecular Genetics-Nutrigenetics, School of Health Science and Education, Department of Nutrition and Dietetics, Harokopio University of Athens

Dimitris Beis, Research Associate Professor, Head of Zebrafish Disease Models, Clinical, Experimental Surgery and Translational Research Center, Biomedical Research Foundation, Academy of Athens

Nikos Yiannakouris, Associate Professor of Biology, School of Health Science and Education, Department of Nutrition and Dietetics, Harokopio University of Athens

Panos (Panagiotis) Deloukas, Professor of Cardiovascular Genomics, Director of the William Harvey Research Institute, Faculty of Medicine and Dentistry, Queen Mary, University of London

Maria Gazouli, Professor of Biology-Nanomedicine, School of Medicine, National and Kapodistrian University of Athens

Manolis Mavroidis, Researcher C, Basic Research Center, Biomedical Research Foundation, Academy of Athens

Loukianos Rallidis, Professor in Cardiology, Second department of cardiology, Medical School, National and Kapodistrian University of Athens, Attikon University Hospital

The approval of the doctoral dissertation by the Department of Nutrition and Dietetics of Harokopio University does not imply the acceptance of the author's point of view.

Publication list of articles supported by the present thesis:

1. **Giardoglou P**, Beis D. On Zebrafish Disease Models and Matters of the Heart. *Biomedicines*. 2019 Feb 28;7(1):15. doi: 10.3390/biomedicines7010015. PMID: 30823496; PMCID: PMC6466020.

2. **Giardoglou P**, Deloukas P, Dedoussis G*, Beis D*. cfdp1 is essential for cardiac development and function. *bioRxiv* 2022.03.21.485062. doi: https://doi.org/10.1101/2022.03.21.485062

3. Graham S.E., Clarke S.L., Wu KH.K., […, **Giardoglou P**,] *et al*. The power of genetic diversity in genome-wide association studies of lipids. *Nature*, 2021. doi: 10.1038/s41586-021-04064-3

4. Aragam GK, [**…, Giardoglou P,**] on behalf of the CARDIoGRAMplusC4D Consortium. Discovery and systematic characterization of risk variants and genes for coronary artery disease in over a million participants. 2021 (Nature Genetics, in press). Medrxiv doi: 10.1101/2021.05.24.21257377

List of articles published during the present thesis:

1. **Giardoglou P**, Bournele D, Park M, Kanoni S, Dedoussis GV, Steinberg SF, Deloukas P, Beis D. A zebrafish forward genetic screen identifies an indispensable threonine residue in the kinase domain of PRKD2. Biol Open. 2021 Mar 9;10(3):bio058542. doi: 10.1242/bio.058542. PMID: 33597201; PMCID: PMC7969590.

2. Serifi I, Besta S, Karetsou Z, **Giardoglou P**, Beis D, Niewiadomski P, Papamarcaki T. Targeting of SET/I2PP2A oncoprotein inhibits Gli1 transcription revealing a new modulator of Hedgehog signaling. Sci Rep. 2021 Jul 6;11(1):13940. doi: 10.1038/s41598-021-93440-0. PMID: 34230583; PMCID: PMC8260731.

3. Leonidis G, Dalezis P, Trafalis D, Beis D, **Giardoglou P**, Koukiali A, Sigala I, Nikolakaki E, Sarli V. Synthesis and biological evaluation of a c(RGDyK) peptide conjugate of SRPIN803. ACS Omega. 2021 Oct. doi: 10.1021/acsomega.1c04576.

Ethics and Copyright Statement

I, Giardoglou Panagiota

Declare responsibly that:

I) I am the owner of the intellectual right of this original work, and to the best of my knowledge, my work does not insult any person, or offends intellectual rights of any third part.

II) I accept that Harokopio University Library and Information Center may, without changing the content of my work, provide it electronically through its Digital Library, copy it by any mean and/or format and hold more than one copies for maintenance and safety reasons.

The heart of a man is very much like the sea,

it has its storms, it has its tides

and in its depths, it has its pearls too.

The letters of Vincent van Gogh

Acknowledgements

"*If you want to lift yourself up, lift up someone else*" – Booker T. Washington

I am extremely grateful to my supervisor, Professor **George Dedoussis** for the opportunity to join his lab right after my homecoming back to Greece upon my return from the Netherlands. I am very thankful as he has always been supportive and open to fruitful collaborations in uncharted waters and gave me the freedom to conduct the main part of my Thesis Dissertation just few kilometers away from Harokopio University, in the BRFAA family. I am thankful for all the discussions we had from which I learnt to 'transform a dream into a goal and then achieve it'.

My deep gratitude goes to my daily supervisor Dr. **Dimitris Beis** for the scientific guidance through all these years, the trust and support in great, good and less good times. For the excellent work environment, discussion and communication that gave me the incredible opportunity to be part of many collaborations along with my Thesis project. I am truly thankful he helped me grow as scientist and learn how to think out of the box.

I would also like to thank Associate Professor **Nikos Yiannakouris** for being in my advisory committee and his valuable comments during the steps of this Dissertation. I am also very grateful to Professor **Panos Deloukas** for sharing his unpublished scientific data in order to initiate the current Thesis, the fruitful collaboration through these years and for participating in the Examination Board.

Also, I would like to thank Professor **Loukianos Rallidis**, Professor **Maria Gazouli** and Dr. **Manolis Mavroidis** for participating in the Examination Board.

A super special thank-you to the Zebrafish Lab that was a second family to me all these years. I am sure nothing would be the same without them!! **Manto** for always being the 'mother' of this family. Her support, the personal and scientific discussions and advice have been of a great value! **Matina**, my senior labmate, who shared with me not only the bench but also so many

moments of laughs, excitement, puzzlement, conference travels and many more! **Vania**, our German-raised postdoc, who instantly brought a new dawn upon her arrival to the Zebrafish Lab! I couldn't have asked for a brighter mind, a true professional, a greater scientist, a more dedicated zebrafish person, a 'please, use this only with gloves' (always accompanied with a smiley face) labmate! I am very grateful for all the moments we shared and the many more that are coming (in and outside the lab), the enthusiasm, willingness, positivity and kindness she offered! **Yiouli**, the young and wild master student who became immediately part of the lab gang. A thank-you for helping with the fish duties whenever it was needed, her fearless attitude and cunning way of thinking that made lab life a bit more interesting. And **Dimitris**, the last addition to the lab who brought his Spanish energy and knowledge not only in zebrafish heart regeneration but also in jamón slicing.

To my multitalented fellow creature **Ani,** I couldn't have gone through this PhD without her. A million thank-you for being such a great friend and life traveler, always there in extremely happy and tough times, she had my back over this long period in light and dark, and was a partner that everybody wishes to have. I am looking forward to all the moments that will come (anywhere in this planet). A huge thank-you to all the **BRFAA family** (Yasemi, Paraskevi, Andrianna, Chrysanthi, George, Sorania), the 3rd floor-PIs, the students, the technicians, the lab managers and everyone who joined to the awesome Developmental Biology department during these years!

Last but definitely not least, most of my sincere gratitude belongs to my **family,** my parents Savvas and Georgia, and my sister Dimitra. For their unlimited patient, unconditional love, utmost support and strong belief in me and what I could achieve. This book is dedicated to them.

Table of Contents

I. Περίληψη

Τα καρδιαγγειακά νοσήματα (ΚΝ) είναι η κύρια αιτία θανάτου σε παγκόσμια κλίμακα. Σύμφωνα με τον Παγκόσμιο Οργανισμό Υγείας, εκτιμάται πως 17.9 εκατομμύρια άνθρωποι κάθε χρόνο χάνουν τη ζωή τους από καρδιαγγειακές παθήσεις, ποσοστό που αντιστοιχεί στο 32% της παγκόσμιας θνησιμότητας. Τα ΚΝ αποτελούν την πιο συχνή μορφή μη-μεταδοτικών ασθενειών και περιγράφουν ένα ευρύ φάσμα παθήσεων που αφορούν στη λειτουργία και μορφογένεση της καρδιάς και των αιμοφόρων αγγείων. Η στεφανιαία νόσος (ΣΝ) αποτελεί μια βασική κλινική μορφή των ΚΝ και περιγράφει τη στένωση των στεφανιαίων αρτηριών λόγω συσσώρευσης αθηρωματικού υλικού στον αυλό τους με αποτέλεσμα να μην τροφοδοτείται επαρκώς η καρδιά με τα απαραίτητα συστατικά και οξυγόνο για τη λειτουργία της. Αποτελώντας μείζον ζήτημα δημόσιας υγείας, το ολικό κόστος των καρδιαγγειακών νοσημάτων μαζί με τις υπόλοιπες μη-μεταδοτικές ασθένειες (όπως ο καρκίνος, ο διαβήτης και η χρόνια πνευμονοπάθεια) αναμένεται να αυξηθεί ακόμα περισσότερο εξαιτίας της αύξησης του μέσου όρου ζωής του πληθυσμού καθώς και των κοινωνικών προτύπων. Συνεπώς, είναι τεράστιας σημασίας η προσπάθεια να οριστεί την πρόγνωση, πρόληψη, εξέλιξη και θεραπεία των καρδιαγγειακών νοσημάτων εντός πλαισίου φάσματος τροποποιήσιμων και μη-τροποποιήσιμων παραγόντων κινδύνου.

Είναι γνωστό πως η εκδήλωση της ΣΝ σχετίζεται με παράγοντες κινδύνου τόσο περιβαλλοντικούς όσο και γενετικούς. Στην πρώτη κατηγορία ανήκουν η αρτηριακή υπέρταση, η δισλιπιδαιμία, το αυξημένο σάκχαρο αίματος, η παχυσαρκία και ο τρόπος ζωής (όπως κάπνισμα, έλλειψη φυσικής δραστηριότητας, κακή διατροφή, άγχος και επιβαρυμένη ψυχική υγεία). Ωστόσο, ιδιαιτέρως σημαντικό ρόλο έχουν και οι γενετικοί παράγοντες που επιδρούν στην εμφάνιση της νόσου. Πληθώρα πληθυσμιακών μελετών έχουν στοχεύσει στην ανακάλυψη της γενετικής αρχιτεκτονικής που καθορίζει τη βάση των καρδιαγγειακών νοσημάτων. Μελέτες συσχέτισης ολόκληρου του γονιδιώματος (Genome-Wide association study - GWAS) έχουν ταυτοποιήσει πάνω από 60 γενετικούς τόπους που σχετίζονται με τη ΣΝ. Τέτοιες γενετικές παραλλαγές έχουν βρεθεί και σε δύο υποψήφια προς μελέτη γονίδια: *craniofacial development protein 1* (*CFDP1*) και *coiled-coil domain containing 92* (*CCDC92*).

Ο σκοπός της παρούσας διατριβής ήταν να μελετήσουμε τον λειτουργικό ρόλο των *CFDP1* και *CCDC92* στην ανάπτυξη της καρδιάς. Στα πλαίσια της έρευνας αυτής, χρησιμοποιήσαμε το zebrafish (*Danio rerio*) που έχει αναδειχθεί ως ένα πολύτιμο μοντέλο-οργανισμός στην έρευνα για τις καρδιαγγειακές παθήσεις, λόγω της υψηλής γενετικής ομολογίας, της ομοιότητας στη φυσιολογία της καρδιάς και την ευκολία του πειραματικού χειρισμού του. Το *CFDP1* ανήκει στη συντηρημένη οικογένεια των Κενταύρων (Bucentaur, BCNT) και έως σήμερα ο μηχανισμός δράσης του στην καρδιακή ανάπτυξη παραμένει άγνωστος. Ως εκ τούτου, δημιουργήσαμε μια *cfdp1* μεταλλαγμένη zebrafish σειρά μέσω του εργαλείου γονιδιωματικής τροποποίησης, CRISPR-Cas9. Ύστερα από ταυτοποίηση του μεταλλαγμένου αλληλομόρφου διαπιστώσαμε πως διαθέτει ένα πρώιμο κωδικόνιο λήξης στο τρίτο εξόνιο το οποίο παράγει ένα ελαττωματικό πρωτεϊνικό προϊόν. Η έλλειψη του *cfdp1* οδηγεί σε έναν θνησιγόνο φαινότυπο, αφού τα πλήρως μεταλλαγμένα άτομα δεν φτάνουν στο ενήλικο στάδιο ζωής. Φαινοτυπικός χαρακτηρισμός έδειξε πως τα μεταλλαγμένα *cfdp1* έμβρυα αναπτύσσουν καρδιακές αρρυθμίες και ελλιπή καρδιακή λειτουργία όπως αυτή αποτυπώνεται από τα μειωμένα επίπεδα του τελοδιαστολικού όγκου, καρδιακής παροχής, κλάσμα εξώθησης και όγκου παλμού. Περαιτέρω ανάλυση σε κυτταρικό επίπεδο έδειξε πως η κοιλιακή δοκίδωση είναι επίσης μειωμένη στα μεταλλαγμένα *cfdp1* έμβρυα, υποδεικνύοντας τον ρυθμιστικό ρόλου του γονιδίου στη μορφογενετική διαδικασία δοκίδωσης κατά την ανάπτυξη της zebrafish εμβρυικής καρδιάς. Τέλος, μετά τη διεξαγωγή knockdown και knockout πειραμάτων δείξαμε πως αποσιώπηση του *cfdp1* οδήγησε σε μειωμένα επίπεδα ενεργοποίησης του Wnt σηματοδοτικού μονοπατιού στις καρδιές εμβρύων κατά τη διάρκεια της δημιουργίας καρδιακών βαλβίδων, χωρίς να επηρεάσει την έκφραση του Notch μονοπατιού στη διαδικασία αυτή.

Το *CCDC92* ανήκει στην υπεροικογένεια των πρωτεϊνών σπειροειδούς ελίκωσης (coiled-coil proteins) και μολονότι πληθυσμιακές μελέτες έχουν αναδείξει πολυάριθμες παραλλαγές του γονιδίου να σχετίζονται με κλινικές μορφές της ανθρώπινης καρδίας, η λειτουργία του δεν έχει εξακριβωθεί, ούτε μελετηθεί επαρκώς. Στην παρούσα διατριβή, δείξαμε πως το zebrafish *ccdc92* εκφράζεται κατά τη διάρκεια την εμβρυικής ανάπτυξης από τα πρώτα στάδια, καταδεικνύοντας το σημαντικό ρόλο του γονιδίου για τη σωστή οργανογένεση και λειτουργία

του οργανισμού. Ακολούθως, διεξήγαμε πειράματα αποσιώπησης της έκφρασης του *ccdc92* (knockdown) σε έμβρυα zebrafish και μέσω φαινοτυπικού χαρακτηρισμού εντοπίσαμε ανάπτυξη περικαρδιακού οιδήματος και δομική δυσμορφία της καρδιάς. Περαιτέρω ανάλυση έδειξε πως αναστολή της έκφρασης του γονιδίου αυτού οδηγεί σε ελλαττωματική καρδιακή περιστροφή (cardiac looping), μια απαραίτητη διαδικασία για τη φυσιολογική μορφογένεση της καρδιάς κατά την ανάπτυξή της.

Η *Protein Kinase D2* (*prkd2*) ανήκει σε οικογένεια εξελικτικά συντηρημένων ενζύμων που ρυθμίζουν πληθώρα βιολογικών διεργασιών. Προσέγγιση ορθόδρομης μεταλλαξιγέννεσης στο μοντέλο zebrafish ανέδειξε μια μεταλλαγή στο γονίδιο *prkd2* (T757A) που προκαλεί στένωση αγωγού καρδιακής εκροής. Στην παρούσα μελέτη, καταγράψαμε την έκτοπη έκφραση του Notch μονοπατιού στην καρδιά μεταλλαγμένων εμβρύων, καθώς επίσης και αυξημένη ευαισθησία στην κυκλοσπορίνη Α (αναστολέας καλσινευρίνης). Ακόμα, αναδείξαμε την πιθανή ρύθμιση του Prkd2 από τον μεταγραφικό παράγοντα Tbx5 στα zebrafish έμβρυα.

Τέλος, στα πλαίσια της παρούσας διατριβής συμμετείχαμε στη συνεργασία GRMIC (Greek Recurrent Myocardial Infarction Cohort), μία προοπτική επιδημιολογική μελέτη με σκοπό τη διαστρωμάτωση των ασθενών ύστερα από εμφάνιση πρώτου επεισοδίου εμφράγματος του μυοκαρδίου, μέσα από τη δημιουργία μοντέλου πρόβλεψης ενσωματώνοντας γενετικούς παράγοντες μαζί με τη δράση βιοδεικτών. Μέχρι την ολοκλήρωση της διατριβής, 66 ασθενείς είχαν επανεξετασθεί μετά το πέρας των έξι μηνών από την εμφάνιση ισχαιμικού επεισοδίου. Ανάλυση επιπέδων γνωστών βιοδεικτών στο πλάσμα ασθενών στις δύο χρονικές περιόδους ανέδειξε πως η ολική χοληστερόλη, η χαμηλής πυκνότητας λιποπρωτεϊνική χοληστερόλη, απολιποπρωτεΐνη Β, C-αντιδρώσα πρωτεΐνη και η φωσφατάση της κρεατίνης παρουσίασαν στατιστικά σημαντικά αυξημένα επίπεδα την περίοδο εμφάνισης επεισοδίου σε σύγκριση με τα επίπεδά τους στο πλάσμα των ασθενών μετά το πέρας των έξι μηνών, επιβεβαιώνοντας τον προγνωστικό τους ρόλο για την πιθανότητα εμφάνισης εμφράγματος του μυοκαρδίου.

Λέξεις κλειδιά: Καρδιαγγειακά Νοσήματα, Στεφανιαία Νόσος, Zebrafish, CRISPR/Cas9 σύστημα, *cfdp1*, *ccdc92, prkd2,* δοκίδωση κοιλίας, καρδιακή περιστροφή, GRMIC

II. Abstract

Cardiovascular disease (CVD) is the prevalent cause of death worldwide and according to the World Health Organization, it is estimated that 17.9 million people die annually from CVDs, which accounts for the 32% of global mortality. CVDs are the most common noncommunicable disease and describe numerous conditions relating to the heart and blood vessel function and morphogenesis. Coronary artery disease (CAD) is the main CVD implication and is developed when inadequate supply of oxygen and nutrients reach the heart through the coronary artery network. The burden of CVDs along with other noncommunicable diseases (such as cancer, diabetes and chronic pulmonary disease) is expected to further increase due to the aging population and lifestyle patterns. Therefore, it is tremendous need to frame CVDs prognosis, prevention, progression and therapy within the spectrum of modifiable and non-modifiable risk factors.

It is well known, that the manifestation of CAD is related with risk factors that can be addressed as behavioral/environmental and genetic effectors. Traditional environmental risk factors include hypertension, dyslipidemia, hyperglycemia, obesity and lifestyle behaviors (smoking, lack of physical activity, poor diet, anxiety and stress-related conditions). In addition to that, it is long recognized that CAD is a heritage disease and plethora of human population studies have aimed to unravel the genetic architecture that underlines the basis of the heart disease. The increase of sample size and genome wide association studies (GWAS) have revealed several susceptibility loci for this multifactorial complex disease. Up to date, there have been identified more than 60 genetic loci correlated with traits of CADs. Such variants associated with the appearance of cardiovascular disease are located to the candidate genes: *craniofacial development protein 1* (*CFDP1*) and *coiled-coil domain containing 92* (*CCDC92*).

The aim of this dissertation was to investigate the functional role of *CFDP1* and *CCDC92* in the cardiac development. For this purpose, we utilized zebrafish (*Danio rerio*), a valuable model organism in Cardiovascular Research due to the high genomic homology, similarity in heart physiology and the ease of experimental manipulation. *CFDP1* belongs to the evolutionary conserved Bucentaur (BCNT) family and up to date, the mechanism of action in cardiovascular

development remains unclear. During this dissertation, we generated a *cfdp1*-null zebrafish line using CRISPR-Cas9 system and identified that the mutated allele carries a pre-mature stop codon at the third exon that produces a predicted truncated protein product. *cfdp1* loss leads to a lethal phenotype since knockout individuals do not reach adulthood. Phenotypic characterization showed that *cfdp1* knockout embryos develop arrhythmic hearts and defective cardiac performance including statistically significant differences in End Diastolic Volume, Cardiac Output, Ejection Fraction and Stroke Volume. Further analysis in cellular level exhibited that myocardial trabeculation is also impaired in *cfdp1* knockout embryonic hearts, suggesting its regulatory role in this essential cardiac developmental process. Finally, conduction of both knockdown and knockout experiments showed that abrogation of *cfdp1* results in downregulation of Wnt signaling in embryonic hearts during valve development but without affecting Notch activation in this process.

CCDC92 belongs to the superfamily of coiled-coil proteins and although a numerous of variants have been identified in human cardiac conditions, its function is still largely unknown. We showed that zebrafish *ccdc92* is expressed during the embryonic development, suggesting its important role in proper organogenesis and function. Following, we performed knockdown experiments by silencing the expression of *ccdc92* at one-cell stage zebrafish embryos. Phenotypic characterization of knockdown embryos revealed that deficiency of *ccdc92* exhibits embryonic cardiac oedema and heart malformation. Further analysis showed that *ccdc92* abrogation results in impaired cardiac looping during embryonic heart morphogenesis, an essential process for the proper structure and function of the heart. More studies are needed to be conducted in order to unravel the mechanism and possible signaling pathways that explain its role in proper cardiac morphogenesis.

Protein Kinase D2 belongs to a family of evolutionarily conserved enzymes regulating several biological processes. In a forward genetic screen for zebrafish cardiovascular mutants, it was identified a mutation in the *prkd2* gene (T757A substitution) which resulted in a complete outflow tract stenosis. In this study, we showed ectopic expression of Notch-activated cells throughout the heart of mutant embryos as well as higher sensitivity to Cyclosporin A (a

Calcineurin inhibitor). Finally, we identify TBX5 as a potential regulator of PRKD2. Our results implicate PRKD2 catalytic activity in outflow tract development in zebrafish.

Finally, we participated in the Greek Recurrent Myocardial Infarction Cohort (GRMIC), which is a prospective epidemiologic study that aims to the stratification of post myocardial infarction (MI) patients by integrating genetic and epigenetic predictors together with biomarkers in a risk prediction model. Up to this stage of the study, sixty-six Greek patients have been recruited at the period of first MI event and re-examined after a six months period. Although the sample size remains small, we analyzed the plasma levels of known biomarkers in patients compared to the two time periods and showed that total cholesterol, low-density lipoprotein cholesterol, apolipoprotein-B, C-reactive protein and creatine phosphokinase are significantly higher at the time of first MI event, confirming their prognostic value for the occurrence of first acute MI event. Taking into account that the design of this study requires the recruitment of 500 re-examined MI patients, our data thus far, represent a premature indication of essential biomarkers for MI. GRMIC is an ongoing prospective study that aims to leverage the power of genetics and biomarkers to design risk models for the post-MI patients, in following future.

Keywords: Cardiovascular Disease, Coronary Artery Disease, Zebrafish, CRISPR/Cas9 genome editing system, *cfdp1*, *ccdc92*, *prkd2*, ventricular trabeculation, cardiac looping, GRMIC

III. Abbreviations

Acronym	Meaning
A	Atrium
AV	Atrio Ventricular
bpm	Beats per minutes
BSA	Bovine Serum Albumin
$CaCl_2$	Calcium Chloride
CAD	Coronary Artery Disease
$CaSO_4.4H_20$	Calcium Sulfate dihydrate
cDNA	Complementary DNA
cmlc2	Cardiac myosin light chain 2
DEPC	Diethyl pyrocarbonate
DMSO	Dimethyl sulfoxide
DNA	Deoxyribonucleic Acid
dNTP	Deoxyribonucleotide triphosphate
dpf	Days post Fertilization
E.coli	Escherichia coli
EDTA	Ethylenediaminetetraacetic acid
EGFP	Enhanced Florescent Protein
fps	Frames per Seconds
gr	Grams
HCl	Hydrochloric acid
hpf	Hours post fertilization
IHC	Immunohistochemistry
ISH	In situ Hybridization

KCl	Potassium chloride
KH_2PO_4	Potassium dihydrogen Phosphate
KOAc	Potassium Acetate
L	Liter
LB	Luria Broth
mCherry	Monomeric red fluorescent protein (mFruit, mRFP)
mg	Milligram
ml	Milliliter
mM	Millimol
MOPS	4-Morpholinepropanesulfonic acid
MS222	Buffer tricaine mathanesulfonate
mRNA	messenger RNA
$MgCl_2$	Magnesium Chloride
$MgSO_4$	Magnesium Sulfate
$MnCl_2$	Manganous Chloride
myl7	Myosin light chain 7
NaCl	Sodium Chloride
NaOH	Sodium Hydroxide
Na_2HPO_4	Disodium Phosphate
ng	nanogram
nl	nanoliter
nls	Nuclear localization signal
OFT	Outflow tract
PFA	Paraformaldehyde
PBS	Phosphate Buffer Saline
PCR	Polymerase Chain Reaction
PTU	N- Phenylthiouria

$RbCl_2$	Rubidium chloride
Real time qRT-PCR	Real time Quantitative Reverse Transcription PCR
RNA	Ribonucleic Acid
rpm	Revolutions per minutes
RT	Room Temperature
RT-PCR	Reverse-transcription PCR
SDS	Sodium dodecyl sulfate
sec	seconds
SEM	Standard error of the mean
SSC	Saline-Sodium Citrate
TAE	Tris acetate EDTA
TCF	T-cell factor
TP1	Terminal protein 1 (of Epstein Barr Virus)
tRNA	Transfer RNA
ul (µl)	Microliter
ug (µg)	Microgram
uM (Mµ)	Micromol
V	Ventricle
wt	Wild-type

IV. List of Figures

List of Tables

1. Introduction

1.1. Cardiovascular diseases under the microscope

Epidemiological transition during the last century and before the ongoing pandemic of SARS-Cov2 refers to the reduction of mortality caused by communicable diseases in favor of the disability and morbidity caused by the noncommunicable diseases (NCD). A possible theory of that transition could lay on prospective population changes regarding demographic and socioeconomic trends and patterns (Rice, 1971). Communicable and noncommunicable diseases are related to low- and high- income countries, reflecting a difference among the poor and the rich populations. Recent data on global scale show that approximately 2.5 million people per year die from HIV and tuberculosis (infectious communicable diseases), while 5 million die only from diabetes mellitus (chronic noncommunicable disease) (Harries *et al.*, 2015). NCD kill approximately 41 million people each year, which represents the 71% of deaths globally. Cardiovascular diseases (CVDs) are the major contributor of NCD deaths, followed by cancers, respiratory diseases and diabetes. According to the World Health Organization (WHO) global observatory data, cardiovascular diseases are the leading cause of mortality and disability for approximately 17.9 million people annually, which is estimated to be 31% of global deaths (Benziger, Roth and Moran, 2016; Wang *et al.*, 2016; Kaptoge *et al.*, 2019). Disability-adjusted life years (DALY) are produced from the years life lost and the years lived with disability and it consists of a factor for global disease burden (Joseph *et al.*, 2017). Cardiovascular diseases account for the 24% of NCD-related DALY and occurred largely in low-income countries (LIC) compared to high-income countries (HIC) affecting mostly the working-age population in the LIC (Alwan and MacLean, 2009; Bovet and Paccaud, 2011; Gheorghe *et al.*, 2018). The vast economic loss due to CVDs is estimated around 3.7 trillion between 2011-2015, which is half the NCD economic burden (Gheorghe *et al.*, 2018). Therefore, it is a global interest and challenge to reduce the cardiovascular disease manifestation and burden by

applying approaches adjusted to diverse economic and social patterns of heterogeneous populations (Leong *et al.*, 2017).

CVD describes a spectrum of diseases affecting the proper function and physiology of the heart and blood vessels. Among those conditions, here we listed ischemic heart disease, hypertensive heart disease, cardiomyopathy and myocarditis, atrial fibrillation, endocarditis, cerebrovascular diseases, aortic aneurysm and peripheral vascular diseases. Though, coronary artery disease (CAD) and its main complication myocardial infarction (MI) are reported to be the leading form of cardiovascular disorders and result in the prevalent cause of total human mortality and morbidity. Over the last decades, a lot of research studies have been conducted in order to dissect the epidemiology regarding the CAD and further identify the causality and the risk factors provoking its appearance.

Coronary artery disease is an outcome of atherosclerotic plaque build-up in the wall of arteries that supply blood (oxygen and nutrients) to the heart, called coronary arteries (Figure 1). The formation of plaques, which consist of cholesterol and other substances, will eventually narrow the arteries over time that will block the blood flow. Specifically, when certain risk factors such as substances involved in hypertension, dyslipidemia, hyperglycemia, proinflammatory cytokines or excess adipose deposition reach arterial endothelial cells, then the later promote the sticking of blood leukocytes in the inner cell wall. Continuous infiltration of lipoprotein-containing particles in the arterial wall provokes inflammatory response by macrophages foam cells. Once all resident in arterial intima, endothelial and smooth muscle cells exchange major signaling messages regarding the mediators of inflammation, immunity and lipids. Smooth muscle cells underlying the vascular wall, proliferate and lead to remodeling of the vessel and the progress of the atherosclerotic lesion. In addition, cell death also occurs and macrophages foam cells die leading to extracellular deposition of lipids. Ultimately, endothelial cells can no longer regulate the vascular tone leading to the narrowing of the vessel, the increase of vascular permeability and the final obstruction of blood flow (Libby and Theroux, 2005; Khera and Kathiresan, 2017).

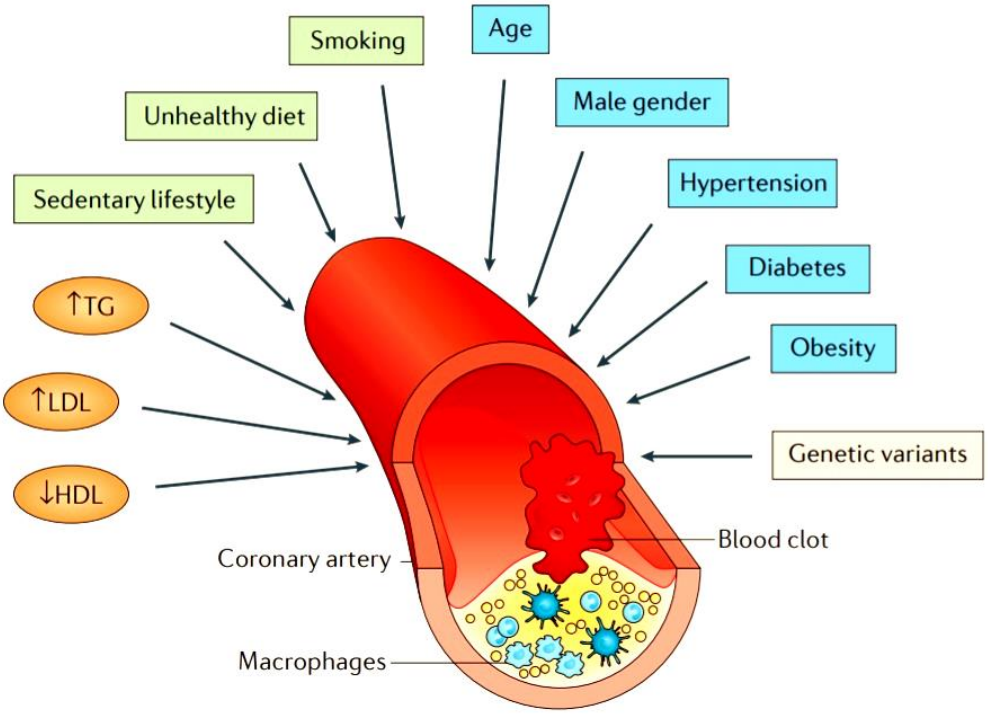

Figure 1: Overview of pathophysiology and risk factors related to coronary artery disease (adjusted from *Khera A.V. and Kathiresan S., Nature Reviews Genetics, 2017*).

As expected from the inestimable sheer burden of CAD and the complexity of the disease architecture, the risk of developing disease is spread to a wide environmental and genetic spectrum and it is modulated by the interplay between them (Figure 2). The Framingham Heart Study was the first attempt to elucidate the underlying risk factors of cardiovascular disease, enrolling its first participant in 1948 (Mahmood *et al.*, 2014). The established, traditional environmental risk factors are divided in modifiable and non-modifiable and up to date, many human studies have been designed aiming to evaluate their contribution to the manifestation of heart diseases. Non-modifiable factors include age, gender, ethnicity, parental history and consanguineous marriage (Tabei *et al.*, 2014; Manfrini *et al.*, 2020). Although, men are at higher risk of CAD occurrence compared to woman, very recent data showed that woman signify higher risk of mortality in obstructive CAD (stenosis ≥ 50%) than men and therefore it is the most life-threatening event of CAD in woman. At the same study, no sex differences in mortality rate was found between patients with non-obstructive CAD

(Makarović *et al.*, 2018; Manfrini *et al.*, 2020). Risk of CAD increases also with age, especially young men are more vulnerable than age-matched women (Grundy *et al.*, 1999; Tabei *et al.*, 2014). In addition, increased cardiovascular risk in women is correlated with peri- and postmenopausal age (Windler, Eidenmüller and Zyriax, 2004; Tabei *et al.*, 2014). Ethnicity, also seems to play a role in the occurrence of CAD. It is indicated that African Americans, Hispanics/Latinos and South Asians have higher proportional mortality rates from heart diseases (Rodriguez *et al.*, 2014; Carnethon *et al.*, 2017; Volgman *et al.*, 2018). The strong association of family history and premature CAD event has also been reported in family studies (Slack and Evans, 1966; Nasir *et al.*, 2007; Bachmann *et al.*, 2012; Tabei *et al.*, 2014). A study on the population of England and Wales, examined the deaths from ischemic heart disease at the first degree relatives of patients (121 men and 96 woman) to those of control healthy individuals and found that they were 7-fold increased (Slack and Evans, 1966). In addition, male relatives of patients showed 5 times higher risk of death compared to relatives of general populations, while woman relatives of patients showed 2 ½ times risk of death than that of the females relatives in the general population (Slack and Evans, 1966). Last, the intrafamilial reproduction as a result of inbreeding raised the risk of cardiovascular disease among other complex diseases. High levels of consanguineous marriage occurs in north Africa, middle East, west and central Asia and account for high the presence of high homozygosity (Bittles and Black, 2010). It is found that death rate in first-cousin offspring is 3.5% higher than the general non-relative progeny derived from nonconsanguineous mating, and of course it is significantly influenced by socioeconomic and demographic factors.

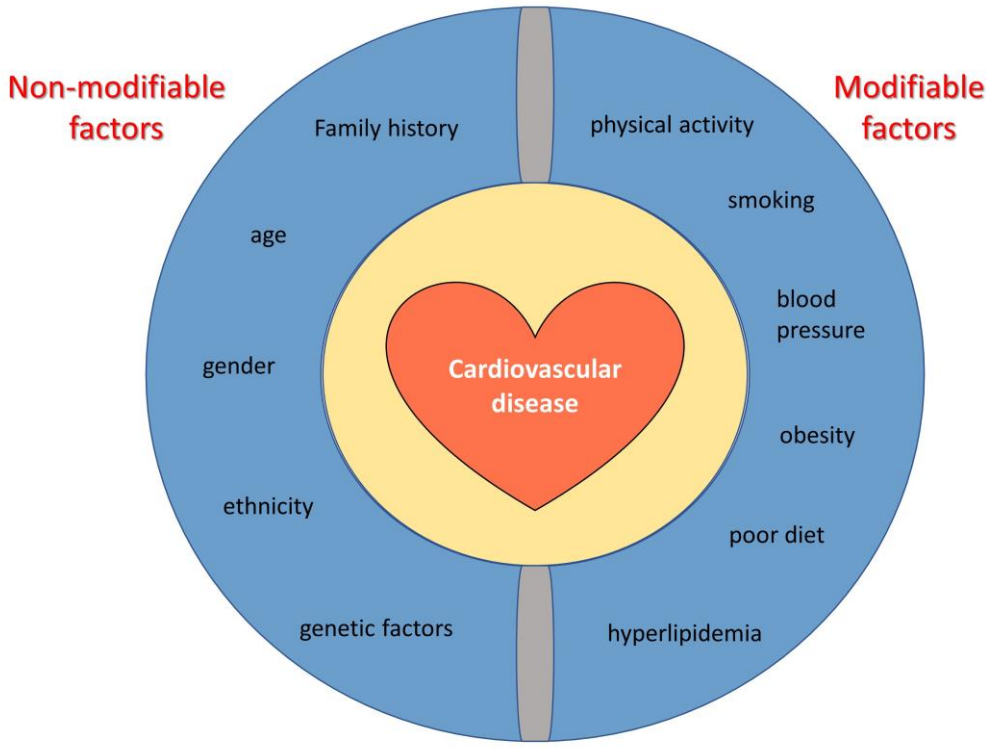

Figure 2: List of risk factors of cardiovascular diseases. Modifiable and non-modifiable factors are presented to the right and left of the chart, respectively.

In parallel, there are also modifiable environmental factors that play smaller (but still very significant) role than non-modifiable, in the development and appearance of heart disease. These are factors that can be altered, estimated, prevented, smoothened or even treated, and are closely related to lifestyle and behavioral patterns. These include hypertension, hyperlipidemia, overweight-obesity, tobacco smoking, poor diet (saturated fat, soft drinks and sweetened beverages, high salt- and sugar- diet, red meat consumption, alcohol use), sedentary life/lack of physical exercise training, as well stress and anxiety levels. Of note, it should be stated that hypertension, hyperlipidemia and blood pressure could as well be categorized as genetic risk factors in cases that altered corresponding genes are involved in the genetic architecture of a person. A comparative study between 12 modifiable factors, showed that high blood pressure and smoking are responsible for the larger portion of deaths in United States (Danaei *et al.*, 2009). Hypertension (≥140/90 mm Hg) increases atherosclerotic events

two- to three fold (Kannel, 2009). A meta-analysis of one million adults in 61 prospective studies showed that 20 mm Hg reduction of systolic blood pressure results to two fold decrease mortality risk from heart diseases at the ages 40-49 and 1/3 fold at the ages of 80-89 (Lewington *et al.*, 2002; Arnett *et al.*, 2019). Another risk factor for cardiovascular disease in hyperlipidemia (Becker, 2008; Ripatti *et al.*, 2020). Specifically, data from 10 perspective studies showed that 0.6 mmol/l (about 10%) reduction of serum cholesterol concentration resulted in the decrease of ischemic heart diseases incident of 54% for the age of 40 years, 39% for the age of 50 years, 27% for the age of 60 years, 20% for the age of 70 years and 10% for the age of 80 years (Law, Wald and Thompson, 1994). Obesity, estimated by body mass index (BMI) provokes a numerous health implications and is associated directly with risk of cardiovascular diseases as well as with other risk factors of CAD, such as hypertension, dyslipidemia and diabetes mellitus type 2 (Jahangir, De Schutter and Lavie, 2014; Medina-Inojosa *et al.*, 2018; Katta *et al.*, 2021). It is worth mentioning, that lot of studies and meta-analysis in heart failure cohorts have revealed the obesity paradox describing that overweight patients have a better prognosis with respect to cardiovascular diseases compared to lean patients, probably influenced by cardiorespiratory fitness (Elagizi *et al.*, 2018; Carbone *et al.*, 2020). Tobacco use and cigarette smoking is another widely known and established risk factor for cardiovascular disease (Huxley, 2015; Manfrini *et al.*, 2020; Levin *et al.*, 2021). Analyses from former smokers support that quitting smoking at any age will reduces the mortality risk related to CAD and other tobacco-related diseases, and also that stop smoking is more effective than reducing the number of cigarettes consumed (Thun *et al.*, 2013). Pharmacological therapies such as nicotine replacement (nicotine gum or nicotine patches) increases the augment of smoking cessation providing additional benefits (however, nicotine replacement affects birth defects and should be avoided during pregnancy) (Larzelere and Williams, 2012; Green, 2015). Alcohol consumption does not have a linear association with CAD relative risk, as a light-drinker (36 grams/d of alcohol) shows a reduced risk of CAD compared to a non-drinker (Yang *et al.*, 2016; Song *et al.*, 2018). Consumption of soft drinks is also related with higher arterial stenosis and considered to have negative relationship with CAD (Bahreini, 2019). Poor diet is a major cause of obesity, diabetes as well as cardiovascular disorders. Mediterranean and vegetarian diet have shown strong evidence that

have a cardiovascular prevention role and can reduce CVD morbidity (Mattioli *et al.*, 2017; Pallazola *et al.*, 2019). Another important risk factor is the sedentary lifestyle. Exercise training enhances blood flow and improves endothelial and smooth muscle cells function in coronary arteries. It increases oxygen demand and promotes systemic and specific adaptations (deactivation of reactive oxygen species, improvement of vasculature, production of endothelial nitrous oxide) that reduce the risk of myocardial infarction and angina (Bruning and Sturek, 2015). Last, psychological interventions are among the risk factors contributing to the occurrence of CAD event, since stress, anxiety and depression have been also reported to effect daily angina (Pimple *et al.*, 2015; Richards *et al.*, 2018; Lu *et al.*, 2021).

Although CAD is strongly associated with behavioral risk factors, siblings and population studies have revealed the genetic basis of the heart diseases as well, and therefore, research interest has been focused in elucidating their genetic causality (Veljkovic *et al.*, 2018). The heredity of CAD was already assessed since 1951, where 100 individuals prior to the age of 40 that have experienced myocardial infarction were examined and showed that the percentage of the parents of patients that had MI event was twice the percentage of the parents of healthy control (Gertler, Garn and White, 1951). Thus, the notion of the theory that "CAD runs in the family" shifted the interest also in the genetic architecture of coronary heart disease. In order to examine the familial occurrence of CAD, studies on twin siblings were conducted (Marenberg *et al.*, 1994; Zdravkovic *et al.*, 2002; Mangino and Spector, 2013). A cohort study in 20.966 twins in Sweden and a 36-years follow-up confirmed the genetic contribution in CAD-mortality both in men and women, and also stated that the genetic effect can be apparent in young age but it remains in operation throughout lifespan (Zdravkovic *et al.*, 2002). The additional advantage of twin studies lays on the integration of additional risk factors such as age and life style, along with family history and genetic background (same at the identical monozygotic twins and high similarity in fraternal dizygotic twins) allowing analysis of gene-gene interactions and epigenetic modifications (Mangino and Spector, 2013). Overall, epidemiological studies unraveling the heredity of CAD, have supported that 40-60% susceptibility is attributed to genetic contribution (Veljkovic *et al.*, 2018).

Advantages of technology via whole genome and exon- sequencing applied in large-scale human studies allowed the discovery of genetic variations that are highly correlated with traits of specific diseases. Genome-wide association studies (GWAS) for cardiovascular and coronary diseases gather invaluable information for loci harboring single nucleotide polymorphisms affecting the outcome of the disease. Familial studies reveal the genetic causality of extreme phenotypes especially at young age without the existence of obvious risk factors. A study on a young man with clinical characteristics of familial hypercholesterolemia and his relatives, unraveled that mutation on a single gene encoding the LDL receptor that deletes exons of transmembrane and cytoplasmatic part of receptor is responsible for the risk of CAD (Lehrman *et al.*, 1985). Another family history study on familial defective apolipoprotein B that is correlated also with CAD risk was conducted in individuals of three families. A mutant allele caused by a single nucleotide change in apo-B resulted in the defect binding in LDL (Soria *et al.*, 1989). Thus, studies in families have been very useful for discovery of genes responsible for CAD risk and mortality. However, CAD is a complex disease and broader correlations and linkages must be performed. Common genetic variants that occurred more frequently are tested in patient-control group studies are mostly covered in GWAS studies for CAD. Progressively larger number of data integration in the pool of genetic and phenotypic data of CAD have led to the dissection of their genetic causality revealing more than 60 correlating loci (Deloukas *et al.*, 2013; Nikpay M, Goel A, Won HH, Hall LM, Willenborg C, Kanoni S *et al.*, 2015; Khera and Kathiresan, 2017; Nelson *et al.*, 2017; Wild *et al.*, 2017; Ntalla *et al.*, 2019). However, the vast majority of the identified variants covers only a part of CAD heritability, raising the issue of the 'missing heritability' in the genome. Therefore, a multifactorial systemic quantitative approach must be applied in the future (So *et al.*, 2011).

Given the aggregating genomic, phenotypic and bioinformative data, the role of databases and biobanks is apparent in order for the collected exome and genome sequencing data from large-scale studies to be broadly available to the scientific community. The Genome Aggregation Data (gnomAD) is such a resource providing genomic information from 76,156 genomes from individuals covering various disease-specific and population studies information. The importance and the need of biobanks is becoming increasingly appreciated, over the last

years. Biobanks are responsible for the biological material collection and aim to identify new factors, biomarkers and therapeutic targets for a wide spectrum of diseases (Malsagova *et al.*, 2020). UK Biobank is a unique resource of genomic data from 500,000 participants along with phenotypic, demographic, transcriptomic and follow-up data (Sudlow *et al.*, 2015; Bycroft *et al.*, 2018). The role of UK Biobank in interrogating CAD pathophysiology, prognosis and prevention has been highlighted through the numerous of studies derived from its data and the impact in cardiovascular research is estimated to be very high.

As next step, biological underpinning of CAD considered to be essential and necessary to unravel the mechanism of action leading to the development of cardiovascular disease. Therefore, functional assessment of candidate variants remains the most powerful and validated strategy to elucidate their specific correlation with the manifestation of the disease. *In vivo* data derived from system models utilized to characterize the clinical phenotype and the mechanism by which the candidate variants are implicated to the pathogenicity of CAD, remains the most precious strategy. The selection of the proper animal is crucial to design the most suitable and appropriate approach in order to address important research questions. Each animal model carries advantages and the limitations depending on the respective biological system aimed to be studied.

During the current dissertation, we utilized zebrafish (*Danio rerio*) as a favorable animal model to study further cardiovascular-candidate genes derived from human population studies. At the next chapter, we will discuss the advantages of the model and its powerful use in cardiovascular field during the last decades. The importance of zebrafish models for the functional analysis of candidate genes derived from large-scale studies has been highlighted via the generation of mutant zebrafish lines and the further analysis in phenotypic, cellular and molecular level.

1.2. Zebrafish (*Danio rerio*): little fish with vast impact in modeling Human Diseases

The zebrafish model has been increasingly used in cardiovascular research field and have augmented the understanding of pathogenic mechanisms which is the primary requirement for the discovery and design of suitable prognostic and therapeutic strategies (reviewed in (Bournele and Beis, 2016; Gut *et al.*, 2017; Giardoglou and Beis, 2019)). Due to the biological advantages that it carries, the easy manipulation, the high genetic similarity to humans and the development of laboratory and bioinformative technologies, it has become an essential vertebrate model to answer fundamental research questions.

Zebrafish is the common name of the scientific *Danio rerio* (Kingdom: Animalia/Metazoa, Phylum: Chordata, Vertabrata, Class: Actinopterygii, Teleostei, Family: Cyprinidae, Genus: Danio, Species: D.rerio) and it is a freshwater fish naturally found in the rivers and streams primarily of south Asia. Although zebrafish is distributed throughout India, Bangladesh and Nepal, it has also been introduced in Florida, California South Mexico and Colombia. Zebrafish are named after the blue stripes throughout the length of its body. Male fish typically have more slender body shape compared to females, who have more protruding belly where eggs are stored. Males also appear to be more gold-pinkish colored than females, who have a silvery streak on the body. The sex of the zebrafish is not fully clarified as it is based both in genetic sex determination (GSD) and environmental sex determination (ESD). GSD includes genetic factors on a polygenic basis, where sex genes are distributed in the whole genome lacking single sex chromosomal pair. Sex determination actually, is based on a gene – environment interaction, since factors such as temperature, population density, hypoxia and food influence the final sex at 28 dpf approximately (Santos, Luzio and Coimbra, 2017). It is a small-sized fish (2-5 cm in length) with high fecundity (each zebrafish adult pair produces large number of offspring, up to 300/week), *ex utero* (monitoring of embryonic stages without sacrificing the female) and transparent embryonic development (offering optical advantage for microscope imaging), as well as short generation time (Figures 3,4).

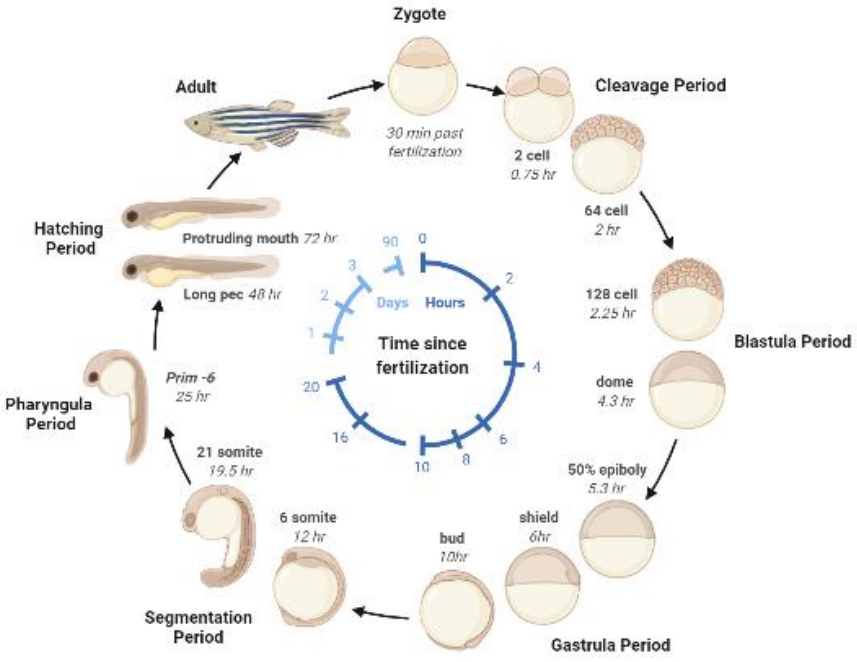

Figure 3: Stages of zebrafish embryonic development (created by *BioRender.com*).

For zebrafish breeding, a pairwise set up must be performed late in the afternoon after feeding where a male and female are placed in the same fish tank filled with system water, with a separator in between them. Initiation of the breeding occurs at the onset of the light, after removal of separator and allowing mating to occur undisturbed for 20 minutes. Collection of eggs with a strainer can be performed then or when sufficient number of eggs are laid, and after removal of unfertilized eggs, the embryos can be monitored at controlled conditions for further manipulation (Avdesh *et al.*, 2012). The high number of embryos is very useful biological advantage especially at experimental strategies that perform molecules- or drug- screenings where large number of animals are needed in order to test different concentrations of wide variation of candidate products. In addition, zebrafish has a low-cost maintenance condition, and therefore can be housed very efficiently in the laboratory aquariums.

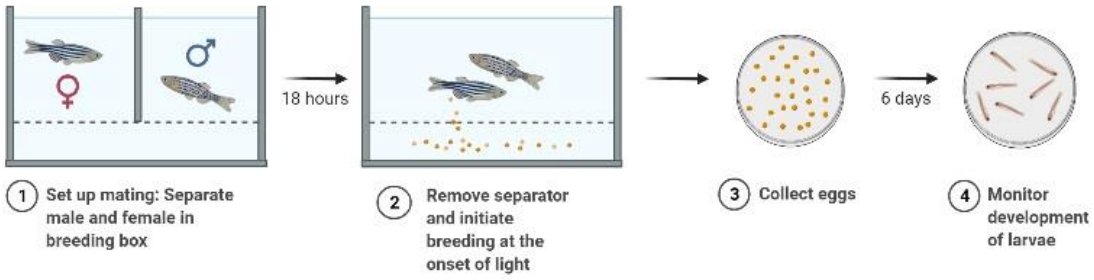

Figure 4: Breeding and collection of zebrafish eggs (created by *BioRender.com*).

Furthermore, the ability of zebrafish to obtain adequate oxygen via passive diffusion through the skin gives them the possibility to fully function without blood circulation up to 4-5 dpf. This biological characteristic is turned into experimental advantage so as to generate zebrafish models and study extreme developmental cardiovascular phenotypes and the underlying mechanisms that affect the pathophysiology of a disorder which can be lethal in mammalian models (Hu *et al.*, 2000; Bakkers, 2011; Bournele and Beis, 2016; Hodgson, Ireland and Grunow, 2018). Zebrafish is a popular animal model for genetic dissection and functional studies related to cardiovascular disorders, also due to the high genetic similarity that it shares with humans. Zebrafish genome sequencing project was initiated from Sanger Institute in 2001 and provided the greatest gene assignment of any vertebrate sequenced (Howe *et al.*, 2013). The zebrafish genetic architecture carries a whole-genome duplication (WGD), and thus gene redundancy must be taken under consideration during the design of experimental strategy (Meyer and Schartl, 1999). According to the Online Mendelian Inheritance in Man (OMIM) database, there are 82% human morbid genes corresponding to zebrafish orthologues, and 72% of zebrafish genes are homologues to human genes related to GWAS analysis (Howe *et al.*, 2013). In addition, zebrafish is suitable for regeneration studies, since it is among the few vertebrates that maintain their high regenerative capacity of several organs, including the heart (Moss *et al.*, 2009; Marques, Lupi and Mercader, 2019; Nguyen, de Bakker and Bakkers, 2021). A property that is lost in high vertebrates or limited at specific tissues (for example skin or liver)

or for a defined time after birth (Porrello *et al.*, 2011). Thus, despite the phylogenetic distance between humans and zebrafish, the high gene conservation led to a boost of zebrafish use for modeling human diseases (Figure 5).

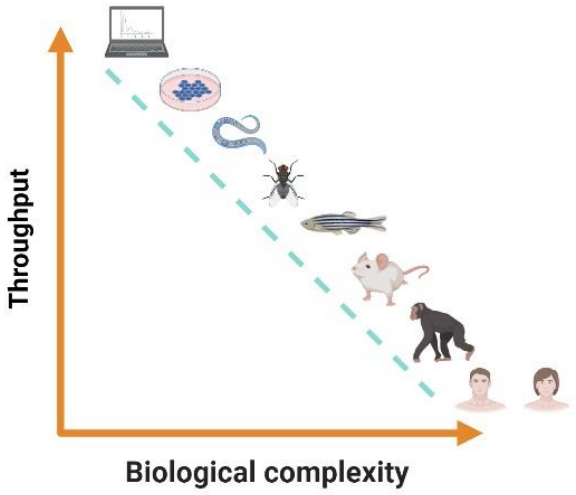

Figure 5: The developing utility of zebrafish as experimental model offers an important position in the biomedical research as a precious vertebrate system among others (*in silico*, *in vitro*, *C.elegans*, *Drosophila melanogaster*, small and large mammal models) (created by *BioRender.com*).

1.2.1 Genetic engineering toolbox

Apart from the aforementioned advantages of zebrafish as an experimental animal model, the development of new technologies for genome engineering, imaging approaches and biochemical tools and strategies brought new insights in zebrafish utilization in the modeling of human diseases. Forward and reverse genetic approaches have been applied in zebrafish in order to elucidate the genetic causality and the function outcome, respectively. Forward genetics include, among other chemical mutagens, the wide use of *N*-ethyl-*N*-nitrosourea (ENU) which induces random mutations in male zebrafish and surpass the technical limitations of other animal models, such as breeding scheme, large-scale husbandry and difficulties in

observing interesting phenotypes during development (Beis, Kalogirou and Tsigkas, 2015). Following to the phenotypic screening of mutants, chromosomal mapping and identification of the responsible genes give new information about the mechanism underlying the manifestation of human disease condition. Up to date, there are more than 50 zebrafish line coming from cardiac phenotype screening which provided new insights in the regulators of heart physiology, morphogenesis and function (Stainier *et al.*, 1996; Sehnert *et al.*, 2002; Beis *et al.*, 2005; Giardoglou *et al.*, 2021).

A toolbox for reverse genetics is also available for large-scale applications using the zebrafish model. A valuable technology which is widely used to target specific gene expression is the use of the Gal4-UAS system from yeast (Asakawa and Kawakami, 2008). This system consists of two components, and the combined use of transgenic lines results in tissue-specific labeling, cell ablation and specific gene expression (Davison *et al.*, 2007; Gawdzik *et al.*, 2018; Iida *et al.*, 2018). The Gal4 gene trap combines Gal4 zebrafish line under the expression of an endogenous promoter (gene A) and a reporter UAS (upstream activation sequence) zebrafish line, so as at the cells that gene A is expressed, Gal4 will bind to UAS region and turn on the gene next to UAS (most often a fluorescent protein to visualize the cells) (Asakawa and Kawakami, 2008). Another strategy is the Cre/lox system which is also widely used for spatiotemporal recombination genetic control, where bacteriophage P1-derived cyclic recombinase (Cre) catalyzes the site-specific recombination between two inverted repeat lox sites (*locus of X-ing over*) (Felker and Mosimann, 2016). The strategy implies an expression of Cre under the promoter of gene A and a *lox*-flanked cassette under a promoter of gene B, followed by a second cassette expressing the gene of interest. Upon activation of Cre at the cell expressing the gene A, excision of *lox*-flanked cassette will be occurred bringing the second cassette at the control of promoter of gene B (Felker and Mosimann, 2016; Carney and Mosimann, 2018).

Reverse genetic approaches also include knockdown approaches and the most commonly applied technique in zebrafish is by injecting morpholino antisense oligomer (MO) molecules at one-cell stage embryos (Nasevicius and Ekker, 2000). MOs are synthetic nucleotide analogs, 25-mer long, which are designed accordingly to the natural nucleotides and contain DNA bases (for

base-pairing ability with the target sequence) to a backbone consisting of morpholine rings instead of deoxyribose or ribose rings. They don't degrade their target RNA but with their high RNA affinity, they block either the proper splicing process by targeting splicing junctions (splicing MOs) or the initiation of translation by blocking translational starting sites (ATG MOs). They are dose-dependent and have been heavily used to study the function of specific genes upon the silencing of their expression via MO-injections. However, there are concerns about off-target effects or p53-induced apoptosis, so a conclusive knockdown strategy design should have appropriate controls and make use of multiple morpholino targets (Kok *et al.*, 2015; Stainier *et al.*, 2017). Undoubtedly, the evolution of a genetic toolbox for genome editing fine-scissoring has facilitated the generation of stable mutant lines and the study of knock-out and knock-in approaches in order to unravel the accurate function of specific genes or even single nucleotide polymorphism. Genome editing requires precise manipulation of DNA sequence in order to improve our understanding of the effect of genes in human genetic diseases and to unravel the mechanism that drive their pathophysiology. DNA-cleaving enzymes have played a crucial role in genome editing techniques, including zing finger nucleases (ZFNs), transcription activator-like effector nucleases (TALENs), and clustered, regularly interspaced, short, palindromic repeats/Cas (CRISPR-associated) (CRISPR/Cas), techniques that have been used for targeted mutagenesis with high successfully rates (Doyon *et al.*, 2008; Meng *et al.*, 2008; Cermak *et al.*, 2011; Bedell *et al.*, 2012; Cade *et al.*, 2012; Hwang *et al.*, 2013; Jao, Wente and Chen, 2013; Sood *et al.*, 2013; Varshney GK, Pei W, LaFave MC, Idol J, Xu L, Gallardo V, Carrington B, K, Jones M, Li M, Harper U, Huang SC, Prakash A, Chen W, Sood R, Ledin J and SM., 2015; Doudna, 2020). CRISPR/Cas9 technologies have brought a real revolution in the field of biotechnology and have been applied in a plethora of studies focusing on the dissection of complex diseases like heart disorders. The most recent methodology for conditional gene inactivation is the alternative approach of Cre-Controlled CRISPR (3C) mutagenesis (Hans *et al.*, 2021). This system is based on Cre effector construct of *floxed* stop cassette followed by open reading frame Cas9/GFP fused sequence cassette upstream of gRNA targeting a gene of interest (GOI) under the *U6a* zebrafish promoter. After exogenous supply of Cre, site-specific

recombination occurs so as expression of Cas9 is activated and together with gRNA synthesis (constituted expressed) the complex Cas9/gRNA is formed leading to mutagenesis in GOI.

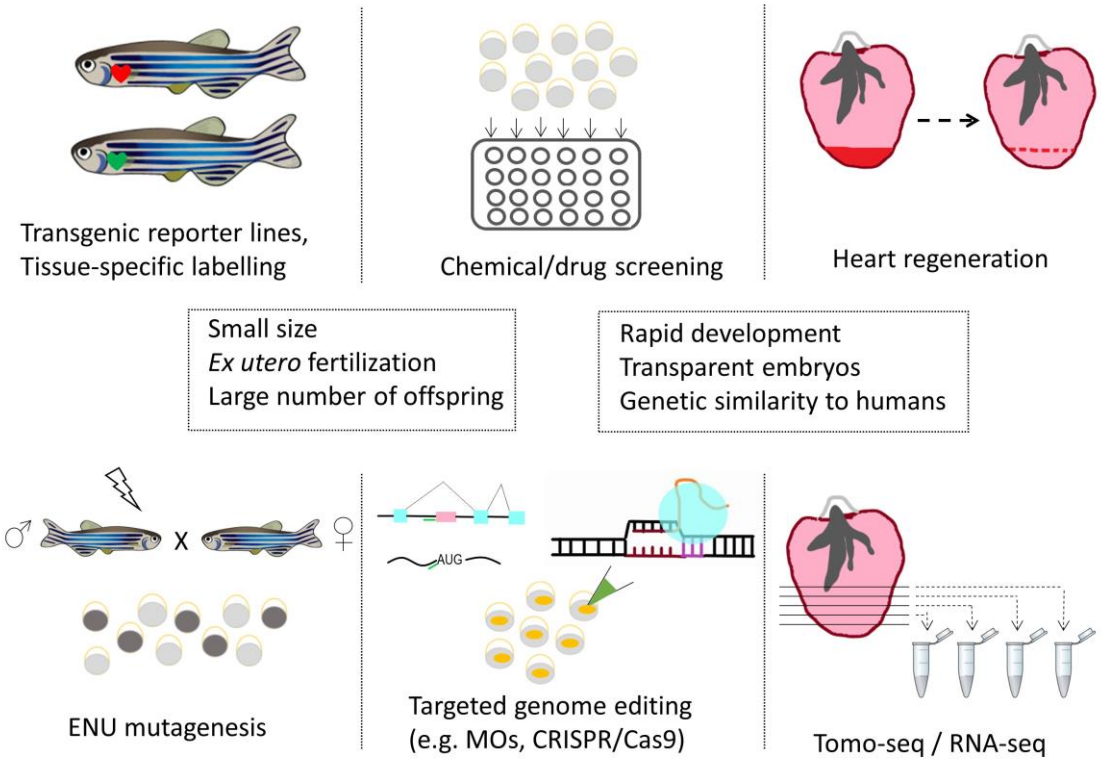

Figure 6: Biological and technical advantages of zebrafish as an animal model for Biomedical Research. Zebrafish are amenable to genomic, biochemical and imaging approaches (*Giardoglou P. and Beis D. Biomedicines, 2019*).

The CRISPR/Cas9 mutagenesis system lies at the core of tailor-mode genomic modifications in many model systems (Gaj, Gersbach and Barbas, 2013; Hsu, Lander and Zhang, 2014). This methodology is modified by the CRISPR/Cas9 prokaryotic adaptive immune system which allows defense against foreign invasion elements (Faure, Makarova and Koonin, 2019; Garcia-Robledo, Barrera and Tobón, 2020). Briefly, this system functions by incorporating mobile fragments of foreign genetic material into specific locus of bacterial DNA, called crispr arrays. This locus contains spacers from foreign elements and when transcribed they proceed

to generate spacer-containing crispr RNA (crRNA) and together with transacting RNA (tracr RNA) molecules, they will form a complex with Cas9 endonuclease protein. Following, the complex RNA/Cas9 will recognize and bind to the foreign genetic material, provoke its cleavage and consequently its inactivation (Figure 7).

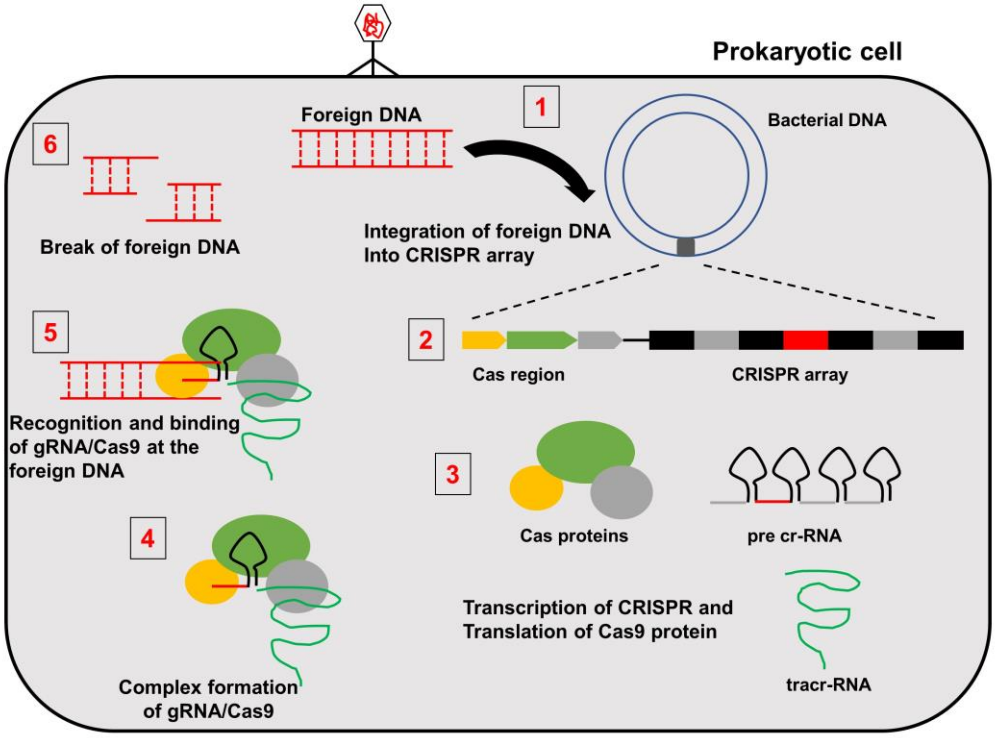

Figure 7: CRSPR/Cas9 system, an adaptive mechanism of prokaryotic cells for defense against invasion.

Based on the principles of CRISPR/Cas9 adaptive system, the corresponding genome editing system CRISPR/Cas9 became an invaluable molecular tool (Chang *et al.*, 2013; Hwang *et al.*, 2013; Jao, Wente and Chen, 2013). According to the strategy of this approach, an annealed oligo product is synthesized bearing 20 nucleotides of the target site immediately before the NGG protospacer adjacent motif (PAM) for efficient Cas9 cleavage and cloned into an expression vector that carries also the sequence of tracrRNA. The T7 RNA polymerase-mediated transcription product will be a single guide RNA (sgRNA), chimaera of crRNA (complementary to target site) and tracrRNA. This complex recruits the Cas9 endonuclease and

it is sufficient to guide the site-specific cleavage of target site upon the binding of sgRNA at the target site and the recognition of PAM sequence. Cas9 endonuclease is expected to cut the DNA sequencing at the PAM or few nucleotides upstream of the PAM sequence. The product of the DNA double-stranded break will activate the error-prone non homologous end joining (NHEJ) DNA repair machinery which will introduce insertions/deletions (indels), probably altering the open reading frame of the gene and introducing an early stop codon in the gene of interest. Alternatively, a precise desired mutation can be introduced by triggering the homologous recombination (HR) repair for an in-frame knock-in modification. For this purpose the insertion of a donor template carrying the desired sequencing flanked by homologous arms to both sides of the break is needed to be inserted together with the gRNA/Cas9 complex (Albadri, Del Bene and Revenu, 2017; Yang *et al.*, 2020) (Figure 8).

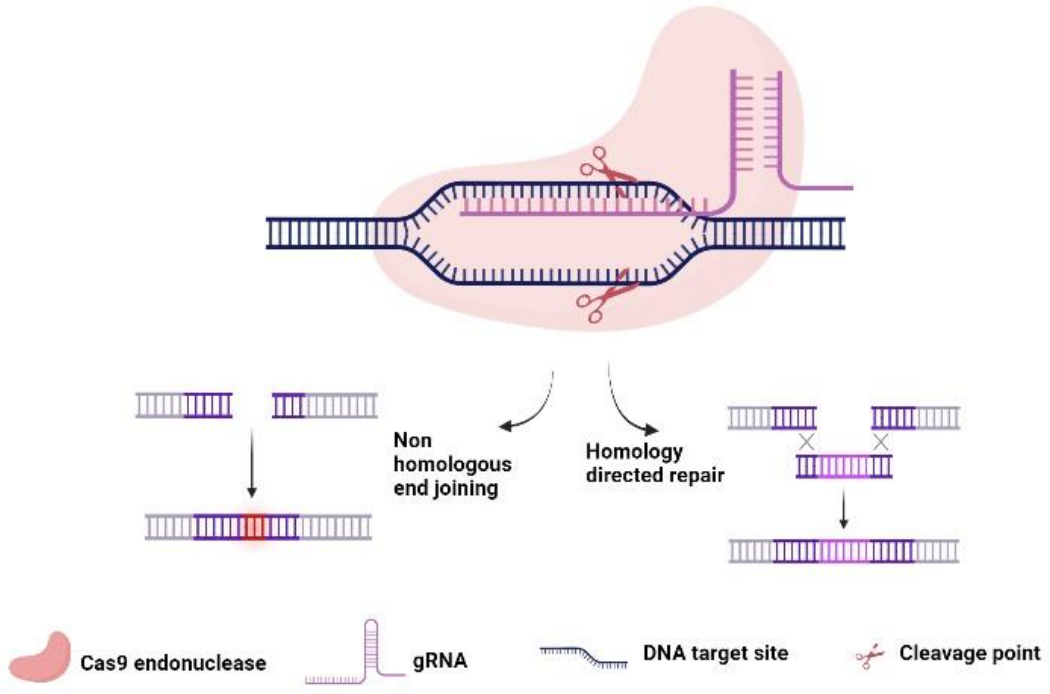

Figure 8: Genome modification induced by CRISPR/Cas9 editing system (created by *BioRender.com*).

1.2.2 Zebrafish heart physiology

The heart physiology and development of zebrafish has given prominence to the strength of its use as an excellent vertebrate model for studying heart disorders. Despite its systematic simplicity, the heart of the zebrafish shares many common features with the human heart regarding the heart rate, contractile dynamics and heart rate (Arnaout *et al.*, 2007; Leong *et al.*, 2010; Yu *et al.*, 2012; Vornanen and Hassinen, 2016; Giardoglou and Beis, 2019). During early cardiogenesis, a complex process that involves proliferation, cellular remodeling, differentiation and morphogenesis, major regulatory signaling pathways are activated to orchestrate such crucial procedures. Molecular pathways such as Notch, Wnt and bone morphogenic protein (BMP) that play crucial role for the proper cardiac development and function are conserved between zebrafish and higher vertebrates (MacGrogan, Münch and de la Pompa, 2018). In addition, although zebrafish heart is a two-chamber organ, it develops fundamental similarities with the human heart with respect to cardiac physiology than other vertebrates, such as heart rate that it's ±150 beats per minutes (bpm) at 72 hpf, whereas mice have ± 300 bpm (Beis, Kalogirou and Tsigkas, 2015).

The zebrafish heart is the first organ that forms and functions during development and in contrast to human heart, it is composed by one atrium and one ventricle, an atrioventricular valve and an outflow valve. During development, myocardial and endocardial progenitor cells are specialized, while two waves of myocardial progenitors are identified, the atrial and the ventricular. At 5 hpf blastula stage, cardiac progenitor cells are placed bilaterally in the marginal zone with atrial progenitor cells placed more ventrally than ventricular progenitors. During gastrulation, progenitor cells move towards the anterior later plate mesoderm and at 16 hpf, the fusion of bilateral heart occurs at the embryonic midline by forming a disc structure with endocardial cells within the center, the ventricular myocytes at the at the center of the disc and the atrial myocytes at the periphery. The formation of a linear cardiac tube follows as a result of cardiac disc morphogenesis. The outer layer of the linear tube consists of myocardial cells, while endocardial cells are forming the inner layer of the tube with the two layers being separated by an acellular extracellular matrix, called cardiac jelly. Already at 24 hpf and after

the formation of the heart tube, rhythmic peristaltic contraction starts. At this stage, venous pole is at the anterior left side, while arterial pole is at the midline. At 36 hpf, cardiac looping is initiated during which the ventricle twists towards the midline forming an S-shaped loop heart. Also, at 36 hpf pumping of the heart transforms from a slow peristaltic rhythm to a sequential construction indicative of the establishment of cardiac conduction system. During cardiac looping (36-48 hpf), the ventricle and atrium become morphologically distinguishable. Epicardium layer spreads around the myocardium of the looped heart at 72 hpf and now the cardiac wall consists of two layers, epicardium, myocardium and endocardium. Just before that stage, ventricular cardiomyocytes start to delaminate in a stochastic way and forming a trabecular layer of cardiomyocytes, and by 72 hpf a trabecular network has been formed (Figure 9) (Bakkers, 2011; Yalcin *et al.*, 2017).

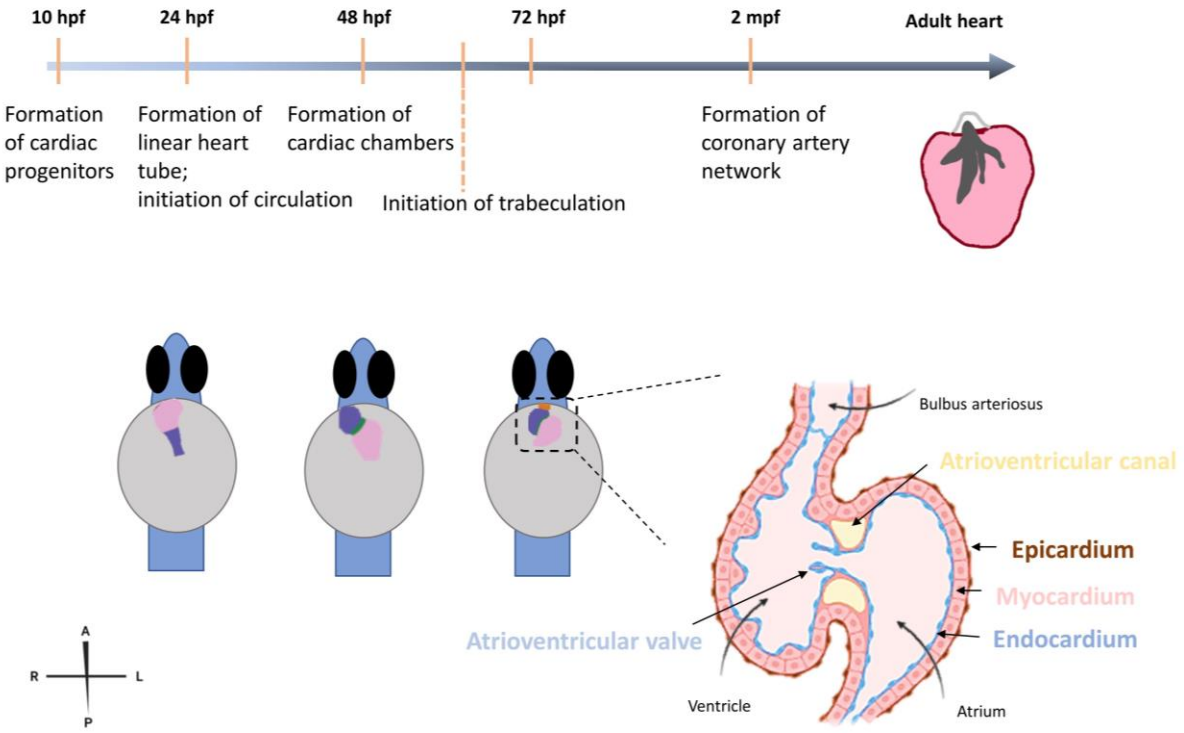

Figure 9: Development of zebrafish heart physiology. During embryonic heart development, distinct phases of cardiac remodeling take place. At 10 hpf, the cardiac progenitor cells are

apparent and gradually form a heart structure with a shape of tube at 24 hpf. Heart undergoes morphogenic transformation via cardiac looping during which ventricle and atrium become distinguishable chambers. At 72 hpf, the heart has established unidirectional blood flow via valve formation and extended trabecular network. Coronary artery network is formed at a later development stage, around 2 months post fertilization (mpf). Orientation cross: (A)Anterior, (P)Posterior, (R)Right, (L)Left.

Cardiac valves are crucial for the unidirectional blood flow in zebrafish. In the embryonic hearts, valvulogenesis starts with the formation of endocardial cushions in atrioventricular canal, a border between atrium and ventricle and occurs at ~36 hpf. The first step of valve formation is after the endocardial cells which are located at the future AV canal, receive signals to undergo an Epithelial- to- Mesenchymal transition (EMT). Then, squamous endocardial cells become cuboidal expressing the cell adhesion molecule Dm-grasp (Beis *et al.*, 2005). The Dm-grasp^{+} cells form protrusions towards the cardiac jelly forming the multicellular cushion structure. Notch signaling pathway plays a major role as it is being restricted to the AV endocardium at around 45 hpf. The formation of valve leaflets is obvious at 105 hpf and the overall procedure is directed and controlled via molecular signaling pathways, but also from the blood flow as sheer-stress is required for the proper formation of the valves (Kalogirou *et al.*, 2014).

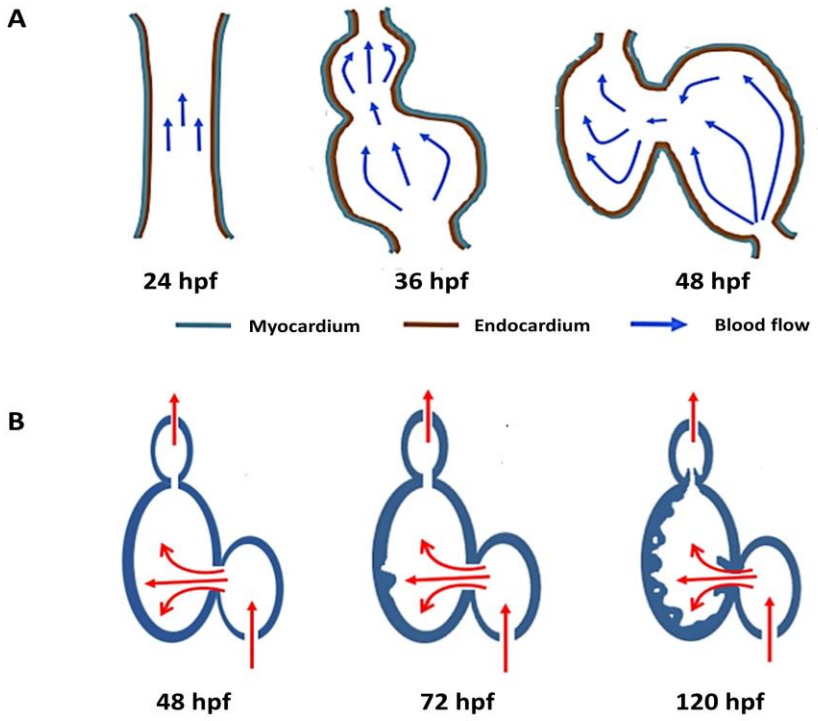

Figure 10: Schematic representation of complex cellular remodeling during cardiac morphogenesis. A. Cardiac looping: at 24 hpf the embryonic heart tube starts to pump, around 36 hpf the heart looping begins and heart transformed gradually from C-shaped to S-shaped, and by 48 hpf the heart has formed two separated chambers, the atrium and the ventricle (adjusted by (Battista *et al.*, 2019)). B. Ventricular trabeculation: at 48 hpf the myocardium forms only a compact cardiomyocyte layer and at 72 hpf some cardiomyocytes delaminate and form an adjusting trabecular cardiomyocyte layer towards the lumen of the ventricle. By the time of 120hpf, the trabecular network has been fully expanded and developed (adjusted from (Vedula *et al.*, 2017)).

As mentioned before, two very crucial cellular remodeling procedures during cardiac development are the cardiac looping and the formation of trabecular network, respectively (Figure 10). Cardiac looping is a complex morphogenic process, which describes the

transformation of an in-line heart tube (or heart cone) into a S-shaped heart asymmetrically positioned between the left/right axis of the body length. When progenitor cells fused at the midline to form the symmetric cardiac tube then, asymmetry procedure begins. During this process, the heart tube rotates and place the venous pole toward the left, a cellular remodeling called cardiac jogging promoting a leftward movement of the tube (Grimes *et al.*, 2020). After jogging, cardiac looping occurs during which, the heart bends rightwards with the ventricle undergoing a D-bending and an atrial bending towards to the left. As a consequence, the two chambers form a dextral S-shaped heart and are placed almost side-by-side with ventricle positioning to the right and atrium to the left of the body axis (Lombardo *et al.*, 2019). Ventricular trabeculation is another essential cardiac remodeling that contributes to the proper morphogenesis and function of the heart. It is a process during which, myocardial wall layers increase and consist of a compact myocardium and a trabecular myocardium. The formation of trabecular myocardium derives from cardiomyocytes lining the compact layer that extrude and expand starting to form ventricular protrusions. During this process, some myocardial cardiomyocytes delaminate in a stochastic way and start seeding the trabecular layer towards to lumen of the ventricular chamber. It has been shown that cardiomyocytes division and proliferation observed during trabeculation play important role to the trabecular growth, rather than trabecular initiation (Uribe *et al.*, 2018). Thus, given the complexity of trabeculation (polarity dynamics, cardiomyocytes remodeling, delamination, oriented cell division and proliferation), it is required an orchestration of regulatory mechanisms that involves signaling pathways (such as Neuregulin/ErbB, Notch and Angiopoetin 1/Tie2), as well as mechanotransducive signals (contractility, fluid sheer stress) (Peshkovsky, Totong and Yelon, 2011; Jiménez-Amilburu *et al.*, 2016; Uribe *et al.*, 2018; Tsata and Beis, 2020). The formation of extended trabecular network is necessary for the increase of myocardium mass in order to permit nutrient and oxygen supply prior the establishment of coronary vascularization, without increasing the size of the heart (Liu *et al.*, 2010; Samsa,Leigh Ann, Yang and Liu, 2014). Failure of trabeculation lead to embryonic lethality and also, even subtle of trabecular projections results in congenital cardiomyopathies (Liu *et al.*, 2010; Dong, Qian and Liu, 2021). Therefore,

the identification of mechanisms and genes involved at the steps of these morphogenic cardiac processes is at the core of biomedical research.

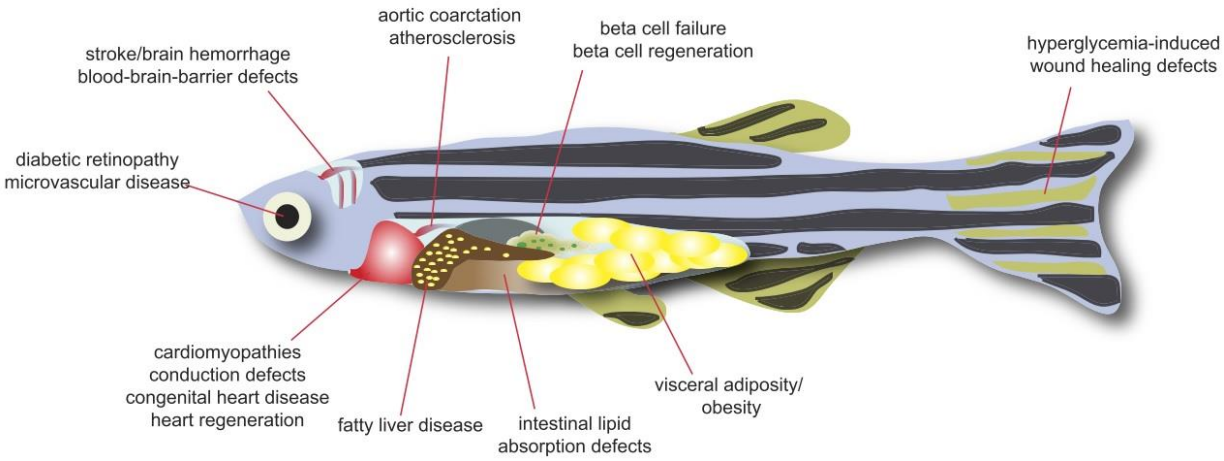

Figure 11: Cardiovascular and metabolic diseases that can be modelled in zebrafish as experimental animal. The anatomy and organogenesis of zebrafish is very similar to higher vertebrates which make is suitable as animal model in cardiovascular research (adjusted from *Gut P. et al., Physiol Rev., 2017*)

1.2.3 The zebrafish as a model for Human Cardiovascular Diseases

Due to all the mentioned biological advantages, cardiac physiology and the existing experimental toolbox, zebrafish has been established as a powerful model for studying cardiovascular diseases. The combination of GWAS studies and the subsequent modeling of genes identified to participate in the CAD manifestation has already shed light to pathways and mechanism involved in diseases pathophysiology. The functional validation of candidate genes derived from GWAS and meta-analysis is the key to our deeper understanding of the basis of heart disorders. Zebrafish acquires all the organs necessary to model cardiovascular and metabolic disorders (Figure 11). Numerous of studies have used zebrafish for the interrogation of specific variants' function that are involved in diseases such as atrial fibrillation,

valvulopathies, congenital heart defects, lipid-associated cardiomyopathies and dilated cardiomyopathy. A representative list of studies, the candidate genes derived from GWAS and the corresponding zebrafish phenotype is presented below (Table 1).

Associated Human Disease	Gene (s)	Zebrafish genotype	References
Atrial Fibrillation	KCNIP1	High atrial rate	Tsai *et al.,* 2016
Long QT syndrome	KCNH2	Severe repolarization	Tanaka *et al.,* 2018
Atrial Fibrillation	PRRX1	Atrial action potential duration	Tucker *et al.,* 2017
Dilated Cardiomyopathy	HSPB7	Cardiac fibrosis, cardiomegaly and sarcomeric abnormalities	Mercer *et al.,* 2018
Congenital Heart Defects	PBX3	Myocardial morphogenesis defects	Farr *et al.,* 2018
Mitral Valve Prolapse	LMCD1, TNS1	Increased atrioventricular regurgitation, moderate reduction in cardiac looping	Dina *et al.,* 2015
Atrioventricular Septal Defect	NFATC1	Cardiac looping defects and altered atrioventricular canal patterning	Ferese *et al.,* 2018
Heart Rate Variability	GNG11, SYT10, RGS6, HCN4, NEO1, KIAA1755	Sinoatrial pauses and arrests, cardiac edema and uncontrolled atrial contractions	von der Heyde *et al.,* 2018
Lipid associated-Cardiomyopathy	APOOP1	Increased the LDL- C levels, increase in the average number of vascular plaques	Montasser *et al.,* 2018
Lipid associated-Cardiomyopathy	PLXND1	Modulate angiogenesis, reduced capacity to store lipid in visceral adipose tissue	Minchin *et al.,* 2017
Congenital Cardiomyopathy	KIF20a	Relative tachycardia, red blood cells proximal to the atrium and cardiac edema	Louw *et al.,* 2018
Cantu syndrome	KCNJ8	Enlarged, hypercontractile ventricles, pericardial edema, reduced blood vein flow velocity	Tessadori *et al.,* 2018

Table 1: A representative table of GWAS-derived cardiomyopathy related genes studied in zebrafish (adjusted from *Giardoglou P. and Beis D. Biomedicines, 2019*)

Zebrafish is a vertebrate model suitable for validation of genes derived from large-scale genome population studies. In addition, it is a model-organism that allows the systemic analyses of rare variants and contributes to the dissection of pathology of multifactorial complex diseases (Figure 12). During this research thesis, zebrafish was utilized in order to

unravel cellular and molecular mechanisms of pathophysiology mediated by the deficiency of genes derived from human studies: CFDP1 and CCDC92. At the following chapter, we will present the information that is available and known regarding these genes that have been identified as modulators of cardiovascular diseases.

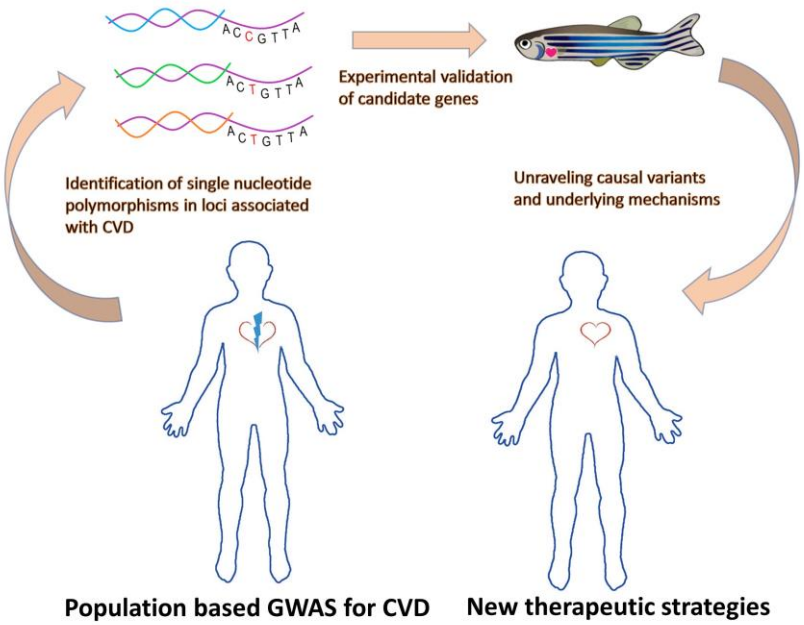

Figure 12: Strategy of research pipeline in order to analyze the function of candidate genes involved in cardiovascular disorders and set the platform for the generation of new therapeutic guidelines (*Giardoglou P. and Beis D. Biomedicines, 2019*).

1.3. Current knowledge about *cfdp1*, *ccdc92* and *prkd2* candidate genes

1.3.1 *CFDP1* gene

Human craniofacial development protein 1 (*CFDP1*) is located at the reverse strand of chromosome 16q23.1, has length size 139.794 base pairs (bp) and harbors 11 exons based on currently annotated genomic sequence reference GRCh38.p13 Primary Assembly (Ensembl:ENSG00000153774 MIM:608108). Alternatively, it is also known as p97; BCNT; CP27; SWC5; Yeti; CENP-29; BUCENTAUR and it is conserved in chimpanzee, Rhesus monkey, dog, cow, mouse, rat, chicken, zebrafish and frog with 400 organisms obtaining orthologs with human gene *CFDP1*. The transcript product (ENST00000283882.4, name CFDP1-201) has length size 1293 bp and codes for a protein product of 299 amino acids (aa) which contains the Bucentaur conserved domain between 222-295 aa (pfam 07572).

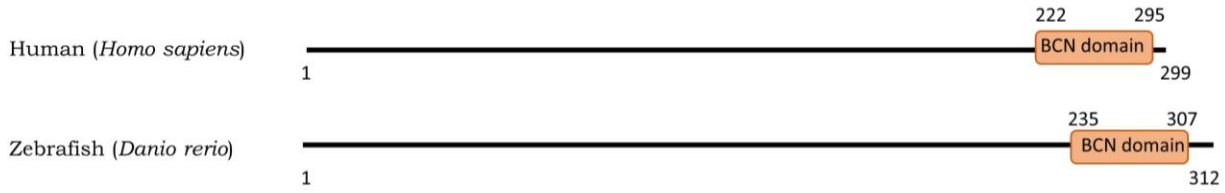

Figure 13: Schematic representation of Human (*Homo sapiens*) CFDP1 and Zebrafish (*Danio rerio*) Cfdp1 protein products.

Zebrafish craniofacial development 1 (*cfdp1*) is located at the forward strand of chromosome 18, has length size 70.717 bp and harbors 7 exons based on the current annotated genomic reference GRCz11 Primary Assembly (ENSDARG00000095086). It is also known (and misassigned) as *rltpr* and has 50,17% protein homology with Human *CFDP1* (with 55% cDNA identity). The transcript product (ENSDART00000115388.3, name cfdp1-201) has length size

1741 bp and codes for a protein product of 312aa which contains the Bucentaur conserved domain between 235-307 aa (pfam 07572).

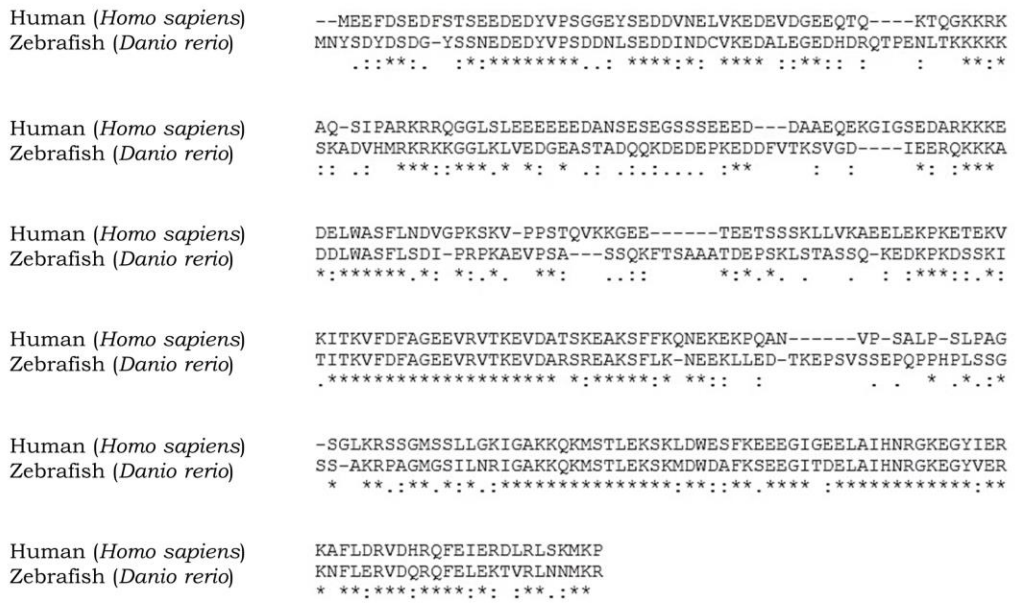

Figure 14: Protein alignment of Human (*Homo sapiens*) *CFDP1* and Zebrafish (*Danio rerio*) *cfdp1* based on reference sequence annotation ((Howe *et al.*, 2013)

A detailed overview of cellular and biological role of *CFDP1* and the corresponding model systems that have been generated for the study of this gene are described and analyzed in Chapter 3, subdivision 3.1.

1.3.2. *CCDC92* gene

Coiled-coil domain-containing 92 (CCDC92) is a coiled-coil protein and belongs to the superfamily of coiled-coil proteins that are found in all three life kingdoms (Truebestein and Leonard, 2016). These proteins are characterized by the their i) pitch (periodicity), ii) pitch angle (angle of helix compared to supercoiled line) and iii) helix angle (with respect to the way two helices are crossing each other). They form polymers with a huge variation in length (from short to very long molecules) and they perform an enormous repertoire of mechanical properties. While these motifs represent a considerable proportion of total proteome, the full-length coiled

coil-containing proteins appear to have an extreme variation of function from simply molecular spacers to molecular rulers. Therefore, the enhanced understanding of the structure, the function and the biological relevance of proteins containing coiled coil motifs remains a future challenge.

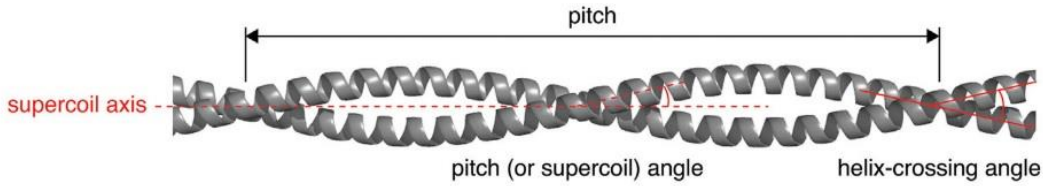

Figure 15: Coiled-coil parameters (adjusted figure Truebestein L. and Leonard T.A., Bioessays 2016)

In the recent years, many genome-wide association studies and large-scale population analysis have highlighted the implication of *CCDC92* gene in a variation of human pathophysiological conditions. Associations studies related to Coronary Artery Heart disease (Van Der Harst and Verweij, 2018; Xiao *et al.*, 2018), Insulin resistance (Klarin *et al.*, 2017), Atrial Fibrillation - the most common heart rhythm disorder - (Roselli, C., Chaffin, M.D., Weng, 2018), type 2 Diabetes (Zhao *et al.*, 2017; Ross, Gerstein and Paré, 2018), plasma Lipid Concentration (Chasman *et al.*, 2009), Adipose storage and Insulin Resistance cardiometabolic disease (Lotta *et al.*, 2017), High HDL (high-density lipoprotein cholesterol) (Khetarpal *et al.*, 2018) and Nephronophthisis-related ciliopathies (NPHP-RC) (Chaki *et al.*, 2012) have underlined the link of *CCDC92* to the manifest of disease traits. Thus, investigating further the effect of *CCDC92* alteration or even depletion is necessary in order to elaborate deeper the mechanisms that are involved in the expression of cardiovascular diseases manifest.

SNIP	Disease	Publication
rs825476	Diabetes type 2 and Coronary Heart Disease	Zhao W. *et al.*, 2017, *Nature Genetics*
rs11057401	Coronary Artery Diseases (and Insulin resistance)	Klarin D. *et al.*, 2017, *Nature Genetics*
rs825476	Coronary Heart disease	Xiao L. *et al.*, 2018, *Lipids in Health and Disease*
rs825452, rs7973683	Insulin resistance	Lotta AL., et al., 2016, *Nature Genetics*
rs7307277	Plasma Lipid Concentration	Chasman DI., et al., 2009, *PLoS Genetics*
rs11057401	Atrial Fibrilllation	Roselli L., et al., 2018, *Nature Genetics*
rs7133378	Adipose Function and Differentiation	Huang l.O., *et al.,* 2021, *Nature Metabolism*
rs11057401	Regional Fat Deposit	Neville MJ., et al., 2019, *PLoS ONE*

Table 2: List of single nucleotide polymorphisms in the CCDC92 gene found in patients participating in genome-wide association studies and analysis and their corresponding disease association.

Human coiled-coil domain containing 92 (*CCDC92*) is located at the reverse strand of chromosome 12q24.31, has length size 44.832 base pairs (bp) and harbors 9 exons based on

currently annotated genomic sequence reference GRCh38.p13 Primary Assembly (Ensembl: ENSG00000119242). Alternatively, it is also known as FLJ2247 and Limkain beta-2, and it is conserved in chimpanzee, Rhesus monkey, dog, cow, mouse, rat, chicken, zebrafish and frog with 414 organisms obtaining orthologs with human gene *CCDC92*. The transcript product (ENST00000238156.8, name CCDC92-201) has length size 2790 bp and codes for a protein product of 331 amino acids (aa), which contains the coiled-coil domain of unknown function between 24-79 aa (pfam 14916) and APG6 (Autophagy protein Apg6) between 45-157 aa (pfam 04111).

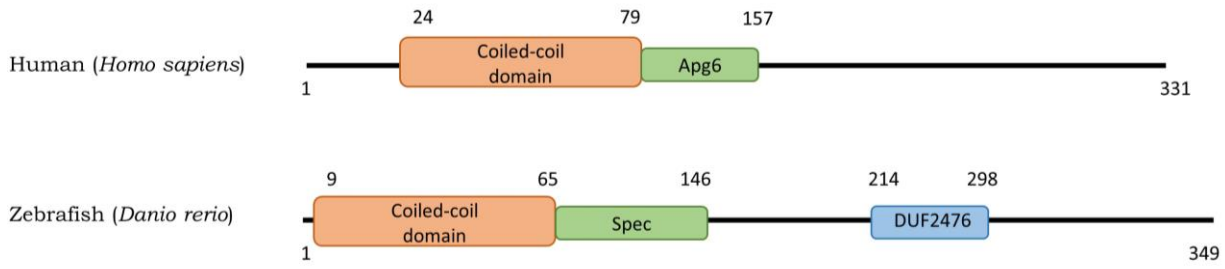

Figure 16: Schematic representation of Human (*Homo sapiens*) CCDC92 and Zebrafish (*Danio rerio*) Ccdc92 protein products.

Zebrafish coiled-coil domain containing 92 (*ccdc92*) is located at the reverse strand of chromosome 8, has length size 62.305 bp and harbors 4 exons based on the current annotated genomic reference GRCz11 Primary Assembly (ENSDARG00000041750). It is also known as *zgc:123269* and has 65,56% protein homology with Human *CCDC92* (with 62% cDNA identity). The transcript product (ENSDART00000134801.2, name ccdc92-201) has length size 2070 bp and codes for a protein product of 349 aa which contains the coiled-coil domain of unknown function between 9-65 aa (pfam 14916), SPEC (Spectrin repeats, found in several proteins involved in cytoskeletal structure) between 23-146 aa (cl02488) and DUF2476 (Protein of unknown function) between 214-298 (pfam 10630).

Figure 17: Protein alignment of Human (*Homo sapiens*) *CCDC92* and Zebrafish (*Danio rerio*) *ccdc92* based on reference sequence annotation.

1.3.3 *PRKD2* gene

PRKD consists of a family of evolutionarily conserved signal-activated enzymes (PRKD1, PRKD2, and PRKD3) (Valverde *et al.*, 1994; Hayashi *et al.*, 1999; Sturany *et al.*, 2001) that play critical roles in fundamental biological processes (Manning *et al.*, 2002) and contribute to the pathogenesis of a large number of clinically important diseases, including pancreatitis (Piscuoglio S, Fusco N, Ng CK, Martelotto LG, da Cruz Paula A, Katabi N and BP, Skálová A, Weinreb I, Weigelt B, 2016), various cancers (Yuan and Pandol, 2016), human heart failure development and cardiac hypertrophy (Wei *et al.*, 2015). PRKD isoforms share a modular domain structure consisting of a C-terminal kinase domain and an N-terminal regulatory domain consisting of tandem C1A/C1B motifs that anchor full-length PRKD to diacylglycerol-

/phorbol ester-containing membranes (Iglesias, Matthews and Rozengurt, 1998; Iglesias and Rozengurt, 1999; Rey and Rozengurt, 2001; Chen *et al.*, 2008) and a pleckstrin homology motif that participates in intramolecular autoinhibitory interactions (Iglesias and Rozengurt, 1998; Waldron, Iglesias and Rozengurt, 1999). PRKD isoform activation is generally attributed to growth factor-dependent mechanisms that promote diacylglycerol accumulation and protein kinase C- (PKC-) dependent trans-phosphorylation of PRKD at serine residues in the activation loop, a highly conserved 20-30 residue flexible segment in kinase domain that sits near the entrance to the active site and functions to structure the enzyme for catalysis (Rozengurt, Rey and Waldron, 2005). Activated PRKD1 and PRKD2 then autophosphorylate at a serine residue in a PDZ domain-binding motif/PRKD consensus phosphorylation motif at the extreme C-terminus. PRKD3 lacks this autophosphorylation site.

While cardiac tissues co-express PRKD1, PRKD2, and PRKD3, and previous studies show that PRKD isoforms can be activated in a stimulus-specific manner in cardiomyocytes (Guo *et al.*, 2011), most studies have focused on the cardiac actions of PRKD1, which is downregulated during normal postnatal development, upregulated in various cardiac hypertrophy/failure models, and contributes to adverse cardiac remodeling and has been implicated in syndromic congenital heart defects (Speliotes *et al.*, 2010; Johnson *et al.*, 2015). Shaheen *et al*. identified a homozygous truncating mutation in *PRKD1* that leads to the generation of a catalytically inactive protein (that contains the entire N-terminal regulatory domain but only the first 35 residues at the N-terminus of the kinase domain) in patients with truncus arteriosus (Shaheen *et al.*, 2015). Studies from Sifrim *et al*. (Sifrim *et al.*, 2016) and more recently Alter *et al*. (Alter *et al.*, 2020) identify heterozygous *de novo* missense mutations in *PRKD1* in 5 patients with syndromic congenital heart disease. Of note, 3 of these patients had identical inactivating missense Gly592Arg mutations in the PRKD1 kinase domain.

Studies of the role of PRKD2 in cardiac function and angiogenesis are more limited, but there is some evidence that defective PRKD2 signaling contributes to the development of human hypertrophic cardiomyopathy (Tsybouleva *et al.*, 2004) and PRKD2 activation of a HDAC5 signaling pathway controls the expression of genes involved in Notch signaling during valve formation in zebrafish embryos (Just *et al.*, 2011). This study uses a zebrafish forward

genetic screen (Beis D, Bartman T, Jin SW, Scott IC, D'Amico LA, Ober EA, Verkade H and J, Field HA, Wehman A, Baier H, Tallafuss A, Bally-Cuif L, Chen JN, Stainier DY, 2005) to identify a mutant line (*s411*) that carries an A to G mutation resulting in a T757A substitution of Prkd2 (T714A in PRKD2) (Figure 18).

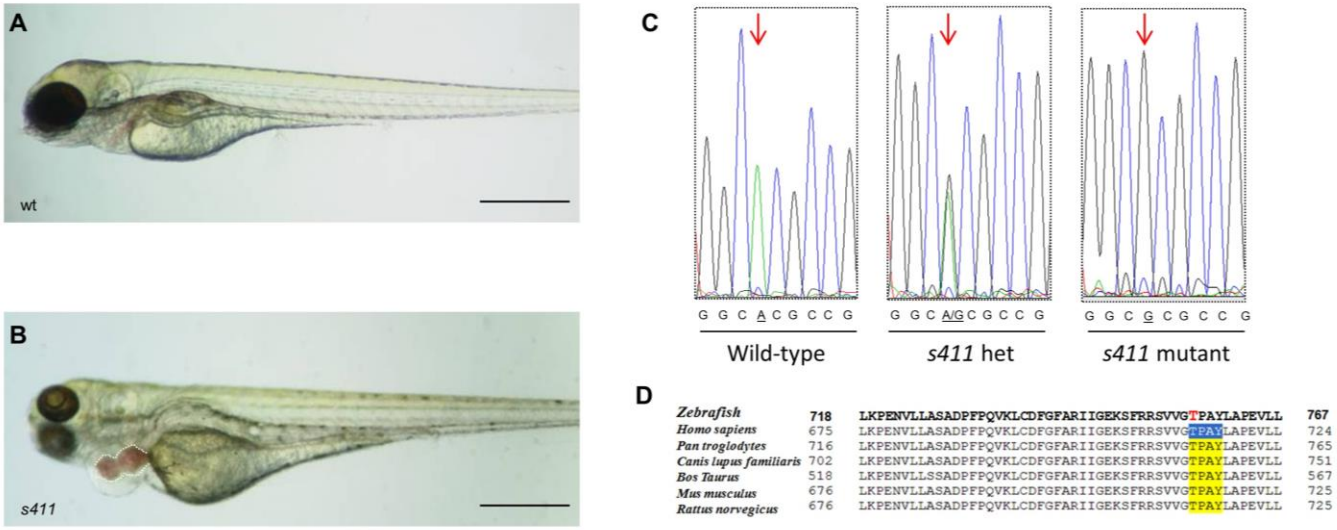

Figure 18: *s411* carry a mutation in the *prkd2* gene. A, B) Bright field image analysis of a wild-type zebrafish embryo compared to an *s411* mutant embryo at 72 hpf. Heterozygous adults that carry the *s411* recessive mutation give 25% offspring mutant embryos exhibiting heart edema, inadequate blood circulation leading to complete outflow tract stenosis and blood regurgitation by 72 hpf. Scale bars: 500 µm. (C) The *s411* embryos carry an A to G mutation that translates to a Threonine (T) to Alanine (A) amino acid change. (D) Blast analysis showed that the threonine T757 (T714 in humans) is a conserved amino acid at a highly conserved region of the C-terminus PRKD2 kinase, between several species. (adjusted by Giardoglou *et al*, 2021)

1.4 GRMIC (Greek Recurrent Myocardial Infarction Cohort)

Undoubtedly, the research focus of Cardiovascular research is lying in the identification of risk factors that influence the presence and development of CVDs. As CAD and its main implication, Myocardial Infraction, account for the leading form of cardiovascular diseases, a plethora of large-scale human studies have highlighted risk factors, related to environmental factors (such as lifestyle, diet, exercise, stress) and genetic heritage that are associated with traits of coronary artery disease. Genome wide association studies (GWAS) have identified genetic loci associated with coronary artery disease risk at the threshold of genome-wide significance ($p = 5 \times 10^{-8}$) (Nikpay *et al.*, 2015; Nelson *et al.*, 2017; Van Der Harst and Verweij, 2018). Inclusion of these variants in a Genetic Risk Score model along with risk score based on traditional risk factors such as family history, smoking, lipid levels, blood pressure and physical activity provide a prognostic value of the disease. Yet, although comprehensive genetic studies have been carried out for disease prognosis, studies based on the post MI patients about the progress of disease manifestation and the risk of a second appearance of disease incident are limited.

Among patients surviving a first MI event, circa 17% will experience a second event within 18-24 months. Furthermore, there seems to be a subgroup of patients with bad prognosis, about 4% will die within 30 days of the first event (Kannel, Sorlie and Mcnamara, 1979; Nauta *et al.*, 2012). In a year after first MI event, mortality levels of patients with recurrent MI can reach approximately 7% (Radovanovic *et al.*, 2016). Mortality related to heart failure and atherosclerotic burden after myocardial infarction remains frequent despite the widespread of acute revascularization (Gerber, Weston, Enriquez-Sarano, Berardi, *et al.*, 2016; Gerber, Weston, Enriquez-Sarano, Manemann, *et al.*, 2016). A study in Swedish population have shown that risk of cardiovascular events are elevated also beyond the first year post-MI, indicating the necessity of a prolong surveillance of patients, especially of those with additionally risk factors (Jernberg *et al.*, 2015). After a myocardial infarction event, patients still remain at the risk of

occurrence of a recurrent ischemic episode or even sudden death. Thus, it is very crucial to investigate the factors that influence the appearance of future MI events in the patients.

Previous studies have shown that family history, Killip class, premature ventricular contractions [PVCs] as well as depression could predict and stratify the risk of MI occurrence and mortality (Miller *et al.*, 2000; Kuyper and Honig, 2008; Rujirachun *et al.*, 2021). Also, moderate and high perceived stress at the period of MI is highly associated to long-term outcomes, such as angina (Arnold *et al.*, 2012). A recent study in New Zealand Cohort using plasma proteomics and single-sell transcriptome from post-MI patients, measured 1035 proteins (possible candidate markers) and identified (the well-established) N-terminal B-type natriuretic peptide and troponin T, as well as the newly emerged angiopoietin-2, thrombospondin-2, latent transforming growth factor-β binding protein-4, and follistatin-related protein-3, as biomarkers for post-MI heart failure (Chan *et al.*, 2020). The left ventricular systolic dysfunction (LVSD) and low ventricular ejection fraction (LVEF) remains an important predictor of arrhythmic hearts and secondary events in post-MI patients (De Luca, 2020).

Little is known about the predictors of recurrent ischemia and thus the need for studies focusing on the risk of recurrent MI event in genetic and environmental level has risen (Al Saleh *et al.*, 2017; Galasso *et al.*, 2021). So far, risk models for post-MI patients have not fully leveraged the power of genetics and epigenetics. The identification of biomarkers has strong potential for patient care and is very timely given the technological advances in RNA sequencing and DNA methylation. The GRMIC (Greek Recurrent Myocardial Infarction Cohort) project serves as a contribution to this purpose and it is a cohort constituted by Harokopio University, Queen Mary University and cardiological clinics of hospitals in Athens (Attikon General University Hospital, General Hospital of Athens Hippokrates and Tzaneio General Hospital of Piraeus). This is a prospective study in which genetic along with demographic and environmental data will be selected from MI patients at the time of the event as well as six (6) months later, after the discharge of hospitalization. The goals of this research study are: i) the identification of novel (or already known) nucleotide polymorphisms and genetic loci in the

Greek population that are related to the MI event (DNA sequencing), ii) stratification for biomarkers of post myocardial infarction patients (measuring of selected plasma markers), iii) possible epigenetic factors that contribute to post-MI events (DNA methylations, histone modifications, microRNAs) and iv) identification of splice variants or allele specific expression pattern (RNA sequencing).

The set of biomarkers that will be tested consists of Total cholesterol (TC), Low-density lipoprotein cholesterol (LDL-C), High-density lipoprotein cholesterol (HDL-C), Triglycerides (TG), Glucose, Uric acid, Apolipoprotein B (Apo-B), Lipoprotein A (LP-A), C-reactive protein (CRP) and Creatine phosphokinase (CPK). The specific selection is based on the current knowledge about environmental (biochemical) factors that are involved in the appearance of coronary artery disease and the last years play important role in prediction of the disease manifestation. Atherosclerosis is the main cause of CAD describing a thickening of arteries due to the formation of atheromatic plague which is consisted of its main substance, cholesterol (Jansen, Samani and Schunkert, 2014). Therefore, lipids are considered to be major contributors to the pathophysiology of the disease (Linton, M. F., Yancey, P. G., Davies, S. S., Jerome, W. G., Linton, E. F., Song, W. L., Doran, A. C., & Vickers, 2019). Plethora of epidemiological studies have highlighted the effect of lipids (total cholesterol, LDL, HDL, TG) and their concentration in plasma, as well as mutations in genes involved in their metabolism on the maintenance of cardiovascular health (Linsel-Nitschke *et al.*, 2008; Teslovich *et al.*, 2010; Voight *et al.*, 2012). The role of LDL-C has been highlighted via a numerous of human studies as CAD biomarker. In a study conducted in Dutch patients with familial hypercholesterolemia carrying mutations in the gene of the LDL-receptor, *LDLR* (Souverein *et al.*, 2007), it was also shown that mutations in the *LDLR* are associated with LDL levels and has high effect on the early onset of coronary atherosclerosis. Apolipoprotein B is a key protein in lipid metabolism and it is tightly connected with the initiation of atherogenesis as high level of plasma apo-B – containing lipoproteins is a risk factor of atherosclerosis while low level could be protective (Benn, 2009; Shapiro and Fazio, 2017; Tani *et al.*, 2017). Apo-B forms a complex with lipoproteins and it is recognized by the LDL receptor and clear the LDL from the plasma. Thus, the concentration of apo-B is representative of the LDL particles in the plasma and reflects a major risk factor for the appearance of CAD.

Low high-density lipoprotein cholesterol levels are associated with risk of cardiovascular events as HDL, a lipid transporter, is the key mediator of reverse transportation of cholesterol and considered to be anti-atherogenic (Bhatt and Rohatgi, 2016). Specifically, it appears to be the lower the HDL concentration, the higher risk for coronary artery disease since HDL is a vehicle for that transfers cholesterol from peripheral cells to the liver for catabolism contributing to lipid homeostasis (Gordon *et al.*, 1977; Ben-Aicha, Badimon and Vilahur, 2020). Large cohort studies have shown that triglyceride-rich lipoproteins are also correlated with atherosclerotic cardiovascular disease risk since they also contribute to the formation of the atherosclerotic plaque and elevated triglycerides are fine predictors of myocardial infarction (Nordestgaard *et al.*, 2007; Sandesara *et al.*, 2019; Langsted, Madsen and Nordestgaard, 2020). In addition, human genome studies have associated polymorphisms in the *LPA* gene and corresponding alterations of lipoprotein A plasma concentration with the occurrence of CAD event (Kamstrup *et al.*, 2009; Trégouët *et al.*, 2009; Enas *et al.*, 2019; König *et al.*, 2019). Therefore, the modulation of LP-a concentration levels consists a therapeutic as well as a preventive measure, in our days. Moreover, it is known that factors involved at the mechanism of inflammation are also important diagnostic markers for CAD as inflammation serves an important role in the initiation and progress of atherosclerosis (Zheng *et al.*, 2020). Among those, C-reactive protein is a powerful candidate marker and has been identified to classify high risk patient group also for recurrent event (Koenig *et al.*, 1999; Kaptoge *et al.*, 2010; Koenig, 2013). Creatine kinase, a key enzyme for energy metabolism, is another tool for diagnosis of acute MI and appears to be in low levels in normal myocardium and several-folds increased in hypoxic myocardium, while its levels are correlated with infarct size (Navin and Hager, 1979; Kruse *et al.*, 2014; Wu *et al.*, 2021). Finally, there are also many epidemiological prospective population-based studies that correlate hyperglycaemia and hyperuricaemia with manifestations of coronary artery disease and life expectancy (Laakso and Kuusisto, 1996; Franco *et al.*, 2007; Riddle, 2010; Palmer *et al.*, 2013). Therefore, glucose variability and uric acid levels could act as markers for progression of coronary artery disease and MI events.

Based on the literature so far, the aim of GRMIC is measure the aforementioned markers in Greek MI patients at two time points and evaluate their prognostic power for a recurrent

event. Together with genetic data, GRMIC aims to identify variants associated with second events or cardiac mortality, construct possible pathways based on the genes that are affected, identify differentially expressed genes at the time of the event and 6 months after and to develop a risk prediction model for post-MI patients by integrating genetic, epigenetic and genomic markers with other known predictors. Our participation in this cohort includes the recruitment of MI patients with longitudinal follow up for 16 months, collection of blood samples and basic questionnaires about life style (diet, physical activity, smoking) at two time points (day 4 from hospital admission and 6 months after), isolation and storage of DNA, RNA and blood plasma in the Biobank of Harokopio University and measurement of candidate biomarkers.

1.5 Research Aims and Objectives

Having highlighted the contribution of genetic architecture to the manifestation of cardiovascular diseases, it is essential to explore the mechanism of action of genes associated with specific traits of CVDs and to elucidate their role in the cardiac pathophysiology. Large-scale human studies have revealed the association of Craniofacial Development Protein 1 (*CFDP1*) and Coiled-Coil Domain Containing 92 (*CCDC92*) with CVDs but their functional role remains unclear. The aim of this Dissertation was to gain a deeper understanding in the function of *CFDP1* and *CCDC92* during heart development and demonstrate the effect of genes abrogation on cellular and organism level. *Danio rerio* (zebrafish) was utilized as model organism due to the high genetic homology and similar heart physiology compared to human. Silencing of zebrafish *cfdp1* and *ccdc92,* respectively*,* was investigated to ascertain whether these genes contribute to early cardiac defects regarding the function and morphology of the heart during development. To achieve this goal the following steps were designed:

a) Demonstration of spatiotemporal expression of *cfdp1* and *ccdc92*, respectively
b) Phenotypic characterization of morpholino-mediated knockdown of *cfdp1* and *ccdc92*
c) Utilization of zebrafish transgenic lines for monitoring cardiomyocytes upon silencing of *cfdp1* and *ccdc92*
d) Utilization of zebrafish transgenic lines for monitoring Wnt-activated cells and Notch-activated cells upon silencing of *cfdp1*
e) Generation of loss-of-function zebrafish mutant lines using CRISPR/Cas9 genome editing tool
f) Determination of potential signaling pathways and morphogenic processes that *cfdp1* and *ccdc92* might be involved in, during cardiac development.

Another goal of this Dissertation was to verify the role of zebrafish Protein Kinase D2 (*prkd2)* in the formation of cardiac valves and identify possible signaling pathways it could cross-link during heart development. Upon applying forward genetic approach to screen for

zebrafish cardiovascular mutants, a mutation, so called *s411*, showed impaired heart performance developing a complete outflow track valve stenosis by 72 hpf which resulted in retrograde blood flow from the ventricle to the atrium and the disruption of blood circulation to the embryo body. It was revealed that the zebrafish *s411* mutants carry a threonine-to-alanine (T757A) mutation in the *prkd2* gene disrupting PRKD2 kinase activity. In order to further analyze the cardiac-specific phenotype, following steps were designed:

a) Phenotypic characterization of morpholino-mediated knockdown of *prkd2*
b) Determination of whether PRKD2 cooperate with Calcineurin/Nuclear Factor of Activated T-cells (CN/NFATc) signaling pathway to regulate proper cardiac valve development
c) Examination of functional association between *tbx5* and *prkd2,* based on the pivotal role of Tbx5 in heart development in vertebrate species.

The third goal of this Dissertation was to highlight the risk factors associated with recurrent ischemic event in Greek population, through our participation in the GRMIC Cohort. The contribution of current research project to the Cohort study included the following stages:

a) Collection and storage of biological human sample (blood sample) derived from MI patients at two time points: i) four days and ii) six months after the ischemic event
b) Analysis of biomarkers levels in the plasma of patients at the aforementioned two time points.

2. Materials and Methods

2.1 Materials

2.1.1 Antibodies

Antibodies that were used during this study are listed below:

Antibodies	Supplier	Working concentration
Phalloidin-conjugated 633	Biotium	1:300
Anti-Digoxigenin-AP, Fab fragments	Roche	1:5000
Islet1	Developmental Studies Hybridoma Bank, clone39.4D5	1:100
Goat anti-mouse, AF555	Invitrogen	1:300

2.1.2 Buffers/Solutions

A list of buffers/solutions and their recipes used at this study is as follows:

50x TAE buffer

- 2.0 M Tris acetate
- 0.05 M EDTA
- 1.0 M Glacial Acetic Acid
- pH 8.2 – 8.4 (at 28˚C)

For 1000ml of 50x TAE buffer, weight 242gr of Tris base (MW=121.1) and transfer to 2 L conical flask. Add 750 ml deionized/Milli-Q water and mix until Tris base dissolves.

Add 100ml of 0.5 M EDTA and 57.1 ml glacial acetic acid and mix again.

Adjust the pH to 8.3.

Adjust the solution volume to 1 L with deionized/Milli-Q water and mix the solution.

OPTIONAL: Filter the solution to remove any undissolved materials

Transfer the solution to autoclave bottle

Sterilize the solution by autoclaving

10x PBS (Phosphate Buffered Saline)

- 80 gr NaCl
- 2.0 gr KCl
- 14.4 gr Na_2HPO_4
- 2.4 gr KH_2PO_4

Dissolve the above in 800 ml distilled H_2O

Adjust pH to 7.4

Adjust solution volume to 1000 ml

Sterilize by autoclaving

EDTA solution (Ethylene Diamine Tetraacetic Acid)

- Commercially available as disodium EDTA dihydrate, CAS Number 6381-92-6, MW 372.24)

For 1000 ml aqueous solution of 0.5 M EDTA, weight 186.12 gr EDTA. $Na_2.2H_2O$

Transfer it to 2 L conical flask

Add 800 ml deionized/Milli-Q water

While stirring vigorously on a magnetic stirrer, add 10 M NaOH to adjust pH 8.0 (pH adjustment is required in order to dissolve EDTA completely)

Adjust the solution volume to 1000 L with deionized/Milli-Q water and mix again

OPTIONAL: Filter the solution to remove any undissolved materials

Transfer the solution to autoclave bottle

Sterilize the solution by autoclaving

PTU (*N*-Phenylthiourea)

- Commercially available: P7629, Sigma-Aldrich, CAS number 103-85-5, MW 152.2 g/mol

Dissolve 1.52 g in 1000 ml to prepare a 10 mM stock solution

Working concentration: 500 ml PTU (stock 10 mM) in 25 ml egg water

Paraformaldehyde 4%

- PFA powder commercially available: P6148, Sigma-Aldrich, CAS number 30525-89-4, MW 30.03

For 1000 ml preparation:

Weight 40g PFA and add it to 700 ml warm DD water

Dissolve PFA in a heat plate using magnetic stirrer

Add drop by drop NaOH 5N to facilitate dissolution

Add 100 ml 10x PBS

Adjust pH to 7.4 with HCl

Adjust solution volume to 1000 ml

Filter sterilize and prepare aliquots of 50 ml

Store at -20˚C

Tricaine 0.4%, MS-222 (Ethyl 3-aminobenzoate methanesulfonate salt)

- Commercially available powder: Cat A-5040, CAS 886-86-2, Sigma-Aldrich

For 1000 ml preparation:

Weight 4 gr tricaine powder

Add 900 ml distilled water

Adjust pH to 7.0 with 1 M Tris (pH 9.0)

Adjust volume to 1000 ml

Prepare aliquots of 50 ml

Store at -20˚C

E3 medium water

For 1000 ml solution:

- 0.3 gr ZM salts
- 0.08 gr $CaSO_4.4H_20$

- 1000 ml distilled H_20
- Methylene blue 0.2‰

DEPC water

For 1000 ml solution:

- 1 ml 0.1% DEPC
- 1000 ml distilled water

Stir solution overnight with magnetic stirrer and then autoclave

MiniPrep Protocol Buffers:

1. **Merlin I (Cell Resuspension solution)**

- 50 mM Tris.HCl, pH 7.5
- 10 mM EDTA
- 100 ug/ml RNAse A (DNAse free)

2. **Merlin II (Cell Lysis solution)**

- 0.2 M NaOH
- 1% SDS

3. **Merlin III (Neutralization solution)**

- 61.35 gr solid potassium acetate
- 35.7 ml glacial acetic acid

For a final volume of 500 ml in Milli-Q

Competent cells Buffers

1. **P.S.I Broth**
    - Bactotryptone 2%
    - Bacto Yeast Extract 0.5%
    - $MgSO_4$ 0.4% (Add before use)
2. **TFB1**

- 100 mM $RbCl_2$
- 50 mM $MnCl_2$
- 10 mM $CaCl_2$
- 30 mM KOAc
- 15% Glycerol

3. **TFB2**
   - 10 mM MOPS pH 7 (with NaOH)
   - 10 mM $RbCl_2$
   - 75 mM $CaCl_2$
   - 15% Glycerol

DNA extraction buffer (for PCR reaction)

- 10 mM Tris, pH 8.0
- 2 mM EDTA
- 0.2% Triton X-100
- 200 mg/ml Proteinase K (add fresh the day of extraction)

Alkaline Lysis Reagent (for DNA preparation from fixed tissue)

- 25mM NaOH
- 0.2 Mm EDTA, pH 12

Keep solution at room temperature. Make fresh every one to two months

Neutralization Reagent (for DNA preparation from fixed tissue)

- 40 mM Tris-HCl, pH 5

Keep solution at room temperature.

PCR Buffer Mix

- 1 M $MgCl_2$
- 1 M Tris-HCl pH 8.4

- 4 M KCl
- 1% Gelatin
- 100 mg/mL BSA (make fresh each time
- Milli-Q water
- dNTP sets (4 x 25 umol in 250 uL) (cat XC111, Roche)

Alkaline Tris buffer

- 100 Mm Tris HCl, pH 9.5
- 50 Mm $MgCl_2$
- 100 mM NaCl
- 0.1% Tween-20

20x SSC

- 175.3 gr NaCl
- 88,2 gr Citric acid trisodium
- 1000 ml water

Hybridization mix (HM)

- 100 ml deionized formamide
- 50 ml 20x SSC
- 1 ml 20% Tween-20
- 460 ul 1M citric acid
- 28,54 ml water

Dissolve into 4 x 45 ml in 50 ml Falcon tubes

To make HM-: Add 5 ml water

To make HM+: Add 500 ug/ml tRNAs and 50 ug/ml heparin and adjust volume to 50 ml

Store at -20˚C

2.1.3 Chemicals

A list of chemicals used during this study is presented below:

Name	Detail
Agarose	Nippon Genetics Europe, AG02
Agarose low- melting	ABT, 1300-25
Bovine serum Albumin (BSA)	Merck, 90604-29-8
Glycerol	EMD Millipore, 356350-500L
Dimethyl Sulfoxide	J.T.Baker, Avantor Performance Materials, 67-68-5
DNA ladder	New England BioLabs
Gel loading dye	New England Biolabs
PFA	Sigma-Aldrich, P6148
Tricaine	Sigma-Aldrich, A-5040,
PTU	Sigma-Aldrich, P7629
EDTA	AppliChem, 6381-92-6
Ethanol	VWR Chemicals, 64-17-5
Methanol	EMD Millipore, 67-56-1
Methylene Blue	Sinclair, ManA 16576
Isopropanol	Fisher, 67-63-0
NBT/BCIP stock solution	Roche Diagnostics, 11681451001
DIG RNA Labeling Mix	Roche Diagnostics, 11277073910
Formamide	Thermo Scientific, 17899

Phenol-chloroform-isoamyl alcohol mixture	Fluka Analytical, BioUltra 77619-100ML
TRI Reagent	Sigma, T9424-200ML
LB-Medium-Powder	AppliChem, A0954
LB-Agar-Powder	AppliChem, A0927
Triton X-100	Sigma, T9284-500ML
HEPES	Sigma, H4034-100G
Heparin	Sigma, H3393
SYBR Safe DNA gel stain	Invitrogen, S33102
DEPC	AppliChem, 1609-47-8
RNase ZAP	Ambion, AM9780
Mineral oil	Sigma, M5310
Tween-20	Sigma, P9416
Yeast extract	Millipore, 70161
tRNA from torula yeast	Sigma, R6625
Sodium hypochlorite solution	Sigma, 425044
Perdrogen 30% H_2O_2	Sigma-Aldrich, 31642

2.1.4 Commercial Kits

The Kits that were used for the conduction of this study are listed below:

Name	Detail
PrimeScript RT reagent kit	TaKaRa, RR037A
Mini Prep DNA isolation	Macherey- Nagel
HiScribe T7 High Yield RNA Synthesis Kit	New England BioLabs, E2040S
mMESSAGE mMACHINE T3 Kit	Invitrogen, AM1348
mMESSAGE mMACHINE SP6 Kit	Invitrogen, AM1340
mMESSAGE mMACHINE T7 Kit	Invitrogen, AM1344
SYBR Kit (for qPCR)	Roche
Gel extraction Kit	Macherey- Nagel
In vitro synthesis of DIG-labeled RNA probes	Roche

2.1.5 Enzymes

A list of enzymes used during this study is presented below:

Name	Details
Pronase Protease	EMD Millipore, Cat 53702-25KU, CAS 9036-06-0
Proteinase K	New England BioLabs, P8108S
Sap I	New England BioLabs, R0569
Exonuclease I (Exo I)	New England BioLabs, M0293S

Shrimps Phosphatase Alkali (SAP)	New England BioLabs, M0371S
Turbo DNase	Ambion, 2238G2
Taq DNA polymerase	Kapa, KE6010
SP6 RNA Polymerase	Invitrogen, 2706G
T7 RNA Polymerase	Invitrogen, 18033-019
T3 RNA Polymerase	Invitrogen, 2736G
T4 DNA Ligase	New England BioLabs, M0202
XbaI	New England BioLabs, R0145
BsmBI	New England BioLabs, R0739
BglII	New England BioLabs, R0144
SalI	New England BioLabs, R0138
BamHI	New England BioLabs, R0136
NcoI	New England BioLabs, R0193
SpeI	New England BioLabs, R0133

2.1.6 Instruments/Equipment

A list of instruments and Lab equipment used during this study is presented below:

Name	Details
Injection needles	Part No TW 100F-4, World Precision Instruments (Thin-wall capillary 4'', w/FiL, 1.0 mm (500), Sonal/Lot No 10c)
	Settings for needles: Pressure 200, Heat 564, Pull 80, Velocity 70, Delay 90

Micropipette Puller	Model P-97/IVF, Sutter Instrument Co.
Microinjector	MM 33 Rechts 00-42-101-0000, M3301R, World Precision Instruments (WPI)
Hybridization Oven	UVP, HB-1000 Hybridizer
PCR machine	Bio-rad, T100 Thermal Cycler
	MJ Research, PTC-200 Peltier Thermal Cycler
Gel electrophoresis (chamber and power supply)	Owl Preparation Systems, models B1a, B2 Thermo Electron Corporation EC1000-90
Centrifuges	Bio-rad C1301, mini centrifuge
	Biofuge Heraeus, *pico*
	Biofuge Heraeus, *fresco*
	Biofuge Heraeus, *stratos*
pH/EC/TDS/°C Portable Meter	HI- 9811-5, HANNA PLUS probe HI-1285-5
Stereoscope	Brightfield stereoscope: SMZ1000, Nikon
	Fluorescent stereoscope: SMZ800, Nikon
Microscope	Brightfield microscope: Leica DMLS2 PLUS Leica DFC-500 Color camera
	Inverted microscope: Leica DMIRE2 PLUS Hamamatsu ORCA-Flash4.0 camera
	Confocal upright microscope: Leica SP5 II on a DM600 CFS Upright microscope
Vibratome	Leica VT10005

Microtome	Leica RM 2265
Heating block	Wealtec Corp., HB2
Hot plate magnetic stirrer	Schott SLR
Bacterial incubator	Orbital Shaker, Thermo Forma 4520
Zebrafish incubator	Lovibond
Nanophotometer	Implen, P-Class
Vortex	Labnet Inernational, VX100
Water bath	Grant Instruments, SUB14
Wight microscale	Sartorius, CP224S

2.1.7 Oligonucleotides

A list of oligonucleotides used during this study is presented below:

Name	Sequencing	Supplier
cfdp1 morpholino	TCTGAATAATTCATTCTTGTGTCGT	GeneTool, LLC
ccdc92 morpholino	ACTCATGAGGCCATGATGAAGATC	GeneTool, LLC
cfdp1 target site 1(exon) (Crispr-Cas)	GGAGGATGCGCTGGAAGGGGAGG Oligo 1: TAGGAGGATGCGCTGGAAGGGG Oligo 2: AAACCCCCTTCCAGCGCATCCT	Macrogen
Genotyping primers for *cfdp1* target site 1 (exon)	For: TTTGCATGTTTGTTTTGTCTCA Rev: AGCCCTACCTCATATGGACATC	Macrogen
cfdp1 target site 2 (exon) (Crispr-Cas)	CAGTAGGAGACATTGAAGAGCGG Oligo 1: TA(GG)CAGTAGGAGACATTGAAGAG	Macrogen

	Oligo 2: AAACCTCTTCAATGTCTCCTACTG	
Genotyping primers for *cfdp1* target site 2 (exon)	For: GGAGGCCTCAAACTGGTGGAG Rev: CTTCTGAGAGCTTGCACTTGG	Macrogen
cfdp1 target site (promoter) (Crispr-Cas)	GATGAAAGAAACGACGAGCCTGG Oligo 1: TA(G)GATGAAAGAAACGACGAGCC Oligo 2: AAACGGCTCGTCGTTTCTTTCAT	Macrogen
Genotyping primers for *cfdp1* target site (promoter)	For: TGCTTTACTACCGTTTGGTTGA Rev: ATACTTGCAAGAAACACTGGGG	Macrogen
ccdc92 target site 1 (exon) (Crispr-Cas)	GGGAGTGGCAGAAGAAGCGATGG Oligo 1: TAGGGAGTGGCAGAAGAAGCGA Oligo 2: **AAAC**TCGCTTCTTCTGCCACTC	Macrogen
Genotyping primers for *ccdc92* target site 1 (exon)	For: GTACTTCGGGATTCGGTAGATG Rev: TGTTCCTTGGACTTGGAGGTAT	Macrogen
ccdc92 target site 2 (exon) (Crispr-Cas)	(G)GAGGGGCGTTCCCTCAACACTGG Oligo 1: TA(G)GAGGGGCGTTCCCTCAACAC Oligo 2: AAACGTGTTGAGGGAACGCCCCT	Macrogen
Genotyping primers for *ccdc92* target site 2 (exon)	For: CTCTCACAACCACTACACTCCG Rev: GTTCCTTGGACTTGGAGGTATGG	Macrogen
ccdc92 target site (promoter) (Crispr-Cas)	CGCGTCTTTCTGGTAGGTGTCGG Oligo 1: TA(GG)CGCGTCTTTCTGGTAGGTGT	Macrogen

	Oligo 2: AAACACACCTACCAGAAAGACGCG	
Genotyping primers for *ccdc92* target site (promoter)	For: CCAGCATGCACCGCTTTATTTAG Rev: CAGCAGACGCACACACAACCTG	Macrogen
Primers for generation of *cfdp1* RNA probe	For: GAGACATTGAAGAGCGGCAG Rev: CGACTTCTCCAGAGTGCTCA	Macrogen
Primers for generation of *ccdc92* RNA probe	For: GGAAAACACCATCCGAGAGC Rev: GAGTGGCAGAAGAAGCGATG	Macrogen

2.1.8 Plasmids

A list of plasmids used during this study is presented below:

Name	Details
p-GEM-T Easy Vector System I	A1360, Promega
pT7-gRNA	46759, Addgene plasmid
pT3TS-nCas9n	46757, Addgene plasmid

2.1.9 Software and data bases

Software

- LAS AF: Leica Microsystems Confocal Microscopy Data acquisition and Analysis
- IMAGEJ/FIJI: quantitative Image Analysis of microscopy Images
- SNAP GENE: Sequence Analysis
- GraphPad: Data Analysis

Data bases

- CHOPCHOP: Identification of CRISP-Cas9 target sites (https://chopchop.cbu.uib.no/)
- ENSEMBL: Genome comparisons (https://www.ensembl.org/index.html)

- NCBI: Literature and gene information (https://www.ncbi.nlm.nih.gov/)
- NEB: Digestion instructions (https://international.neb.com/)
- ZFIN: Zebrafish Information (protocols, publications, husbandry) (https://zfin.org/)

2.1.10 Zebrafish lines

The zebrafish lines that were utilized for the conduction of this thesis are as follows:

Name	Detail	Reference
AB	Wild-type	
Tg(*myl7:GFP*)	Myocardial cells	Huang et al., 2003
Tg(*fli1:EGFP*)	Endothelial cells	Lawson et al., 2002
Tg(*Tp1:mCherry*)	Notch reporter	Ninov et al., 2012
Tg(7x*TCF-Xla.Siam:nlsmCherry*)	Wnt reporter	Moro et al., 2012

2.1.11 Zebrafish Food

Zebrafish larvae, juveniles and adults were fed at least two times per day. For juveniles and adults, the daily nutrition included both live food (Brine shrimp cysts) alongside with fry food. The larvae were fed exclusively with dry food as an alternative to paramecia and small rotifers, by tapping it onto the water surface. The fish food is listed below according to the developmental stage of the animal.

Fish Age	Food	Supplier
7dpf – up to 1 month	ZM-000 fry food (Protein 56.0%, Oil 8.0%, Ash 11.0%, Fibre 2.0%)	ZM Fish Food and Equipment
	ZM-100 fry food (Protein 55.0%, Oil 13.0%, Ash	ZM Fish Food and Equipment

1 month – 3 months (juveniles)	12%, Moisture 7.0%, Fibre 1.0% Vit. A: 20,000 IU/kg, Vit. D3: 2,500 IU/kg, Vit. E: 700mg/kg, Vit. C: 2,000 mg/kg, w3 HUFA 30mg/g dwt)	
	Polarized Sep-Art Artemia Cysts (Brine Shrimp Cysts) (>225,000 hatched shrimp per g)	Ocean Nutrition, ZM Fish Food and Equipment
Adult (≥ 3 months)	ZM-400 fry food (Protein 58.0%, Oil 14.5%, Ash 11.5%, Moisture 7.0%. Vit. A. 30,000 I.U./kg, Vit. D3 2,500 I.U./kg, Vit. E 400 mg/kg, Vit. C 2,000 mg/kg, w3 HUFA 30 mg/g dwt)	ZM Fish Food and Equipment
	Polarized Sep-Art Artemia Cysts (Brine Shrimp Cysts) (>225,000 hatched shrimp per g)	Ocean Nutrition, ZM Fish Food and Equipment

2.2 Methods

2.2.1 Bleaching of zebrafish embryos

Commercially available: Sodium hypochlorite solution 10-15%, 425044, Sigma

1. Prepare bleaching solution by adding 180 ul stock NaOCl in 500 ml E3 medium (0.0045% final working solution)
2. Transfer embryos to a Petri dish using tea strainer and incubate them in bleaching solution for 5 minutes
3. Wash embryos in E3 medium water for 5 minutes
4. Repeat steps 2 and 3
5. Wash one additional time with E3 medium water

Ideally, embryos should be bleached at 2-6 hpf. After 24 hpf, chorion is getting degraded and NaOCl could damage the embryo. Since bleaching interferes with hatching, Pronase treatment should follow to facilitate the dechorionation.

2.2.2 cDNA synthesis (PrimeScript RT reagent kit, TaKaRa RR037A)

1. Prepare on ice the master mix for cDNA synthesis
    - For one reaction:

      2 ul 5x PrimeScript Buffer

      0.5 ul Enzyme mix

      0.5 ul Oligo dT primer (50 uM)

      0.5 ul Random 6 mers (1000 uM)

      ------ RNA (500ng)

      ------ water (up to 10 ul final volume)
2. Add in a 0.5 ml tube first the RNA and the water to volume 6.5 ul. Then dispense the mix to the tubes
3. Incubate at 37˚C for 15 minutes and then at 85˚C for 5 seconds.
4. Store at 4˚C or -20˚C

2.2.3 Competent Cells

1. Pick up one colony and dilute in 5 ml P.S.I. Broth. Incubate at 37˚C until $O.D_{550} = 0.3$
2. In 100 ml P.S.I. Broth, pre-heated at 37˚C, add the above 5 ml and incubate until $O.D_{550} = 0.48$
3. Incubate in ice for 10 minutes
4. Place cells in 50 ml Falcon tubes and centrifuge at 4˚C, 2500 rpm for 5 minutes (from this point forward all steps in ICE)
5. Dilute pellets in 30 ml cold TFB1. The solution must be set at pH 5.8 with HOAc 0.2 M. If it gets more acidic, do not try to fix it with any base but make a new solution from the beginning
6. Incubate DH5α cells on ice for 15 min. If there is another type of cells, incubate on ice accordingly:
   DH1 centrifuge immediately
   C600 incubate for 5 minutes
   HB101 incubate for 90-120 minutes
7. Centrifuge DH5α cells at 4˚C, 2500 rpm for 5 minutes
8. Dilute pellets in 4 ml of cold TFB2
9. Split 100 ul in pre-frozen tubes with pre-frozen pipette tips and store in -80˚C. It is very important the tubes to be frozen before use and to immediately store them in -80˚C

2.2.4 CRISPR-Cas9 protocol

1. **Identification of CRISPR targets**
   - Choice of target site either in exon close to the 5’ end or inside the promoter region of gene of interest by using the online program CHOP-CHOP
   - Cas9 mechanism requires the target site to have the following sequence: 5’-GG(N_{18})NGG-3’

2. **Design of oligos for RNA synthesis**

   - The oligos should have the following structure in order to be cloned to the backbone vector pT7-gRNA:

     Oligo 1: 5'- **TA** GG(N_{18}) -3' (should not contain PAM NGG sequence)

     Oligo 2: 5' - **AAAC** (N_{18}) -3 (should not contain PAM NGG sequence)

3. **Annealing of target oligos**

   - Primer Anneal mix:

     2 ul Oligo 1 (100 uM)

     2 ul Oligo 2 (100 uM)

     2 ul NEB3.1 10x

     14 ul water

   Incubate mixture at 95˚C for 5 minutes, ramping down to 50˚C at 0.1˚C /second, incubating at 50˚C for 10 minutes and chilling to 4˚C at normal ramp speed (1˚C /second)

4. **Cloning (one- step digestion/ligation)**

1 ul	Annealed ds oligo
400 ng	pT7-gRNA vector
1 ul	NEB3.1 10x
1 ul	T4 ligase buffer 10x
0.5 ul	BsmBI
0.3 ul	BglII
0.3 ul	SalI
0.5 ul	T4 Ligase
(up to 10 ul final volume)	water

   Incubate in thermal cycler: 3 cycles of 20 minutes at 37 ˚C/15 minutes at 16 ˚C, followed by 10 minutes at 37 ˚C, 15 minutes at 55 ˚C and 15 minutes at 80 ˚C

5. **Transformation**

   - Use 2 ul of the ligation product and plate 10% of the transformants to a LB/Ampicillin plate. Incubate at 37 ˚C overnight

6. **Identification of the correct clones**

   - Pick 10 single colonies for inoculation of liquid mini prep cultures (5 ml LB/Ampicillin)

7. **Plasmid DNA extraction and diagnostic test**

   - Perform miniprep isolation of plasmid DNA and keep a bacto stock of each colony for later (In 1 ml cryovial: 500 ul bacterial culture + 500 ul sterile 50% glycerol. Store at -80˚C)
   - Perform diagnostic test with BglII in order to screen for colonies that have lost their BglII-cutting site. So, successful transformation product will be uncut by this enzyme:

     3 ul DNA

     2 ul BglII

     2 ul NEB3.1 10x

     13 ul DD water

     Incubate at 37 ˚C for 3 hours

     Load 10 ul digestion product (plus 2 ul 6x purple loading dye in each sample) in 1% agarose gel for electrophoresis and visualization of digestion
   - Send for sequencing the DNA samples from positive clones (Macrogen requirements: 5 ul plasmid DNA 100ng/ul PLUS 3 ul For. Primer M13 PLUS 2 ul water)

8. **Bacterial inoculation and DNA plasmid isolation**

   - After confirmation of insert, pick the corresponding bacterial stock and inoculate in plate with LB/Ampicillin using sterilized inoculation loop. Dip the inoculation stick in the bacterial stock and then place it on the plate and create discrete bacterial lines. Incubate at 37˚C overnight.
   - Pick single colonies with a sterile tip and place it into liquid mini cultures (5 ml LB/Ampicillin). Incubate at 37˚C overnight in shaking machine
   - Perform MiniPrep DNA plasmid isolation using the Nucleo Spin Plasmid, Macherey-Nagel

9. Linearization of the gRNA vector

Linearize the isolated DNA plasmid by the following reaction:

5 ug	plasmid
2.5 ul	BamHI
5 ul	NEB3.1
(up to 50 ul final volume)	nuclease-free water

Incubate at 37 ˚C for 3 hours

Check the digestion by running 1 ul on 1% agarose gel

10. Precipitation of the DNA

6 ul (0.1 vol)	3 M NaOAc, pH 5.2
4 ul	nuclease-free water, Mix well
120 ul (2 vol)	Ethanol, Mix well

Chill at -20 ˚C for 30 minutes or overnight

Spin for 30 minutes at high speed at 4 ˚C

Discard supernatant

Add 500 ul 70% Ethanol

Spin 15 minutes at high speed at 4 ˚C

Take off all supernatant

Air dry pellet

Resuspend in nuclease-free water to about 500 ng/ul concentration

11. *In vitro* transcription of the gRNA

Use of T7 High Yield RNA Synthesis Kit (NEB) following the manufacturer's instruction.

Briefly:

1.5 ul	10x Reaction Buffer
1.5 ul	NTP (7.5 mM final each)
1 ug	Template DNA linearized
1.5 ul	T7 RNA Polymerase Mix
(up to 20 ul final volume)	Nuclease-free water

Incubate at least 4 hours at 37 ˚C in dry incubator

12. (Optional) DNase treatment

Treat with 1 ul TURBO DNase and TURBO DNase Buffer, incubate for 10 minutes at 37 ˚C

13. Purification of gRNA

20 ul	3 M NaOAc, pH 5.2
200 ul	Isopropanol
160 ul	nuclease-free water

Mix well and chill for 30 minutes at -20 ˚C or overnight (you can store RNAs as RNA/isopropanol mixes to protect RNAs from freeze/thaw cycle damages)

Spin for 30 minutes at high speed at 4˚C

Discard supernatant

Add 500 ul 70% Ethanol

Spin for 15 minutes at high speed at 4 ˚C

Take off all supernatant

Air dry the pellet

Resuspend in 30 ul nuclease-free water

Store at -80˚C

14. Linearization of the Cas9 vector

5 ug	pT3TS-nls-zCas9-nls
2.5 ul	XbaI
5 ul	CutSmart
(Up to 50 ul final volume)	nuclease-free water

Incubate at 37˚C for 3 hours

15. Precipitate the DNA

2 ul 0.5 M EDTA pH 8.0

6 ul (0.1 vol) 3 M NaOAc, pH 5.2

4 ul nuclease-free water

Mix well

120 ul (2 vol) Ethanol

Mix well and chill for 30 minutes at -20˚C or overnight

Spin 30 minutes at high speed at 4 ˚C and discard supernatant

Add 500 ul 70% Ethanol, spin 15 minutes at high speed at 4 ˚C

Remove the supernatant and air dry the pellet

Resuspend in nuclease-free water to about 500 ng/ul concentration

16. *In vitro* synthesis of capped mRNA of nls-zCas9-nls

(Using mMESSAGE mMACHINE T3 Kit). Briefly:

(up to 20 ul final volume)	nuclease-free water
10 ul	2x NTTP/CAP
2 ul	10x buffer
X ul(1 ug)	linearized pT3TS-nls-zCas9-nls
2 ul	T3 RNA polymerase enzyme mix

Incubate for 2 hours at 37˚C

DNase treatment: Add 0.5 ul Turbo DNase, incubate for 15 minutes at 37˚C

RNA cleanup: Add 115 ul nuclease-free water and 15 ul Ammonium Acetate Stop Solution, mix well and then add 150 ul Isopropanol

Mix well and chill for 30 minutes at -20˚C or overnight

Spin for 30 minutes at high speed at 4 ˚C, discard supernatant

Add 500 ul 70% Ethanol, spin 15 minutes at high speed at 4 ˚C

Remove supernatant and air dry the pellet

Resuspend in nuclease-free water and store at -80˚C

2.2.5 DH5α Bacterial transformation

1. Defrost 100 ul *Escherichia coli* (E.coli) in ice for 5 minutes
2. Add 4 ul ligation/insert product (plasmid) in the bacterial suspension
3. Incubate on ice for 10 minutes
4. Heat sock at 42 ˚C for 45 seconds (water bath or thermocycler)
5. Place on ice for 2 minutes
6. Add 1 ml LB (without antibiotic)
7. Incubate at 37 ˚C for 1 hour in shaking machine

8. Place 110 ul of bacterial culture onto a plate with LB plus antibiotic
9. (optional) Spin the rest of the bacterial culture at 3000 rpm for 5 minutes, discard the supernatant and leave approximately 100 ul medium. Dissolve bacterial pellet by gently pipetting up and down. Place 100 ul bacterial culture onto a plate with LB plus antibiotic
10. Incubate the transformed bacteria at 37˚C, overnight

2.2.6 DNA extraction (fixed tissue and after ISH-genotyping)

1. Incubate fixed tissue in 50 ul Alkaline Lysis Reagent (make sure tissue is completely submerged)
2. Incubate at 95˚C for 1-2 hour and store at 4˚C until you proceed to the next step
3. Add 50 ul Neutralization Reagent in each sample and mix well

2.2.7 DNA extraction (fresh tissue)

(Large sample number, very quick and dirty, adequate for RCR)

1. Transfer zebrafish embryos into microfuge tube and remove excess liquid
2. Add DNA extraction buffer (50 ml for pool of embryos or adult fin tail and 20ml for single embryo)
3. Incubate at 55˚C for 3hrs
4. Boil at 98˚C for 15min to inactivate Proteinase K
5. Spin samples for 1 min at room temperature
6. Store at - 20˚C

2.2.8 DNase treatment

1. Transfer RNA to 0.5 ml tube
2. Add to the RNA
    - 2 ul 10x DNase buffer (TURBO)
    - 0.5 ul TURBO DNase
3. Incubate at 37˚C for 30 minutes and then at 75˚C for 10 minutes

2.2.9 ExoSap PCR cleaning reaction (prior sequencing)

Before sequencing of PCR products, residual nucleotides must be removed. Cleaning Protocol follows:

- 0.025 ul ExoI
- 0.25 ul rSAP
- 4.725 ul DD water
- 15 ul PCR product

Incubate samples at 37˚C for 30 minutes and then 85˚C for 20 minutes in a PCR machine
Store at 4˚C or -20˚C until needed

2.2.10 Immunohistochemistry

For fixed sections or whole mount staining, antibodies concentration and incubation time is adjusted. The basic protocol that was followed during this study is as indicated below:

1. Washes/Permeabilization
    - 3 rinses with 0.5-0.8% PBT (0.5-0.8% Triton X-100 in 1x PBS)
    - 3 washes for 15 minutes with 0.5-0.8% PBT
2. Blocking
    - Incubation in blocking solution (4% BSA in 0.5-0.8% PBT) for 1 hour at room temperature
3. Primary antibody incubation
    - Incubation with primary antibody (diluted in blocking solution) for at least one O/N (overnight) at 4˚C
4. Remove primary antibody
5. Washes
    - 3 rinses with 0.5-0.8% PBT (0.5-0.8% Triton X-100 in 1x PBS)
    - 6 washes for 15 minutes with 0.5-0.8% PBT
7. Secondary antibody incubation
    - Incubation with secondary antibody (diluted in 0.5-0.8% PBT) for 2 hours at room temperature or O/N at 4˚C. Wrap with aluminum foil for light protection

8. Washes
    - 3 rinses with 0.5-0.8% PBT (0.5-0.8% Triton X-100 in 1x PBS)
    - 3 washes for 15 minutes with 0.5-0.8% PBT
9. Mounting
    - Mount samples on slides with 70% glycerol or Ibidi mounting medium

2.2.11 Injection preparation

1. Injection plates

Prepare 1% agarose gel in E3 medium by heating in microwave. Pour the solution in a 10cm Petri dish and gently place a mold with lines until gel is solidified. After removal of the mold, the generated grooves will utilize the alignment of zebrafish embryos prior the microinjection.

2. Injections needles

Glass capillaries of certain features are placed in needle puller. The center of the capillary is melted by heat and pulled apart from the two side-ends forming two needles in each round of pull. The needles are stored carefully for microinjections purposes.

3. Injection mixture

For CRISPR-Cas9:

- 150 ng/ul Cas9 mRNA
- 50-100 ng/ul sgRNA
- 120 mM KCl
- 20 mM HEPES, pH 7.0
- 1 ul phenol red
- (up to 5 ul final volume) water

For morpholino:

- 2-4 ul MO
- 1 ul phenol red
- (up to 5 ul final volume) water

4. Injection set up

The tip of the injection needle is carefully trimmed by cutting its end using forceps in order to create a needle diameter to efficiently enter the embryo without provoke any further damage. The needle is filled with mineral oil and placed into the microinjector manipulator and 4.6 nl injection droplet is set to be released in each injection pulse. Following, needle is filled with 5 ul injection mixture and embryos are collected and injected at one-cell stage.

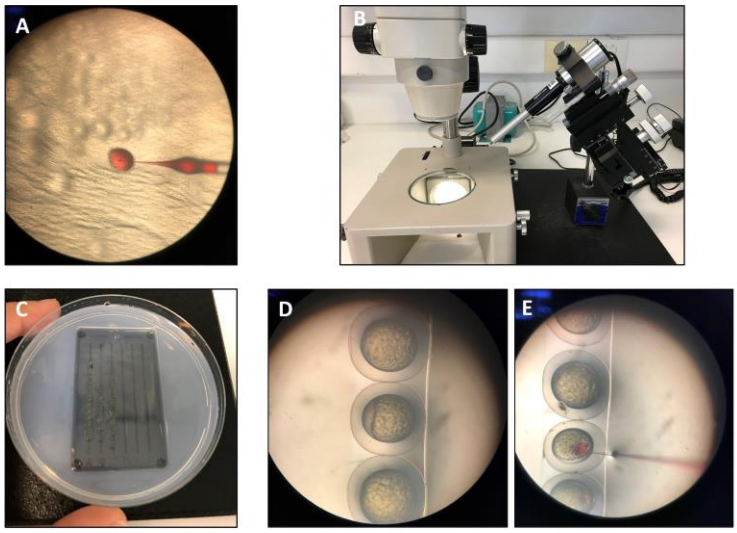

Figure 19: Microinjections in one-cell stage zebrafish embryos. A, Loading the injection needle with injection mix. B, Microinjector. C, Zebrafish embryos are placed in agarose mold straight in a line for better manipulation. D, Zebrafish embryos under the stereoscope before the microinjection (yolk is yellow and one cell embryo is transparent attached to the yolk). E, Injection needle pass through the chorion and injection mixed is released either in the cell or at the animal pole of the yolk.

2.2.12 Whole mount *In Situ* Hybridization

Transfer Methanol (MeOH)-stored embryos in 6-well plate. For the dilution and buffers, use DEPC-treated water whenever is needed)

1. Rehydration

   1 x 5 min 100% MeOH wash

   1 x 5 min 75% MeOH – 25% PBS

   1 x 5 min 50% MeOH – 50% PBS

   1 x 5 min 25% MeOH – 75% PBS

   4 x 5 min PBT (1xPBS pH 5.5, 0.1% Tween20)

2. Permeabilization

   Prepare 10 ug/ml Proteinase K in PBT, use a fresh aliquot each time. Incubate at room temperature for a duration that is dependent on the developmental stage of the emryo:

   No Proteinase K embryos up to 16 hpf

   5 min embryos up to 32 hpf

   45 min embryos 30 hpf and later

   20 minutes post fixation 4% PFA in PBS

   1 rinse PBT

   5 x 5 min PBT

3. Hybridization (in hybridization oven with horizontal shaker)

   2-5 hours Pre-hybridization: Incubate embryos in HM+ at 70˚C

   Probe incubation: probe dilution 1:300 in HM, overnight at 70˚C. Seal plate with wet paper and wrap it with aluminum foil to prevent evaporation.

4. Washes (in hybridization oven with horizontal shaker)

   Take off HM+/probe and save for 2-3 more uses, store at -20 ˚C

   1 rinse HM- at 70˚C

   10 min 75% HM- / 25% 2x SSC at 70˚C

   10 min 50% HM- / 50% 2x SSC at 70˚C

   10 min 25% HM- / 75% 2x SSC at 70˚C

10 min 2x SSC at 70˚C

2x 30 min 0.2x SSC at 70˚C

5. Washes (at room temperature on horizontal shaker)

   10 min 75% 0.2x SSC / 25% PBT at RT

   10 min 50% 0.2x SSC / 50% PBT at RT

   10 min 25% 0.2x SSC / 75% PBT at RT

   10 min PBT at RT

6. Blocking and Incubation of anti-DIG

   3-4 hours Blocking Solution: 1x Blocking Reagent in PBT

   Anti-DIG incubation: Incubate at 4˚C with anti-DIG in blocking solution at 1:5000, overnight and wrap in aluminum foil

7. Washes

   1 rinse PBT

   6 x 15 min PBT

   1 rinse Alkaline Tris buffer

   3 x 5 min Alkaline Tris buffer

8. Staining

   Staining solution: 200 ul NBT/CIP per 10 ml Alkaline Tris buffe. Add 600 ul of staining solution and observe reaction under stereoscope every 10 minutes

9. Stop Labeling reaction

   1 rinse PBS pH 5.5, 1 mM EDTA

   2 x 5 min PBS pH 5.5, 1 mM EDTA

   1 x 5 min 25% MeOH - 75% PBS pH 5.5, 1 mM EDTA

   1 x 5 min 50% MeOH - 50% PBS pH 5.5, 1 mM EDTA

   1 x 5 min 75% MeOH - 25% PBS pH 5.5, 1 mM EDTA

   2 x 20 min 100% MeOH

   1 x 5 min 75% MeOH - 25% PBS pH 5.5, 1 mM EDTA

   1 x 5 min 50% MeOH - 50% PBS pH 5.5, 1 mM EDTA

   1 x 5 min 25% MeOH - 75% PBS pH 5.5, 1 mM EDTA

2 x 5 min PBS pH 5.5, 1 mM EDTA

10. Mounting

    Add 500 ul 1x PBS, pH 5.5 in glycerol

2.2.13 MiniPrep Protocol (MERLIN)

1. Harvest bacterial cells
    - Spin the overnight LB culture at 10.000g for 3 minutes at room temperature (fill and spin twice)
    - Remove all the medium and let the pellet dry
2. Cell lysis
    - Add 200 ul MERLIN I, vortex to resuspend the pellet until it is homogeneous
    - Add 250 ul MERLIN II, mix gently by inverting the tube. Do NOT vortex. Keep the tubes on ice
    - Incubate at room temperature for 3 minutes
    - Add 250 ul MERLIN III, mix gently by inverting the tube 6-8 times. Do NOT vortex
    - Incubate on ice for 5-10 minutes
3. Clarification of lysate
    - Spin max speed for 10 minutes at room temperature
    - Transfer supernatant in a new tube
4. Precipitate and wash the DNA
    - Add 700 ul pre-chilled isopropanol and mix by inverting the tube 6-8 times
    - Spin max speed for 30 minutes at 4˚C
    - Discard the supernatant
    - Add 700 ul 70% Ethanol
    - Spin max speed for 15 minutes at room temperature
    - Discard supernatant
    - Air dry the pellet for 10 minutes
    - Add 30-50 ul elution buffer or water
    - Measure concentration in nanodrop

- Store at 4˚C or -20˚C

2.2.14 PCR Buffer Mix

1. Mix the ingredients in a flask that is at least two times the final volume of the solution to avoid boil over during sterilization

   343.800 ml Milli-Q water

   0.745 ml 1 M $MgCL_2$

   4.975 ml 1 M Tris-HCl pH 8.4

   6.220 ml 4 M KCl

   0.500 ml 1% Gelatin
2. Autoclave the above solution
3. While the solution is cooling, thaw the nucleotides (dATP, dTTP, dGTP, dCTP)
4. Briefly centrifuge the nucleotides
5. Add the nucleotides to the solution
6. Add 3.5 ml of the 100 mg/ml BSA to the solution
7. Swirl flask to mix and pour solution off into 50 ml Falcon tubes.
8. Aliquot 950 ul per Eppendorf tube for long-term storage at - 20˚C

2.2.15 PCR reaction

The mix of PCR reaction for genotyping is as follows:

- 2.5 ul DNA sample
- 20 ul PCR Buffer mix
- 1 ul Forward Primer
- 1 ul Reverse Primer
- 0.125 ul Taq DNA Polymerase
- 0.375 ul DD water

At a final volume reaction of 25 ul

2.2.16 Pronase dechorionation of zebrafish embryos

1. Transfer up to 50 zebrafish 24hpf embryos in a petri dish containing 20 ml E3 medium H_20
2. Add 100ul of Pronase (20 mg/ml stock solution) and incubate for approximately 20 minutes
3. Embryos will have been hatched by the end of the incubation time or can be hatched by gently pipetting up and down up to 4 times
4. Pour off the Pronase solution and refill with fresh E3 medium H_20

2.2.17 RNA isolation using TRIzol reagent

1. Homogenize tissue in 500 ul TRIzol using syringes 21G
2. Allow samples to stand for 5 minutes at room temperature
3. Add 0.1 ml chloroform in each sample (0.2 ml/ml TRIzol)
4. Shake vigorously for 15 seconds
5. Incubate 20 minutes at room temperature
6. Centrifuge at 12000x g for 20 minutes at 4˚C
7. Centrifugation separates the mixture into 3 phases:
    - A red organic phase (protein)
    - An interphase (DNA)
    - A colorless upper aqueous phase (RNA)
8. Transfer the aqueous phase on a new tube
9. Add 0.250 ml pre-chilled isopropanol and mix well (0.5 ml/ml TRIzol)
10. Allow samples to stand for 5-10 minutes at room temperature
11. Centrifuge at 12000x g for 20 minutes at 4˚C
12. Remove supernatant
13. Wash RNA pellet by adding 1 ml 75% Ethanol
14. Vortex and centrifuge at 12000x g for 10 minutes at 4˚C (samples can be stored in 75% Ethanol at -20˚C, before centrifugation)
15. Remove Ethanol

16. Air dry RNA pellet for 10 minutes (do not let RNA dry completely)
17. Dissolve RNA in 25 ul DEPC water
18. Measure RNA concentration
19. Store RNA samples at -80˚C

2.2.18 RNA probe synthesis

1. Generation of the desired insert by performing PCR reaction using zebrafish cDNA template and primers designed based on the cDNA sequence
2. Cloning of the PCR product into pGEM-T Easy vector in the ratio of 3:1 (PCR product:vector)

pGEM-T Easy vector is a linearized plasmid of 3015 bp (~3.0Kb). The mass of the insert is calculated based on the follow formula:

$$\frac{\text{(ng vector x Kb size insert)}}{\text{Kb size vector}} \quad X \quad \text{(insert : vector) ratio}$$

Ligation reaction mixture:

5ul	2x Rapid buffer T4
1 ul	Vector (50 ng)
X ul	PCR product (25 ng)
1 ul	T4 DNA ligase
(up to 10 ul final volume)	dH_2O

Incubate for 1 hour at room temperature

3. Bacterial transformation (insertion of the ligation product into competent DH5α cells)
4. Selection of 5 single colonies and inoculation in liquid 5 ml LB/Ampicillin culture overnight at 37˚C
5. DNA plasmid extraction (miniprep isolation)
6. IMPORTANT: Identification of the insert orientation in order to transcribe the RNA using the appropriate RNA polymerase. For the generation of antisense RNA (mRNA complementary), transcript must be synthesized by RNA polymerase corresponding to

the promoter at the 3', or carboxy-terminal side of the coding region pf the protein. For the generation of sense RNA (negative control), transcript must be synthesized by RNA polymerase corresponding to the promoter at the 5', or amino-terminal side of the coding region pf the protein (use T7/SP6 RNA polymerases from mMESSAGE mMACHINE kit)

7. Linearization of plasmid by using *NcoI* and *SpeI*:

For transcription with SP6 RNA polymerase		For transcription with T7 RNA polymerase	
DNA (5 ug)	X ul	DNA (5 ug)	X ul
NcoI	3 ul	*SpeI*	3 ul
Cut Smart buffer	5 ul	Cut Smart buffer	5 ul
dH_2O	Up to 50 ul	dH_2O	Up to 50 ul

Incubate for 1 ½ hours at 37˚C

8. Precipitation of linearized DNA plasmid

2 ul	0.5 M EDTA, pH 8.0
5 ul (0.1 vol)	3 M NaOAc, pH 5.2, mix well
50 ul (1 vol)	Isopropanol

Chill at -20 ˚C overnight

Spin for 30 minutes at high speed at 4 ˚C

Discard supernatant

Add 500 ul 70% Ethanol

Spin for 30 minutes at high speed at 4 ˚C

Discard supernatant

Air dry the pellet

Resuspend in 40 ul of dH_20

Measure the concentration of digested products

9. Transcription of RNA probes

X ul (1 ug)	template

2 ul	10x NTP/DIG labeling mix
2 ul	10x Transcription buffer
1 ul	RNase inhibitor
2 ul	T7/SP6 RNA Polymerase
(up to 20 ul final volume)	nuclease-free water

Incubate at 37˚C for 2 hours

10. DNase treatment for removal of DNA template)
11. Add HM+ buffer (Hybridization Mix) and store at -80˚C

3. Results

3.1. A CRISPR/Cas9-induced mutant zebrafish line reveals the essential role of *cfdp1* in cardiac development and function

Cardiovascular diseases (CVD) lay in an extensive and broad spectrum of cardiac defects and clinical characteristics. Several factors contribute to the coincidence of CVD traits and it still remains unclear in which extend the genetic roots together with environmental elements lead to the disease manifest. The suggested predisposition of the CVD appearance is currently on the main focus of research interest. Genome-wide association studies have identified thousand robust associations (genome-wide significance, $p < 5x10^{-8}$) between disease traits and genetic loci and to date, especially for coronary artery disease (CAD), 66 loci have been unraveled which can explain approximately 12% of CAD heritability (Deloukas *et al.*, 2013; Nelson *et al.*, 2017; Webb *et al.*, 2017; Ntalla *et al.*, 2019). Moreover, it has also been reported that a larger number of putative loci is found at the false discovery rate (FDR) of 5%. Recently, a study that used UK Biobank data (Sudlow *et al.*, 2015) to evaluate the validity of FDR loci and conducted meta-analysis using CAD GWAS identified new loci at GWAS significance that were previously on 5% FDR providing support that variants in this threshold could hold the key for higher percentage of heritability (Nelson *et al.*, 2017).

Findings from human studies trying to analyze the genetic architecture of normal heart physiology, link the cardiac structure and function with SNPs (single nucleotide polymorphisms) in identified genetic loci. A list of recent publications derived from analysis of GWAS human data have highlighted the involvement of *CFDP1* (craniofacial development protein 1) in the determinants of risk factors for CAD, blood pressure, aortic diameter and carotid intima-media thickness raising the interest for deeper understanding of the functional analysis of *CFDP1* gene (Gertow *et al.*, 2012; Sabater-Lleal *et al.*, 2014; Boardman-Pretty *et al.*, 2015; Sung *et al.*, 2018; Aragam *et al.*, 2021).

The human *CFDP1* is a protein coding gene belonging to the evolutionary conserved Bucentaur (BCNT) superfamily which is classified by the uncharacterized BCNT domain of 80

amino acids (aa) at the C-terminal region. It is located on chromosome 16, consists of 7 exons which encodes for a protein product of 299 aa and it is flanked by the *BCAR1* (breast cancer antiestrogen resistance 1) and *TMEM170A* (transmembrane protein 170A) genes. The BCNT protein family is widespread among the species and their orthologues are also found in yeast *Saccharomyces cerevisiae* (SWC5), fruit fly *Drosophila melanogaster* (YETI), mouse *Mus musculus* (CP27) and zebrafish *Danio rerio* (RLTPR or CFDP1)(Messina *et al.*, 2015). The fact that BCNT is evolutionary conserved implies the important role of this superfamily, which was first detected in bovine brain extracts using monoclonal antibodies against a rat GTPase-activating protein with the same epitope (Nobukuni *et al.*, 1997). Although *CFDP1* gene is highly conserved, there is limited knowledge about its function and role not only at cellular level but also at the organism level. Yeast *Swc5* gene is essential for the optimal function of chromatin remodeler SWR which has histone exchange activity in an ATP-dependent manner (Wu *et al.*, 2009; Sun and Luk, 2017; Chu and Wang, 2021). Studies in *Drosophila melanogaster* have shown that loss of BCNT gene, *Yeti* causes lethality before pupation and that mechanistically provides a chaperon-like activity that is required in higher-order chromatin organization by its interaction with histone variant H2A.V and chromatic remodeling machinery (Messina *et al.*, 2014). In the same context, functional analysis of zebrafish *cfdp1* has shown evidence for its role in craniofacial structure and bone development (Celauro *et al.*, 2017a). Mammalian BCNT proteins have also been characterized as molecular epigenetic determinants via their association with chromatin-related proteins (Iwashita *et al.*, 2015). Mouse BCNT gene, *cp27* was suggested to mediate early organogenesis and high level of its expression was demonstrated in developing mouse teeth, heart, lung and liver (Diekwisch *et al.*, 1999; Diekwisch, Luan and McIntosh, 2002; Luan and Diekwisch, 2002). Thus, while there are sparse studies accessing the role of *cfdp1* in chromatin remodeling complex via the maintenance of chromosome organization (Messina *et al.*, 2017; Iwashita *et al.*, 2020), little is known about not only its function and the mechanism it is involved in but also its role in heart physiology and morphogenesis.

Since, GWAS studies have revealed the implication of *CFDP1* in the risk of CAD in humans, it is essential to unravel how *cfdp1* affects the proper development and function of the

heart. For this purpose, we utilized zebrafish, a valuable animal model of human cardiovascular development and diseases (Bakkers, 2011; Bournele and Beis, 2016; Giardoglou and Beis, 2019). The physiology of the zebrafish heart offers several advantages to gain deeper knowledge about cardiac diseases derived from mutations that result in early embryonic lethality. For instance, although the severe heart-specific zebrafish line *sih* (*silent heart*) develop a non-contractile heart phenotype, the *sih* embryos survive up to 7 dpf (days post fertilization) as they uptake adequate oxygen through diffusion and are not dependent on circulating blood until that developmental stage (Sehnert *et al.*, 2002). This characteristic provides the ability to study mutations lethal to other vertebrate models.

For proper heart function, orchestrated myocardial cellular behavior and molecular signaling pathways are needed. The sequence of complicated events of early cardiac morphogenesis in vertebrate species includes heart tube formation, rightward heart looping, chamber establishment, cushion and valve development (Miquerol and Kelly, 2013). Initially, the cardiac tube consists of the outer one or two cells layer thick myocardium, the acellular cardiac jelly and the inner endocardium (Sedmera *et al.*, 2000). Cardiac trabeculation is among the most crucial process in developing heart which increases muscle mass and maximizes oxygen and nutrient exchange prior the establishment of coronary circulation network. Trabeculation is a highly regulation process during which ventricular cardiomyocytes expand towards the lumen of ventricle forming a sponge-like structure. Ventricular trabeculation occurs in a stochastic manner and requires an orchestration of cellular remodeling regulating changes in polarity (Crb2a), adhesion (N-cadherin, ZO-1), and tension (vinculin, active myosin) that are sufficient to promote the delamination of some cardiomyocytes in order to exit the compact layer and seed the trabecular layer (Cherian *et al.*, 2016; Jiménez-Amilburu *et al.*, 2016; Jiménez-Amilburu and Stainier, 2019; Priya *et al.*, 2020). The maintenance of myocardial architecture is highly crucial for the proper cardiac development and embryonic survival as *erbb2* mutant zebrafish lacking trabeculation suffer from heart dysfunction and progressively heart failure (Liu *et al.*, 2010). Therefore, it is fundamental to illustrate the factors that modulate ventricular trabeculation and cardiac morphogenic changes.

In this work, we aim to focus for the first time on the deeper study of the previously unanticipated role of *cfdp1* during development of the embryonic heart in order to elucidate its involvement in proper cardiac function. We show evidence that the expression of *cfdp1* is apparent during early developmental stages and plays an important role in cardiac trabeculation. As a consequence of *cfdp1* abrogation, embryos display heart dysfunction and contractility impairment supporting its role on proper cardiac performance. In addition, mutant *cfdp1* embryonic hearts exhibit downregulation of Wnt signaling pathway in the mesenchymal cells of the inner valve region during valvulogenesis without affecting Notch activation in this process. Thus, it is also suggested that *cfdp1* is possibly associated with canonical Wnt activation during valve development.

3.1.1. Effect of *cfdp1* abrogation

3.1.1.1 Expression profile of zebrafish *cfdp1* gene during embryonic development

Albeit, the BCNT (Bucentaur) protein superfamily is highly conserved between species, their functional role remains unclear (Messina *et al.*, 2015). Previous studies, on model systems such as yeast *Saccharomyces cerevisiae* (SWC5) (Wu *et al.*, 2005, 2009) , *Drosophila melanogaster* (YETI) (Messina *et al.*, 2014) and human cell lines (CFDP1) (Messina *et al.*, 2017) homologues have shown an important role during development by providing activity in chromatin remodeling organization. A recent study on zebrafish *cfdp1* linked the function of the gene with proper osteogenesis and craniofacial development focusing on the abundant *cfdp1* expression at the region of head (Celauro *et al.*, 2017b). In our study, we first analyzed the spatiotemporal expression of *cfdp1* during the development of zebrafish embryos, focusing on the cardiac area.

For this purpose, we performed semi-quantitative reverse transcription PCR with total RNA extracted from wild-type zebrafish embryos at different developmental stages (5 hpf – 120 hpf). We observed that *cfdp1* transcripts are detected from the first stages of development suggesting an important role in the proper development of the early embryo. The zygotic expression of *cfdp1* is as well apparent at later stages compared to the expression of *actinb2* housekeeping gene.

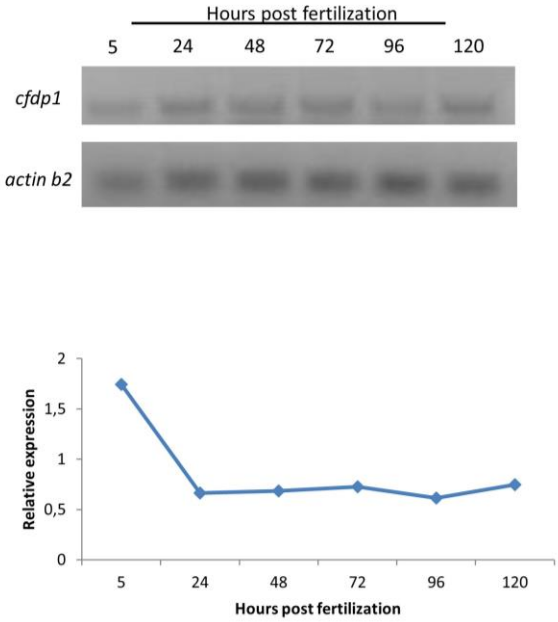

Figure 20: Expression analysis of *cfdp1* in different development stages via RT-PCR show that *cfdp1* is apparent during early development.

Furthermore, we performed whole mount *in situ* hybridization (WISH) with specific *cfdp1* antisense RNA probe in wild-type embryos to investigate the expression pattern during development. At the first developmental stages, *cfdp1* expression is observed at the anterior part of the organism and at 120 hpf the *cfdp1* expression is mainly detected at the cephalic region and the developing heart. Findings that are in accordance to the rt-PCR results in temporal matter. Control embryos that were hybridized with sense *cfdp1* RNA probe showed no staining pattern.

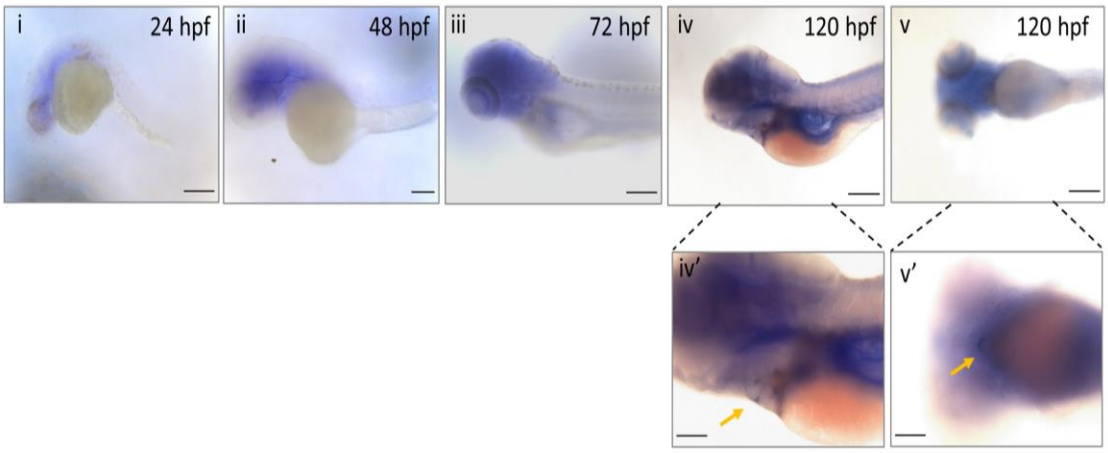

Figure 21: *In situ* hybridization using *cfdp1* RNA probe shows spatial expression during embryonic development. The expression of the gene is apparent from the 24 hpf and is restricted at the region of the head and the heart by 120 hpf. Scale bar (i-v) 150 µm, Scale bar (iv'-v') 200 µm

To further investigate the cardiac *cfdp1* expression at this later developmental stage, 120 hpf ISH-stained embryos were collected, embedded in paraffin and cut in 5 µm tissue sections via microtome. The histology analysis confirmed that *cfdp1* is expressed at the surrounding layer of the heart. These data reveal, for first time, that *cfdp1* plays an important role in zebrafish developing heart.

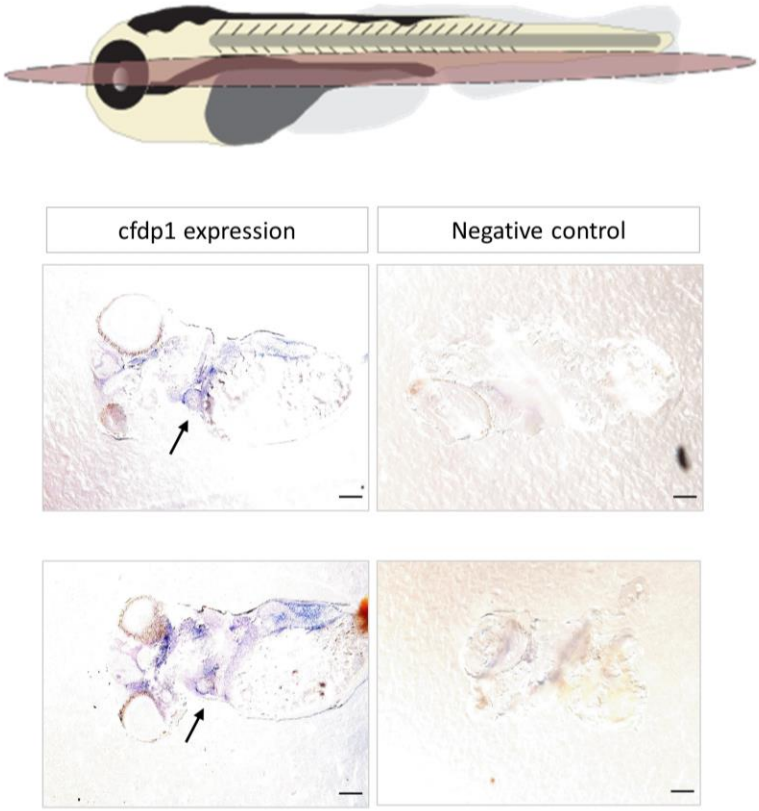

Figure 22: Upper: schematic representation of cutting plane of fixed *cfdp1*-ISH stained embryo. Lower: Paraffin section of ISH stained embryos with *cfdp1* antisense RNA probe and *cfdp1* sense RNA (negative control). Arrows point at the stained embryonic heart. Scale bar: 50 µm

3.1.1.2 Silencing of *cfdp1* expression reduces activation of Wnt pathway in the embryonic heart but Notch signaling remains unaffected

After the demonstration that *cfdp1* is also expressed in the zebrafish heart, it became important to address what is its function during development. To achieve this, we investigated *in vivo* the phenotype of embryos upon silencing of *cfdp1* expression via antisense morpholino oligonucleotide (MO)-mediated knockdown experiments. Therefore, we injected *cfdp1* translation-blocking MO in one-cell stage wild-type embryos and then incubate them at 28℃ up

to 120 hpf for monitoring. Figure 22 shows the phenotypic scoring of *cfdp1* morphants compared to the control sibling embryos. The majority of injected embryos develop pericardial oedema, from severe heart balloon shape to moderate oedema, along with craniofacial malformations, defects in otoliths and body curvature. The heart malformations of the *cfdp1* morphants phenotype affirmed the role of *cfdp1* in proper cardiac function and morphology.

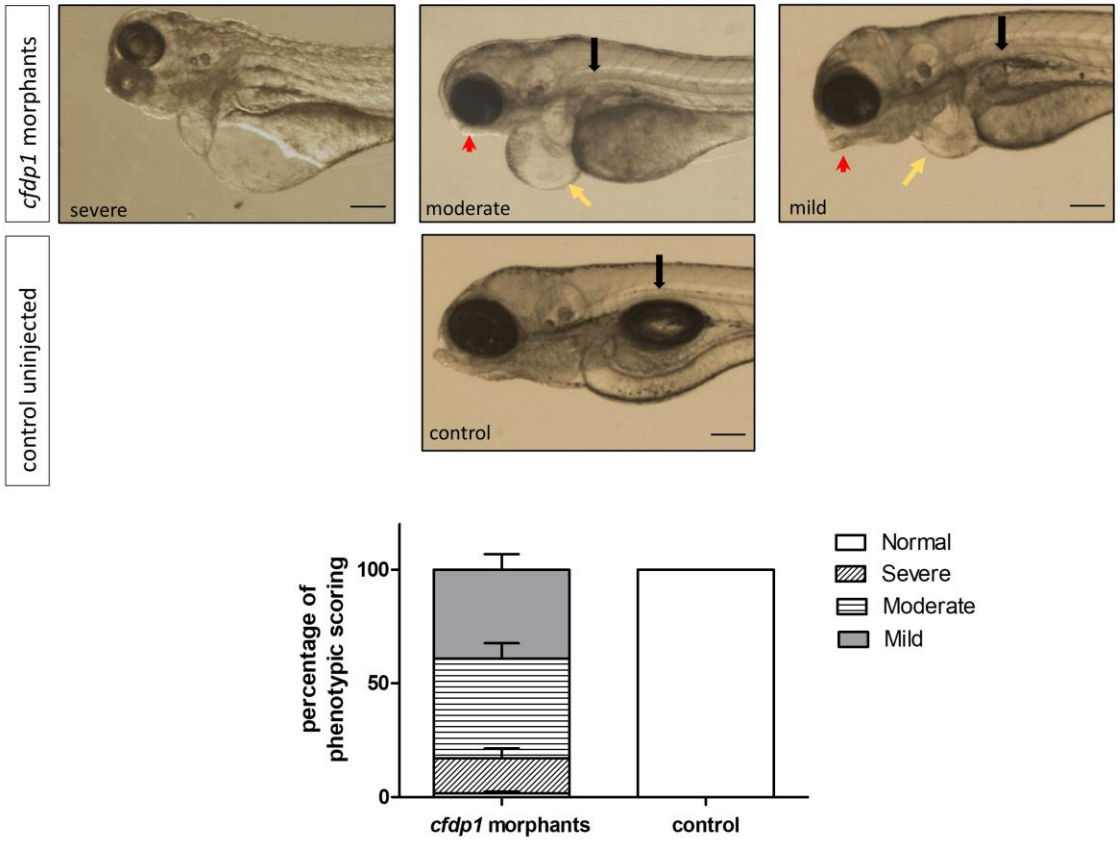

Figure 23: Silencing of *cfdp1* expression via morpholino microinjections. Stereoscopic images of representative 5dpf *cfdp1*-MO injected and uninjected control embryos. Quantification of phenotypic scoring via GraphPad Prism. Black arrows point swim bladder, yellow arrows point pericardiac oedema, red arrows point mouth opening position. Scale bar 150 µm.

Next, based on the importance of Notch and Wnt signaling pathways during development, morphogenesis and function of the embryonic heart, we investigated whether these major regulator pathways are affected in *cfdp1* morphant embryos. First, we utilized the transgenic lines: Tg(*myl7:GFP*) to visualize myocardial cells and Tg(*Tp1:mCherry*) which indicate Notch-activated cells as the expression of *mCherry* is driven by the Notch-responsive element *Tp1*. It is known that *notch1b* is initially expressed throughout the endocardium of the heart and then becomes restricted at the valve-forming region and more specifically at the luminal endocardial cells of immature valve leaflets (Walsh and Stainier, 2001; Pestel *et al.*, 2016). Therefore, we mated individual fish of the aforementioned reporter lines and performed *cfdp1*-MO injections at one-cell stage offspring embryos in order to monitor the activity of Notch signaling in the zebrafish heart. Our results showed that Notch activation is not affected in *cfdp1* morphants compared to control siblings at 72 hpf and the expression of the Notch reporter is found at the ventricular endocardial cells.

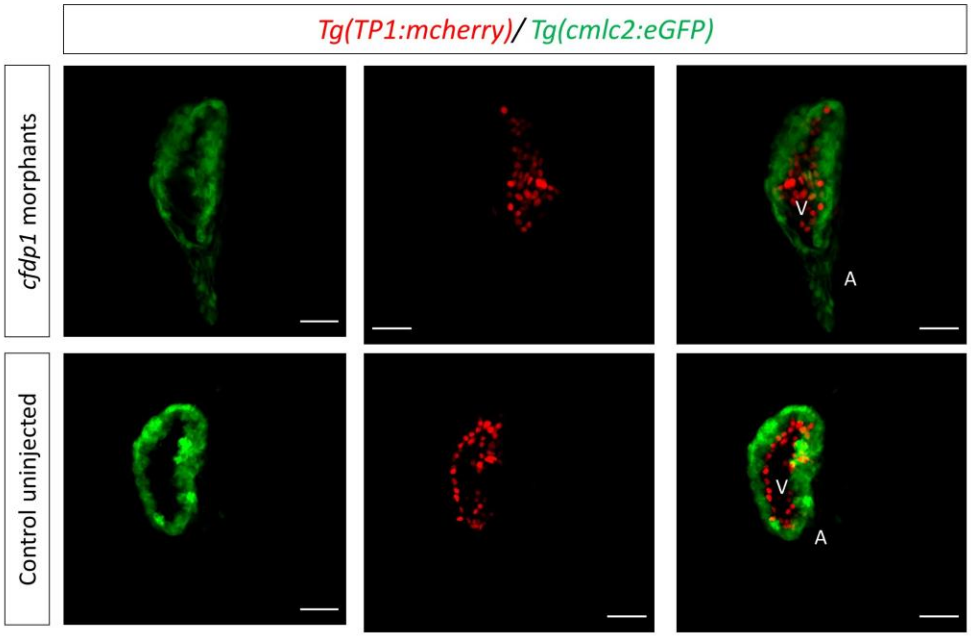

Figure 24: Notch signaling remains unaffected in *cfdp1* morphants compared to the uninjected sibling controls. Max projection of z-stack confocal images of 3dpf *cfdp1*-MO embryos. Ventricular cardiomyocytes are labeled with green (Tg(*myl7:GFP*)) and Notch-activated cells are labeled with red (Tg(*Tp1:mCherry*)). Scale bar 150 μm

Next, we investigated the Wnt/β-catenin signaling activity, another major pathway that facilitates heart morphogenesis and cellular behaviors during cardiac and valve development. It was previously shown that Notch and Wnt have different activity patterns since Wnt activity is primary located at the abluminal cells of the valves possibly mediating Epithelial-to-Mesenchymal Transition (EMT) of endocardial cells by increasing cell invasion during valve formation (Pestel *et al.*, 2016). In order to study the Wnt/β-catenin signaling in *cfdp1* morphants, we mated the following reporter zebrafish lines: Tg(*fli1:EGFP*) (enhanced *GFP* expression under the endothelial specific promoter *fli1*) with Tg(7x*TCF-Xla.Siam:nlsmCherry*) and injected *cfdp1*-MO at one-cell stage offspring embryos. Interestingly, in contrast to the Notch reporter data, we observed a significant disturbance of Wnt activity in *cfdp1* morphants as they appear to have from reduced-to-complete absent signal of Wnt reporter in the region of the heart (whereas reporter signal remains unaffected at the rest of the embryo). Collectively, these findings show that *cfdp1* silencing affects Wnt/β-catenin but not Notch signaling indicating that *cfdp1* plays different role in these two sets of cells and it might mediate in the activity of Wnt pathway.

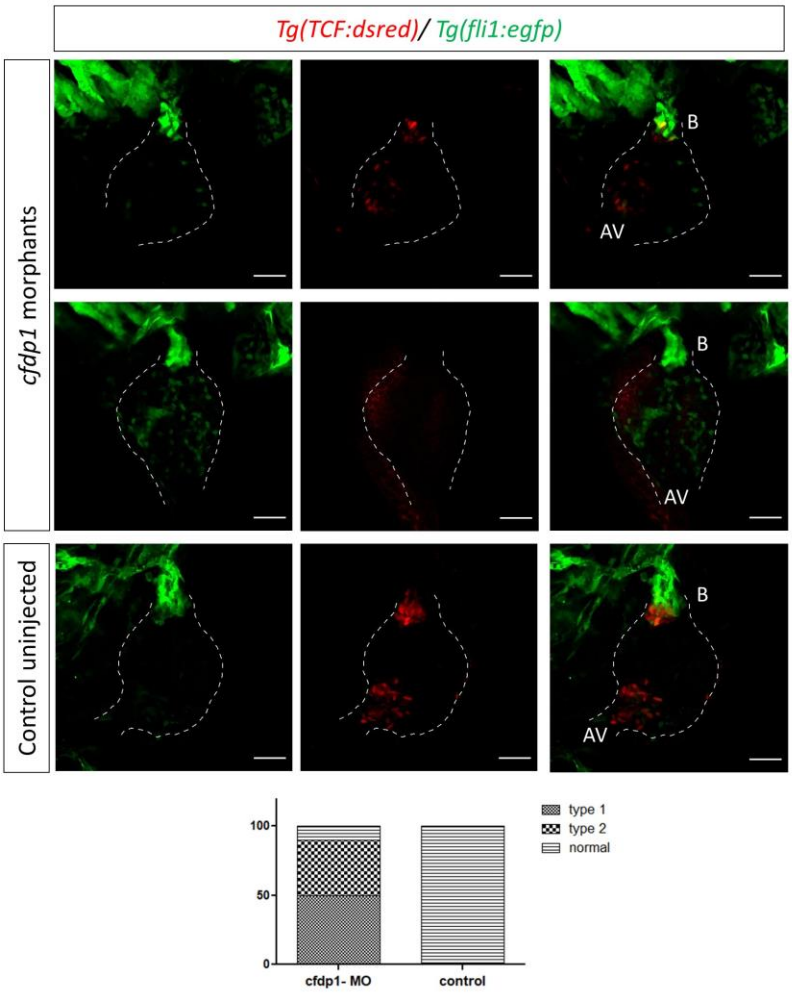

Figure 25: Wnt/β-catenin activity is diminished in *cfdp1* morphants compared to the uninjected sibling controls. Max projection of z-stack confocal images of 3dpf *cfdp1*-MO embryos. Endothelial cells are labeled with green (Tg(*fli1:EGFP*)) and Wnt-activated cells are labeled with red (Tg(7x*TCF-Xla.Siam:nlsmCherry*)). Lower: percentage of phenotypic scoring. AV, atrioventricular valve. B, bulbus arteriosus. Scale bar 150 µm

3.1.1.3 Generation of zebrafish *cfdp1* mutant line

After the *in vivo* characterization of *cfdp1* morphants that shed light to the role of *cfdp1* in the developing heart of zebrafish embryos which was previously unknown, we aimed to generate knock-out *cfdp1* mutant line in order to analyze in deep the effect of *cfdp1* abrogation

in early cardiac development. Due to phenotypic discrepancies between morphants and mutants which have been widely reported (Rossi *et al.*, 2015), the study on a stable genetic loss during embryonic development is indispensable for deeper understanding of *cfdp1* function.

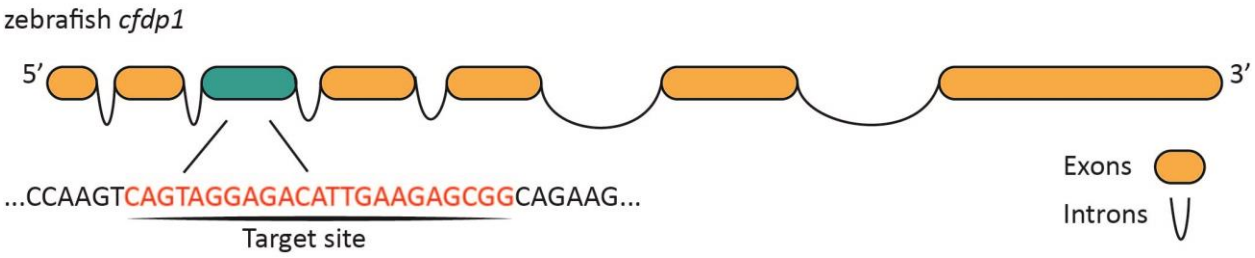

Figure 26: Schematic representation of zebrafish *cfdp1* gene. For generation of CRISPR/Cas9-mediated mutant line, a target site in exon 3 was selected.

Zebrafish *cfdp1* gene is located at chromosome 18 and consists of 7 exons which encode for a protein of 312 aa. In order to generate a mutation within the gene, we designed *cfdp1* guide RNAs (gRNAs) for CRISPR-Cas9-induced mutagenesis to target specific location according to published instructions (Jao *et al.*, 2013)(Jao, Wente and Chen, 2013). To successfully design gRNAs, we utilized the online tool CHOPCHOP (https://chopchop.cbu.uib.no/) and we targeted the exon three as it was at the highest ranking and efficiency rate. The mixture of *cfdp1* gRNA and Cas9 mRNA was then injected at one-cell stage embryos of Tg(*myl7:EGFP*) line and the efficiency of the induced mutation was verified by Sanger sequencing of the flanking region around the target site of the injected embryos. Specifically, at 24 hpf a pool of injected embryos was collected, DNA was extracted and a 350 bp fragment across the target site was PCR amplified and the activity of guide RNA (and therefore the induction efficiency of somatic mutation) was assessed via DNA sequencing. Following, F0 fish were raised until adulthood when they were crossed with wild-type individuals to identify the founders and confirm that the induced mutation is germline transmitted.

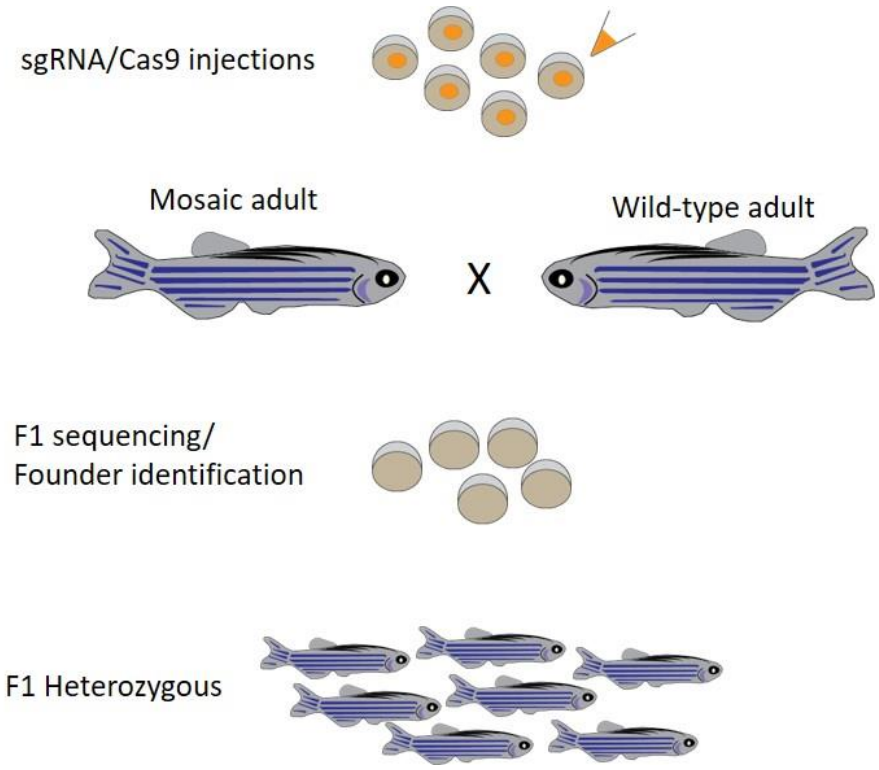

Figure 27: Schematic representation of CRISPR/Cas9-mediated zebrafish line. The injection mix of gRNA /Cas9 in injected at the one-cell stage embryos. The crispants (F0 injected) grow until adulthood and are crossed with wild-type adults. The F1 generation is being genotyped in order to identify possible Founders of the line. After the identification, the corresponding F1 heterozygous generation in kept for further analysis.

A zebrafish line of F1 carriers was recovered and the responsible mutated allele was identified to carry a deletion of five nucleotides that caused a frameshift leading to an introduction of premature stop codon and as a result to the production of a truncated protein. More specifically, the deletion of AAGA before the PAM sequence of target site is predicted to result in a truncated product of 114aa which carries 107 aa of the wild-type *cfdp1* protein and seven new aa insertions before harboring a premature stop codon. Here, we mention that the highly conserved BCNT domain that resides at the C-terminal domain (exon six and exon seven) is also absent in the resulting truncated product.

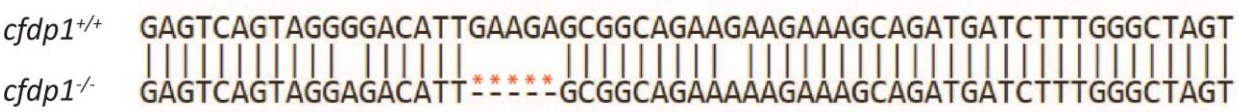

Figure 28: Identification of *cfdp1* mutant allele. Nucleotide alignment between *cfdp1* mutant and *cfdp1* wild-type sequence. A 5bp deletion in *cfdp1* mutant is detected.

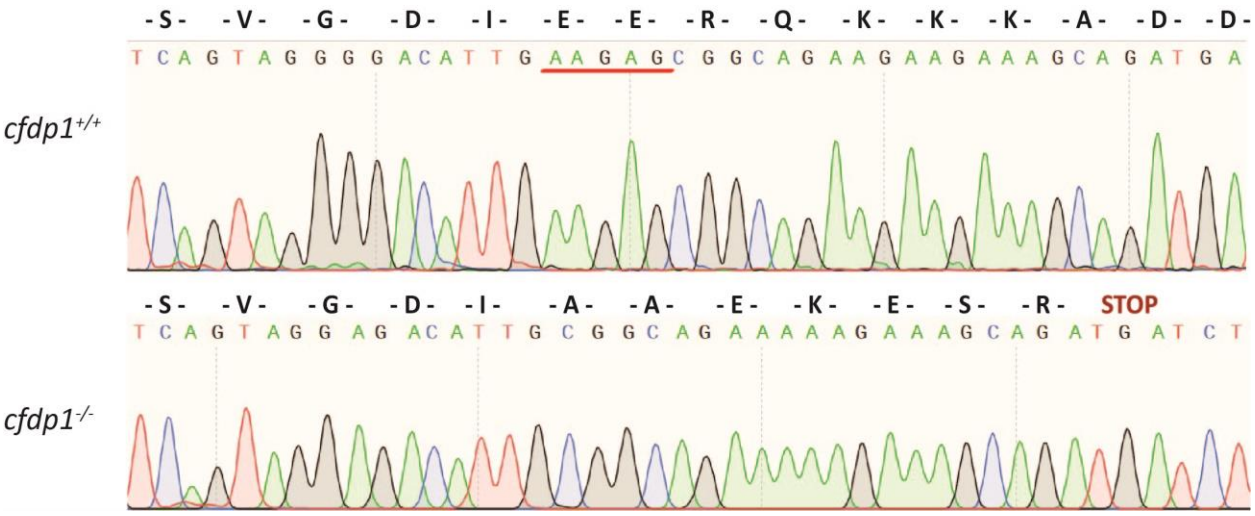

Figure 29: Identification of *cfdp1* mutant allele. Chromatogram of sanger sequencing of *cfdp1* mutant and *cfdp1* wild-type sequence and the corresponding aa they encode. In *cfdp1* mutant, at the point of DNA break, there is an insertion of seven novels aa and an early stop codon.

Additionally, the deletion of mutant allele led to the loss of the unique *SapI* cutting site in the surrounding area of the target site which was a verification of *cfdp1* genotyping after diagnostic digestion of extracted DNA samples of *cfdp1* siblings.

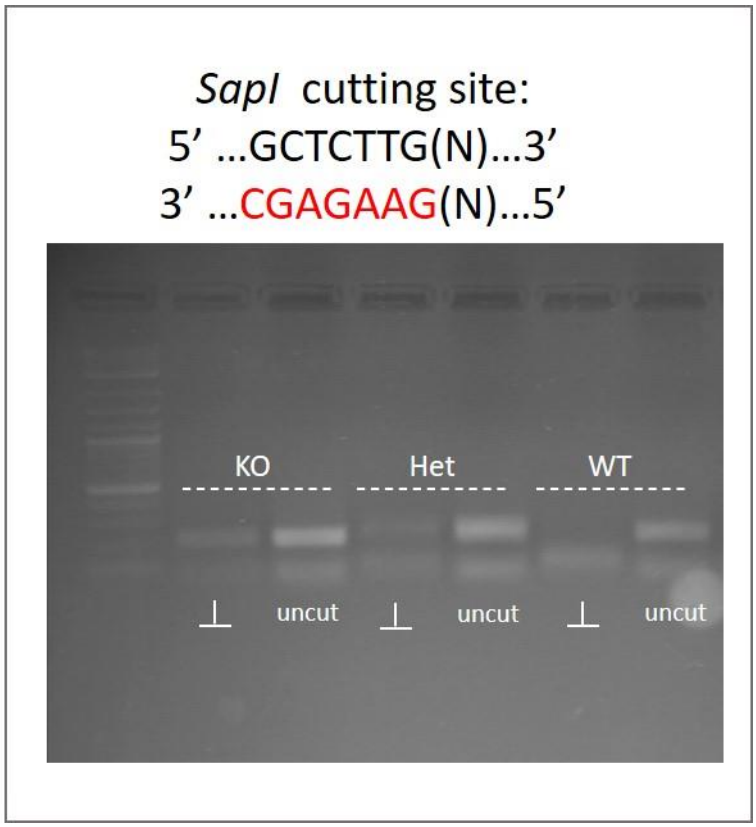

Figure 30: Diagnostic test after digestion of samples with *SapI* restriction enzyme. KO, knockout, Het, heterozygous, WT, wild-type.

3.1.1.4 Zebrafish *cfdp1* mutants show impaired cardiac performance

Following the generation of *cfdp1* mutant line, we examined the phenotype of homozygous individuals. Intriguing, the fully knockout larvae did not reach adulthood and survived up to 10-15 dpf, whereas only adult heterozygous and wild-type siblings were viable and fertile. Thus, we proceeded to study the *cfdp1* role during development and early heart morphogenesis and function. Sibling *cfdp1* embryos did not develop phenotypic cardiac morphogenic malformations but when monitored at 5 dpf, we detected that a 27,8% of embryos suffered from cardiac arrhythmias, while the rest developed normally (N=3, n=141). We, then carefully selected the individuals that have manifested the observed heart

dysfunction and sequenced the samples in order to identify their genotype. Interesting, we discovered that not only homozygous *cfdp1*$^{\Delta/\Delta}$ but also a small portion of heterozygous *cfdp1*$^{\Delta/+}$ siblings developed the observed heart dysfunction, while homozygous *cfdp1*$^{+/+}$ (wild-type siblings) and also heterozygous *cfdp1*$^{\Delta/+}$ genotyped group were corresponding to the embryos without cardiac abnormalities. These findings highlight the importance of *cfdp1* to the proper heart function since null mutation arrests development and even the haplo-insufficient condition provokes specific pathophysiology at an extend that might be dependent on the number of mutated copies. In order to distinguish the homozygous *cfdp1*$^{\Delta/\Delta}$ from the heterozygous individuals that are mimicking the severe phenotype of null mutants, we sequenced retrospectively the sibling embryos (Fin Clipping) and proceeded further with the analysis (anterior embryo) based on the genotyping.

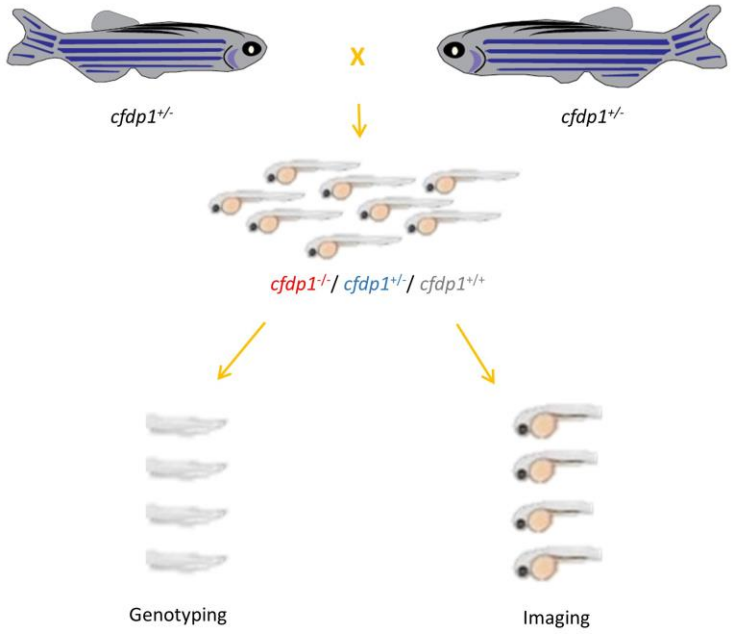

Figure 31: Schematic representation of genotyping the pool of embryos. After a cross of heterozygous *cfdp1*$^{+/-}$ fish, the offspring consist of a pool of three genotypes: *cfdp1*$^{-/-,}$ *cfdp1*$^{+/-,}$ *cfdp1*$^{+/+}$. For the identification of the corresponding genotype, we label the single embryos and keep a part of fin tail for DNA extraction, while storing the rest of the embryo at 4 ˚C until further use.

Following, in order to verify the production of a non-functional protein product of the mutated *cfdp1* allele, we performed *cfdp1*-MO injections in one-cell stage embryos from F2 *cfdp1*$^{\Delta/+}$ adult individuals in-cross. Data showed that 22,3% of injected embryos developed arrhythmic hearts, 42,1% exhibited moderated phenotype with pericardial oedema, reduced size of head/eyes, malformations of mouth opening and flat or non-fully inflated swim bladder and 7,2% were scored as severe phenotype with gross abnormalities (N=4, n= 152). Therefore, the percentage of *cfdp1*-MO injected *cfdp1* sibling embryos that develop arrhythmic hearts is slightly reduced compared to the corresponding percentage observed to *cfdp1* siblings, while the appearance of moderate and severe phenotype scoring in *cfdp1*-MO injected *cfdp1* siblings is in accordance with the corresponding observed phenotypes in *cfdp1*-MO injected wild-type embryos.

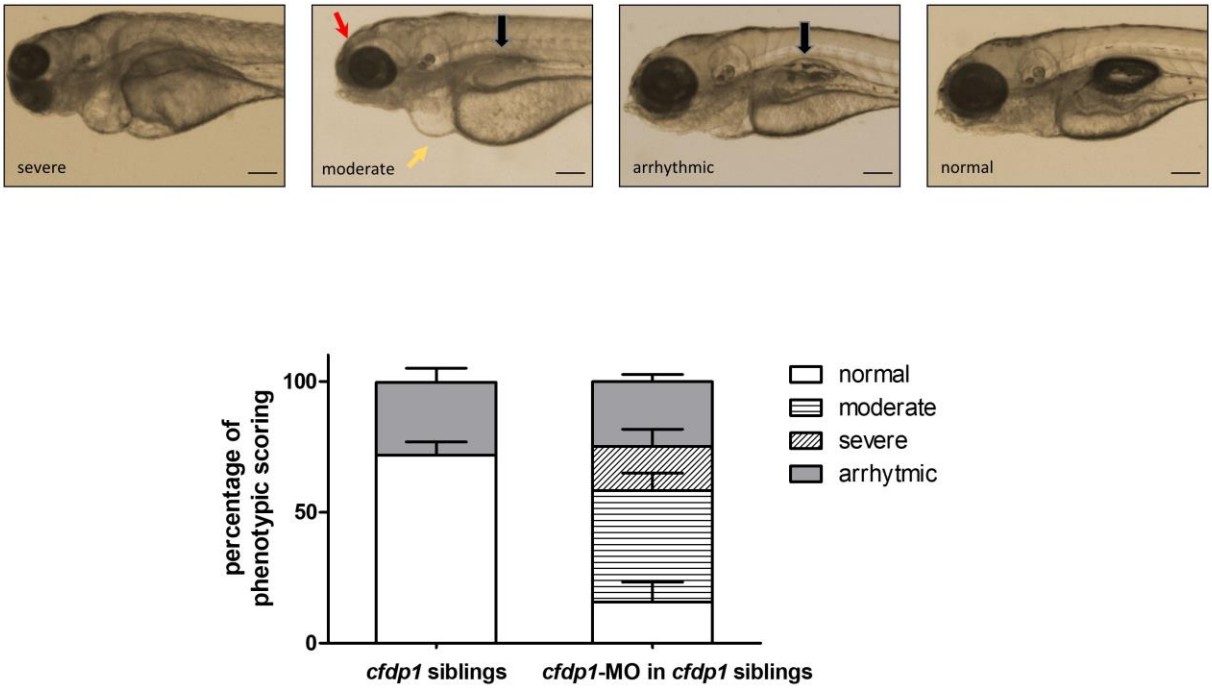

Figure 32: *cfdp1*-MO injections in siblings embryos derived from cross between heterozygous *cfdp1* adult fish. Black arrows point swim bladder, yellow arrows point pericardiac oedema, red arrows point mouth opening position. Lower: Quantification of phenotype scoring of *cfdp1* siblings (pool of all three genotypes: $cfdp1^{-/-}$, $cfdp1^{+/-}$, $cfdp1^{+/+}$) and *cfdp1*-MO injected *cfdp1* sibling embryos. Scale bar 150 µm.

In order to elucidate the functional characterization of homozygous $cfdp1^{\Delta/\Delta}$ individuals , we exclusively focused on the larvae stage and continued by monitoring and quantifying heart features through high-speed video imaging of single individuals (a method that was previously described by Hoage et al.,2012) (Hoage, T.; Ding, Y.; Xu, 2012). Since, among the sibling group of embryos developing cardiac arrhythmias, homozygous $cfdp1^{\Delta/\Delta}$ and heterozygous $cfdp1^{\Delta/+}$ were phenotypically inconspicuous, we recorded videos of all F3 *cfdp1* siblings at 5 dpf

acquiring brightfield and fluorescent images due to the fact that *cfdp1* mutant line was generated utilizing Tg(*myl7:EGFP*) reporter line and carries *myl7*-driven GFP expression for cardiomyocytes visualization. Embryos were then sacrificed and retrospectively analyzed after identification of genotype via DNA sequencing of single larvae. Remarkably, *cfdp1*$^{\Delta/\Delta}$ showed significantly reduced end-diastolic volume and stroke volume as well as cardiac output and ejection fraction, compared to wild-type *cfdp1*$^{+/+}$ siblings. This strongly demonstrates that *cfdp1* abrogation inhibits proper ventricular function and stands as a strong effector in embryonic cardiac physiology.

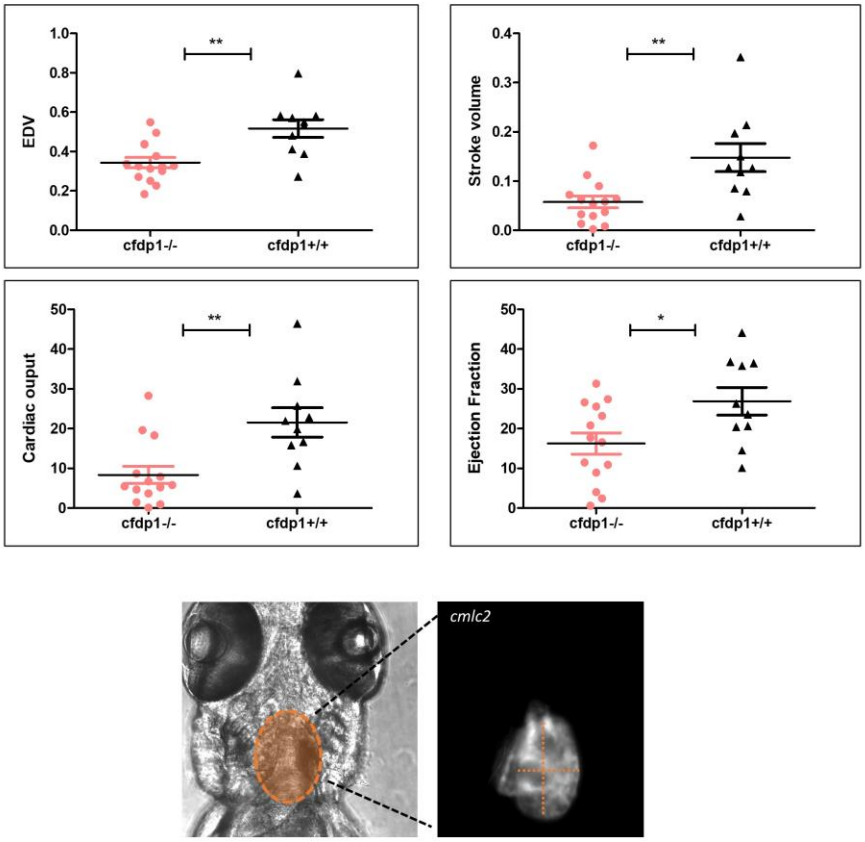

Figure 33: Defective cardiac performance of *cfdp1*$^{-/-}$ embryos compared to their siblings *cfdp1*$^{+/+}$ 5dpf based on ventricular measurements after recording heart rate utilizing the Tg(*myl7:EGFP*) background they carry.

3.1.1.5 Zebrafish *cfdp1* heterozygous develop variation in phenotype at embryonic stage

Due to the phenotypic heterogeneity in the group of heterozygous *cfdp1*$^{\Delta/+}$, we initially examined whether this is result of considerable different levels of *cfdp1* expression within the corresponding genotype group. For this, we performed whole mount ISH with *cfdp1* RNA probe in a group of F3 *cfdp1* siblings 5 dpf which contained a mixed of genotypes. Following, images of all ISH-stained embryos were captured and the expression levels of *cfdp1* were quantified via measuring ISH-staining pixel intensity that was analyzed using Fiji software (Dobrzycki, Krecsmarik and Monteiro, 2020). This method represents an unbiased way of quantification of expression without prior knowledge of genotype. Therefore, after imaging, embryos were labelled and their genomic DNA was extracted and sequenced in order to retrospectively correlate their genotype to the quantified *cfdp1* expression levels. As expected, the heterozygous *cfdp1*$^{\Delta/+}$ showed a variation range of *cfdp1* expression between low and middle levels of intensity which could explain the demonstration of the corresponding phenotypic variation within this genotype group.

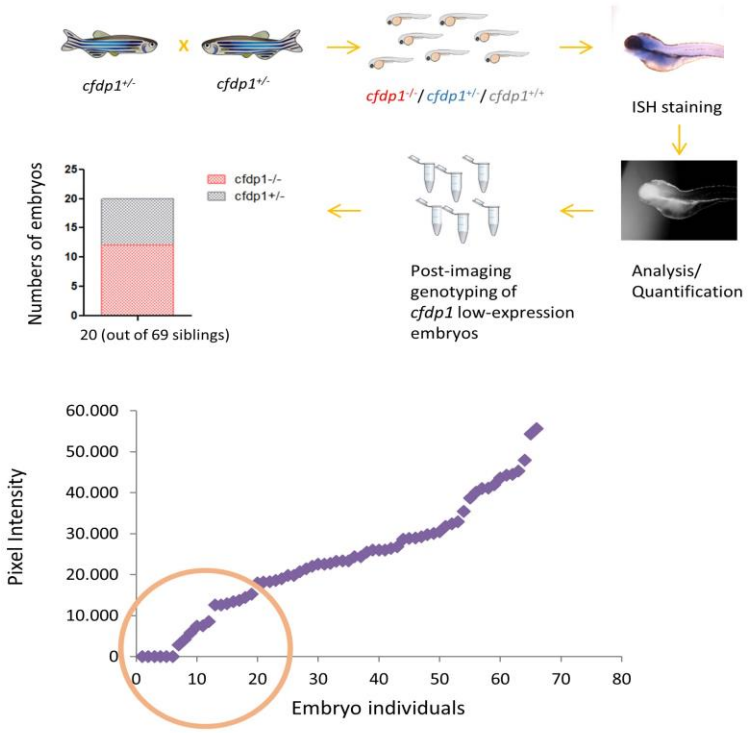

Figure 33: Expression of *cfdp1* in *cfdp1* siblings (pool of three genotypes: *cfdp1*$^{-/-}$, *cfdp1*$^{+/-}$, *cfdp1*$^{+/+}$). After performing in situ hybridization using cfdp1 RNA probe in cfdp1 siblings at 5dpf, we labeled the embryos and quantified the ISH signal intensity. The low- and no- ISH signal of *cfdp1* were genotyped and it was confirmed that they corresponded to *cfdp1*$^{-/-}$ and *cfdp1*$^{+/-}$ embryos.

Since, some heterozygous *cfdp1*$^{\Delta/+}$ reach adulthood (heterozygous escapers), we then examine the structure of the heart of adult *cfdp1*$^{\Delta/+}$ compared to age-matched *cfdp1*$^{+/+}$ individuals. Here, 7 months old adult fish were sacrificed and hearts were removed, sectioned and stained with Hematoxylin and Eosin for nuclear and ECM/cytoplasm staining, respectively. For accurate assessment, images of all heart sections were captured and analysis was performed on sections revealing the cardiac valves and the largest ventricular area. Interesting,

we observed that heterozygous *cfdp1*$^{\Delta/+}$ showed dilated ventricle, with thinner compact myocardium and sparse trabecular myocardium, with respect to wild-type control adult fish. Overall, these findings show that the respective phenotypic variability of heterozygous is reflected to the levels of *cfdp1* expression and even so, the individuals that reach adulthood develop defects in heart morphology.

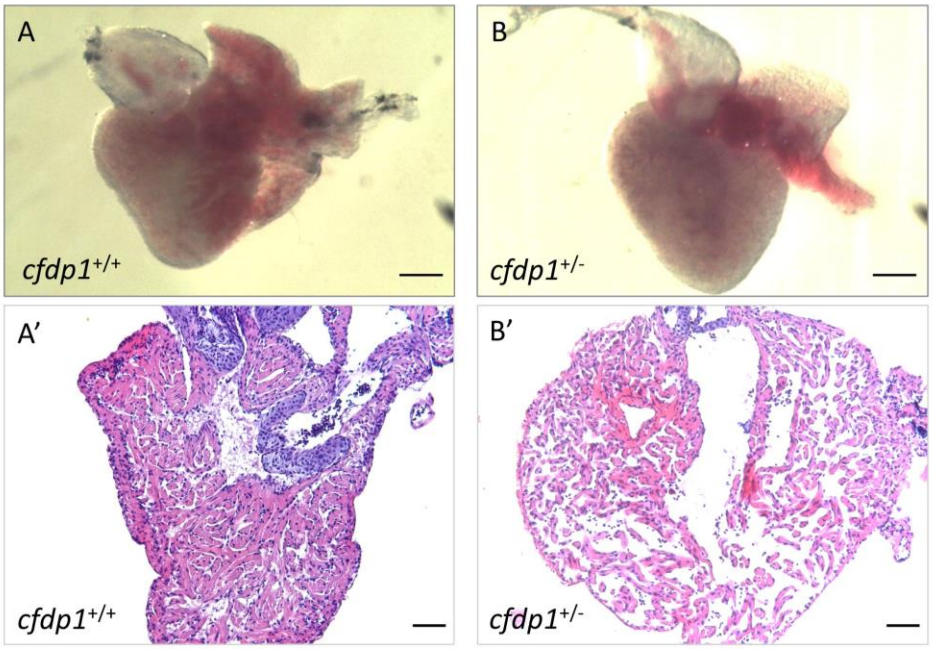

Figure 35: Study of adult heart of *cfdp1* heterozygous and wild type sibling fish. Upper: Stereoscopic image capturing of extracted heart before fixation. Lower: H&E staining of 5μm paraffin embedded cardiac slices. Scale bar (A, B) 200μm. Scale bar (A', B') 50μm.

3.1.1.6 Zebrafish *cfdp1* mutants appear to downregulate Wnt pathway but Notch signaling remains unaffected

After the findings derived from the knockdown experiments that demonstrated a severe disturbance of Wnt pathway, while the expression pattern of Notch signaling was not altered,

we continued by investigating whether that could also be confirmed at the *cfdp1* mutant embryos. For this purpose, we first mated adult heterozygous *cfdp1*$^{\Delta/+}$ (generated in Tg(*myl7:EGFP*) reporter line) with Tg(7x*TCF-Xla.Siam:nlsmCherry*) individuals and then raised the double positive egfp^{+}/mCherry^{+} , *cfdp1*$^{\Delta/+}$ offspring (for cardiomyocytes and *TCF*-activated cells visualization, respectively). Following, 120 hpf siblings from an in-cross of adult *cfdp1*$^{\Delta/+}$/Tg(*myl7:EGFP*)/Tg(7x*TCF-Xla.Siam:nlsmCherry*) were screened under fluorescent microscope and double positive egfp^{+}/mCherry^{+} larvae were genotyped (DNA samples derived from fin tail tissue) while the anterior part of the embryos was further proceeded and imaged after the identification of the corresponding phenotype (figure 35). As illustrated at the figure 36, maximum projection of z-stack imaging reveals that Wnt pathway is significantly downregulated in mutant *cfdp1*$^{\Delta/\Delta}$ compared to their wild-type *cfdp1*$^{+/+}$ siblings, which is appropriately in line with the observed Wnt disruption in *cfdp1* morphants.

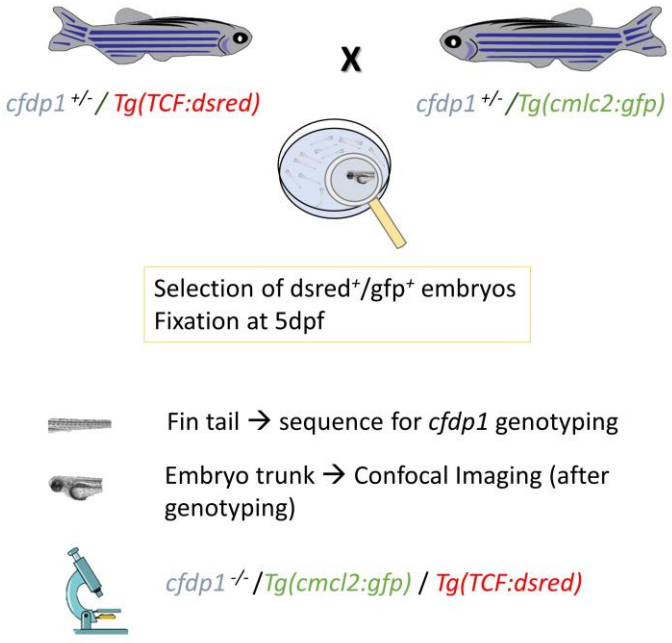

Figure 36: Schematic representation of genotyping strategy before imaging. Adult heterozygous fish *cfdp1*$^{\Delta/+}$/Tg(*myl7:EGFP*)/Tg(7x*TCF-Xla.Siam:nlsmCherry*) are set up for mating. The 120 hpf offspring are being selected under the fluorescent microscope and double egfp^{+}/mCherry^{+} are selected. After proper labeling, the tip of the fin tail is cut for DNA sanger sequencing and genotyping, while the rest of the trunk embryo is kept at 4˚C. Embryos with the same genotype are being pooled and processed for further analysis.

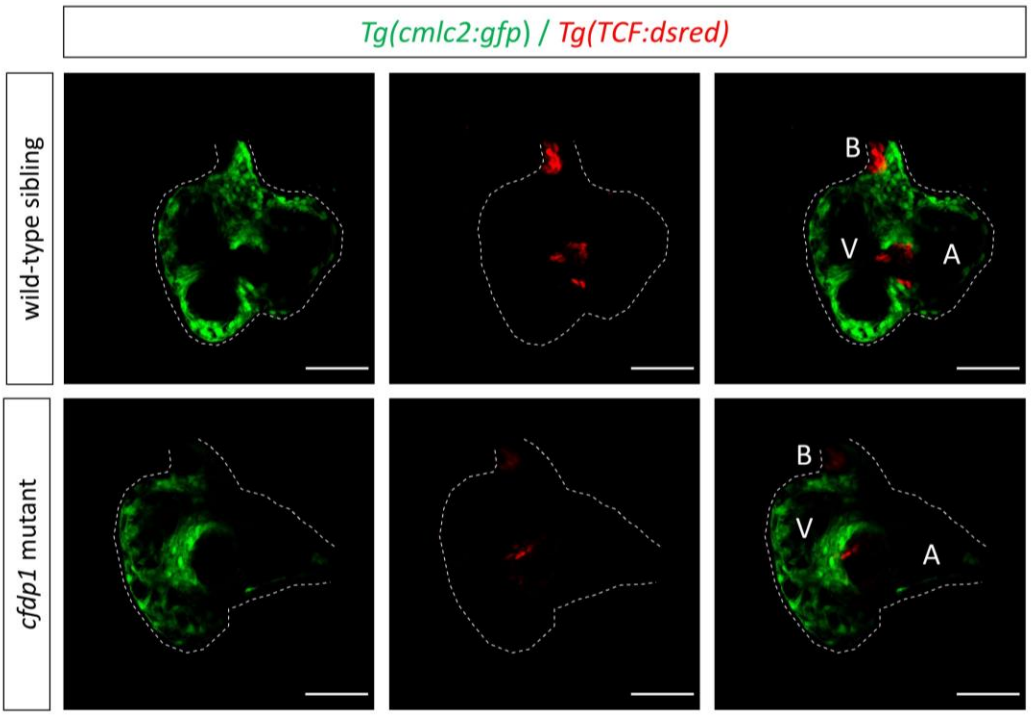

Figure 37: canonical Wnt/β-catenin signaling impairment upon *cfdp1* deletion. Confocal images of 5dpf *cfdp1* mutant and wild-type siblings expressing *Tg(Tcf:dsred)* in Wnt-activated cells and *Tg(cmlc2:eGFP)* in all cardiomyocytes. A:atrium, V: ventricle, B: bulbus arteriosus, Scale bar: 50μm.

To this effect, we tested whether Notch signaling and valve formation are unaffected after *cfdp1* loss, with respect to the corresponding findings in *cfdp1* morphants. Hence, we followed the same strategy as before and we mated adult heterozygous *cfdp1*$^{\Delta/+}$ with

Tg(*Tp1:mCherry*) individuals and generated a zebrafish *cfdp1*$^{\Delta/+}$/Tg(*myl7:EGFP*)/Tg(*Tp1:mCherry*) line (figure 37). Remarkably, analogous to *cfdp1* morphants results, Notch activation is restricted to the valve forming cells at 120 hpf and expression pattern is not indifferent to the wild-type *cfdp1*$^{+/+}$ siblings suggesting that *cfdp1* is dispensable for valve formation (figure 38). In summary, TCF-positive endocardial cells have lower expression levels while Notch-expressing valves are normally formed indicating that *cfdp1* plays a role in activation of Wnt signaling in atrioventricular endocardium independently of Notch pathway activation. It is not a surprise that endocardial valvular cells have different cellular behaviors and are ruled by different cell signaling pathways (Pestel *et al.*, 2016). Therefore, our data support that Notch and Wnt/β-catenin signaling are influenced by distinct regulators in order to orchestrate cellular and molecular processes for proper cardiac and valvular function and formation and *cfdp1* is for first time demonstrated to be involved in Wnt/β-catenin pathway.

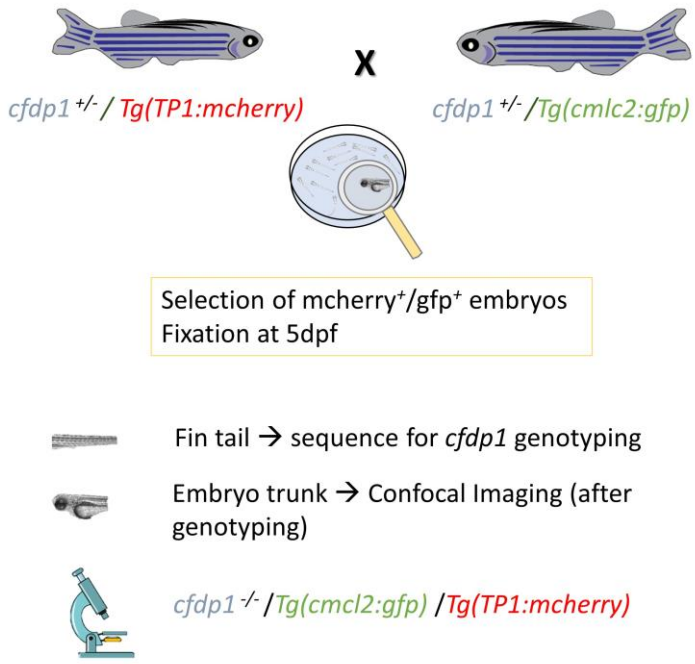

Figure 38: Schematic representation of genotyping strategy before imaging. Adult heterozygous fish *cfdp1*$^{\Delta/+}$/Tg(*myl7:EGFP*)/Tg(*Tp1:mCherry*) are set up for mating. The 120 hpf offspring are

being selected under the fluorescent microscope and double egfp^{+}/mCherry^{+} are selected. After proper labeling, the tip of the fin tail is cut for DNA sanger sequencing and genotyping, while the rest of the trunk embryo is kept at 4˚C. Embryos with the same genotype are being pooled and processed for further analysis.

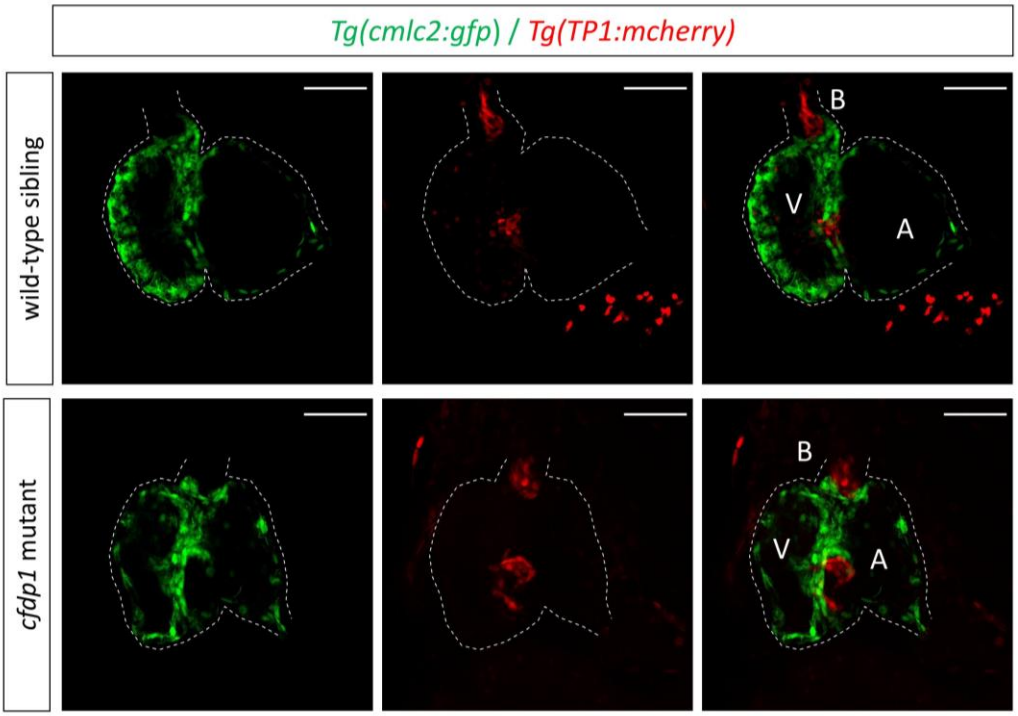

Figure 39: Notch signaling activation upon *cfdp1* abrogation. Confocal images of 5dpf *cfdp1* mutant and wild-type siblings expressing *Tg(TP1:mcherry)* in Notch-activated cells and *Tg(cmlc2:eGFP)* in all cardiomyocytes. A:atrium, V: ventricle, B: bulbus arteriosus, Scale bar: 50μm.

3.1.1.7 Cardiac trabeculation in developing zebrafish ventricle is defective in *cfdp1* mutants

Prior studies have shown that orchestration of cardiac trabeculation is highly significant for the proper function of the heart and the survival of the embryo since defects during the complex morphogenic events occurring at trabeculation lead to embryonic lethality or adult dilated cardiomyopathies (Liu *et al.*, 2010; Rasouli and Stainier, 2017). It has been also shown that zebrafish *erbb2* mutant embryos lack trabeculation but they develop normal valves (Liu *et al.*, 2010). To this end, we examined the levels of cardiac trabeculation in *cfdp1* mutant embryos at 120 hpf when the entire length of luminal side of ventricle has developed extensive trabeculation. Single sibling *cfdp1* embryos were genotyped at 120 hpf and groups of wild-type and mutant embryos were further stained with phalloidin for filamentous actin staining. Interestingly, while *cfdp1* sibling wild-type embryos develop an extensive normal pattern of trabeculation, *cfdp1* mutant embryos exhibit less complex trabeculation. This finding suggests the requirement of *cfdp1* for the proper initiation and formation of trabecular cardiomyocyte layer. As we have already shown, the *cfdp1* mutant hearts do not show signs of valve malformations, so the impairment of ventricle trabeculation doesn't appear to be a secondary effect to a defective valvulogenesis. Taken together, our data show the *cfdp1* role specifically in cardiac trabeculation while it is dispensable for valve formation.

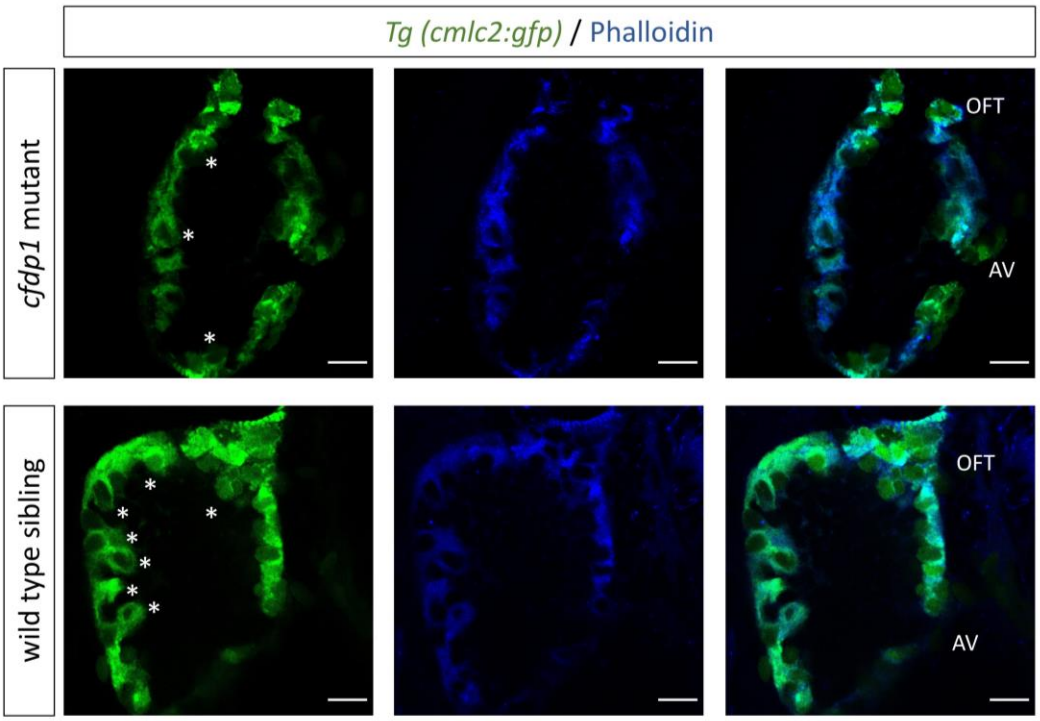

Figure 40: *cfdp1* is required for cardiac trabeculation. Single confocal plane of fluorescent phalloidin staining (actin filaments) in 120 hpf *cfdp1* embryos, expressing *Tg(cmlc2:eGFP)* in all cardiomyocytes. Asterisks: trabeculae cardiomyocytes, AV: atrioventricular, OFT: outflow tract. Scale bar:50µm.

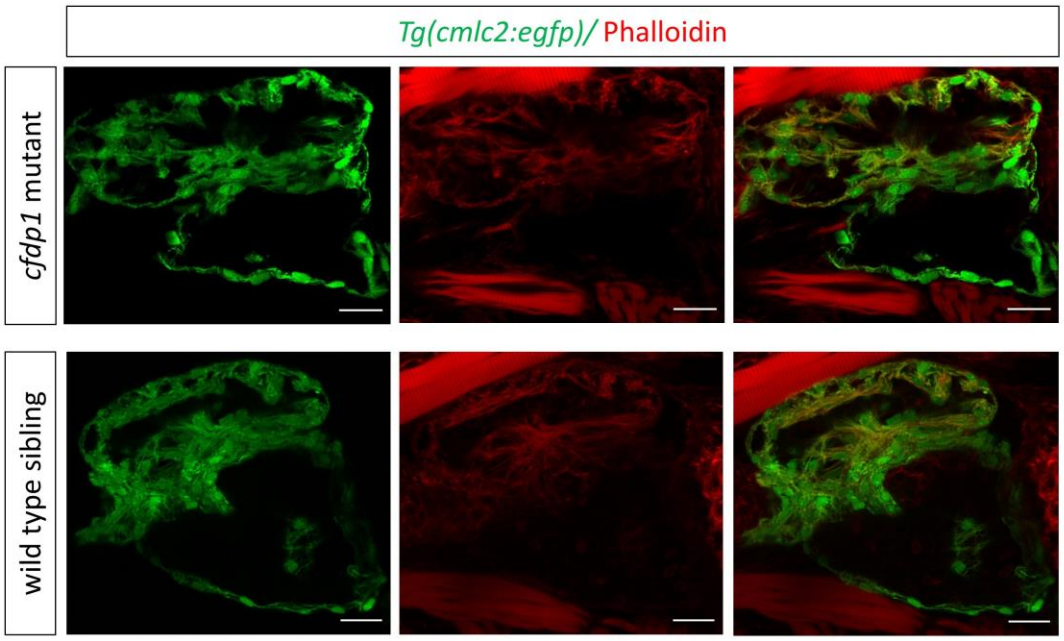

Figure 41: *cfdp1* is required for cardiac trabeculation. Maximum projection of z-stack confocal planes of fluorescent phalloidin staining (actin filaments) in 120 hpf *cfdp1* embryos, expressing *Tg(cmlc2:eGFP)* in all cardiomyocytes., AV: atrioventricular, OFT: outflow tract. Scale bar:50µm.

3.1.1.8 Depletion of *cfdp1* does not affect *islet1*$^{+}$ cells

We have shown that *cfdp1* mutant embryos develop arrhythmic hearts, indicating of a defect in cardiac conduction system. Previous characterization of cardiac pacemaker cells in zebrafish showed that Islet1-expressing cells (*isl1*) hold a pacemaker activity in adult zebrafish heart (Tessadori *et al.*, 2012). Same study showed that *isl1* is also expressed in sinoatrial node (SAN) region of the heart of 48 hpf zebrafish embryos. To investigate whether the arrhythmias observed in *cfdp1* mutant hearts correlate with the *isl1*-expressing cells, we performed whole

mount immunohistochemistry analysis in 120 hpf *cfdp1* mutant and wild-type siblings. Our data show no significant differences in the expression pattern of *isl1* between the two genotyping groups of embryos. Of note, *isl1*$^{+}$ cells at this developmental stage are detected at the region of AV node, as well as the outflow tract of embryonic hearts. We couldn't detect *isl1*$^{+}$ cells at the SAN, probably due to the limited number of *isl1*$^{+}$ cardiomyocytes or the later developmental stage we investigated.

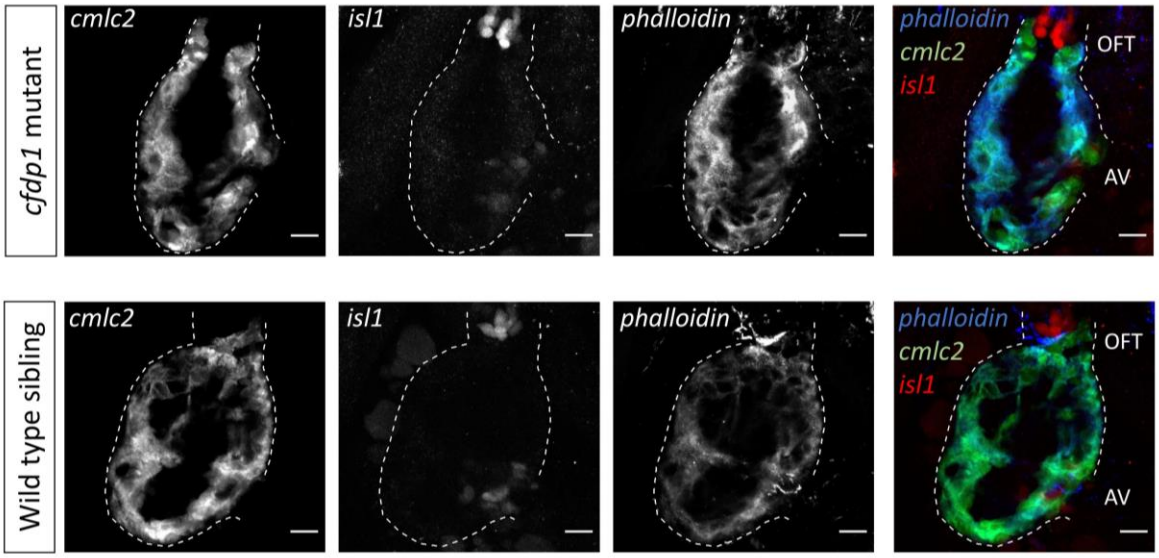

Figure 42: Islet1 expression in embryonic zebrafish heart. Confocal z-stack images of fluorescent antibody staining of Isl1, phalloidin (for actin filaments staining) in 120 hpf *cfdp1* embryos, expressing *Tg(cmlc2:eGFP)* in all cardiomyocytes. AV atrioventricular, OFT outflow tract. Scale bar:15µm.

3.2 Study of *ccdc92* role in zebrafish embryos

A plethora of recent human studies have revealed the implication of *CCDC92* in the manifestation of clinical pathophysiological conditions. Population-based studies, phenome-wide associations, as well as cellular models support the *CCDC92* involvement in cardiovascular disease and pinpoint the importance of unraveling the link with the mechanism of action. Phenome-wide association combining UK Biobank data, mRNA transcripts phenotypes and GWAS results identified the CAD risk variant of *CCDC92* to be associated with the disease trait of waist-hip ratio (Body Mass Index), triglycerides levels (Klarin *et al.*, 2017) and other traits of CAD, such levels of HDL (Khetarpal *et al.*, 2018). All these data so far highlight the role of *CCDC92* but there is only limited number of experimental studies that have investigated the actual function of the gene.

Lotta LA. *et al*., have conducted experimental validation of *Ccdc92* as an effector gene in cellular mouse model (Lotta *et al.*, 2017). They performed knockdown approach by using small interfering RNA (siRNA) against *Ccdc92* in OP9-K mouse adipocyte cell line and showed reduced levels of lipid accumulation in accordance to the association with insulin-raising allele. This analysis is consistent with the implication of *CCDC92* and the impaired adipogenesis and circulating levels of large HDL particles (Chasman *et al.*, 2009). Human primary adipose tissue samples showed effect on visceral fat mass (visceral adipose tissue, VAT) but not on subcutaneous abdominal fat mass (subcutaneous adipose tissue, SAT), suggesting a role in adipose tissue distribution (Neville *et al.*, 2019). Another GWAS study that uncouples adiposity and obesity from their cardiometabolic comorbidities showed a mechanistic role of CCDC92 to the specific trait of adipocyte function and differentiation (Huang *et al.*, 2021).

CCDC92 is a nuclear protein that interacts with other proteins at centriole-ciliary interface (Gupta *et al.*, 2015) and may also be involved in DNA repair (Chaki *et al.*, 2012). Another study have shown that CCDC92 is the substrate of Tau tubulin kinase 2 (TTBK2), which is a key regulator in cilium assembly pathway (Bernatik *et al.*, 2020). Primary cilia are organelles necessary for proper development and homeostasis and play a central role cardiovascular heart disease (Klena, Gibbs and Lo, 2017; Pala *et al.*, 2018). The determinant mechanism through

which CCDC92 functions and influences the exhibition of the aforementioned traits of cardiovascular disease remains to be elucidated.

In this study, we utilize zebrafish (*Danio rerio*) as experimental model organism to investigate deeper the role of the *ccdc92* candidate gene involved in cardiovascular disease and the results are presented at the following section. Since, there are no other *ccdc92* models available, this study constitutes the first experimental evidence derived from a novel *in vivo* model regarding the role of *ccdc92* in embryo development.

3.2.1 Effect of *ccdc92* silencing

3.2.1.1. Identification of *ccdc92* zebrafish orthologue

Firstly, we searched for zebrafish orthologue of the human *CCDC92* gene and we found that in zebrafish genome, there is a clone previously named *zgc:123269* and is registered in many data bases (ZFIN: https://zfin.org/, Ensembl: https://www.ensembl.org/index.html, NCBI: https://www.ncbi.nlm.nih.gov/gene). The zebrafish *ccdc92* contains the coiled-coil domain that characterizes the function and structure of the gene, similar to human *CCDC92* orthologue. In addition, zebrafish *ccdc92* has two domains that are not in human orthologue: a SPEC domain (spectrin repeats found in proteins of cytoskeletal structure; other family members include spectrin, a-actinin and dystrophin) and a DUF2476 domain (domain rich in proline residues which is found in family of proteins with unknown function till today). On the other hand, human *CCDC92* obtains a domain that is not found in zebrafish orthologue and that is APG6 domain (found in proteins that coordinate the formation of autophagosomes in yeasts). Notably, there are no available data regarding the structure, the expression pattern, the tissue-specificity nor the phenotype associated with this gene. It remains an important cardiovascular-involved candidate gene that its function has not been studied and carefully investigated. Thus, we will provide evidence for the phenotypical characterization of its zebrafish *ccdc92* orthologue.

3.2.1.2. Spatiotemporal expression of *ccdc92*

After identifying the *ccdc92* zebrafish orthologue, we investigated whether it is expressed during early organism development. To do so, we extracted total RNA from zebrafish samples at distinct embryonic developmental stages of 5, 24, 48, 72 and 120 hpf. We then reverse transcribed it into cDNA and performed RT-PCR, using oligonucleotide primers designed with high binding specificity in *ccdc92* mRNA sequence. We could confirm that its expression is detected from 24 hpf and becomes apparent up to 120 hpf (final embryonic stage we tested during this experiment). Relative expression levels of the gene were calculated compared to the expression levels of housekeeping gene *b-actin* at the corresponding developmental stages and quantification is represented at the following figure using ImageJ software.

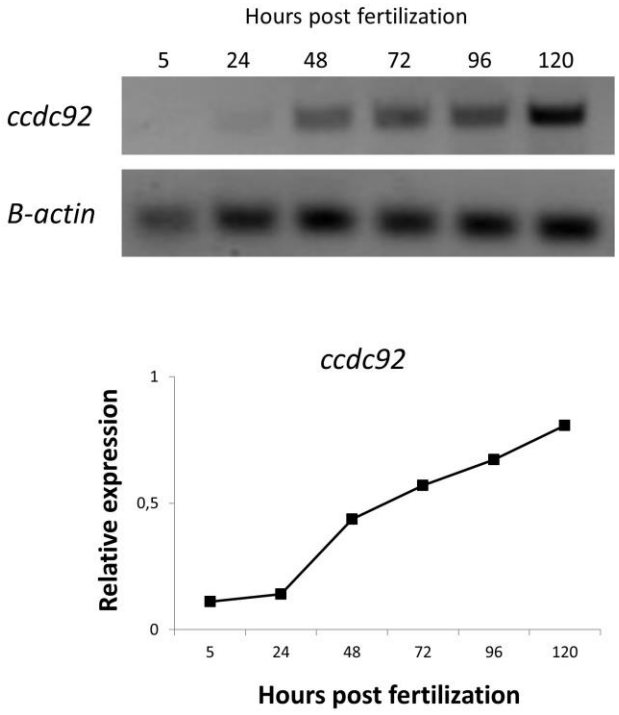

Figure 43: Temporal expression of zebrafish *ccdc92*. Relative expression of the gene during embryonic development compared to *b-actin* housekeeping gene via RT-PCR.

Next, we investigated the expression pattern of *ccdc92* during embryonic development. We performed whole mount *in situ* hybridization using the specific anti-sense RNA probe in order to observe the tissue specificity of *ccdc92* expression in zebrafish embryos at different developmental stages. In accordance to the temporal expression results, we observed relatively low expression levels at the first development stages (up to 48 hpf) but an increase at later stages. Specifically, we monitor ubiquitous expression of *ccdc92* which is being restricted at the region of the head at 120 hpf.

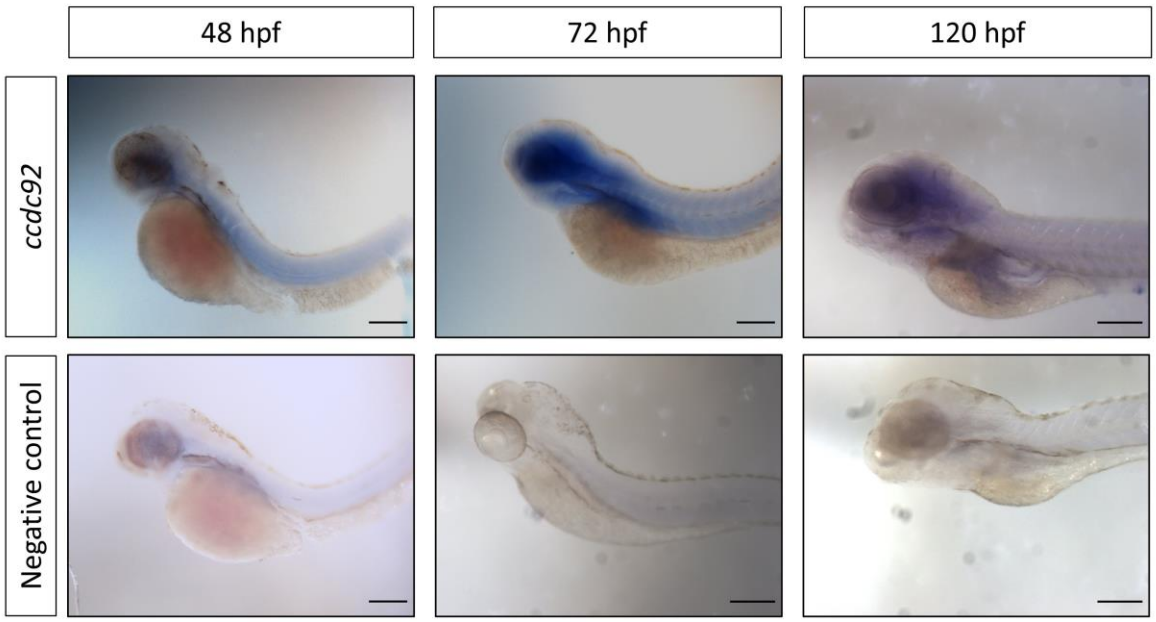

Figure 44: Spatial expression of zebrafish *ccdc92*. Whole mount *in situ* hybridization for monitoring the expression pattern of the gene during embryonic development using *ccdc92* antisense RNA probe (Upper panel) and sense RNA probe as negative control (Lower panel). Scale bars 150 μm.

3.2.1.3. Knockdown approach via morpholino-induced *ccdc92* silencing

In order to investigate the phenotype induced by the depletion of *ccdc92*, we first conducted knockdown *in vivo* experiment in wild-type zebrafish embryos. We designed morpholino oligonucleotide (MO) which blocks the initiation of *ccdc92* translation so as to monitor the phenotype of the injected embryos at the absence of *ccdc92* protein product during development. We prepared the injection mix by adding 2.5 µl antisense MO 1 mM stock solution, 1.5 µl dd H_20 and 1 µl Phenol Red (final MO: 4 ng/nl) and injected 4.6 nl injection mix per embryo at one-cell stage. After, removing the non-successfully injected and non-fertilized eggs, we placed injected and control embryos in egg water at 28^oC, monitored their development and captured representative images under the stereoscope up to 120 hpf. We observed a classification of phenotypes from severe to normal looking embryos. The severe/truncated phenotype represents the 18% of injected embryos which are embryos developmentally stalled and removed from the experiment. Interestingly, 41.6% of injected embryos are categorized as mild and represent embryos that develop pericardial oedema, head oedema and bend body axis, whereas 10,5% exhibit extreme malformation in heart development showing stretched, non-functional embryonic heart which fails to loop and remains at heart tube stage, along with the display of huge pericardial heart oedema (moderate phenotype). The phenotypic observation and scoring suggest an important role of *ccdc92* in the cardiac development of zebrafish embryos and accounts for the first *in vivo* evidence that *ccdc92* affects cardiac morphogenesis and function. Moreover, it displays the fact that deficiency in *ccdc92* provoking cardiac disorders is retained in fish as well.

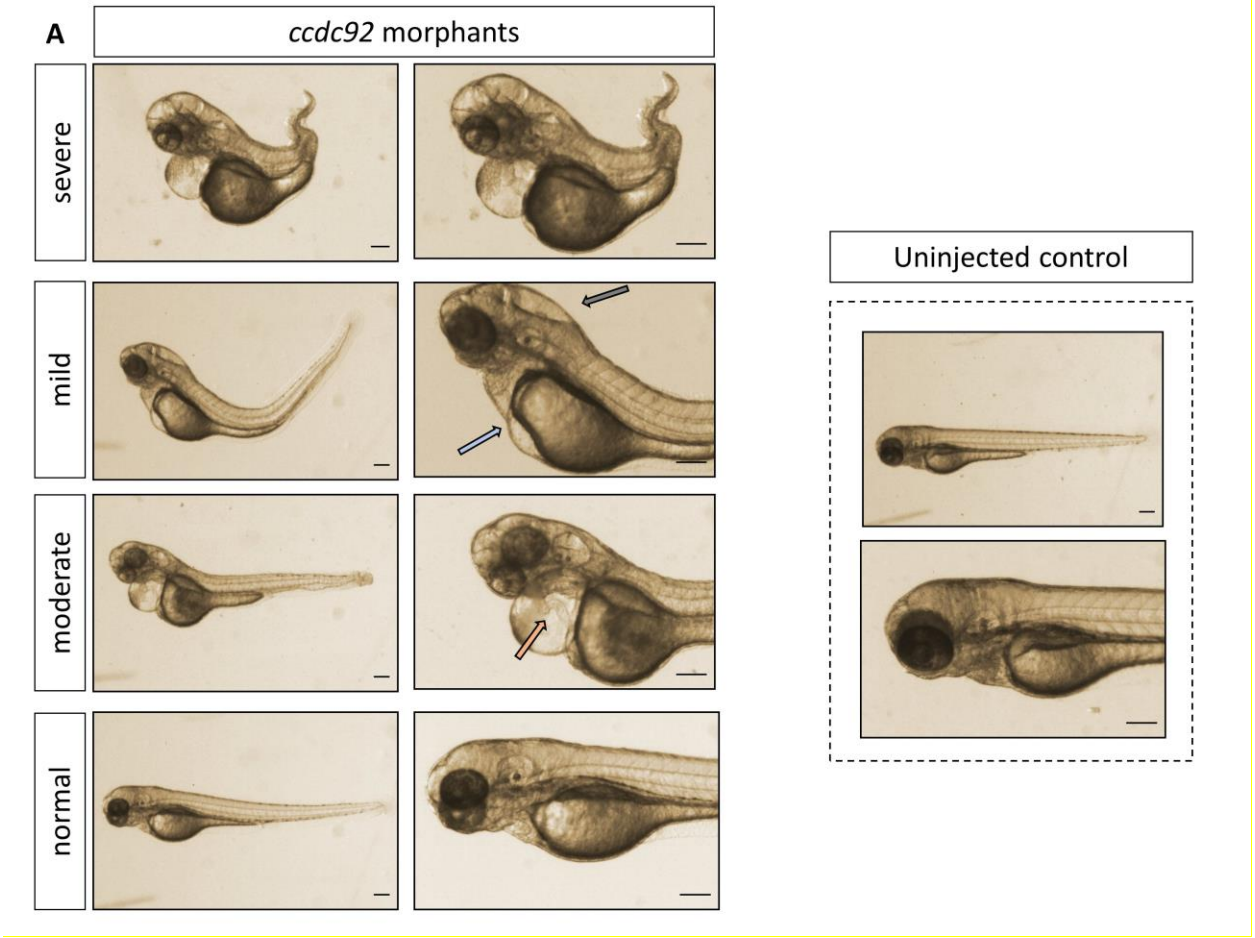
A
ccdc92 morphants
severe
mild
moderate
normal
Uninjected control
B
percentage of phenotypic scoring
100
80
60
40
20
0
ccdc92 morphants
control
normal
severe
moderate
mild

Figure 45: A. Phenotypic representation of 72 hpf *ccdc92* morphants compared to age-matched uninjected zebrafish embryos. Grey arrow: head oedema, Blow arrow: heart oedema, Orange arrow: heart string phenotype. Scale bar 150 μm. B. Quantification of embryonic phenotype scoring in *ccdc92* morphants at 72 hpf. GraphPad Prism Software was used for the design of the corresponding graph.

Following, we aimed to study the effect of *ccdc92* silencing in the embryonic hearts at a cellular level. Therefore, we utilized the zebrafish transgenic line *Tg(cmlc2:eGFP)* in which all cardiomyocytes express green fluorescent protein and we performed *ccdc92* MO-injections in one-cell stage embryos. Following, *ccdc92* morphants and uninjected control embryos were grown up to 72 hpf, monitored and imaged under stereoscope and sacrificed in order to investigate cardiac morphogenesis via confocal imaging. First, we observed that control siblings complete the ventricular rotation around the longitudinal axis of the heart forming an asymmetrical dextral S-shape looping along the Left/Right axis and a mature functioning heart. Interestingly, in *ccdc92* morphants this ventricular D-looping is compromised since they fail to completely bend to the right resulting in a midline positioned heart. Given the morphogenetic complexity of this process, it is important to further interrogate whether *ccdc92* affects directly the heart looping or it is a secondary response to a primary defect in other cellular mechanism in heart or other tissues, during future experiments.

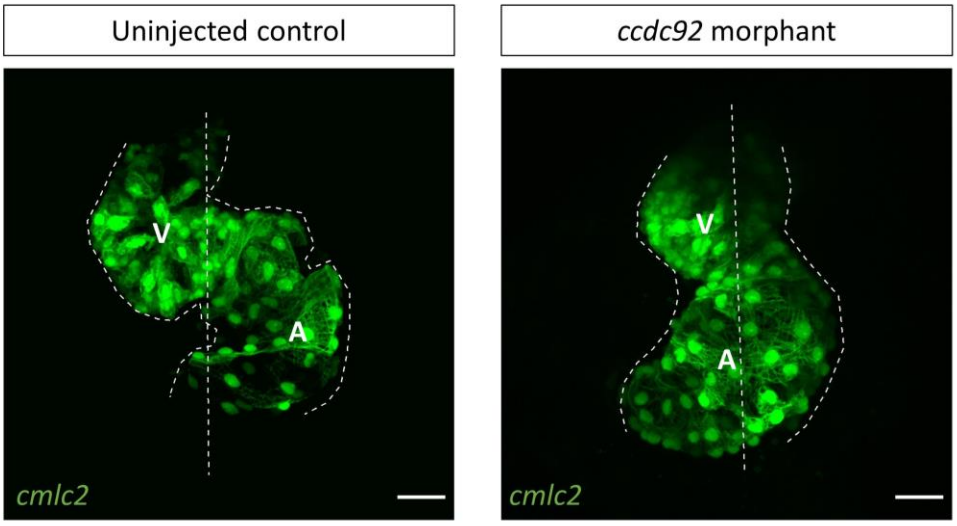

Figure 46: Embryonic hearts of *ccdc92* morphants and control embryos at 72 hpf. Confocal images of embryonic heart presented in maximum projection of z-stack. While uninjected control embryos complete heart looping and form two chambers, *ccdc92* morphants prevent proper looping. A: atrium, V: ventricle. Scale bar 25 µm.

3.2.1.4. Strategy for generation of mutant zebrafish *ccdc92* zebrafish line via CRISPR-Cas9 editing tool

Having highlighted the phenotypic outcome in zebrafish heart lacking a functional *ccdc92* product based on knockdown approach, we then proceeded on generating a genetically stable mutant zebrafish line using CRISPR/Cas9 system as a molecular editing tool. We first designed two target sites in *ccdc92* zebrafish gene based on the online tool CHOPCHOP for selecting specific regions for Crispr/Cas9-directed mutagenesis. We selected target sites into the last exon of the gene (4th) since the previous three are very short and didn't contain 23-noucleotide sequence meeting the strategy requirements (Jao, Wente and Chen, 2013), with no predicted off-target sites and high efficiency rate.

Target site	Exon	Off-targets	Efficiency
GGGAGTGGCAGAAGAAGCGATGG	4	0	0.72
(G)GAGGGGCGTTCCCTCAACACTGG	4	0	0.64

Table 3: Properties of CRISPR/Cas9 selection sites in *ccdc92* for induced mutagenesis

After the *in vitro* transcription of the corresponding gRNAs according to the protocol described earlier, the mixture of each *ccdc92* gRNA along with Cas9 mRNA was injected at one-cell-stage wild-type embryos. Non-successfully injected embryos and non-fertilized were removed. Injected and control embryos were grown in egg water at 28^{o}C and monitored under the stereoscope for phenotypic observation. In order to assess the efficiency of induced mutagenesis, we genotyped the F0 injected embryos at the flanking region around the target site via Sanger sequencing. Specifically, pools of injected embryos were collected at 24 hpf, DNA was isolated, the fragment across the target site was PCR amplified and the activity of guide RNAs (and therefore the induction efficiency of somatic mutation) was assessed via DNA sequencing. Unfortunately, we didn't detect any change in nucleotide sequence of injected embryos from both gRNAs injections. Therefore, due to insufficient genome editing, we couldn't proceed further with the generation of the *ccdc92* mutant line during the conduction of the current research study. Design of new target sites, optimization of editing strategy and performance of corresponding microinjections should be included in future experiments in order to create a zebrafish mutant line to study in deep the function of the *ccdc92* gene.

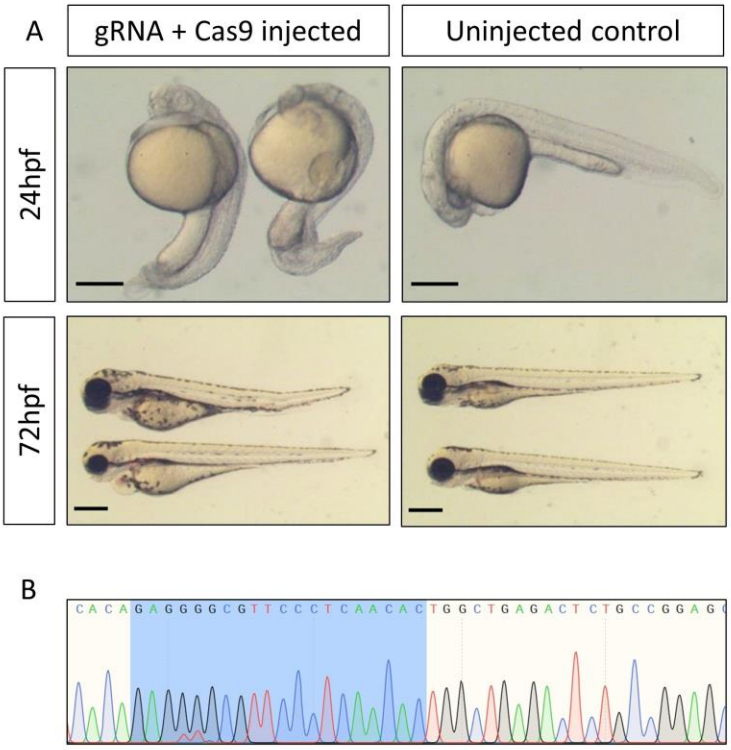

Figure 47: F0 embryos after microinjections with *ccdc92* gRNA/Cas9 injection mix. A. Phenotypic observation of injected and control siblings at 24 hpf (upper) and 72 hpf (lower). B. Representative sequence result of injected embryos that depicts single peak in each nucleotide position without change induction in the wildtype sequence. Scale bar 150 µm.

3.3. The role of T757A in the kinase domain of PRKD2 in cardiovascular development

3.3.1 *s411* zebrafish mutant

The zebrafish *s411* mutant was identified during a large-scale zebrafish ENU-mutagenesis forward genetics screen (Beis D, Bartman T, Jin SW, Scott IC, D'Amico LA, Ober EA, Verkade H and J, Field HA, Wehman A, Baier H, Tallafuss A, Bally-Cuif L, Chen JN, Stainier DY, 2005). *s411* is a recessive mutation that results in embryonic lethality by 120 hpf. *s411* mutants initially appear morphologically as wild-type, but they show a reduced circulation and a heart-specific phenotype at 48 hpf which becomes progressively more severe. Specifically, *s411* mutants develop outflow tract stenosis by 72 hpf that leads to retrograde blood flow from the ventricle to the atrium and disruption of blood circulation to the rest of the embryo body. As a result, a severe pericardial edema starts developing from 72 hpf. The *s411* mutation causes an adenine to guanine conversion, and the substitution of a conserved Threonine to Alanine at position 757, in the Prkd2 catalytic domain (corresponding to Thr714 in human *PRKD2*) (Giardoglou *et al.*, 2021). This threonine, located in the kinase domain activation loop, is evolutionarily conserved across *PRKD2* homologs from zebrafish to rodent and human. The aim of this project was to examine the effect of *prkd2* abrogation on the expression of major signaling pathways during valve formation.

3.3.1.1 *prkd2* knockdown phenocopies *s411* phenotype

In order to confirm that the impaired heart development of *s411* mutants derives from the T757A mutation of Prkd2, we injected a *prkd2*-targeting morpholino at the one-cell stage of wild-type embryos to block the *prkd2* mRNA splicing. Morpholino was designed to impair the splicing site of exon 11 with the following intron. Accordingly, the injected embryos display similar phenotype to *s411* mutants at a rate of 80% (Figure 48). They exhibited outflow blood stenosis and blood regurgitation without developing any other phenotypic characteristics phenocopying *s411* homozygous mutants. This structure corresponds to a truncated protein

that entirely misses the catalytic site of the enzyme (Figure 48). In addition, a previously identified mutation in Tyrosine 849 shows a similar phenotype (Just *et al.*, 2011) (Figure 48).

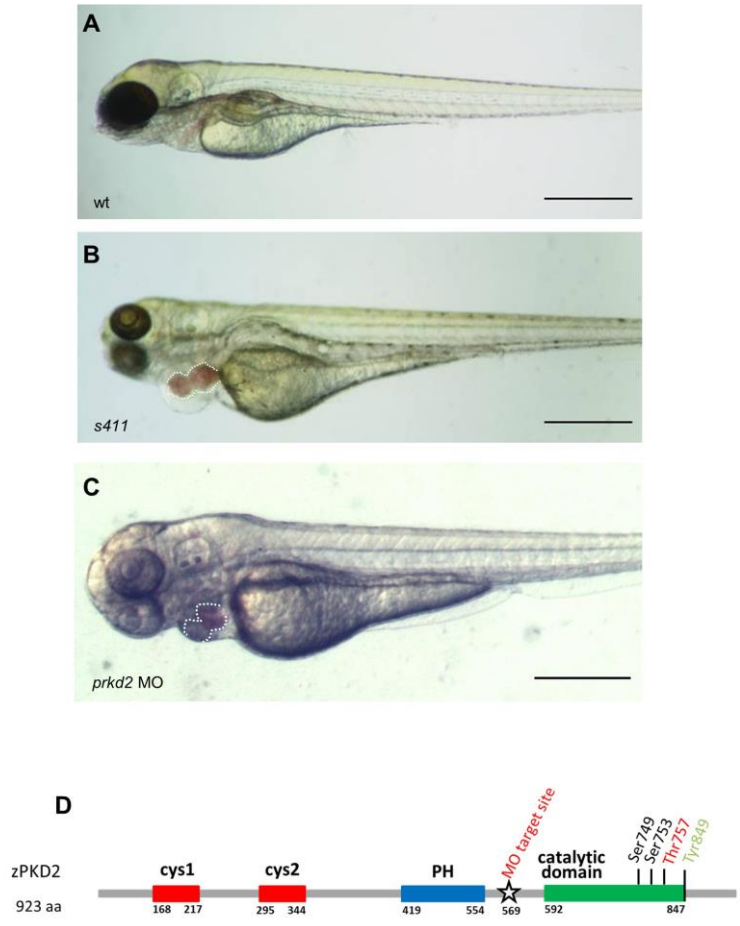

Figure 48: *s411* carry a mutation in the *prkd2* gene. A, B) Bright field image analysis of a wild-type zebrafish embryo compared to an s411 mutant embryo at 72 hpf. Heterozygous adults that carry the *s411* recessive mutation give 25% offspring mutant embryos exhibiting heart edema, inadequate blood circulation leading to complete outflow tract stenosis and blood regurgitation by 72 hpf. Scale bars: 500 µm. (C) Bright-field image analysis *prkd2*-targeted morpholino injected embryo at 72 hpf. MO-*prkd2*-injected embryos resemble the *s411* phenotype possessing the same features as *s411* mutants (three replicates, n>50). Scale bar: 200 µm. (D) Schematic representation of zebrafish Prkd2 kinase. It consists of 923 amino acids

and the main domains of the enzyme are indicating: two cysteine-rich motif domains (cys1 and cys2), a pleckstrin homology domain (PH), and the C-terminal catalytic domain where the PKC-phosphorylation sites, Ser749 and Ser753 reside. It is also highlighted the position of *s411* mutation (A to G), a previously identified zebrafish mutation with a similar phenotype (Y849) and the position of premature stop codon after MO injection resulting to defective splicing.

3.3.1.2 *s411* mutants exhibit ectopic expression of AV markers

The expression of *notch1*, *bmp4* and *klf2a* is initially throughout the heart and gets restricted to the AV canal cells by 72 hpf. These are the first hallmarks of AV differentiation, and a reliable indicator of proper valve development (Stainier *et al.*, 2002; Beis D, Bartman T, Jin SW, Scott IC, D'Amico LA, Ober EA, Verkade H and J, Field HA, Wehman A, Baier H, Tallafuss A, Bally-Cuif L, Chen JN, Stainier DY, 2005). It was shown that all the three markers (*notch1b*, *klf2a*, and *bmp4*) remain ectopically expressed throughout the heart of *s411* mutants (Giardoglou *et al.*, 2021).

In addition, *s411* mutants carrying the *Tg(TP1:mCherry)* (a transgenic reporter line used as a biomarker for Notch signaling activation) show ectopic activation throughout the ventricular endocardium (Figure 49 C', compare to 49 C). This confirms the *in situ hybridization* data as well as previous reports that Prkd2 controls Notch signaling via HDAC regulation. Notably, Notch signaling remains unaffected in non-cardiac tissue (Figure 49 B' compare with B). These results reveal the critical role of Prkd2 in cardiac valve morphogenesis during early development.

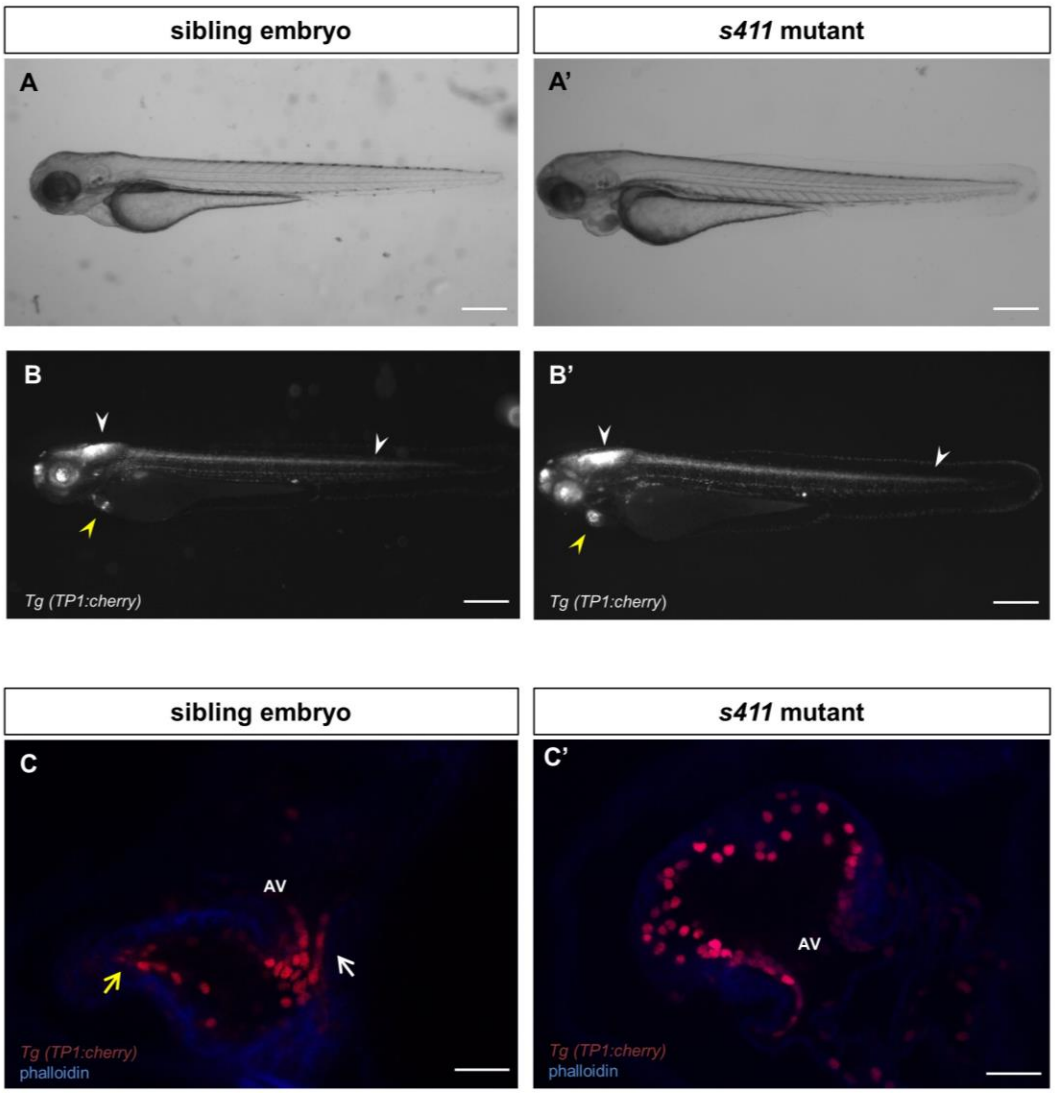

Figure 49: Ectopic activation of endocardial Notch signaling in *s411* embryos carrying the T757A PRKD2 mutation**.** Bright field (A,A') and fluorescence (B,B') analysis of *s411* sibling and mutant embryos carrying the *Tg(Tp1:mCherry)* (pseudo-colored grey). Scale bars: 500 µm. Confocal analysis of 150 µm cardiac slices of *s411* sibling and mutant embryos carrying the *Tg(Tp1:mCherry)* co-stained with 633-phalloidin (blue) (C,C'); Scale bar: 25 µm. Notch signaling is active in several tissues and organs throughout the embryo and restricted to the AV canal and OFT of wild-type embryos at 72 hpf (B, C). In *s411* mutants, Notch signaling appears unaffected in the embryo (B', white arrowheads) but remains active throughout the ventricular

endocardium (B', yellow arrowheads, C'). White and yellow arrows (C) indicate the Notch positive cells at AV canal and OFT, respectively. AV, atrioventricular; OFT, outflow tract. n=10 in each of three independent experiments.

3.3.1.3 PRKD2 and Calcineurin (CN) cooperate to regulate heart development

The Calcineurin/Nuclear Factor of Activated T-cells (CN/NFATc) signaling pathway plays a crucial role in cardiac valve morphogenesis (de la Pompa JL, Timmerman LA, Takimoto H, Yoshida H, Elia AJ, Samper E and J, Wakeham A, Marengere L, Langille BL, Crabtree GR, 1998). Studies in embryonic mouse and fish heart valve remodeling link this pathway to the production of soluble factors such as vascular endothelial growth factor (VEGF) that regulate EMT (Timmerman *et al.*, 2004; Gunawan *et al.*, 2020). Since NFAT enters the nucleus and drives the transcription of genes involved in heart formation only when dephosphorylated, NFAT activation can result from either enhanced dephosphorylation (by activated calcineurin) or reduced phosphorylation (by a PKC/PRKD-dependent mechanism) (Prasad and Inesi, 2009). WT and heterozygous *s411* mutant zebrafish embryo were treated with Cyclosporine (CsA), a Calcineurin inhibitor (under conditions that abrogate CN activity) to test the hypothesis that CN and PRKD2 cooperate to regulate zebrafish valve development. Figure 50 A shows that WT CsA-treated embryos display heart defects nearly identical to those identified in *s411* mutant embryos. Interestingly, heterozygous *s411* embryos from an heterozygous cross showed enhanced sensitivity to CsA, displaying a phenotype at a CsA dose that does not affect wild-type embryos (2µg ml^{-1}). The observation that CsA treatment of WT embryos recapitulates the *s411* Prkd2 T757A phenotype suggests that CN and PRKD2 act in a reciprocal manner to control the phosphorylation of signaling proteins that regulate valve development.

Finally, wild-type zebrafish embryos were treated with CID755673, an inhibitor of PRKD activity. While early treatment with the inhibitor led to severely dysmorphic embryos (implicating PRKD activity in overall embryo development), CID755673 treatment initiated at 30 hpf resulted in the appearance of embryos that phenocopied the *s411* morphology (outflow blood stenosis and blood regurgitation), (Figure 50 D compare to 50 A). These findings identify a specific time-window in which PRKD activity is required for cardiac development in zebrafish.

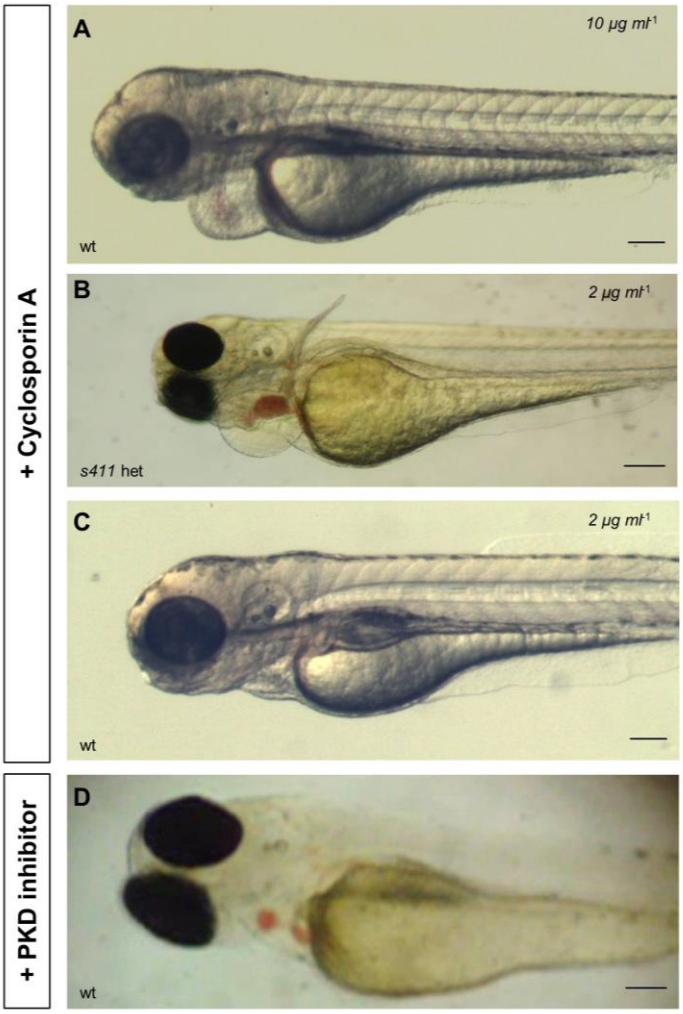

Figure 50: Disruption of calcineurin/NFATc signaling and blocking PRKD activity exhibits a similar phenotype to *s411* mutant embryos. Incubation of wild type (A) with 10 µg ml^{-1} cyclosporine A (CsA) results to a *s411* phenotype. *s411* heterozygous (B) embryos treated with cyclosporine A, at 2 µg ml^{-1}, a sublethal dose of CsA show phenotype while there is no effect in wild-type embryos (C) when treated at this dose. (D) Treatment of wild-type embryos with a protein kinase D family inhibitor, 2,3,4,5 -Tetrahydro-7-hydroxy- 1H-benzofuro[2,3-c]azepin-1-one between 30–72 hpf phenocopies *s411* mutants showing that this is the critical window of *prkd2* activity in the heart. n=20 in each of three independent experiments. Scale bars: 100 µm.

3.3.1.4 Translational implications for a Tbx5-Prkd2 axis

PRKD2 is significantly associated with coronary heart disease, but doesn't reach the genome-wide threshold. It is interesting to note that the associated variant rs425105 is an eQTL for PRKD2 in various human tissues.

There are two SNPs in perfect LD in the region (r2 = 1) rs425105 and rs60652743. The latter, rs60652743,https://pubs.broadinstitute.org/mammals/haploreg/detail_v4.1.php?query=&id=rs60652743 may be of interest as it will affect TBX5 binding sites. *Tbx5* encodes for a T-box containing transcription factor (TF), which plays a pivotal role in heart, eyes and forelimb development in many vertebrate species (Chapman *et al.*, 1996; Gibson-Brown *et al.*, 1998; Begemann and Ingham, 2000). Homozygous mutation of *tbx5a* in zebrafish embryos leads to lethal cardiac looping defects and impair of fin initiation and morphogenesis (also known as *heartstrings*) (Garrity, Childs and Fishman, 2002). In order to evaluate the potential functional association between *tbx5a* and *prkd2*, we first examined whether *prkd2* area in zebrafish contains Tbx5a TF binding sites (TFBS) using the Bio-tool of TFBS identification across species, ConTra v3 (Kreft *et al.*, 2017). This database visualizes and identifies TFBS in any region surrounding a gene of interest. An analysis of a promoter region set 3000bp upstream and 300bp downstream of the first exon of *prkd2* identified several sites correspond to Tbx5a DNA binding motifs (Figure 51 A,B). Moreover, *tbx5a* morpholino treatment recapitulated the *s411* mutant phenotype, with *tbx5a* morphants exhibiting a failure of heart looping and absence of pectoral fin budding (Figure 51 C, with the cardiac defects appearing earlier and being more severe when compared to the *s411* mutants) and reduced *prkd2* expression (Figure 51 D). These results are consistent with the notion that Tbx5a regulates *prkd2* expression.

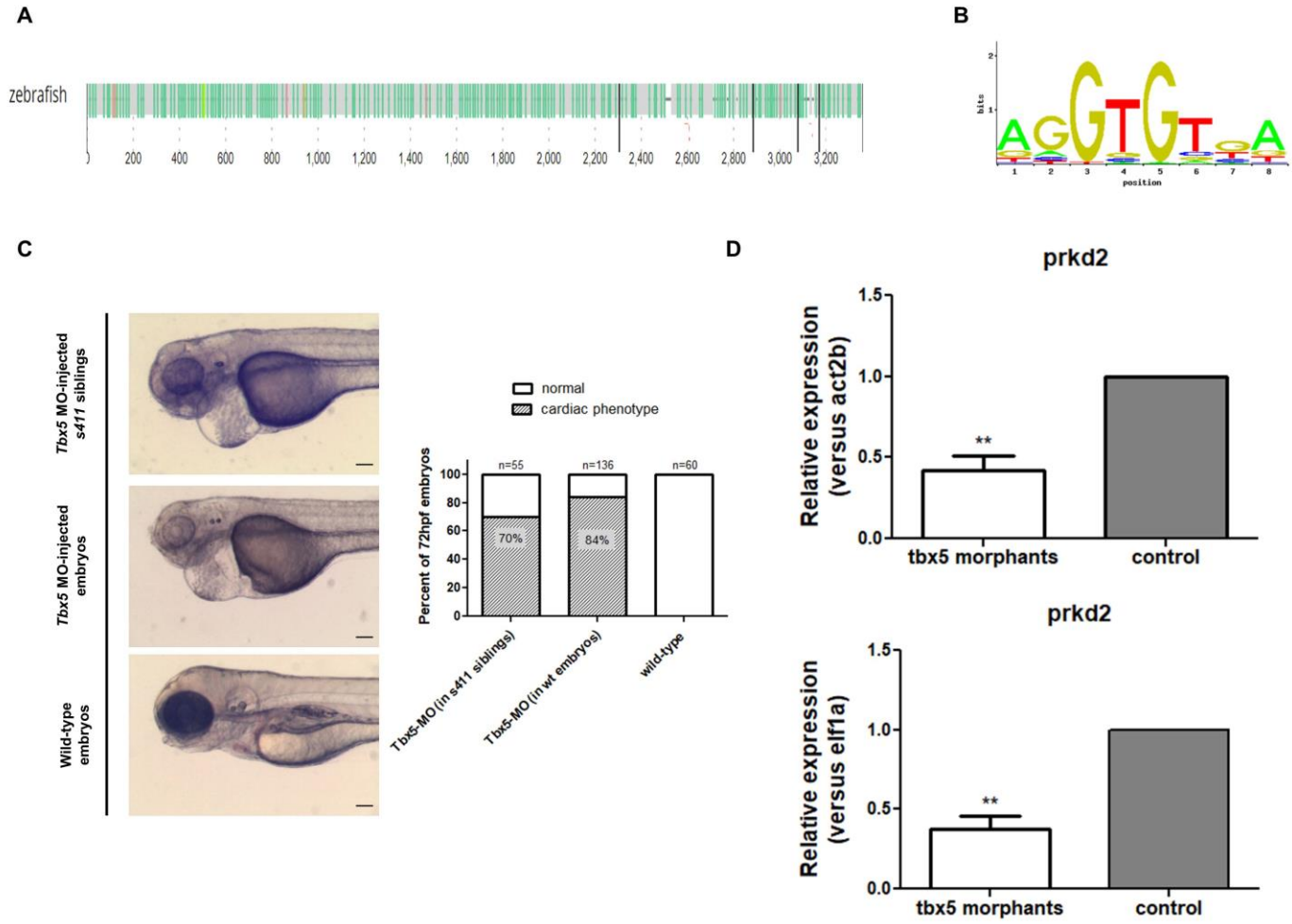

Figure 51: PRKD2 association with TBX5a regulation. Multiple predicted transcription factor Tbx5a binding sites in the promoter region of zebrafish Prkd2 via the ConTraV3 web server (A) and the possible DNA binding motif (B). Brightfield image analysis and quantification of 72 hpf *tbx5a*-morpholino injected *s411* siblings, *tbx5a*-morpholino injected wild-type and control wild-type embryos (C). *tbx5*-morpholino injected *s411* mutant embryos exhibit an earlier more severe phenotype reminiscent to the tbx5 morphants and mutants. Scale bars: 100 µm. As measured via rt-qPCR, *prkd2* expression levels in *tbx5* morphants are reduced compared to uninjected siblings at 56 hpf, normalized both to *act2b* and *elf1a* as reference genes (D). n=6 independent replicates, 15 larvae per sample, Student's t-test (two-tailed distribution, paired), ** significantly different P-value <0.01, error bars +s.e.m.

3.4. Predictive capacity of traditional cardiovascular risk factors in Greek population: an ongoing prospective study

3.4.1 Study population

The prospective study was conducted on patients who had experienced a first cardiovascular (CV) event in the era of coronary artery disease (CAD). It was carried out in Athens, Greece and the recruited patients were hospitalized in the Cardiology Department of 'Attikon' University Hospital, 'Tzaneio' General Hospital and 'Hippocrates' General Hospital. A total of 396 patients was enrolled: 327 males and 67 females; age raging between 36 - 84 years for males and 41 - 83 years for females. A total of 66 patients was re-examined 6 months after the first recruitment: 58 males and 8 females; age raging between 38 - 73 years for males and 48 - 75 years for females. At the subgroup of 66 patients that were re-examined, only 3 had a recurrent MI event. Since the first recruitment, 9 patients with additional medical conditions were excluded and the rest of the patients recruited at the first MI event (321) didn't consent to continue their participation in the study, were not available for an appointment or died at the 6 months period after MI event. All diagnosed CAD patients were participants of the GRMIC (Greek Recurrent Myocardial Infarction Cohort). This study which is on-going prospective, hospital-based registry is investigating the prognostic value of cardiovascular risk factors in the course of the appearance of second CV events. All individuals were informed about the study and voluntarily signed a written consent.

3.4.2 Data collection

On the recruitment day, all the study participants were interviewed based on a validated study purpose-oriented questionnaire including self-declared information regarding demographic characteristics, medical records, family history, dietary habits and condition of their lifestyle (smoking behavior, physical activity, and psychological state). In parallel, blood specimen was collected in specialized vacuum vials for biochemistry laboratory tests requiring blood serum. The same procedure was repeated during the follow-up voluntary appointments, 6 months after hospital discharge.

3.4.3 Biochemical measurements and analysis

Freshly isolated blood specimen was centrifuged at 12000g for 30min at 4^0C and following, separated serum was subtracted and kept separately in cryovial tubes at -80^0C at the Harokopio University Biobank. Serum testing [glucose, total cholesterol, triglycerides, high density lipoprotein cholesterol (HDL), low density lipoprotein cholesterol (LDL), uric acid (UA), apolipoprotein B (Apo-B), lipoprotein a (LP-A), C-reactive protein (CRP) and creatine phosphokinase (CPK)] was performed in external medical clinic, 'Bioiatriki'.

Due to the small number of samples and the corresponding data in the re-examination, no conclusive results regarding the prognosis of a recurrent event could be drawn, during the conduction of the current dissertation. However, GRMIC is an ongoing study and sufficient data will be collected until its future completion. Although, the limitation of data so far, we aimed to test the tendency of the candidate biomarkers in 66 samples of Greek MI-patients between the two time points, considering t=0 the time of the first MI event, and t=6 the time of the re-examination (6 months after). Our results showed the total cholesterol, low-density lipoprotein cholesterol, apolipoprotein-B, C-reactive protein and creatine phosphokinase are significantly reduced after the first myocardial infarction event, whereas the levels of the other candidate markers that were tested in the plasma were not altered at the time of blood collection compared to the two different time-points. These results show the strength of traditional risk factors (lipids together with C-reactive protein and creatine phosphokinase) as indicators of risk for CAD occurrence. Undoubtedly, the requirements of the recruitment of 500 patients in this study will empower the potential of cohort scope and contribute to a better understanding of the risk of post-MI recurrent event, as well as the identification of variations related to CAD in the Greek population.

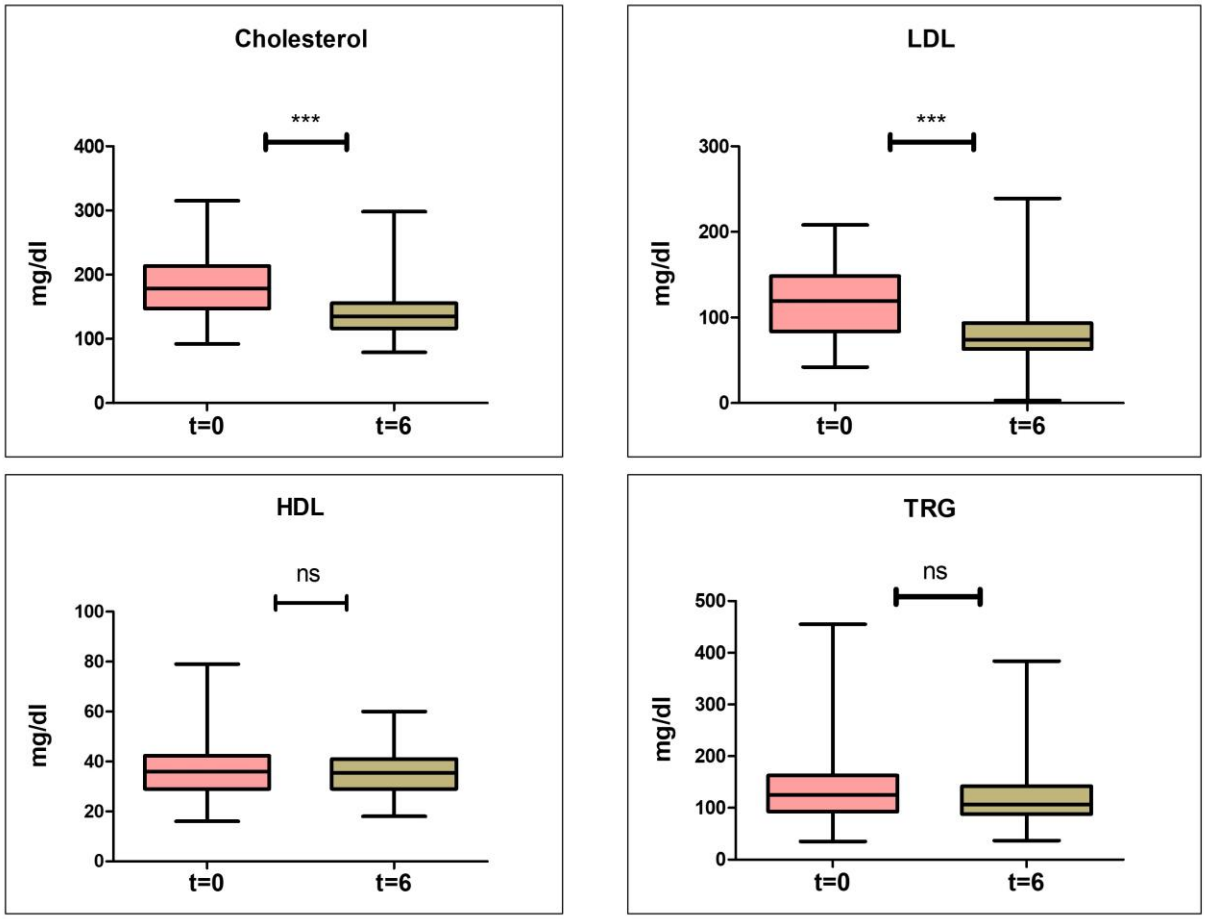

Figure 52 (continues at the next page)

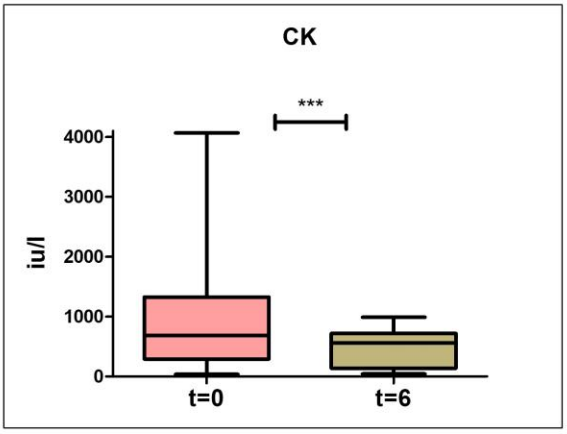
CK
***
4000
3000
2000
1000
0
iu/l
t=0
t=6

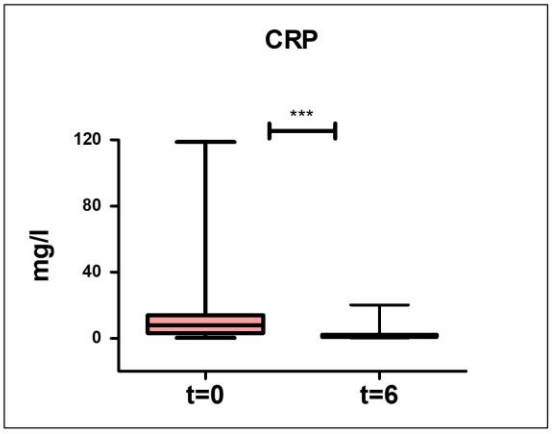
CRP
***
120
80
40
0
mg/l
t=0
t=6

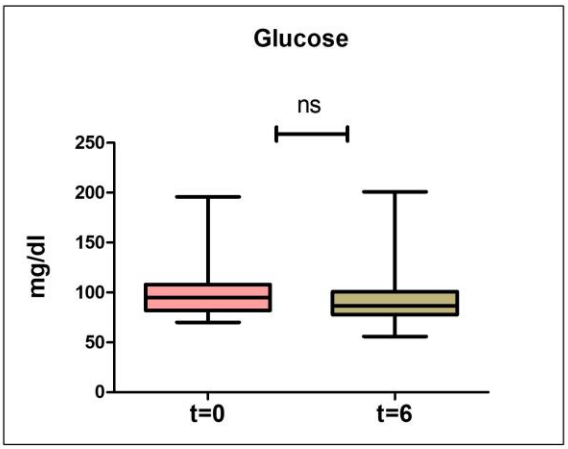
Glucose
ns
250
200
150
100
50
0
mg/dl
t=0
t=6

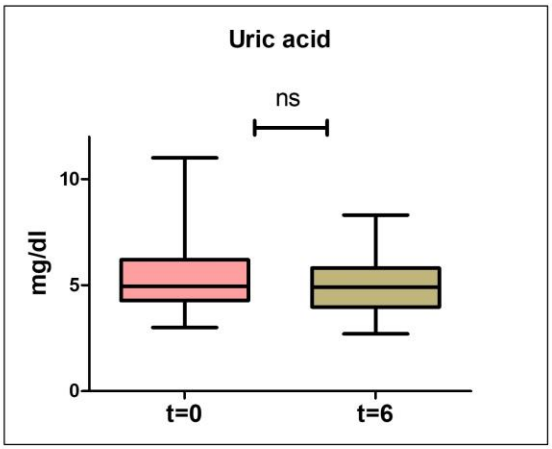
Uric acid
ns
10
5
0
mg/dl
t=0
t=6

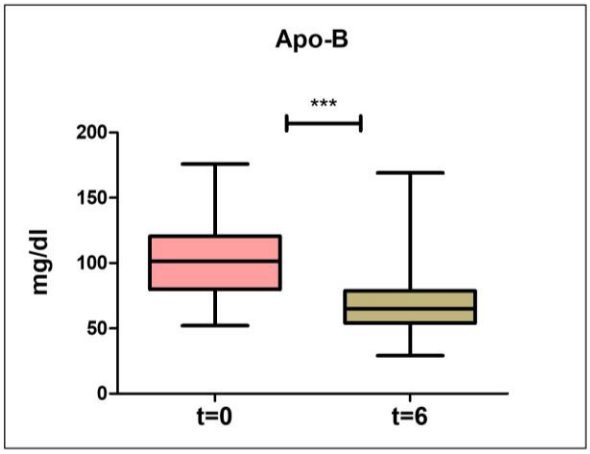
Apo-B
***
200
150
100
50
0
mg/dl
t=0
t=6

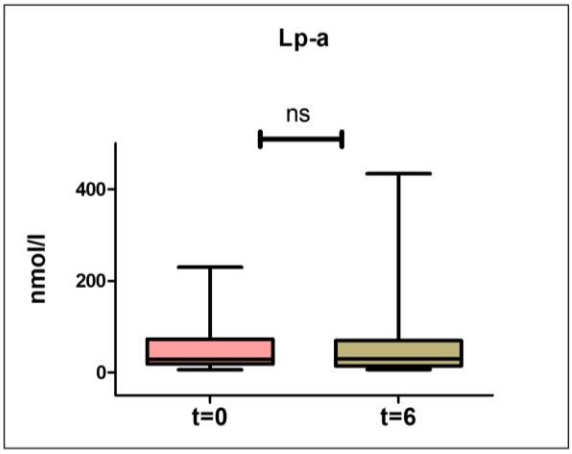
Lp-a
ns
400
200
0
nmol/l
t=0
t=6

Figure 52: Plots of candidate markers measured after biochemical analysis of plasma samples of myocardial infarction Greek patients at the at the time of the occurrence of the event (t=0) and the re-examination, 6 months after the hospital discharge (t=6). Graphs were designed using GraphPad Prism tool. Student's *t*-test (two-tailed distribution, paired), ns: non-significant, *** significantly different *P*-value ≤ 0.001, error bars ± s.e.m

4. Discussion

In this study, we studied for the first time the role of *cfdp1* in cardiac development and proper function of the heart. We successfully generated a CRISPR/Cas9 - induced *cfdp1* mutant line by deleting five nucleotides around the PAM sequence resulting in alteration of reading frame, introduction of seven novel amino acids followed by an early stop codon and coding of a truncated protein product (missing the evolutionary conserved BCNT domain). This was achieved by targeting an oligonucleotide region on the third exon of zebrafish *cfdp1* orthologue and identification of mutant allele after sequencing. Our work demonstrated the cardiac dysfunction upon *cfdp1* abrogation which was reflected in decreased heart features of end-diastolic volume, stoke volume, cardiac output and ejection fraction. The *cfdp1*$^{\Delta/\Delta}$ embryos do not reach adulthood as they die at approximately 10-15 dpf. We presented *in vivo* evidence of decreased ventricular trabeculation in *cfdp1* mutant hearts, while age-matched wild-type siblings showed normally developed trabecular network. In addition*, cfdp1* mutant embryos as well as a portion of *cfdp1* heterozygous embryo exhibited impaired contractility and bradycardia, indicating a partially penetrant haploinsufficiency. Interestingly, we showed that Wnt signaling in mesenchymal valvular cells is downregulated in *cfdp1* mutant hearts while they do not affect Notch activation and valve formation. This is an indication that *cfdp1* act as an effector of Wnt pathway during cardiac physiology.

4.1.1 Providing a valuable novel tool for phenotypic and functional characterization of *cfdp1* gene.

Biochemical and functional analysis of CFDP1 (hBCNT/CFDP1) in human cell lines (HeLa, U2OS and MRC5) identified two isoforms of 50 kDa and 35 kDa (spliced variants) found in the nucleus of the cells (Messina *et al.*, 2017). The same study suggested that the 50 kDa variant has chromatin-binding activity (while the shorter isoform obtains different characteristics) and plays an important role in chromatin remodeling and organization affecting the progression of cell cycle. Interestingly, the truncated construct Flag-CFDP1-Nt containing only the N-terminal

and lacking the conserved BCNT domain (C-terminal region) was able to enter the nuclei but lost the chromatin binding activity resulting in a defective truncated product (Messina *et al.*, 2017). In our zebrafish model, the mutated *cfdp1* allele generated via CRISRP/Cas9 system lacks also the BCNT domain since early stop codon is inserted close to the N-terminal region of the protein product. Based on the fact that this domain is highly evolutionary conserved between species, it is expected that z*cfdp1*$^{\Delta/\Delta}$ loses the chromatin binding activity as well, and therefore its subcellular mechanical function but this needs to be further clarified and confirmed.

The characterization of orthologous *cfdp1* has been studied in different species and sparse evidence have shown that *cfdp1* plays a role in organism development but the specified function and the mechanism of action is largely unexplored. Both *in vitro* and *in vivo* studies on yeast (*Saccharomyces cerevisiae*) BCNT orthologue SWC5, have shown that SWC5-deleted mutants lack SWC1-mediated Htz1 histone replacement suggesting that SWC5 is required for chromatin remodeling which can impair transcription and other cellular responses (Wu *et al.*, 2005; Morillo-Huesca *et al.*, 2010). In the same context, studies in *Drosophila melanogaster* have demonstrated YETI, the BCNT member to be a multifaceted chromatin protein found in cell nuclei whereas its depletion in *Yeti* mutants leads to lethality before pupation (Messina *et al.*, 2014). *Yeti* binds to chromatin via its BCNT domain and interacts with both H2A.V variant and HP1a and it is proposed that YETI participates in the control of transcription initiation or the chromatin integrity. The first evidence of heart localization of BCNT genes during development comes from embryonic mouse studies revealing that CP27, the BCNT orthologue, is expressed in the developing heart (E8-E10), as well as organs like brain neuroepithelium, teeth, retina of the eye, otic vesicles, cerebellum and periosteum developing bones and in most cases, CP27 signal expression is found in epithelial-mesenchymal boundary in developing tissues (except dental pulp and periosteum) (Diekwisch *et al.*, 1999). Later on, CP27 loss of function in mouse embryonic fibroblast cell line BALB/c 3T3 showed reduction in fibronectin matrix composition and redistribution of extracellular matrix (ECM) organization, suggesting that CP27 has a regulative effect on ECM and cellular changes (Luan and Diekwisch, 2002). It is known that ECM synthesis and remodeling promotes trabecular rearrangements and trabecular network growth in non-compaction cardiomyopathy (NCC) mouse model and it has been shown

that fibronectin exhibit similar pattern to *Has2*, *Vcan* and CD44 (a hyaluronan receptor), which are ECM synthesis genes essential for trabeculation (Monte-nieto *et al.*, 2018). Therefore, a possible involvement of CP27 in ECM remodeling during ventricular trabeculation in mice, should also be investigated.

Genome-wide association studies have unraveled multiple genome loci associated with human diseases. A recent study performed deep transcriptomic analysis of genotyped primary human coronary artery smooth muscle cells (HCASMCs) and coronary endothelial cells (HCAECs) from the same subjects and analyzed GWAS loci associated with vascular disease and CAD risk, in these two coronary cell types (Nurnberg *et al.*, 2020). Researchers found *CFDP1* (along with *YAP1* and *STAT6*) for HCAECs that passed the 5% false discovery level (FDR) correction at the gene level which associates *CFDP1* with artery disease traits (Nurnberg *et al.*, 2020). Another study which applied a 2-stage discovery and replication study design with more than 15000 individuals, identified an association of a novel SNP in the last 3' intron of *CFDP1*, rs4888378, with carotid intima-media thickness (cIMT), an established marker for subclinical atherosclerotic cardiovascular disease (Gertow *et al.*, 2012). A different study identified another *CFDP1* variant, rs3851738, as CAD-associated locus after analysis from UK Biobank and CARDIoGRAMplusC4D 1000 Genomes imputation study, and following 'phenome-wide association study' (PheWas) correlated this variant with systolic blood pressure (Klarin *et al.*, 2017). In the same context, GWAS studies have shown correlation of human *CFDP1* with aortic root diameter, as well as CAD risk (Sabater-Lleal *et al.*, 2014; Wild *et al.*, 2017).

Thus far, *in vivo* studies clarifying specifically the involvement of *cfdp1* in cardiac development are voided. A detailed phenotypical and functional analysis of the GWAS-derived *CFDP1* is essential to shed light to the way of action and its determinant role in cardiovascular physiology. The present work provides evidence for first time about the fundamental effect of *cfdp1* in proper heart morphogenesis and function via the generation of CRISRP/Cas9-induced zebrafish mutant line which accounts as a novel and valuable platform for the deeper understanding of *cfdp1* activity in embryonic heart physiology.

4.1.2 *cfdp1* knockdown and knockout zebrafish models demonstrated similar but not identical results.

Targeted knockdown of genes via MO injections is distinguishable from stable genetic lines which inherit the induced change, since MOs are gradually degraded within few days and therefore result in a transient effect. Despite that fact, knockdown approach in zebrafish remain an *in vivo* phenotypic assay to investigate the effect of gene depletion upon blocking mRNA translation. Our data showed that *cfdp1* morphants develop phenotypic abnormalities, such as pericardial oedema, craniofacial malformations and hypoplastic swim bladder (arrest of swim bladder inflation has been proposed to be a secondary event to heart failure, since in *silent heart* morphants that lack heart contractility, heart-specific constitutively activated AHR signaling and TCDD-exposed zebrafish models which develop heart failure, the swim bladder development is inhibited in the same manner (Yue, Peterson and Heideman, 2015)). Interestingly, the *cfdp1* mutants, although they do not survive to adulthood, they exhibit a milder phenotype by developing arrhythmic embryonic hearts but not pericardial oedema or extreme craniofacial disorders compared to *cfdp1* morphants at 120 hpf. At the same context, when we investigated the effect of *cfdp1* depletion in Wnt signaling pathway at *cfdp1* morphant hearts, we observed major reduction in signal intensity or even complete blockage of expression pattern in Wnt-activated cells of Tg(7x*TCF-Xla.Siam:nlsmCherry*) reporter line, while *cfdp1* mutant hearts showed strong inhibitory effect without total silence of Wnt pathway. The differences in the manifestation of *cfdp1* depletion between knockout and knockdown embryos could possibly be due to the activation of a genetic compensation response, which has been previously proposed to explain phenotypic discrepancies in morphants and mutant models (Rossi *et al.*, 2015). Knowing that *cfdp1* is expressed during development and *cfdp1* mutation leads to lethality at larvae stage, it is expected that morphants will exhibit more severe developmental defects and an earlier phenotype. Overall, practical approaches to confirm the observed phenotype includes analysis of multiple alleles, genetic rescue and combination of both mutants and morphants. In our strategy, we combined *cfdp1* knockdown and knockout

data and future experiments could include rescue of observed phenotype with *cfdp1* mRNA injections or study of an alternative *cfdp1* mutated allele.

4.1.3 Variation of *cfdp1* heterozygous phenotype manifestation.

The generation of stable *cfdp1* zebrafish mutant line resulted in the induction of a deleterious mutation caused by harboring a premature termination codon (PTC) in *cfdp1* sequence. Detailed phenotypic study of *cfdp1* sibling embryos unveiled the arrhythmic hearts of $cfdp1^{\Delta/\Delta}$ embryos. Notably, the same phenotype emerged in a range of heterozygous $cfdp1^{\Delta/+}$ embryos that made them undistinguished from the *cfdp1* mutants. We further investigated whether this could be a result of variation in *cfdp1* expression levels and indeed, we detected differences in signal intensity within $cfdp1^{\Delta/+}$ embryo pool, suggesting that this could modulate the phenotypic variation of heterozygous zebrafish. Our data support the existence of heterogeneity (variation of phenotype) in heterozygous *cfdp1* siblings (same genotyping group) and the possible correlation of wild-type/mutated copies and phenotypic outcome. A proposed scenario for this variation holds on the activation of quality control nonsense-mediated mRNA decay (NMD) that targets flawed messenger RNAs. Since, our *cfdp1* mutation induces a PTC that is not at the last exon and is ~ 50 nucleotides upstream of the last exon-exon junction, it is well assumed that triggers NMD machinery (Kurosaki and Maquat, 2016). It is generally known that, NMD is a surveillance pathway that degrades transcripts containing PTCs in order to maintain transcriptome homeostasis (Khajavi, Inoue and Lupski, 2006; Miller and Pearce, 2014). Although NMD plays a beneficial role by limiting the dominant-negative effect of mutant proteins, there is a variation in the efficiency of NMD activity in cell-, tissue- and transcript-specific differences that modulates the manifestation of a disorder (Khajavi, Inoue and Lupski, 2006; Miller and Pearce, 2014). Interestingly, it has also been suggested that NMD variation potentially leads to different clinical outcomes in individuals carrying the same PTC-containing mutated transcript (Nguyen, Wilkinson and Gecz, 2014). For instance, patients containing the same mutation in *X*-chromosome develop markedly different phenotypes (Duchene Muscular Dystrophy and Becker Muscular Dystrophy, respectively) upon differentially activation of NMD, allowing the accumulation of truncated protein in one case (Kerr *et al.*, 2001; Nguyen, Wilkinson and Gecz, 2014). Thus, efficacy of NMD vary between individuals which acts as potential modifier of

disease phenotype. Therefore, the observed variability between *cfdp1*$^{\Delta/+}$ individuals could also be a consequence of incomplete NMD resulting in *cfdp1* haploinsufficiency and heterogeneity observed in the same genotype group but it needs to be investigated and further elaborated in follow-up research study.

4.1.4 The role of *cfdp1* in ventricular trabeculation and cardiac function.

After cardiac chamber formation, cellular remodeling leads to a formation of an intricate architecture through the initiation and growth of ventricular trabeculation. Numerous of signaling pathways in endocardium, myocardium and cardiac ECM are involved in the regulation of this process, such as Notch (Grego-Bessa *et al.*, 2007; Monte-nieto *et al.*, 2018), Semaphorin 3E/PlexinD1(Sandireddy *et al.*, 2019), angiopoietin/Tyrosine kinase with immunoglobulin-like and EGF-like domains (Tie2) (Qu, Harmelink and Scott Baldwin, 2019), Bone morphogenic protein (BMP) (Chen *et al.*, 2004), EphrinB2/EphB4 (Gerety *et al.*, 1999), and most importantly Neuregulin (nrg) signaling which operates through ErbB receptor tyrosine kinase. E10.5 days postcoitum (dpc) *nrg1*$^{-/-}$ mice suffer from severe impaired trabeculation, as well as increased apoptotic levels at the region of the head, reflecting its role also in cranial neurogenesis (Lai *et al.*, 2010). Similarly, null mutations in ErbB2 and ErbB4 result in abrogation of ventricular trabeculation that lead to lethality between E10.5 and E11.5 in mice (Gassmann *et al.*, 1995; Lee *et al.*, 1995). Zebrafish *erbb2* mutant embryos lack cardiac trabeculation and develop progressive cardiac dysfunction and fatal heart failure, showing the functionally conserved role of Nrg/ErbB signaling in heart morphogenesis (Liu *et al.*, 2010). Interestingly, *erbb2* mutants exhibit normal valve morphogenesis, indicating a direct and cell-autonomous regulation of ErbB2 in cardiac trabeculation. In addition, while in *nrg1* zebrafish mutant larvae trabeculation appears unaffected and *nrg1*$^{-/-}$ survive to fertile adults, *nrg2a* (another member of Nrg family) mutants hearts fail to form trabeculation and suffer defects similar to *erbb2* mutants (Rasouli and Stainier, 2017). Notably, *nrg2a*$^{-/-}$ are recognized morphologically by their aberrant jaw and swim bladder inflation disorders, reminiscing of the phenotypic characterization of *cfdp1* morphant embryos. In accordance to what it was observed in *erbb2* mutants, *nrg2a* zebrafish mutants develop normal atrioventricular (AV) valves, indicating that Nrg2a/ErbB2 is dispensable for AV valve formation and it is required for proper cardiac

trabeculation. Interestingly, zebrafish *tomo*-seq genome-wide transcriptional profiling (Wu *et al.*, 2016) revealed similar expression pattern of *cfdp1* (previously misassigned as *rltpr*) and *nrg1* in regenerating heart 3 days after injury, indicating a possible functional association between the two genes. Whether c*fdp1* mechanism of action and its role in trabeculae cardiomyocytes regulation crosslinks with Nrg signaling pathway remains to be further investigated.

We have shown that *cfdp1* zebrafish mutants suffer from impaired trabecular network. Defects of this complex cardiac remodeling lead to embryonic lethality which illustrates the importance of this process and the need to fully unravel the signaling molecules regulating the trabeculation in cardiac development. Mechanical forces and contractility are also important factors for the proper trabeculation network formation. Both reduction of blood flow in *weak atrium* (*myh6*) (Peshkovsky, Totong and Yelon, 2011; Sidhwani and Yelon, 2019) mutants and disrupted contractility in *silent heart* (*tnnt2a)* (Chi *et al.*, 2008) mutants result in severe defects in trabeculation, as well as *tnnt2a* morphants that do extend ventricular protrusions but they are less stable and frequently retract (Staudt *et al.*, 2014). Disorder in trabeculae layer shown in *cfdp1* mutant embryos could be a secondary event of reduced contractility which is demonstrated by reduced stroke volume and ejection fraction cardiac performances. It would be interesting to utilize the zebrafish transgenic line *Tg(cmlc2:gCaMP)* (Chi *et al.*, 2008), a cardiac-specific fluorescent calcium indicator line to monitor the cardiac conduction signal travel in *cfdp1* mutants in order to further investigate the correlation of contractility and trabeculation in *cfdp1* embryonic mutant hearts.

Since previous studies have illustrated that Notch and canonical Wnt/β-catenin signaling pathways expressed in endocardial cell are influenced by blood flow and contractility (Pestel *et al.*, 2016), we investigated how modulation of contractility in *cfdp1* mutants affects the activation of these major molecular pathways. We demonstrated that Wnt/β-catenin signaling reporter line exhibited disrupted expression pattern, while Notch-activated cells in the corresponding reporter line didn't show any effect. The different activities of Notch and Wnt/β-catenin observed in *cfdp1* mutant hearts indicate the composition of two different cell subsets, in accordance to previously reported Notch-activated luminal AV cells and Wnt/β-catenin-

activated abluminal AV cells during valve formation (Pestel *et al.*, 2016; Paolini *et al.*, 2021). Moreover, it has been shown that although Notch and Wnt signaling intersect in order to promote the TCF-positive endocardial cells ingression into cardiac jelly during valvulogenesis, inhibition of Erk5-Klf2 pathway impairs canonical Wnt signaling without affecting Notch nor Dll4 activation in atrioventricular endocardial cells, confirming that these pathways are regulated independently (Paolini *et al.*, 2021).

Cardiac conduction system is composed by the pacemaker cells in sinoatrial junction, atrioventricular node and ventricular conduction system, and canonical Wnt pathway has been implied to contribute during specific stages of conduction (Gao and Ren, 2021). Canonical Wnt5b signaling has been reported to play an important role in heart contractility by promoting pacemakers cardiomyocytes differentiation transcription factors Isl1 and Tbx18 and inhibiting Nkx2.5, both in zebrafish and human pluripotent stem cells (hPSCs) (Ren *et al.*, 2019). Likewise, Wnt signaling activation (via Wnt3 ligand) promotes pacemaker lineage in mouse and human embryonic stem cells (Liang *et al.*, 2020). In *Isl1*-deficient zebrafish and mouse embryos, there is a progressive failure of contractility leading to arrhythmias and bradycardia (De Pater *et al.*, 2009) and it is reported that canonical Wnt/β-catenin signaling in zebrafish is activated in *isl1*$^{+}$ cells in sinoatrial region affecting the control of heart rate (Burkhard and Bakkers, 2018). In addition, Wnt/β-catenin signaling in AV canal regulates specific electrophysiological properties of AVC and AV node by slowing down conduction velocity (Gillers *et al.*, 2014). We reported that *cfdp1* embryonic mutant hearts exhibit arrhythmias, a phenotype indicating of defects in contractility and pacemaker activity. Having highlighted the significant role of Wnt in regulating pacemaker development in zebrafish, *cfdp1* seems to function in regulatory mechanism upstream of Wnt pathway involved in cellular specification of conductivity. The mechanism of how *cfdp1* cooperates with canonical Wnt/β-catenin signaling remain to be elucidated.

In summary, the CRISPR/Cas9-induced *cfdp1* zebrafish mutant line provides an unprecedented tool to unveil novel mechanisms that regulate cardiac physiology and function, as well as ventricular trabeculation during embryonic development. It is worth mentioning that according to the Mouse Genome Informatics database (www.informatics.jax.org) the phenotype of *BCAR1* mouse line is related to abnormal heart development (Aragam *et al.*, 2021). Since

BCAR1 and *CFDP1* belong to the same locus, it is very interesting to identify the causal variant associated with CAD and to further analyze the relevant phenotypes of genes that belong to this specific gene synteny in order to better assess the prospective clinical significance.

4.2. New insights in current knowledge of the role of *ccdc92* in cardiovascular field

In the present study, we aimed to interrogate the effect of *ccdc92* abrogation in heart development using *Danio rerio* as model organism. We identified the zebrafish orthologue and investigated its spatiotemporal pattern during development. Once, we confirmed that *ccdc92* is expressed at early developmental stages, we suggest that it plays an important role in the proper organism development and physiology. Previous studies in human population-level analyses have underlined the implication of *CCDC92* in cardiovascular disorders but its function remains poorly characterized. Although there are notions that the link of *CCDC92* with cardiovascular diseases is associated with insulin resistance, adipose distribution and lipid metabolism, there are still no further studies providing evidence about the mechanism of action of the gene and its molecular link with cardiometabolic risk. There is limited knowledge derived from model systems regarding the phenotypic characterization and the molecular function of *ccdc92* in the developing heart, thus here we provide *in vivo* evidence of the effect of *ccdc92* depletion in zebrafish model.

Knockdown approach via morpholino-induced silencing of zebrafish *ccdc92* exhibit cardiac abnormalities with pericardial oedema and heart malformation along with head oedema and body axis malformations. This clearly suggests that the absence of *ccdc91* product has a major effect in cardiac development and proper function. In addition, in *ccdc92* morphants we observed yolk retention indicating that yolk-derived nutrients were not consumed at a physiological rate as in wild-type embryos. The phenotypic observation of morphants raised the necessity to investigate deeper the role of *ccdc92* in early developing in cellular level as well as to generate a stable mutant *ccdc92* zebrafish line for an in-depth functional study.

To do so, we first imaged the *ccdc92* morphant hearts in comparison with control sibling embryos at 72 hpf. To analyze cardiac morphologies, we utilized transgenic reporter line *Tg (cmlc2:egfp)* that labels cardiomyocytes to perform microinjection of *ccdc92* MO. Our findings

support that *ccdc92*-deficient zebrafish embryos show cardiac looping disorder since morphant hearts fail to complete heart looping and maintain a cardiac tube-shaped heart. The cellular changes during this complex process through which heart tube deforms towards an S-shaped loop are orchestrated and tightly regulated by specific molecular pathways as well as tissue-intrinsic and extrinsic factors (Noël *et al.*, 2013; Lombardo *et al.*, 2019). BMP (bone morphogenetic protein) (Lombardo *et al.*, 2019) signaling and Nodal signaling mechanisms (Baker, Holtzman and Burdine, 2008) have been shown to regulate heart looping chirality and asymmetric position of the heart along L/R body axis. Extrinsic factors affecting cardiac looping could be hemodynamic forces ruled by blood flow (Auman *et al.*, 2007) or mechanical forces derived from restrains in surrounding tissue, since continuously elongation of heart tube in the defined space of pericardial cavity could eventually result in morphological changes (Bayraktar and Männer, 2014). It has been shown that the zebrafish null mutant, *southpaw* (*spaw*), a Nodal-related gene affects the geometry of the heart and exhibits randomized positioning of the heart chambers ((Kalogirou *et al.*, 2014; Grimes *et al.*, 2020). Injections of *ccdc92* MO in *spaw* mutant line or expression of bmp/nodal genes in *ccdc92* morphants (and mutants) could be test a possible functional mechanism of *ccdc92* and investigate its role in cardiac looping.

Findings from knockdown approaches should be confirmed by studying the role of a gene in a stable mutant line. The indication of cardiac looping defect in *ccdc92* morphants has to be further investigated in the *ccdc92* mutant hearts in order to compare the phenotype between morphants and mutants, assess the extent of phenotypic similarity and whether there are phenotypic discrepancies, study in-depth the cardiac formation and function and present conclusive data. To do so, our next step was to generate a CRISPR/Cas9-induced *ccdc92* mutant line. During this study, we designed and injected two different gRNAs including target site sequences according to the protocol instructions. Despite the optimization of the microinjections (concentration rate, primers specificity), we could not succeed on provoking alterations on *ccdc92* sequence after gRNA/Cas9 injections, and therefore we were not able to generate a corresponding mutant line. The efficiency of genome editing approach can vary due to many reasons such as target sequence, technical strategy and model organism. Single nucleotide polymorphisms and sequence alterations such as methylation and other

modifications could very well influence the effectiveness of genome editing tools. For CRISPR/Cas9, the sequence requirement of target potential site adjacent to PAM sequence can limit the sequence options for editing target (Sertori *et al.*, 2016). Zebrafish genome is highly polymorphic and possible mismatches in target site or even in PAM sequence can be detrimental to editing success (K. Liu *et al.*, 2019). To overcome the low effectiveness of our genome editing in *ccdc92* gene, we could design new target sites and corresponding gRNAs in regions without high variation that would still meet the sequence requirements of CRISPR/Cas9 technology. In addition, to further increase the efficiency of CRISPR/Cas9 editing, we could co-inject together with gRNA, directly the Cas9 endonuclease (gRNA/Cas9 protein) instead of Cas9 mRNA as an alternative injection mix to bypass endogenous transcription of Cas9 RNA (Gagnon *et al.*, 2014; Sung *et al.*, 2014). Alternatively, other strategies that could be followed are i) a potential deletion of promoter by designing target sites in the *ccdc91* promoter region and inhibition of synthesis of any RNA product (Hoshijima *et al.*, 2019; Quick *et al.*, 2021) or ii) deletion of entire open reading frame in the locus of interest by co-injecting a pair of gRNAs (targeting up- and downstream of a chosen cluster) in order to delete a genomic region and avoid alternative translational start sites (Schwarzer *et al.*, 2017).

After generating a potential *ccdc92* mutant zebrafish line, it is essential to characterize the phenotype and monitor whether there are same cardiac specifications with those we observed when we silenced the expression of *ccdc92* via morpholino injections in knockdown experiments. Having highlighted the importance and complexity of cardiac morphogenesis, it would be a possible future approach to investigate whether the effect of *ccdc92* abrogation in heart morphogenesis is a direct or secondary effect. Based on current literature, a following step would be to investigate adipose deposit and insulin signaling pathway in *ccdc92* zebrafish model. Adipocytes can be visualized by Oil Red O or Nile Red fluorescent staining dyes allowing live-imaging of adipocytes formation and expansion under controlled nutrient conditions (Flynn, Trent and Rawls, 2009; Minchin and Rawls, 2011; Seth, Stemple and Barroso, 2013). In addition, it would be also interesting to study insulin resistance and glucose homeostasis in *ccdc92* depletion. Quantitative analysis of glucose homeostasis could be performed either by whole-blood analysis in mature zebrafish (Moss *et al.*, 2009) or by measuring the glucose levels

in embryonic extracts (Jurczyk *et al.*, 2011). Also, expression levels of *pck1* (insulin inhibits its expression) or genes involved in insulin pathway such as *insr, irs1, irs2*, could be calculated in order to test whether *ccdc92*-deficient individuals lose insulin sensitivity and develop resistance. Moreover, insulin intravenous injections could be performed in *ccdc92* morphant or mutant larvae (since zebrafish are sensitive to human insulin and provoke transient hypoglycemia, whereas high dose of insulin develops insulin resistance (Marín-Juez *et al.*, 2014)), followed by glucose measurement to test whether *ccdc92* interferes with glucose metabolism and insulin signaling.

In future experiments, what could also be tested is whether genes involved in lipid metabolism, such as apolipoproteins (*apoA, apoB, apoC, apoE*), cholesterol transporters (*npc1l1*), fatty-acid transporters (*fatp3, cav1, cd36, slc27a1, slc27a2*), long-chain Acyl-CoA synthetases (*acsl1a/b, acsl2, acsl3a/b, acsl4a/b, acsl5, acsl6*) (Quinlivan and Farber, 2017) show any differences in *ccdc92* depleted individuals in order to assess possible effect on lipid composition and/or update at embryonic (yolk absorption) or adult (gut, liver, intestine) stage. In addition, delivery of fluorescent lipid substrates by yolk-injection or feeding and subsequent monitor of their transport and metabolism along with native lipids offer another tool for interrogating a potential mechanism of *ccdc92* in lipid regulation (Miyares, De Rezende and Farber, 2014).

4.3. An indispensable threonine residue in the kinase domain of zebrafish PRKD2

Heart valve defects are a leading cause of CHD, providing a strong rationale for studies that dissect the genetic and molecular factors that underlie heart valve formation. Zebrafish embryos survive early stages of embryo development without a functional cardiovascular system and therefore provide a particularly useful model to elucidate mechanisms of valve formation. This study uses the zebrafish *s411* mutant (that harbors a T757A substitution that inactivates Prkd2) which have been identified to develop a complete outflow tract stenosis.

Previous studies implicate a Prkd2-HDAC5 pathway in valve formation (Just *et al.*, 2011). However, the observation that BMP signaling is impaired in *s411* mutants and

that *s411* heterozygous embryos are hypersensitive to sublethal concentrations of the Calcineurin inhibitor cyclosporine would suggest that PKD regulates additional signaling pathways that control AV specification. Both PRKD1 and PRKD3 have been reported to exhibit a synergistic effect with the calcineurin signaling pathway to promote the expression of specific genes (Kim *et al.*, 2008; Li *et al.*, 2011). Although, it was demonstrated *in vivo* that PRKD1 stimulates myocyte enhancer factor-2 (MEF2) activity and it's involved in pathological cardiac remodeling in mice (Fielitz *et al.*, 2008), it was then studied in skeletal muscle a possible mechanism through which PRKD1 cooperates with calcineurin to drive MEF2 expression and slow-twitch fiber phenotype (Kim *et al.*, 2008). In addition, another study showed that PRKD3 is required for the NFATc4, Nkx2.5, and GATA4 expression while acting downstream of calcineurin-activated NFATc1 and c3 in pathological cardiac hypertrophy (PCH) model (Li *et al.*, 2011). Therefore, the signaling cascade clacineurin-NFATc1/c3-PKD3-NFATc4 is proposed for the PCH model. Our findings propose that PRKD2 acts synergistically with calcineurin pathway for the fine-tuning of heart development and function.

Moreover, *PRKD2* expression has been correlated with key genes involved in Notch pathway in newly diagnosed acute myeloid leukemia (AML) patients (Q. Liu *et al.*, 2019) and there is evidence that PRKD2 promotes proliferation and chemo-resistance of human AML cell lines through a mechanisms involving Notch activity (Q. Liu *et al.*, 2019). The observation that *notch1b, bmp4,* and the flow responsive transcriptional factor *klf2a* (factors that have been implicated in AV valve formation (Kalogirou *et al.*, 2014) are detected throughout the hearts of *s411* mutants - these factors do not localize to the AV region – reinforces the notion that PKD2 sits at a nodal point controlling a number of signaling pathways that regulate AV valve formation. In addition, another study has recently revealed a PRKD1-HDAC4/5-TBX5 regulatory pathway via PRKD1 relief of HDAC4/5-mediated post-translational suppression of TBX5 transcriptional activity (Ghosh *et al.*, 2019). In our study, we also showed an interaction of PRKD2 with TBX5, a novel regulatory interaction in heart development, which warrants further investigation of the underlying mechanism.

The origin of congenital heart defects has been linked with the properties of cardiac progenitor cells and the mechanisms of their development. Myocardial specification and

differentiation during the initial growth of the heart tube, its elongation and the cardiac looping are well-orchestrated processes. In mammals, early cardiomyocytes that contribute to the formation of the left ventricle, atrioventricular canal and atria arise from a collection of progenitor cells named the first heart field (FHF). Subsequent addition of cardiomyocytes to the early cardiac tube that forms the outflow tract, right ventricle, and inflow region occurs via a second distinct cell lineage termed the second heart field (SHF) (Buckingham, Meilhac and Zaffran, 2005; Rochais *et al.*, 2009). Thus, the embryonic heart development occurs by cardiomyocytes deriving from two cell lineages corresponding to the contribution of HFH and SHF. Despite the difference of heart morphology between the two-chamber zebrafish heart and mammalian heart, it has been shown that similar regulatory networks drive the fish cardiac cell fate. In the fish model, FHF is the source of cells for the formation of the primitive heart tube, and cells derived from SHF are added to the heart tube and build structures at the inflow and outflow tract (De Pater *et al.*, 2009; Hami *et al.*, 2011; Musso *et al.*, 2015). The discrete cardiomyocyte differentiation phases of zebrafish heart revealed that the two-cell lineage model is a conserved mechanism.

Studies have shown the critical role of cardiac neural crest cells in regulating the second heart field differentiation and that the absence of neural crest-derived mesenchyme in the pharyngeal impacts negatively on heart tube elongation. SHF cells contribute to the outflow tract and the structure and morphology of bulbus arteriosus in zebrafish. Several signaling pathways emerge in regulating this complex morphogenetic process where the heart and endocardium continues to the outflow tract endothelium, which is supported by smooth muscle cells. Pathways that play crucial role in atrioventricular development are emerging to be involved also in shaping the outflow tract. These include the Yap1 klf2a/Notch axis (Duchemin, Vignes and Vermot, 2019) as well as Tgfβ (Boezio *et al.*, 2020). Based on that, it is not surprising that *prkd2* mutants show defects both in the bulbus arteriosus (initially) and the atrioventricular valve. *prkd2* knockout could cause a similar phenotype in mice as in *s411* mutant zebrafish embryos, but conditional and inducible knockouts would be necessary in order to validate and study the respective murine phenotype.

As it has been already mentioned, zebrafish Prkd family consists of three members of (*prkd1*, *prkd2*, *prkd3*). *prkd2* is located on chromosome 15, whereas both *prkd1* and *prkd3* are found on chromosome 17. Previous studies implicate zebrafish Prkd1 in the regulation of angiogenesis and lymphangiogenesis during development and as essential for tumor angiogenesis; silencing of *prkd1* results in reduced formation of the intersomitic vessels and parachordal lymphangioblasts and abolished tumor angiogenesis (Hollenbach *et al.*, 2013). Of note, while the overall homology of Prkd1, Prkd2, and Prkd3 is between 60-70%, their catalytic domains show 91% amino acid similarity. However, the identification of an inactivating Prkd2-T757A substitution that drives the *s411* mutant phenotype, argues that the Prkd family enzymes play non-redundant roles during zebrafish development and it also validates the forward genetic screen mutagenesis approach.

5. Conclusive remarks

Cardiovascular diseases are the prevalent cause of mortality worldwide affecting million of individuals every year. CVDs are not only extremely life-threatening diseases but also influence the quality of life of patients (and their relatives, as a consequence, in a broad manner of thinking). The socioeconomic impact of the disease is reflected to a variety of fields in personal, community and globally level. More people die from CVDs than any other cause and shockingly, every 34 seconds a person experiences a myocardial infarction or death due to cardiac issue (Bruning and Sturek, 2015). The economic burden of the CVDs is extremely enormous due to high-cost therapies, the health examination, the medical costs and the drug therapies/medication. The annual cost per patient for CVD, coronary artery disease and heart failure is 112%, 107% and 59% higher in comparison with the corresponding costs for patient with Type 2 Diabetes Mellitus (Acs *et al.*, 2017). Therefore, the interest of interrogating the characteristic of this complex set of heart diseases and unraveling step by step the regulators of their pathogeny is in the high priority of the community and subsequently of the science as a whole.

Cardiovascular disease is a general term describing disorders affecting the proper function and morphogenesis of the heart and blood vessels, and forms an umbrella underneath which a variety of heart diseases lay. Coronary artery disease is the often implication of CVDs and it is caused by the production of plaques (containing a combination of mainly lipids, fat, calcium among other substances) in the arteries that supply oxygen to the heart, the coronary arteries. The formation of such atherosclerotic plaques reduces the oxygen-rich blood cells of the coronary circulation that reach the tissue of the heart and it can provoke either chest pain (angina) or extremely severe blockage of blood supply, and therefore the damage of the heart or even cardiac death. Thus, coronary disease narrows or blocks the arteries and results in a variation of disease outcomes. Types of CAD includes stable angina or unstable angina (a discomfort or pain), myocardial infarction and sudden cardiac death. The most severe complication derives from the prolonged deprivation of oxygen that can lead to myocardial cell death and necrosis (when MI or heart attack occur).

Through time, several research studies provided evidence about the risk factors that accompany the manifestation of the CAD and they are divided in environmental and genetic factors. The traditional environmental factors include hypertension, high blood cholesterol, high sugar levels, obesity, lifestyle and behavioral choices (smoking, bad diet, absence of physical activity) and psychological disturbances. However, epidemiological human studies have revealed also the importance of genetic causality of CAD confirming that 'you cannot run away from your genes and your DNA'. Genome-wide association studies and large-scale analysis based on patient-control genomic comparisons, and meta-analysis estimating the presence of risk factors and statistical/experimental methodology adjustments, have identified more that 60 genetic loci associated with CAD development.

Despite the burst of technological techniques, advantages and improvements that facilitated the recognition of genetic causal factors, the prediction of pathogenesis and the role of each genetic variant in clinical outcomes remain a challenge. Several strategies have been employed in order to validate the role and unravel the function of candidate genes that have derived from human population studies (like bioinformatic tool that prioritized the genes via computational analysis). However, the utilization of the appropriate animal model is by far, the most preferable way to characterize the phenotype and study the mechanism by which a gene or a variant is implied in the CAD occurrence. The choice of the right animal model is based on the designed experimental strategy and the questions that needs to be answered. The physiology of the experimental animal and the available biotechnical toolbox are two of the most important factors to seek the system model suitable for the research plan.

The purpose of this original work was to validate the function and the implication to cardiac phenotype of two genes derived from CAD-associated human studies, *CFDP1* and *CCDC92*. The evidence of contribution of both of these genes derives from published GWAS studies related to different traits of CAD and were studied during the current work as separated cases. However, the *CARDIoGRAMplusC4D* Consortium (Coronary ARtery DIsease Genome wide Replication and Meta-analysis (CARDIoGRAM) plus The Coronary Artery Disease (C4D) Genetics) (http://www.cardiogramplusc4d.org/) conducted a meta-analysis of multiple large scale genetic studies and UK Biobank genetic data (https://www.ukbiobank.ac.uk/) that resulted in the

identification of CAD-associated SNPs harboring to *CFDP1* and *CCDC92* genes. Thus far, up to the writing date of this Doctoral Dissertetion, these are still unpublished data that remain to be further analyzed and published so as to be openly available.

For the scope of our research, we used zebrafish (Danio rerio) to generate knockdown and knockout lines in order to assess the impact of the abrogation of the genes in cardiac physiology. Over the last decades, zebrafish has emerged as a valuable animal model and has provided significant evidence underlying the genetic causuality of human cardiovascular diseases. The small size of the adults, the external embryo development, the large numbers of offsprings, the optical transparenct at the early steps of embryonic developmnet, their regenerative capacity, the high genetic similarity to human genome and the ease of genetic manipulation are some from the significant advantages that has established zebrafish as a powerful teleost model. Due to the fact that zebrafish and human share homologues genes and molecular pathways regulating cardiac morphogenesis and function, this animal model can recapitulate the mammalian cardiac features and characteristics during development and adulthood.

The role of cfdp1 in cardiogenesis: First, we indentified the zebrafish *cfdp1* orthologue and observed the hight conservation of the gene between species and then based on the sequence of zebrafish *cfdp1*, we designed specific RNA probes in order to study its spatial expression during development in wild-type embryos. We confirmed that *cfdp1* is expressed at the early developmental stages and is mainly located at the region of the head and the heart. Having confirmed the cardiac expression, we applied forward genetic approaches (Morpholino for silencing of gene expression and CRISPR/Cas9 editing tool for genome modification). From the *cfdp1* morphants, we observed that silencing of *cfdp1* expression provokes, apart form decreased size of head and eyes, as well as cartilage malformations, pericardial oedema, indicating of cardiac disorder. We further investigated *cfdp1* morphant hearts in cellular level, and we observed that the expression of Wnt/β-catenin activated cells is reduced or even abolished. Based on the pre-screening results derived from the kockdown technique, we generated a CRISPR-Cas9-induced *cfdp1* zebrafish mutant line. The mutated allele carries an insertion of seven novel aa followed by an early stop codon leading to coding of a truncated

protein product. Studying mutant embryos revealed that *cfdp1* is an essential gene and *cfdp1*$^{-/-}$ embryos do not reach adulthood as they die at around 12-15 dpf. Phenotypic monitoring and imaging showed that mutant embryos exhibit arrhythmic hearts (or even bradycardias) without appearing any gross phenotypic abnormalities. Following analysis of *cfdp1*$^{-/-}$ embryos showed that they develop impaired heart features (reduced end-diastolic volume and stroke volume as well as cardiac output and ejection fraction) which confirms the ventricular dysfunction and the developed cardiac disorder. Interestingly, it was discovered that *cfdp1* depleted embryonic hearts have impaired ventricular trabeculation, a crucial cardiac process for the survival of the organism. In addition, detailed analysis of mutant embryonic heart confrimed that Wnt/β-catenin pathway in mesechymal-like valve cells is downregulated when *cfdp1* is depleted, while there is no efect on valvulogenesis (Notch signaling activation in endocardial valve cells is not affected).

So, in conclusion of our findings and what it was presented and discussed at the former chapter of this book:

- *cfdp1* is **expressed during early embyonic development** at the anterior body part at the region of the head and the heart
- The CRISPR/Cas9-mediated ***cfdp1* mutant zebrafish line** is the first *cfdp1* animal model and serves as a tool for deeper understanding of its function
- *cfdp1* loss results in a **lethal** phenotype
- **Heterozygous *cfdp1* individuals exhibit variation** in cardiac development and function
- Depletion of *cfdp1* results in a **defective cardiac performance**
- Abrogation of *cfdp1* leads to **impaired ventricular trabeculation**
- **Wnt/β-catenin signaling pathway is downregulated** in abluminal valve cells of mutant embryonic hearts
- Mutant heart forms **functional AV valves** and Notch signaling is not affected

Future experimental strategy should unravel the specific role of *cfdp1* in the regulation of trebaculation and how it is functionally linked to the known pathways that control the

formation of trabeculation network, such as Nrg/ErbB. Moreover, as *cfdp1* derives from human studies unraveling CAD candidate genes, the initial strategy was to visualize coronary artery network in mutant juvenile hearts (by using zebrafish reporter line that marks with green fluorescent protein the coronary arteries, *Tg(fli1:egfp)*), since coronary arteries are established at 2 months post fertilization. Unfortunately, mutants do not reach that age, so it was worth it to visualize the coronary artery in heterozygous *cfdp1* hearts, since this genotype also develops a variation in phenotype mimicking either the mutant contition or the wild-type.

The role of ccdc92 in cardiogenesis: First, we indentified the zebrafish *ccdc92* orthologue and then based on its sequence, we designed specific RNA probe in order to study its spatial expression during development in wild-type embryos. We observed low expression levels at the first development stages (up to 48 hpf) and an increased expression at later stages in a ubiquitous manner up to 120 hpf. The same finding was confirmed by temporal expression of *ccdc92* (via RT-PCR) at specific embryonic stages. Following, we study the *ccdc92* knockdown model (via ATG-blocking morpholino). Interestingly, we observed that *ccdc92* morphant embryos developed pericardiac oedema (at some cases, even "cardiac balloons") and defects in cardiac morphogenesis maintaining the cardiac tube structure even at 72 hpf. Confocal imaging of *ccdc92* morphants confirmed that they exhibit heart looping defects and cardiomyocytes of the two chambers are not fully positioned asymmetrically in a R/L axis. Following, we attepmted to create a stable *ccdc92* mutant line via CRISPR/Cas9 genome editing tool, but unfortunately we did not succeed to induce mutagenesis.

So, in conclusion to our findings and what it was presented and discussed at the former chapter of this book:

- Zebrafish orthologue *ccdc92* is **expressed during embyonic development** and it is mostly apparent from 48 hpf onwards.
- Silencing of *ccdc92* expression induce **severe cardiac phenotype** which is described by pericardial oedema and defective heart structure

- *In vivo* study of *ccdc92* morphant heart in cellular level revealed **impaired cardiac looping** and developmentally staled heart at the heart tube or C-shaped heart

The current research study analyze an *in vivo ccdc92* model for first time, and provide phenotypic information derived from the knockdown approach. The characteristic cardiac phenotype of *ccdc92* morphants that we describe shows a very promising field of future study regarding the cardiovascular development. Although, morpholino are widely used for silencing of a gene expression, it is necessary to generate a stable *ccdc92* mutant line and confirm the findings from the knockdown model and study in depth its mechanism of function.

The role of Threonine residue in the Kinase Domain of PRKD2: Protein Kinase D2 belongs to a family of evolutionarily conserved enzymes regulating several biological processes. In a forward genetic screen for zebrafish cardiovascular mutants, a mutation in the *prkd2* gene was identified. *s411* mutants exhibit severe impaired heart development with outflow tract stenosis by 72hpf that leads to retrograde blood flow. As a follow up, we investigated further the possible mechanism and pathways that are involved in s411 phenotype and in summary:

- **Knockdown of *prkd2* phenocopies *s411* mutants** which confirms impaired cardiac phenotype of *s411* derives from *prkd2* mutation
- *s411* mutants show **ectopic expression of Notch signaling** pathway
- **PRKD2 and calcineurin** cooperate to regulate heart development in zebrafish
- There might be a functional **Tbx5-Prkd2 axis** regulating the *s411* phenotype, a novel interaction that warrands further investigation.

GRMIC participation: GRMIC is a cohort that have designed a prospective human study. The aim of this ongoing study is the recruitment of 500 Greek participants with first myocardial infarction event and their re-examination six months after the hospital discharge. During the appointments of both time periods, human sample (fresh blood) is collected and a questionaire- driven interview is conducted directly with the patients and according to self-

report, the questionaire is filled out. At the first only appointment, we explain the aim and the purposes of the study to the patients, they voluntarily sign a consent form and each of them receive a code name. The files with the personal details are kept at the center of Harokopio University and stored under strict confidentiality. The scope of this cohort is to stratify patients for the appearance of a second post-MI event, the genomic sequence of patients in order to unravel novel genetic locus involved in MI and the transcriptomic profile of a patient right after the MI event and six months after in order to compare upregulation or downregulation of genes indicating the corresponding mechanisms that are activated after MI.

Our participation in the GRMIC cohort was the recrutiment of patients via collaborations with General Hospitals in Athens, the sample collection, manipulation and storage, the questionaire-based interview for recording information about environmental risk factors and the stratification of the biomarkers after measuring their corresponding levels in the plasma of each patient. Thus far, the number of recruited patients who were re-examined is quite small (66 patients) and this study is open and ongoing till the appropiate sample number is collected in order to proceed with the designed analyses. Nevertheless, we did measure the concentration levels of selected biomarkers from the plasma of 66 pair samples and compared the two time points in all patients, independently of whether they had a post-MI event during the six moth period (since only 3 patients had a recurrent event)

- Total cholesterol, low-density lipoprotein cholesterol, apolipoprotein-B, C-reactive protein and creatine phosphokinase are **significantly higher at the time of first MI event**, whereas
- High-density lipoprotein cholesterol, glucose, triglycerides, uric acid and lipoprotein a **didn't show alteration** to plasma levels between the two time points

It is not a surprise, that at the time of myocardial infarction event, the traditional risk factors of lipids and C-reactive protein and creatine phosphokinase were elevated. It is a confirmation that these biomarkers are indicative of risk for CAD occurrence and can act as prognostic measure. The rest of the biomarkers that were measured didn't change their

concentration levels. This could be due to the small size that covered possible minor changes or that these factors do not play such a drastic role in the acute appearance of CAD. It will be confirmed at the completion of the study when the sample size meets the required patient recruitment. GRMIC is an onward prospective population study which has been designed based on the limited knowledge about the recurrent MI events after the occurrence of the first. Thorough study needs to be conducted in order to fill the missing information about the post-MI events in combination with other traditional environmental risk factors and GRMIC aims to contribute to that in the near future.

6. References

Acs, A. *et al.* (2017) 'Economic Burden of Cardiovascular Disease In Type 2 Diabetes: A Systematic Review', *Value in Health*, 20(9), pp. A476–A477. doi: 10.1016/j.jval.2017.08.443.

Albadri, S., Del Bene, F. and Revenu, C. (2017) 'Genome editing using CRISPR/Cas9-based knock-in approaches in zebrafish', *Methods*, 121–122(March 2017), pp. 77–85. doi: 10.1016/j.ymeth.2017.03.005.

Alter, S. *et al.* (2020) 'Telangiectasia-ectodermal dysplasia-brachydactyly-cardiac anomaly syndrome is caused by de novo mutations in protein kinase D1', *Journal of Medical Genetics*, pp. 1–7. doi: 10.1136/jmedgenet-2019-106564.

Alwan, A. and MacLean, D. R. (2009) 'A review of non-communicable disease in low- and middle-income countries', *International Health*, 1(1), pp. 3–9. doi: 10.1016/j.inhe.2009.02.003.

Aragam, K. G. *et al.* (2021) 'Discovery and systematic characterization of risk variants and genes for coronary artery disease in over a million participants', *medRxiv*. doi: 10.1101/2021.05.24.21257377

Arnaout, R. *et al.* (2007) 'Zebrafish model for human long QT syndrome', *Proceedings of the National Academy of Sciences*, 104(27), pp. 11316–11321. doi: 10.1073/pnas.0702724104.

Arnett, D. K. *et al.* (2019) *2019 ACC/AHA Guideline on the Primary Prevention of Cardiovascular Disease: A Report of the American College of Cardiology/American Heart Association Task Force on Clinical Practice Guidelines*, *Circulation*. doi: 10.1161/CIR.0000000000000678.

Arnold, S. V. *et al.* (2012) 'Perceived stress in myocardial infarction: Long-term mortality and health status outcomes', *Journal of the American College of Cardiology*, 60(18), pp. 1756–1763. doi: 10.1016/j.jacc.2012.06.044.

Asakawa, K. and Kawakami, K. (2008) 'Targeted gene expression by the Gal4-UAS system in zebrafish', *Development Growth and Differentiation*, 50(6), pp. 391–399. doi: 10.1111/j.1440-169X.2008.01044.x.

Auman, H. J. *et al.* (2007) 'Functional modulation of cardiac form through regionally confined cell shape changes', *PLoS Biology*, 5(3), pp. 0604–0615. doi: 10.1371/journal.pbio.0050053.

Avdesh, A. *et al.* (2012) 'Regular care and maintenance of a Zebrafish (Danio rerio) laboratory: An introduction', *Journal of Visualized Experiments*, (69). doi: 10.3791/4196.

Bachmann, J. M. *et al.* (2012) 'Association between family history and coronary heart disease death across long-term follow-up in men: The cooper center longitudinal study', *Circulation*, 125(25), pp. 3092–3098. doi: 10.1161/CIRCULATIONAHA.111.065490.

Bahreini, A. (2019) 'Association between Dietary Intakes of Tea , Coffee , and Soft Drinks in Patients Undergoing Coronary Angiography with Coronary Artery Stenosis', *international journal of preventive medicine*, 10(172), pp. 1–5. doi: 10.4103/ijpvm.IJPVM.

Baker, K., Holtzman, N. G. and Burdine, R. D. (2008) 'Direct and indirect roles for Nodal signaling in two axis conversions during asymmetric morphogenesis of the zebrafish heart', *Proceedings of the National Academy of Sciences of the United States of America*, 105(37), pp. 13924–13929. doi: 10.1073/pnas.0802159105.

Bakkers, J. (2011) 'Zebrafish as a model to study cardiac development and human cardiac disease', *Cardiovascular Research*, 91(2), pp. 279–288. doi: 10.1093/cvr/cvr098.

Battista, N. A. *et al.* (2019) *Vortex dynamics in trabeculated embryonic ventricles*, *Journal of Cardiovascular Development and Disease*. doi: 10.3390/JCDD6010006.

Bayraktar, M. and Männer, J. (2014) 'Cardiac looping may be driven by compressive loads resulting from unequal growth of the heart and pericardial cavity. Observations on a physical simulation model', *Frontiers in Physiology*, 5 APR(April), pp. 1–15. doi: 10.3389/fphys.2014.00112.

Becker, J. (2008) 'Cardiovascular Risk Assessment and Hyperlipidemia', *Critical Care Nursing Clinics of North America*, 20(3), pp. 277–285. doi: 10.1016/j.ccell.2008.03.014.

Bedell, V. M. *et al.* (2012) 'In vivo genome editing using a high-efficiency TALEN system', *Nature*, 491(7422), pp. 114–118. doi: 10.1038/nature11537.

Begemann, G. and Ingham, P. W. (2000) 'Developmental regulation of Tbx5 in zebrafish embryogenesis', *Mechanisms of Development*, 90(2), pp. 299–304. doi: 10.1016/S0925-4773(99)00246-4.

Beis D, Bartman T, Jin SW, Scott IC, D'Amico LA, Ober EA, Verkade H, F. and J, Field HA, Wehman A, Baier H, Tallafuss A, Bally-Cuif L, Chen JN, Stainier DY, J. B. (2005) 'Genetic and cellular analyses of zebrafish atrioventricular cushion and valve development', *Development*, 132(18), pp. 4193–4204. doi: 10.1242/dev.01970.

Beis, D. *et al.* (2005) 'Genetic and cellular analyses of zebrafish atrioventricular cushion and valve development', *Development*, 132(18), pp. 4193–4204. doi: 10.1242/dev.01970.

Beis, D., Kalogirou, S. and Tsigkas, N. (2015) *Insights into Heart Development and Regeneration*, *Introduction to Translational Cardiovascular Research*. doi: 10.1007/978-3-319-08798-6.

Ben-Aicha, S., Badimon, L. and Vilahur, G. (2020) 'Advances in HDL: Much more than lipid transporters', *International Journal of Molecular Sciences*, 21(3). doi: 10.3390/ijms21030732.

Benedikt von der Heyde, Anastasia Emmanouilidou, Tiffany Klingström, Eugenia Mazzaferro, Silvia Vicenzi, Sitaf Jumaa, Olga Dethlefsen, Harold Snieder, Eco de Geus, Erik Ingelsson, Amin Allalou, Hannah L Brooke, M. den H. In Vivo Characterization of Candidate Genes for Heart Rate Variability Identifies Culprits for Sinoatrial Pauses and Arrests. *bioRxiv* **2018**, 1–5. https://doi.org/https://doi.org/10.1101/385500.

Benn, M. (2009) 'Apolipoprotein B levels, APOB alleles, and risk of ischemic cardiovascular disease in the general population, a review', *Atherosclerosis*, 206(1), pp. 17–30. doi: 10.1016/j.atherosclerosis.2009.01.004.

Benziger, C. P., Roth, G. A. and Moran, A. E. (2016) 'The Global Burden of Disease Study and the Preventable Burden of NCD', *Global Heart*, 11(4), pp. 393–397. doi: 10.1016/j.gheart.2016.10.024.

Bernatik, O. *et al.* (2020) 'Phosphorylation of multiple proteins involved in ciliogenesis by Tau Tubulin kinase 2', *Molecular Biology of the Cell*, 31(10), pp. 1032–1046. doi: 10.1091/MBC.E19-06-0334.

Bhatt, A. and Rohatgi, A. (2016) 'HDL Cholesterol Efflux Capacity: Cardiovascular Risk Factor and Potential Therapeutic Target', *Current Atherosclerosis Reports*, 18(1), pp. 1–8. doi: 10.1007/s11883-015-0554-1.

Bittles, A. H. and Black, M. L. (2010) 'Consanguinity, human evolution, and complex diseases', *Proceedings of the National Academy of Sciences of the United States of America*, 107(SUPPL. 1), pp. 1779–1786. doi: 10.1073/pnas.0906079106.

Boardman-Pretty, F. *et al.* (2015) 'Functional Analysis of a Carotid Intima-Media Thickness Locus Implicates BCAR1 and Suggests a Causal Variant', *Circulation: Cardiovascular Genetics*, 8(5), pp. 696–706. doi: 10.1161/CIRCGENETICS.115.001062.

Boezio, G. L. M. *et al.* (2020) 'Endothelial TGF-β signaling instructs smooth muscle development in the cardiac outflow tract', *bioRxiv*, pp. 1–32. doi: 10.1101/2020.01.30.925412.

Bournele, D. and Beis, D. (2016) 'Zebrafish models of cardiovascular disease', *Heart Failure Reviews*, 21(6), pp. 803–813. doi: 10.1007/s10741-016-9579-y.

Bovet, P. and Paccaud, F. (2011) 'Cardiovascular Disease and the Changing Face of Global Public Health: A Focus on Low and Middle Income Countries', *Public Health Reviews*, 33(2), pp. 397–415. doi: 10.1007/bf03391643.

Bruning, R. S. and Sturek, M. (2015) 'Benefits of Exercise Training on Coronary Blood Flow in Coronary Artery Disease Patients', *Progress in Cardiovascular Diseases*, 57(5), pp. 443–453. doi: 10.1016/j.pcad.2014.10.006.

Buckingham, M., Meilhac, S. and Zaffran, S. (2005) 'Building the mammalian heart from two sources of myocardial cells', *Nature Reviews Genetics*, 6(11), pp. 826–835. doi: 10.1038/nrg1710.

Burkhard, S. B. and Bakkers, J. (2018) 'Spatially resolved RNA-sequencing of the embryonic heart identifies a role for Wnt/β-catenin signaling in autonomic control of heart rate', *eLife*, 7, pp. 1–19. doi: 10.7554/eLife.31515.

Bycroft, C. *et al.* (2018) 'The UK Biobank resource with deep phenotyping and genomic data', *Nature*, 562(7726), pp. 203–209. doi: 10.1038/s41586-018-0579-z.

Cade, L. *et al.* (2012) 'Highly efficient generation of heritable zebrafish gene mutations using homo-and heterodimeric TALENs', *Nucleic Acids Research*, 40(16), pp. 8001–8010. doi: 10.1093/nar/gks518.

Carbone, S. *et al.* (2020) 'The Impact of Obesity in Heart Failure', *Heart Failure Clinics*, 16(1), pp.

71–80. doi: 10.1016/j.hfc.2019.08.008.

Carnethon, M. R. *et al.* (2017) *Cardiovascular Health in African Americans: A Scientific Statement From the American Heart Association*, *Circulation*. doi: 10.1161/CIR.0000000000000534.

Carney, T. J. and Mosimann, C. (2018) 'Switch and Trace: Recombinase Genetics in Zebrafish', *Trends in Genetics*, 34(5), pp. 362–378. doi: 10.1016/j.tig.2018.01.004.

Celauro, E. *et al.* (2017a) 'Functional analysis of the cfdp1 gene in zebrafish provides evidence for its crucial role in craniofacial development and osteogenesis', *Experimental Cell Research*, 361(2), pp. 236–245. doi: 10.1016/j.yexcr.2017.10.022.

Celauro, E. *et al.* (2017b) 'Functional analysis of the cfdp1 gene in zebrafish provides evidence for its crucial role in craniofacial development and osteogenesis', *Experimental Cell Research*, 361(2), pp. 236–245. doi: 10.1016/j.yexcr.2017.10.022.

Cermak, T. *et al.* (2011) 'Efficient design and assembly of custom TALEN and other TAL effector-based constructs for DNA targeting', *Nucleic Acids Research*, 39(12), pp. 1–11. doi: 10.1093/nar/gkr218.

Chaki, M. *et al.* (2012) 'Exome capture reveals ZNF423 and CEP164 mutations, linking renal ciliopathies to DNA damage response signaling', *Cell*, 150(3), pp. 533–548. doi: 10.1016/j.cell.2012.06.028.

Chan, M. Y. *et al.* (2020) 'Prioritizing Candidates of Post-Myocardial Infarction Heart Failure Using Plasma Proteomics and Single-Cell Transcriptomics', *Circulation*, pp. 1408–1421. doi: 10.1161/CIRCULATIONAHA.119.045158.

Chang, N. *et al.* (2013) 'Genome editing with RNA-guided Cas9 nuclease in Zebrafish embryos', *Cell research*, 23(4), pp. 465–472. doi: 10.1038/cr.2013.45.

Chapman, D. L. *et al.* (1996) 'Expression of the T-box family genes, Tbx1-Tbx5, during early mouse development', *Developmental Dynamics*, 206(4), pp. 379–390. doi: 10.1002/(SICI)1097-0177(199608)206:4<379::AID-AJA4>3.0.CO;2-F.

Chasman, D. I. *et al.* (2009) 'Forty-three loci associated with plasma lipoprotein size, concentration, and cholesterol content in genome-wide analysis', *PLoS Genetics*, 5(11). doi: 10.1371/journal.pgen.1000730.

Chen, H. *et al.* (2004) 'BMP10 is essential for maintaining cardiac growth during murine cardiogenesis', *Development*, 131(9), pp. 2219–2231. doi: 10.1242/dev.01094.

Chen, J. *et al.* (2008) 'Selective binding of phorbol esters and diacylglycerol by individual C1 domains of the PKD family', *Biochemical Journal*, 411(2), pp. 333–342. doi: 10.1042/BJ20071334.

Cherian, A. V. *et al.* (2016) 'N-cadherin relocalization during cardiac trabeculation', *Proceedings of the National Academy of Sciences of the United States of America*, 113(27), pp. 7569–7574. doi: 10.1073/pnas.1606385113.

Chi, N. C. *et al.* (2008) 'Genetic and physiologic dissection of the vertebrate cardiac conduction system', *PLoS Biology*, 6(5), pp. 1006–1019. doi: 10.1371/journal.pbio.0060109.

Chu, W. T. and Wang, J. (2021) 'Influence of sequence length and charged residues on Swc5 binding with histone H2A-H2B', *Proteins: Structure, Function and Bioinformatics*, 89(5), pp. 512–520. doi: 10.1002/prot.26035.

Danaei, G. *et al.* (2009) 'The preventable causes of death in the United States: Comparative risk assessment of dietary, lifestyle, and metabolic risk factors', *PLoS Medicine*, 6(4). doi: 10.1371/journal.pmed.1000058.

Davison, J. M. *et al.* (2007) 'Transactivation from Gal4-VP16 transgenic insertions for tissue-specific cell labeling and ablation in zebrafish', *Developmental Biology*, 304(2), pp. 811–824. doi: 10.1016/j.ydbio.2007.01.033.

Deloukas, P. *et al.* (2013) 'Large-scale association analysis identifies new risk loci for coronary artery disease', *Nature Genetics*, 45(1), pp. 25–33. doi: 10.1038/ng.2480.

Diekwisch, T. G. H. *et al.* (1999) 'Cloning, gene expression, and characterization of CP27, a novel gene in mouse embryogenesis', *Gene*, 235(1–2), pp. 19–30. doi: 10.1016/S0378-1119(99)00220-6.

Diekwisch, T. G. H., Luan, X. and McIntosh, J. E. (2002) 'CP27 localization in the dental lamina basement membrane and in the stellate reticulum of developing teeth', *Journal of Histochemistry and Cytochemistry*, 50(4), pp. 583–586. doi: 10.1177/002215540205000416.

Dina C, Bouatia-Naji N, Tucker N, Delling FN, Toomer K, Durst R, Perrocheau M, Fernandez-Friera L, Solis J; PROMESA investigators, Le Tourneau T, Chen MH, Probst V, Bosse Y, Pibarot P, Zelenika D, Lathrop M, Hercberg S, Roussel R, Benjamin EJ, Bonnet F, L, J. X. L. T. M. N. Genetic Association Analyses Highlight Biological Pathways Underlying Mitral Valve Prolapse. *Nat. Genet.* **2015**, *47* (10), 1206–1211. https://doi.org/10.1161/CIRCULATIONAHA.114.010270.Hospital.

Dobrzycki, T., Krecsmarik, M. and Monteiro, R. (2020) 'Genotyping and quantification of in situ hybridization staining in zebrafish', *Journal of Visualized Experiments*, (155), pp. 1–7. doi: 10.3791/59956.

Dong, Y., Qian, L. and Liu, J. (2021) 'Molecular and cellular basis of embryonic cardiac chamber maturation', *Seminars in Cell and Developmental Biology*, 118(January), pp. 144–149. doi: 10.1016/j.semcdb.2021.04.022.

Doudna, J. A. (2020) 'The promise and challenge of therapeutic genome editing', *Nature*, 578(7794), pp. 229–236. doi: 10.1038/s41586-020-1978-5.

Doyon, Y. *et al.* (2008) 'Heritable targeted gene disruption in zebrafish using designed zinc-finger nucleases', *Nature Biotechnology*, 26(6), pp. 702–708. doi: 10.1038/nbt1409.

Duchemin, A. L., Vignes, H. and Vermot, J. (2019) 'Mechanically activated Piezo channels modulate outflow tract valve development through Yap1 and Klf2-Notch signaling axis', *bioRxiv*,

pp. 1–27. doi: 10.1101/529016.

Elagizi, A. *et al.* (2018) 'An Overview and Update on Obesity and the Obesity Paradox in Cardiovascular Diseases', *Progress in Cardiovascular Diseases*, 61(2), pp. 142–150. doi: 10.1016/j.pcad.2018.07.003.

Enas, E. A. *et al.* (2019) 'Lipoprotein(a): An independent, genetic, and causal factor for cardiovascular disease and acute myocardial infarction', *Indian Heart Journal*, 71(2), pp. 99–112. doi: 10.1016/j.ihj.2019.03.004.

Farr GH 3rd, Imani K, Pouv D, M. L. Functional Testing of a Human PBX3 Variant in Zebrafish Reveals a Potential Modifier Role in Congenital Heart Defects. *Dis. Model. Mech.* **2018**, *11* (10). https://doi.org/10.1242/dmm.035972.

Faure, G., Makarova, K. S. and Koonin, E. V. (2019) 'CRISPR–Cas: Complex Functional Networks and Multiple Roles beyond Adaptive Immunity', *Journal of Molecular Biology*, 431(1), pp. 3–20. doi: 10.1016/j.jmb.2018.08.030.

Felker, A. and Mosimann, C. (2016) *Contemporary zebrafish transgenesis with Tol2 and application for Cre/lox recombination experiments*, *Methods in Cell Biology*. Elsevier Ltd. doi: 10.1016/bs.mcb.2016.01.009.

Ferese, R.; Bonetti, M.; Consoli, F.; Guida, V.; Sarkozy, A.; Lepri, F. R.; Versacci, P.; Gambardella, S.; Calcagni, G.; Margiotti, K.; et al. Heterozygous Missense Mutations in NFATC1 Are Associated with Atrioventricular Septal Defect. *Hum. Mutat.* **2018**, *39* (10), 1428–1441. https://doi.org/10.1002/humu.23593

Fielitz, J. *et al.* (2008) 'Requirement of protein kinase D1 for pathological cardiac remodeling', *Proceedings of the National Academy of Sciences of the United States of America*, 105(8), pp. 3059–3063. doi: 10.1073/pnas.0712265105.

Flynn, E. J., Trent, C. M. and Rawls, J. F. (2009) 'Ontogeny and nutritional control of adipogenesis in zebrafish (Danio rerio).', *Journal of lipid research*, 50(8), pp. 1641–52. doi: 10.1194/jlr.M800590-JLR200.

Franco, O. H. *et al.* (2007) 'Associations of diabetes mellitus with total life expectancy and life expectancy with and without cardiovascular disease', *Archives of Internal Medicine*, 167(11), pp. 1145–1151. doi: 10.1001/archinte.167.11.1145.

Gagnon, J. A. *et al.* (2014) 'Efficient mutagenesis by Cas9 protein-mediated oligonucleotide insertion and large-scale assessment of single-guide RNAs', *PLoS ONE*, 9(5), pp. 5–12. doi: 10.1371/journal.pone.0098186.

Gaj, T., Gersbach, C. A. and Barbas, C. F. (2013) 'ZFN, TALEN, and CRISPR/Cas-based methods for genome engineering', *Trends in Biotechnology*. Elsevier Current Trends, pp. 397–405. doi: 10.1016/j.tibtech.2013.04.004.

Galasso, G. *et al.* (2021) 'Predictors of Recurrent Ischemic Events in Patients With ST-Segment Elevation Myocardial Infarction', *American Journal of Cardiology*, 159, pp. 44–51. doi:

10.1016/j.amjcard.2021.08.019.

Gao, R. and Ren, J. (2021) 'Zebrafish Models in Therapeutic Research of Cardiac Conduction Disease', *Frontiers in Cell and Developmental Biology*, 9(August), pp. 1–10. doi: 10.3389/fcell.2021.731402.

Garcia-Robledo, J. E., Barrera, M. C. and Tobón, G. J. (2020) 'CRISPR/Cas: from adaptive immune system in prokaryotes to therapeutic weapon against immune-related diseases: CRISPR/Cas9 offers a simple and inexpensive method for disease modeling, genetic screening, and potentially for disease therapy', *International Reviews of Immunology*, 39(1), pp. 11–20. doi: 10.1080/08830185.2019.1677645.

Garrity, D. M., Childs, S. and Fishman, M. C. (2002) 'The heartstrings mutation in zebrafish causes heart/fin Tbx5 deficiency syndrome', *Development*, 129(19), pp. 4635–4645.

Gassmann, M. *et al.* (1995) 'Aberrant neural and cardiac development in mice lacking the ErbB4 neuregulin receptor', 378(November), pp. 390–394.

Gawdzik, J. C. *et al.* (2018) 'sox9b Is Required in Cardiomyocytes for Cardiac Morphogenesis and Function', *Scientific Reports*, 8(1), pp. 1–16. doi: 10.1038/s41598-018-32125-7.

Gerber, Y., Weston, S. A., Enriquez-Sarano, M., Manemann, S. M., *et al.* (2016) 'Atherosclerotic burden and heart failure after myocardial infarction', *JAMA Cardiology*, 1(2), pp. 156–162. doi: 10.1001/jamacardio.2016.0074.

Gerber, Y., Weston, S. A., Enriquez-Sarano, M., Berardi, C., *et al.* (2016) 'Mortality Associated with Heart Failure after Myocardial Infarction: A Contemporary Community Perspective', *Circulation: Heart Failure*, 9(1), pp. 1–9. doi: 10.1161/CIRCHEARTFAILURE.115.002460.

Gerety, S. S. *et al.* (1999) 'Symmetrical mutant phenotypes of the receptor EphB4 and its specific transmembrane ligand ephrin-B2 in cardiovascular development', *Molecular Cell*, 4(3), pp. 403–414. doi: 10.1016/S1097-2765(00)80342-1.

Gertler, M. M., Garn, S. M. and White, P. D. (1951) 'Young candidates for coronary heart disease', *JAMA*, 147(7), pp. 621–625.

Gertow, K. *et al.* (2012) 'Identification of the BCAR1-CFDP1-TMEM170A locus as a determinant of carotid intima-media thickness and coronary artery disease risk', *Circulation: Cardiovascular Genetics*, 5(6), pp. 656–665. doi: 10.1161/CIRCGENETICS.112.963660.

Gheorghe, A. *et al.* (2018) 'The economic burden of cardiovascular disease and hypertension in low- and middle-income countries: A systematic review', *BMC Public Health*, 18(1), pp. 1–11. doi: 10.1186/s12889-018-5806-x.

Ghosh, T. K. *et al.* (2019) 'HDAC4 and 5 repression of TBX5 is relieved by protein kinase D1', *Scientific Reports*, 9(1), pp. 1–10. doi: 10.1038/s41598-019-54312-w.

Giardoglou, P. *et al.* (2021) 'A zebrafish forward genetic screen identifies an indispensable threonine residue in the kinase domain of PRKD2', *Biology Open*, 10(3), pp. 1–11. doi: 10.1242/bio.058542.

Giardoglou, P. and Beis, D. (2019) 'On zebrafish disease models and matters of the heart', *Biomedicines*. MDPI AG. doi: 10.3390/biomedicines7010015.

Gibson-Brown, J. J. *et al.* (1998) 'Expression of T-box genes Tbx2–Tbx5 during chick organogenesis', *Mechanisms of Development*, 74(1–2), pp. 165–169. doi: 10.1016/S0925-4773(98)00056-2.

Gillers, B. S. *et al.* (2014) 'Canonical Wnt signaling regulates atrioventricular junction programming and electrophysiological properties', *Circulation Research*, 116(3), pp. 398–406. doi: 10.1161/CIRCRESAHA.116.304731.

Gordon, T. *et al.* (1977) 'High density lipoprotein as a protective factor against coronary heart disease. The Framingham study', *The American Journal of Medicine*, 62(5), pp. 707–714. doi: 10.1016/0002-9343(77)90874-9.

Green, G. (2015) 'Nicotine replacement therapy for smoking cessation', *American Family Physician*, 92(1), pp. 24A-24B.

Grego-Bessa, J. *et al.* (2007) 'Notch Signaling Is Essential for Ventricular Chamber Development', *Developmental Cell*, 12(3), pp. 415–429. doi: 10.1016/j.devcel.2006.12.011.

Grimes, D. T. *et al.* (2020) 'Left-right asymmetric heart jogging increases the robustness of dextral heart looping in zebrafish', *Developmental Biology*, 459(2), pp. 79–86. doi: 10.1016/j.ydbio.2019.11.012.

Grundy, S. M. *et al.* (1999) 'Assessment of cardiovascular risk by use of multiple-risk-factor assessment equations: A statement for healthcare professionals from the American Heart Association and the American College of Cardiology', *Circulation*, 100(13), pp. 1481–1492. doi: 10.1161/01.CIR.100.13.1481.

Gunawan, F. *et al.* (2020) 'Nfatc1 promotes interstitial cell formation during cardiac valve development in Zebrafish', *Circulation Research*, pp. 968–984. doi: 10.1161/CIRCRESAHA.119.315992.

Guo, J. *et al.* (2011) 'Protein kinase D isoforms are activated in an agonist-specific manner in cardiomyocytes', *Journal of Biological Chemistry*, 286(8), pp. 6500–6509. doi: 10.1074/jbc.M110.208058.

Gupta, G. D. *et al.* (2015) 'A Dynamic Protein Interaction Landscape of the Human Centrosome-Cilium Interface', *Cell*, 163(6), pp. 1484–1499. doi: 10.1016/j.cell.2015.10.065.

Gut, P. *et al.* (2017) 'Little Fish, Big Data: Zebrafish As a Model for Cardiovascular and Metabolic Disease', *Physiological Reviews*, 97(3), pp. 889–938. doi: 10.1152/physrev.00038.2016.

Hami, D. *et al.* (2011) 'Zebrafish cardiac development requires a conserved secondary heart field', *Development*, 138(11), pp. 2389–2398. doi: 10.1242/dev.061473.

Hans, S. *et al.* (2021) 'Cre-Controlled CRISPR mutagenesis provides fast and easy conditional gene inactivation in zebrafish', *Nature Communications*, 12(1125), pp. 1–12. doi: 10.1038/s41467-021-21427-6.

Harries, A. D. *et al.* (2015) 'Communicable and non-communicable diseases: connections, synergies and benefits of integrating care', *Public Health Action*, 5(3), pp. 156–157.

Van Der Harst, P. and Verweij, N. (2018) 'Identification of 64 novel genetic loci provides an expanded view on the genetic architecture of coronary artery disease', *Circulation Research*, 122(3), pp. 433–443. doi: 10.1161/CIRCRESAHA.117.312086.

Hayashi, A. *et al.* (1999) 'PKCν, a new member of the protein kinase C family, composes a fourth subfamily with PKCμ', *Biochimica et Biophysica Acta (BBA) - Molecular Cell Research*, 1450(1), pp. 99–106. doi: 10.1016/S0167-4889(99)00040-3.

Hoage, T.; Ding, Y.; Xu, X. (2012) 'Cardiovascular development: structure and molecular mechanism', *Anatomical science international*, 84(3), pp. 65–66. doi: 10.1007/978-1-61779-523-7.

Hodgson, P., Ireland, J. and Grunow, B. (2018) 'Fish, the better model in human heart research? Zebrafish Heart aggregates as a 3D spontaneously cardiomyogenic in vitro model system', *Progress in Biophysics and Molecular Biology*. doi: 10.1016/j.pbiomolbio.2018.04.009.

Hollenbach, M. *et al.* (2013) 'Different Regulation of Physiological and Tumor Angiogenesis in Zebrafish by Protein Kinase D1 (PKD1)', *PLoS ONE*. Edited by K. Datta, 8(7), p. e68033. doi: 10.1371/journal.pone.0068033.

Hoshijima, K. *et al.* (2019) 'Highly Efficient CRISPR-Cas9-Based Methods for Generating Deletion Mutations and F0 Embryos that Lack Gene Function in Zebrafish', *Developmental Cell*, 51(5), pp. 645-657.e4. doi: 10.1016/j.devcel.2019.10.004.

Howe, K. *et al.* (2013) 'The zebrafish reference genome sequence and its relationship to the human genome', *Nature*, 496(7446), pp. 498–503. doi: 10.1038/nature12111.

Hsu, P. D., Lander, E. S. and Zhang, F. (2014) 'Development and applications of CRISPR-Cas9 for genome engineering', *Cell*. Elsevier B.V., pp. 1262–1278. doi: 10.1016/j.cell.2014.05.010.

Hu, N. *et al.* (2000) 'Structure and Function of the Developing Zebrafish Heart', *The Anatomical Record*, 260(July), pp. 148–157. doi: 10.1002/1097-0185(20001001)260:2<148::AID-AR50>3.0.CO;2-X.

Huang, L. O. *et al.* (2021) 'Genome-wide discovery of genetic loci that uncouple excess adiposity from its comorbidities', *Nature Metabolism*, 3(2), pp. 228–243. doi: 10.1038/s42255-021-00346-2.

Huxley, R. (2015) 'Risk factors: Smoking and CAD - What's plaque got to do with it?', *Nature Reviews Cardiology*, 12(5), pp. 265–266. doi: 10.1038/nrcardio.2015.37.

Hwang, W. Y. *et al.* (2013) 'Efficient genome editing in zebrafish using a CRISPR-Cas system.', *Nature biotechnology*, 31(3), pp. 227–9. doi: 10.1038/nbt.2501.

Iglesias, T., Matthews, S. and Rozengurt, E. (1998) 'Dissimilar phorbol ester binding properties of the individual cysteine-rich motifs of protein kinase D', *FEBS Letters*, 437(1–2), pp. 19–23. doi: 10.1016/S0014-5793(98)01189-2.

Iglesias, T. and Rozengurt, E. (1998) 'Protein kinase D activation by mutations within its pleckstrin homology domain', *Journal of Biological Chemistry*, 273(1), pp. 410–416. doi: 10.1074/jbc.273.1.410.

Iglesias, T. and Rozengurt, E. (1999) 'Protein kinase D activation by deletion of its cysteine-rich motifs', *FEBS Letters*, 454(1–2), pp. 53–56. doi: 10.1016/S0014-5793(99)00772-3.

Iida, A. *et al.* (2018) 'Integrin β1 activity is required for cardiovascular formation in zebrafish', *Genes to Cells*, 23(11), pp. 938–951. doi: 10.1111/gtc.12641.

Iwashita, S. *et al.* (2015) 'Mammalian Bcnt/Cfdp1, a potential epigenetic factor characterized by an acidic stretch in the disordered N-terminal and Ser250 phosphorylation in the conserved C-terminal regions', *Bioscience Reports*, 35(4), pp. 1–12. doi: 10.1042/BSR20150111.

Iwashita, S. *et al.* (2020) 'Overcoming off-targets: Assessing Western blot signals for Bcnt/Cfdp1, a tentative component of the chromatin remodeling complex', *Bioscience Reports*, 40(6), pp. 1–16. doi: 10.1042/BSR20194012.

Jahangir, E., De Schutter, A. and Lavie, C. J. (2014) 'The relationship between obesity and coronary artery disease', *Translational Research*, 164(4), pp. 336–344. doi: 10.1016/j.trsl.2014.03.010.

Jansen, H., Samani, N. J. and Schunkert, H. (2014) 'Mendelian randomization studies in coronary artery disease', *European Heart Journal*, 35(29), pp. 1917–1924. doi: 10.1093/eurheartj/ehu208.

Jao, L. E., Wente, S. R. and Chen, W. (2013) 'Efficient multiplex biallelic zebrafish genome editing using a CRISPR nuclease system', *Proceedings of the National Academy of Sciences of the United States of America*, 110(34), pp. 13904–13909. doi: 10.1073/pnas.1308335110.

Jernberg, T. *et al.* (2015) 'Cardiovascular risk in post-myocardial infarction patients: Nationwide real world data demonstrate the importance of a long-term perspective', *European Heart Journal*, 36(19), pp. 1163-1170a. doi: 10.1093/eurheartj/ehu505.

Jiménez-Amilburu, V. *et al.* (2016) 'In Vivo Visualization of Cardiomyocyte Apicobasal Polarity Reveals Epithelial to Mesenchymal-like Transition during Cardiac Trabeculation', *Cell Reports*, 17(10), pp. 2687–2699. doi: 10.1016/j.celrep.2016.11.023.

Jiménez-Amilburu, V. and Stainier, D. Y. R. (2019) 'The transmembrane protein Crb2a regulates cardiomyocyte apicobasal polarity and adhesion in zebrafish', *Development (Cambridge)*, 146(9). doi: 10.1242/dev.171207.

Johnson, K. R. *et al.* (2015) 'Genome-Wide Gene Expression Analysis Shows AKAP13-Mediated PKD1 Signaling Regulates the Transcriptional Response to Cardiac Hypertrophy', *PLOS ONE*. Edited by S. Gupta, 10(7), p. e0132474. doi: 10.1371/journal.pone.0132474.

Joseph, P. *et al.* (2017) 'Reducing the global burden of cardiovascular disease, part 1: The epidemiology and risk factors', *Circulation Research*, 121(6), pp. 677–694. doi: 10.1161/CIRCRESAHA.117.308903.

Jurczyk, A. *et al.* (2011) 'Dynamic glucoregulation and mammalian-like responses to metabolic and developmental disruption in zebrafish', *General and Comparative Endocrinology*, 170(2), pp. 334–345. doi: 10.1016/j.ygcen.2010.10.010.

Just, S. *et al.* (2011) 'Protein kinase D2 controls cardiac valve formation in zebrafish by regulating histone deacetylase 5 activity', *Circulation*. doi: 10.1161/CIRCULATIONAHA.110.003301.

Kalogirou, S. *et al.* (2014) 'Intracardiac flow dynamics regulate atrioventricular valve morphogenesis', *Cardiovascular Research*, 104(1), pp. 49–60. doi: 10.1093/cvr/cvu186.

Kamstrup, P. R. *et al.* (2009) 'Genetically Elevated Lipoprotein (a)', *The Journal of the American Medical Association*, 301(22), pp. 2331–2339.

Kannel, W. B. (2009) 'Hypertension: Reflections on Risks and Prognostication', *Medical Clinics of North America*, 93(3), pp. 541–558. doi: 10.1016/j.mcna.2009.02.006.

Kannel, W. B., Sorlie, P. and Mcnamara, P. M. (1979) 'Prognosis after initial myocardial infarction: The Framingham study', *The American Journal of Cardiology*, 44(1), pp. 53–59. doi: 10.1016/0002-9149(79)90250-9.

Kaptoge, S. *et al.* (2010) 'C-reactive protein concentration and risk of coronary heart disease, stroke, and mortality: An individual participant meta-analysis', *The Lancet*, 375(9709), pp. 132–140. doi: 10.1016/S0140-6736(09)61717-7.

Kaptoge, S. *et al.* (2019) 'World Health Organization cardiovascular disease risk charts: revised models to estimate risk in 21 global regions', *The Lancet Global Health*, 7(10), pp. e1332–e1345. doi: 10.1016/S2214-109X(19)30318-3.

Katta, N. *et al.* (2021) 'Obesity and Coronary Heart Disease: Epidemiology, Pathology, and Coronary Artery Imaging', *Current Problems in Cardiology*, 46(3), p. 100655. doi: 10.1016/j.cpcardiol.2020.100655.

Kerr, T. P. *et al.* (2001) 'Long mutant dystrophins and variable phenotypes: Evasion of nonsense-mediated decay?', *Human Genetics*, 109(4), pp. 402–407. doi: 10.1007/s004390100598.

Khajavi, M., Inoue, K. and Lupski, J. R. (2006) 'Nonsense-mediated mRNA decay modulates clinical outcome of genetic disease', *European Journal of Human Genetics*, 14(10), pp. 1074–1081. doi: 10.1038/sj.ejhg.5201649.

Khera, A. V. and Kathiresan, S. (2017) 'Genetics of coronary artery disease: Discovery, biology and clinical translation', *Nature Reviews Genetics*, 18(6), pp. 331–344. doi: 10.1038/nrg.2016.160.

Khetarpal, S. A. *et al.* (2018) 'Multiplexed Targeted Resequencing Identifies Coding and Regulatory Variation Underlying Phenotypic Extremes of High-Density Lipoprotein Cholesterol in Humans', *Circulation. Genomic and precision medicine*, 11(7), p. e002070. doi: 10.1161/CIRCGEN.117.002070.

Kim, M.-S. *et al.* (2008) 'Protein Kinase D1 Stimulates MEF2 Activity in Skeletal Muscle and Enhances Muscle Performance', *Molecular and Cellular Biology*, 28(11), pp. 3600–3609. doi: 10.1128/mcb.00189-08.

Klarin, D. *et al.* (2017) 'Genetic analysis in UK Biobank links insulin resistance and transendothelial migration pathways to coronary artery disease', *Nature Genetics*, 49(9), pp. 1392–1397. doi: 10.1038/ng.3914.

Klena, N. T., Gibbs, B. C. and Lo, C. W. (2017) 'Cilia and ciliopathies in congenital heart disease', *Cold Spring Harbor Perspectives in Biology*, 9(8). doi: 10.1101/cshperspect.a028266.

Koenig, W. *et al.* (1999) 'C-Reactive Protein, a Sensitive Marker of Inflammation, Predicts Future Risk of Coronary Heart Disease in Initially Healthy Middle-Aged Men Results From the MONICA (Monitoring Trends and Determinants in Cardiovascular Disease) Augsburg Cohort Study, 1984 ', *Circulation*, pp. 237–243.

Koenig, W. (2013) 'High-sensitivity C-reactive protein and atherosclerotic disease: From improved risk prediction to risk-guided therapy', *International Journal of Cardiology*, 168(6), pp. 5126–5134. doi: 10.1016/j.ijcard.2013.07.113.

Kok, F. O. *et al.* (2015) 'Reverse genetic screening reveals poor correlation between morpholino-induced and mutant phenotypes in zebrafish', *Developmental Cell*, 32(1), pp. 97–108. doi: 10.1016/j.devcel.2014.11.018.

König, M. *et al.* (2019) 'Cohort profile: Role of lipoproteins in cardiovascular disease - The LipidCardio study', *BMJ Open*, 9(9), pp. 1–6. doi: 10.1136/bmjopen-2019-030097.

Kreft, L. *et al.* (2017) 'ConTra v3: A tool to identify transcription factor binding sites across species, update 2017', *Nucleic Acids Research*, 45(W1), pp. W490–W494. doi: 10.1093/nar/gkx376.

Kruse, J. M. *et al.* (2014) 'Weak diagnostic performance of troponin, creatine kinase and creatine kinase-MB to diagnose or exclude myocardial infarction after successful resuscitation', *International Journal of Cardiology*, 173(2), pp. 216–221. doi: 10.1016/j.ijcard.2014.02.033.

Kurosaki, T. and Maquat, L. E. (2016) 'Nonsense-mediated mRNA decay in humans at a glance', *Journal of Cell Science*, 129(3), pp. 461–467. doi: 10.1242/jcs.181008.

Kuyper, A. M. G. and Honig, A. (2008) 'Treatment of post-myocardial infarction depressive disorder', *Expert Review of Neurotherapeutics*, 8(7), pp. 1115–1123. doi: 10.1586/14737175.8.7.1115.

de la Pompa JL, Timmerman LA, Takimoto H, Yoshida H, Elia AJ, Samper E, P. and J, Wakeham A, Marengere L, Langille BL, Crabtree GR, M. T. (1998) 'Role of the NF-ATc transcription factor in morphogenesis of cardiac valves and septum', *Nature*, 392(December), pp. 182–186.

Laakso, M. and Kuusisto, J. (1996) 'Epidemiological evidence for the association of hyperglycaemia and atherosclerotic vascular disease in non-insulin-dependent diabetes mellitus', *Annals of Medicine*, 28(5), pp. 415–418. doi: 10.3109/07853899608999101.

Lai, D. *et al.* (2010) 'Neuregulin 1 sustains the gene regulatory network in both trabecular and nontrabecular myocardium', *Circulation Research*, 107(6), pp. 715–727. doi: 10.1161/CIRCRESAHA.110.218693.

Langsted, A., Madsen, C. M. and Nordestgaard, B. G. (2020) 'Contribution of remnant cholesterol to cardiovascular risk', *Journal of Internal Medicine*, 288(1), pp. 116–127. doi: 10.1111/joim.13059.

Larzelere, M. M. and Williams, D. E. (2012) 'Promoting smoking cessation', *American Family Physician*, 85(6), pp. 591–598. doi: 10.1038/sj.bdj.4812328.

Law, M. R., Wald, N. J. and Thompson, S. G. (1994) 'By how much and how quickly does reduction in serum cholesterol concentration lower risk of ischaemic heart disease?', *Bmj*, 308(6925), p. 367. doi: 10.1136/bmj.308.6925.367.

Lee, K.-F. *et al.* (1995) 'Requirement for neuregulin receptor erbB2 in neural and cardiac development', *Nature*, 378(November), pp. 394–398. doi: 10.1007/978-3-662-22192-1_2.

Lehrman, M. A. *et al.* (1985) 'Mutation in LDL receptor: Alu-Alu recombination deletes exons encoding transmembrane and cytoplasmic domains', *Science*, 227(4683), pp. 140–146. doi: 10.1126/science.3155573.

Leong, D. P. *et al.* (2017) 'Reducing the global burden of cardiovascular disease, part 2: Prevention and treatment of cardiovascular disease', *Circulation Research*, 121(6), pp. 695–710. doi: 10.1161/CIRCRESAHA.117.311849.

Leong, I. U. S. *et al.* (2010) 'Zebrafish as a model for long QT syndrome: The evidence and the means of manipulating zebrafish gene expression', *Acta Physiologica*, 199(3), pp. 257–276. doi: 10.1111/j.1748-1716.2010.02111.x.

Levin, M. G. *et al.* (2021) 'Genetics of Smoking and Risk of Atherosclerotic Cardiovascular Diseases: A Mendelian Randomization Study', *JAMA network open*, 4(1), p. e2034461. doi: 10.1001/jamanetworkopen.2020.34461.

Lewington, S. *et al.* (2002) 'Age-specific relevance of usual blood pressure to vascular mortality: a meta-analysis of individual data for one million adults in 61 prospective studies Prospective', *Lancet*, 360(9349), pp. 1903–1913.

Li, C. *et al.* (2011) 'Protein kinase D3 is a pivotal activator of pathological cardiac hypertrophy by selectively increasing the expression of hypertrophic transcription factors', *Journal of Biological Chemistry*, 286(47), pp. 40782–40791. doi: 10.1074/jbc.M111.263046.

Liang, W. *et al.* (2020) 'Canonical Wnt signaling promotes pacemaker cell specification of cardiac mesodermal cells derived from mouse and human embryonic stem cells', *Stem Cells*, 38(3), pp. 352–368. doi: 10.1002/stem.3106.

Libby, P. and Theroux, P. (2005) 'Pathophysiology of coronary artery disease', *Circulation*, 111(25), pp. 3481–3488. doi: 10.1161/CIRCULATIONAHA.105.537878.

Linsel-Nitschke, P. *et al.* (2008) 'Lifelong reduction of LDL-cholesterol related to a common

varriant in the LDL-receptor gene decreases the risk of coronary artery disease - A Mendelian randomisation study', *PLoS ONE*, 3(8), pp. 1–9. doi: 10.1371/journal.pone.0002986.

Linton, M. F., Yancey, P. G., Davies, S. S., Jerome, W. G., Linton, E. F., Song, W. L., Doran, A. C., & Vickers, K. C. (2019) 'The Role of Lipids and Lipoproteins in Atherosclerosis', *Endotex*, p. 2019.

Liu, J. *et al.* (2010) 'A dual role for ErbB2 signaling in cardiac trabeculation', *Development*, 137(22), pp. 3867–3875. doi: 10.1242/dev.053736.

Liu, K. *et al.* (2019) 'Expanding the CRISPR toolbox in zebrafish for studying development and disease', *Frontiers in Cell and Developmental Biology*, 7(MAR), pp. 1–15. doi: 10.3389/fcell.2019.00013.

Liu, Q. *et al.* (2019) 'Prkd2 promotes progression and chemoresistance of aml via regulating notch1 pathway', *OncoTargets and Therapy*, 12, pp. 10931–10941. doi: 10.2147/OTT.S233234.

Lombardo, V. A. *et al.* (2019) 'Morphogenetic control of zebrafish cardiac looping by Bmp signaling', *Development (Cambridge)*, 146(22). doi: 10.1242/dev.180091.

Lotta, L. A. *et al.* (2017) 'Integrative genomic analysis implicates limited peripheral adipose storage capacity in the pathogenesis of human insulin resistance', *Nature Genetics*, 49(1), pp. 17–26. doi: 10.1038/ng.3714.

Louw, J. J.; Nunes Bastos, R.; Chen, X.; Verdood, C.; Corveleyn, A.; Jia, Y.; Breckpot, J.; Gewillig, M.; Peeters, H.; Santoro, M. M.; et al. Compound Heterozygous Loss-of-Function Mutations in KIF20A Are Associated with a Novel Lethal Congenital Cardiomyopathy in Two Siblings. *PLoS Genet.* **2018**, *14* (1), 1–17. https://doi.org/10.1371/journal.pgen.1007138.

Lu, Y. *et al.* (2021) 'Genetic liability to depression and risk of coronary artery disease, myocardial infarction, and other cardiovascular outcomes', *Journal of the American Heart Association*, 10(1), pp. 1–8. doi: 10.1161/JAHA.120.017986.

Luan, X. and Diekwisch, T. G. H. (2002) 'CP27 affects viability, proliferation, attachment and gene expression in embryonic fibroblasts', *Cell Proliferation*, 35(4), pp. 207–219. doi: 10.1046/j.1365-2184.2002.00238.x.

De Luca, L. (2020) 'Established and Emerging Pharmacological Therapies for Post-Myocardial Infarction Patients with Heart Failure: a Review of the Evidence', *Cardiovascular Drugs and Therapy*, 34(5), pp. 723–735. doi: 10.1007/s10557-020-07027-4.

MacGrogan, D., Münch, J. and de la Pompa, J. L. (2018) 'Notch and interacting signalling pathways in cardiac development, disease, and regeneration', *Nature Reviews Cardiology*, 15(11), pp. 685–704. doi: 10.1038/s41569-018-0100-2.

Mahmood, S. S. *et al.* (2014) 'The Framingham Heart Study and the epidemiology of cardiovascular disease: a historical perspective', *The Lancet*, 383(9921), pp. 999–1008. doi: 10.1016/S0140-6736(13)61752-3.

Makarović, Z. *et al.* (2018) 'Nonobstructive coronary artery disease – Clinical relevance, diagnosis, management and proposal of new pathophysiological classification', *Acta Clinica*

Croatica, 57(3), pp. 528–541. doi: 10.20471/acc.2018.57.03.17.

Malsagova, K. *et al.* (2020) 'Biobanks-A platform for scientific and biomedical research', *Diagnostics*, 10(7). doi: 10.3390/diagnostics10070485.

Manfrini, O. *et al.* (2020) 'Sex differences in modifiable risk factors and severity of coronary artery disease', *Journal of the American Heart Association*, 9(19). doi: 10.1161/JAHA.120.017235.

Mangino, M. and Spector, T. (2013) 'Understanding coronary artery disease using twin studies', *Heart*, 99(6), pp. 373–375. doi: 10.1136/heartjnl-2012-303001.

Manning, G. *et al.* (2002) 'The Protein Kinase Complement of the Human Genome', *Science*, 298(5600), pp. 1912–1934. doi: 10.1126/SCIENCE.1075762.

Marenberg, M. E. *et al.* (1994) 'Genetic susceptibility to death from coronary heart disease in a study of twins', *The new england journal of medicine*, 330(15), pp. 1041–1046.

Marín-Juez, R. *et al.* (2014) 'Hyperinsulinemia induces insulin resistance and immune suppression via Ptpn6/Shp1 in zebrafish', *Journal of Endocrinology*, 222(2), pp. 229–241. doi: 10.1530/JOE-14-0178.

Marques, I. J., Lupi, E. and Mercader, N. (2019) 'Model systems for regeneration: Zebrafish', *Development (Cambridge)*, 146(18). doi: 10.1242/dev.167692.

Mattioli, A. V. *et al.* (2017) 'Mediterranean diet impact on cardiovascular diseases: A narrative review', *Journal of Cardiovascular Medicine*, 18(12), pp. 925–935. doi: 10.2459/JCM.0000000000000573.

Medina-Inojosa, J. R. *et al.* (2018) 'Relation of Waist-Hip Ratio to Long-Term Cardiovascular Events in Patients With Coronary Artery Disease', *American Journal of Cardiology*, 121(8), pp. 903–909. doi: 10.1016/j.amjcard.2017.12.038.

Meng, X. *et al.* (2008) 'Targeted gene inactivation in zebrafish using engineered zinc-finger nucleases', *Nature Biotechnology*, 26(6), pp. 695–701. doi: 10.1038/nbt1398.

Mercer, E. J.; Lin, Y. F.; Cohen-Gould, L.; Evans, T. Hspb7 Is a Cardioprotective Chaperone Facilitating Sarcomeric Proteostasis. *Dev. Biol.* **2018**, No. December 2017, 1–15. https://doi.org/10.1016/j.ydbio.2018.01.005.

Messina, G. *et al.* (2014) 'Yeti, an essential Drosophila melanogaster gene, encodes a protein required for chromatin organization', *Journal of Cell Science*, 127(11), pp. 2577–2588. doi: 10.1242/jcs.150243.

Messina, G. *et al.* (2015) 'The Bucentaur (BCNT) protein family: a long-neglected class of essential proteins required for chromatin/chromosome organization and function', *Chromosoma*, 124(2), pp. 153–162. doi: 10.1007/s00412-014-0503-8.

Messina, G. *et al.* (2017) 'The human Cranio Facial Development Protein 1 (Cfdp1) gene encodes a protein required for the maintenance of higher-order chromatin organization',

Scientific Reports, 7(September 2016), pp. 1–10. doi: 10.1038/srep45022.

Meyer, A. and Schartl, M. (1999) 'Gene and genome duplications in vertebrates: The one-to-four (-to-eight in fish) rule and the evolution of novel gene functions', *Current Opinion in Cell Biology*, 11(6), pp. 699–704. doi: 10.1016/S0955-0674(99)00039-3.

Miller, J. N. and Pearce, D. A. (2014) 'Nonsense-mediated decay in genetic disease: Friend or foe?', *Mutation Research - Reviews in Mutation Research*, 762(605), pp. 52–64. doi: 10.1016/j.mrrev.2014.05.001.

Miller, W. L. *et al.* (2000) 'Improved survival after acute myocardial infarction in patients with advanced Killip class', *Clinical Cardiology*, 23(10), pp. 751–758. doi: 10.1002/clc.4960231012.

Minchin JEN, R. J. Elucidating the Role of Plexin D1 in Body Fat Distribution and Susceptibility to Metabolic Disease Using a Zebrafish Model System. *Adipocyte* **2017**, *6* (4), 277–283. https://doi.org/10.1080/21623945.2017.1356504.

Minchin, J. E. N. and Rawls, J. F. (2011) *In vivo Analysis of White Adipose Tissue in Zebrafish*. Third Edit, *Methods in Cell Biology*. Third Edit. Elsevier Inc. doi: 10.1016/B978-0-12-381320-6.00003-5.

Miquerol, L. and Kelly, R. G. (2013) 'Organogenesis of the vertebrate heart', *Wiley Interdisciplinary Reviews: Developmental Biology*, 2(1), pp. 17–29. doi: 10.1002/wdev.68.

Miyares, R. L., De Rezende, V. B. and Farber, S. A. (2014) 'Zebrafish yolk lipid processing: A tractable tool for the study of vertebrate lipid transport and metabolism', *DMM Disease Models and Mechanisms*, 7(7), pp. 915–927. doi: 10.1242/dmm.015800.

Montasser, M. E.; O'Hare, E. A.; Wang, X.; Howard, A. D.; McFarland, R.; Perry, J. A.; Ryan, K. A.; Rice, K.; Jaquish, C. E.; Shuldiner, A. R.; et al. An *APOO* Pseudogene on Chromosome 5q Is Associated With Low-Density Lipoprotein Cholesterol Levels. *Circulation* **2018**, *138* (13), 1343–1355. https://doi.org/10.1161/CIRCULATIONAHA.118.034016.

Monte-nieto, G. *et al.* (2018) 'Control of cardiac jelly dynamics by NOTCH1 and NRG1 defines the building plan for trabeculation', *Nature*, 557(1), pp. 439–445.

Morillo-Huesca, M. *et al.* (2010) 'The SWR1 histone replacement complex causes genetic instability and genome-wide transcription misregulation in the absence of H2A.Z', *PLoS ONE*, 5(8). doi: 10.1371/journal.pone.0012143.

Moss, J. B. *et al.* (2009) 'Regeneration of the pancreas in adult zebrafish', *Diabetes*, 58(8), pp. 1844–1851. doi: 10.2337/db08-0628.

Musso, G. *et al.* (2015) 'Generating and evaluating a ranked candidate gene list for potential vertebrate heart field regulators', *Genomics Data*, 6, pp. 199–201. doi: 10.1016/J.GDATA.2015.09.015.

Nasevicius, A. and Ekker, S. C. (2000) 'Effective targeted gene "knockdown" in zebrafish', *Nature Genetics*, 26(2), pp. 216–220. doi: 10.1038/79951.

Nasir, K. *et al.* (2007) 'Family history of premature coronary heart disease and coronary artery calcification: Multi-Ethnic Study of Atherosclerosis (MESA)', *Circulation*, 116(6), pp. 619–626. doi: 10.1161/CIRCULATIONAHA.107.688739.

Nauta, S. T. *et al.* (2012) 'Sex-related trends in mortality in hospitalized men and women after myocardial infarction between 1985 and 2008: Equal benefit for women and men', *Circulation*, 126(18), pp. 2184–2189. doi: 10.1161/CIRCULATIONAHA.112.113811.

Navin, T. R. and Hager, W. D. (1979) 'Creatine kinase MB isoenzyme in the evaluation of myocardial infarction', *Current Problems in Cardiology*, 3(12), pp. 1–32. doi: 10.1016/0146-2806(79)90010-0.

Nelson, C. P. *et al.* (2017) 'Association analyses based on false discovery rate implicate new loci for coronary artery disease', *Nature Genetics*, 49(9), pp. 1385–1391. doi: 10.1038/ng.3913.

Neville, M. J. *et al.* (2019) 'Regional fat depot masses are influenced by protein-coding gene variants', *PLoS ONE*, 14(5), pp. 1–17. doi: 10.1371/journal.pone.0217644.

Nguyen, P. D., de Bakker, D. E. M. and Bakkers, J. (2021) 'Cardiac regenerative capacity: an evolutionary afterthought?', *Cellular and Molecular Life Sciences*, 78(12), pp. 5107–5122. doi: 10.1007/s00018-021-03831-9.

Nguyen, S. L., Wilkinson, F. M. and Gecz, J. (2014) 'Nonsense-mediated mRNA decay: inter-individual variability and human disease', *Neurosci Biobehav Rev.*, 46(2), pp. 175–86. doi: 10.1016/j.neubiorev.2013.10.016.

Nikpay M, Goel A, Won HH, Hall LM, Willenborg C, Kanoni S, S. D. *et al.* (2015) 'A comprehensive 1000 Genomes – based genome-wide association meta-analysis of coronary artery disease', *Nature Genetics*, 47(10), pp. 1121–1130. doi: 10.1038/ng.3396.

Nikpay, M. *et al.* (2015) 'A comprehensive 1000 Genomes-based genome-wide association meta-analysis of coronary artery disease', *Nature Genetics*, 47(10), pp. 1121–1130. doi: 10.1038/ng.3396.

Nobukuni, T. *et al.* (1997) 'An Alu-linked repetitive sequence corresponding to 280 amino acids is expressed in a novel bovine protein, but not in its human homologue', *Journal of Biological Chemistry*, 272(5), pp. 2801–2807. doi: 10.1074/jbc.272.5.2801.

Noël, E. S. *et al.* (2013) 'A Nodal-independent and tissue-intrinsic mechanism controls heart-looping chirality', *Nature Communications*, 4. doi: 10.1038/ncomms3754.

Nordestgaard, B. G. *et al.* (2007) 'Nonfasting triglycerides and risk of myocardial infarction, ischemic heart disease, and death in men and women', *Journal of the American Medical Association*, 298(3), pp. 299–308. doi: 10.1001/jama.298.3.299.

Ntalla, I. *et al.* (2019) 'Genetic Risk Score for Coronary Disease Identifies Predispositions to Cardiovascular and Noncardiovascular Diseases', *Journal of the American College of Cardiology*, 73(23), pp. 2932–2942. doi: 10.1016/j.jacc.2019.03.512.

Nurnberg, S. T. *et al.* (2020) 'Genomic profiling of human vascular cells identifies TWIST1 as a

causal gene for common vascular diseases', *PLoS Genetics*, 16(1), pp. 1–22. doi: 10.1371/journal.pgen.1008538.

Pala, R. *et al.* (2018) 'The roles of primary cilia in cardiovascular diseases', *Cells*, 7(12), pp. 1–18. doi: 10.3390/cells7120233.

Pallazola, V. A. *et al.* (2019) 'A Clinician's Guide to Healthy Eating for Cardiovascular Disease Prevention', *Mayo Clinic Proceedings: Innovations, Quality & Outcomes*, 3(3), pp. 251–267. doi: 10.1016/j.mayocpiqo.2019.05.001.

Palmer, T. M. *et al.* (2013) 'Association of plasma uric acid with ischaemic heart disease and blood pressure: Mendelian randomization analysis of two large cohorts', *BMJ (Online)*, 347(7919), pp. 1–10. doi: 10.1136/bmj.f4262.

Paolini, A. *et al.* (2021) 'Mechanosensitive Notch-Dll4 and Klf2-Wnt9 Signaling Pathways Intersect in Guiding Valvulogenesis in Zebrafish', *Cell Reports*, 37(1). doi: 10.1016/j.celrep.2021.109782.

De Pater, E. *et al.* (2009) 'Distinct phases of cardiomyocyte differentiation regulate growth of the zebrafish heart', *Development*, 136(10), pp. 1633–1641. doi: 10.1242/dev.030924.

Peshkovsky, C., Totong, R. and Yelon, D. (2011) 'Dependence of cardiac trabeculation on neuregulin signaling and blood flow in zebrafish', *Developmental Dynamics*, 240(2), pp. 446–456. doi: 10.1002/dvdy.22526.

Pestel, J. *et al.* (2016) 'Real-time 3D visualization of cellular rearrangements during cardiac valve formation', *Development (Cambridge)*, 143(12), pp. 2217–2227. doi: 10.1242/dev.133272.

Pimple, P. *et al.* (2015) 'Angina and mental stress-induced myocardial ischemia', *Journal of Psychosomatic Research*, 78(5), pp. 433–437. doi: 10.1016/j.jpsychores.2015.02.007.

Piscuoglio S, Fusco N, Ng CK, Martelotto LG, da Cruz Paula A, Katabi N, R. and BP, Skálová A, Weinreb I, Weigelt B, R.-F. J. (2016) 'Lack of PRKD2 and PRKD3 kinase domain somatic mutations in PRKD1 wild-type classic polymorphous low-grade adenocarcinomas of the salivary gland', *Histopathology*, 68(7), pp. 1055–1062. doi: 10.1111/his.12883.

Porrello, E. R. *et al.* (2011) 'Transient Regenerative Potential of the Neonatal Mouse Heart', *Science*, 331(12), pp. 2–4.

Prasad, A. M. and Inesi, G. (2009) 'Effects of thapsigargin and phenylephrine on calcineurin and protein kinase C signaling functions in cardiac myocytes', *American Journal of Physiology - Cell Physiology*, 296(5), pp. 992–1002. doi: 10.1152/ajpcell.00594.2008.

Priya, R. *et al.* (2020) 'Tension heterogeneity directs form and fate to pattern the myocardial wall', *Nature*, 588(7836), pp. 130–134. doi: 10.1038/s41586-020-2946-9.

Qu, X., Harmelink, C. and Scott Baldwin, H. (2019) 'Tie2 regulates endocardial sprouting and myocardial trabeculation', *JCI Insight*, 4(13). doi: 10.1172/jci.insight.96002.

Quick, R. E. *et al.* (2021) 'Highly Efficient Synthetic CRISPR RNA/Cas9-Based Mutagenesis for

Rapid Cardiovascular Phenotypic Screening in F0 Zebrafish', *Frontiers in Cell and Developmental Biology*, 9(October). doi: 10.3389/fcell.2021.735598.

Quinlivan, V. H. and Farber, S. A. (2017) 'Lipid uptake, metabolism, and transport in the larval zebrafish', *Frontiers in Endocrinology*, 8(NOV), pp. 1–11. doi: 10.3389/fendo.2017.00319.

Radovanovic, D. *et al.* (2016) 'Treatment and outcomes of patients with recurrent myocardial infarction: A prospective observational cohort study', *Journal of Cardiology*, 68(6), pp. 498–503. doi: 10.1016/j.jjcc.2015.11.013.

Rasouli, S. J. and Stainier, D. Y. R. (2017) 'Regulation of cardiomyocyte behavior in zebrafish trabeculation by Neuregulin 2a signaling', *Nature Communications*, 8(May), pp. 1–11. doi: 10.1038/ncomms15281.

Ren, J. *et al.* (2019) 'Canonical Wnt5b Signaling Directs Outlying Nkx2.5+ Mesoderm into Pacemaker Cardiomyocytes', *Developmental Cell*, 50(6), pp. 729-743.e5. doi: 10.1016/j.devcel.2019.07.014.

Rey, O. and Rozengurt, E. (2001) 'Protein Kinase D Interacts with Golgi via Its Cysteine-Rich Domain', *Biochemical and Biophysical Research Communications*, 287(1), pp. 21–26. doi: 10.1006/BBRC.2001.5530.

Rice, E. L. (1971) 'The epidemiologic transition. A Theory of the Epidemiology of Population Change', *The Milbank Memorial Fund Quarterly*, 49(4), pp. 509–538.

Richards, S. H. *et al.* (2018) 'Psychological interventions for coronary heart disease: Cochrane systematic review and meta-analysis', *European Journal of Preventive Cardiology*, 25(3), pp. 247–259. doi: 10.1177/2047487317739978.

Riddle, M. C. (2010) 'Effects of intensive glucose lowering in the management of patients with type 2 diabetes mellitus in the Action to Control Cardiovascular Risk in Diabetes (ACCORD) trial', *Circulation*, 122(8), pp. 844–846. doi: 10.1161/CIRCULATIONAHA.110.960138.

Ripatti, P. *et al.* (2020) 'Polygenic Hyperlipidemias and Coronary Artery Disease Risk', *Circulation: Genomic and Precision Medicine*, (April), pp. 59–65. doi: 10.1161/CIRCGEN.119.002725.

Rochais, F. *et al.* (2009) 'Hes1 Is Expressed in the Second Heart Field and Is Required for Outflow Tract Development', *PLoS ONE*. Edited by M. H. Sham, 4(7), p. e6267. doi: 10.1371/journal.pone.0006267.

Rodriguez, C. J. *et al.* (2014) *Status of cardiovascular disease and stroke in hispanics/latinos in the united states: A science advisory from the american heart association*, *Circulation*. doi: 10.1161/CIR.0000000000000071.

Roselli, C., Chaffin, M.D., Weng, L. et al. (2018) 'Multi-Ethnic Genome-wide Association Study for Atrial Fibrillation', *Nature Genetics*, 50, pp. 1225–1233. doi: 10.1038/s41588-018-0133-9.

Ross, S., Gerstein, H. and Paré, G. (2018) 'The Genetic Link Between Diabetes and Atherosclerosis', *Canadian Journal of Cardiology*, 34(5), pp. 565–574. doi:

10.1016/j.cjca.2018.01.016.

Rossi, A. *et al.* (2015) 'Genetic compensation induced by deleterious mutations but not gene knockdowns', *Nature*, 524(7564), pp. 230–233. doi: 10.1038/nature14580.

Rozengurt, E., Rey, O. and Waldron, R. T. (2005) 'Protein kinase D signaling', *Journal of Biological Chemistry*, 280(14), pp. 13205–13208. doi: 10.1074/jbc.R500002200.

Rujirachun, P. *et al.* (2021) 'Association of premature ventricular complexes and risk of ischemic stroke: A systematic review and meta-analysis', *Clinical Cardiology*, 44(2), pp. 151–159. doi: 10.1002/clc.23531.

Sabater-Lleal, M. *et al.* (2014) 'Common genetic determinants of lung function, subclinical atherosclerosis and risk of coronary artery disease', *PLoS ONE*, 9(8). doi: 10.1371/journal.pone.0104082.

Al Saleh, A. S. *et al.* (2017) 'Predictors and Impact of In-Hospital Recurrent Myocardial Infarction in Patients with Acute Coronary Syndrome: Findings from Gulf RACE-2', *Angiology*, 68(6), pp. 508–512. doi: 10.1177/0003319716674855.

Samsa,Leigh Ann, Yang, B. and Liu, J. (2014) 'Embryonic Cardiac Chamber Maturation: Trabeculation, Conduction and Cardiomyocyte Proliferation', *Am j Med Genet Semin Med Genet*, 163(3), pp. 157–168. doi: 10.1002/ajmg.c.31366.Embryonic.

Sandesara, P. B. *et al.* (2019) 'The forgotten lipids: Triglycerides, remnant cholesterol, and atherosclerotic cardiovascular disease risk', *Endocrine Reviews*, 40(2), pp. 537–557. doi: 10.1210/er.2018-00184.

Sandireddy, R. *et al.* (2019) 'Semaphorin 3E/PlexinD1 signaling is required for cardiac ventricular compaction', *JCI Insight*, 4(16). doi: 10.1172/jci.insight.125908.

Santos, D., Luzio, A. and Coimbra, A. M. (2017) 'Zebrafish sex differentiation and gonad development: A review on the impact of environmental factors', *Aquatic Toxicology*, 191(August 2016), pp. 141–163. doi: 10.1016/j.aquatox.2017.08.005.

Schwarzer, S. *et al.* (2017) 'Dlx3b/4b is required for early-born but not later-forming sensory hair cells during zebrafish inner ear development', *Biology Open*, 6(9), pp. 1270–1278. doi: 10.1242/bio.026211.

Sedmera, D. *et al.* (2000) 'Developmental patterning of the myocardium', *Anatomical Record*, 258(4), pp. 319–337. doi: 10.1002/(SICI)1097-0185(20000401)258:4<319::AID-AR1>3.0.CO;2-O.

Sehnert, A. J. *et al.* (2002) 'Cardiac troponin T is essential in sarcomere assembly and cardiac contractility', *Nature Genetics*, 31(1), pp. 106–110. doi: 10.1038/ng875.

Sertori, R. *et al.* (2016) 'Genome editing in zebrafish: A practical overview', *Briefings in Functional Genomics*, 15(4), pp. 322–330. doi: 10.1093/bfgp/elv051.

Seth, A., Stemple, D. L. and Barroso, I. (2013) 'The emerging use of zebrafish to model metabolic disease', *DMM Disease Models and Mechanisms*, 6(5), pp. 1080–1088. doi:

10.1242/dmm.011346.

Shaheen, R. *et al.* (2015) 'Positional mapping of PRKD1, NRP1 and PRDM1 as novel candidate disease genes in truncus arteriosus', *Journal of Medical Genetics*, 52(5), pp. 322–329. doi: 10.1136/JMEDGENET-2015-102992.

Shapiro, M. D. and Fazio, S. (2017) 'Apolipoprotein B-containing lipoproteins and atherosclerotic cardiovascular disease', *F1000Research*, 6, pp. 1–8. doi: 10.12688/f1000research.9845.1.

Sidhwani, P. and Yelon, D. (2019) *Fluid forces shape the embryonic heart: Insights from zebrafish*. 1st edn, *Current Topics in Developmental Biology*. 1st edn. Elsevier Inc. doi: 10.1016/bs.ctdb.2018.12.009.

Sifrim, A. *et al.* (2016) 'Distinct genetic architectures for syndromic and nonsyndromic congenital heart defects identified by exome sequencing', *Nature Genetics*, 48(9), pp. 1060–1065. doi: 10.1038/ng.3627.

Slack, J. and Evans, K. A. (1966) 'The increased risk of death from ischaemic heart disease in first degree relatives of 121 men and 96 women with ischaemic heart disease.', *Journal of medical genetics*, 3(4), pp. 239–257. doi: 10.1136/jmg.3.4.239.

So, H. C. *et al.* (2011) 'Evaluating the heritability explained by known susceptibility variants: A survey of ten complex diseases', *Genetic Epidemiology*, 35(5), pp. 310–317. doi: 10.1002/gepi.20579.

Song, R. J. *et al.* (2018) 'Alcohol Consumption and Risk of Coronary Artery Disease (from the Million Veteran Program)', *American Journal of Cardiology*, 121(10), pp. 1162–1168. doi: 10.1016/j.amjcard.2018.01.042.

Sood, R. *et al.* (2013) 'Efficient Methods for Targeted Mutagenesis in Zebrafish Using Zinc-Finger Nucleases: Data from Targeting of Nine Genes Using CompoZr or CoDA ZFNs', *PLoS ONE*, 8(2). doi: 10.1371/journal.pone.0057239.

Soria, L. F. *et al.* (1989) 'Association between a specific apolipoprotein B mutation and familial defective apolipoprotein B-100', 86(January), pp. 587–591.

Souverein, O. W. *et al.* (2007) 'Influence of LDL-receptor mutation type on age at first cardiovascular event in patients with familial hypercholesterolaemia', *European Heart Journal*, 28(3), pp. 299–304. doi: 10.1093/eurheartj/ehl366.

Speliotes, E. K. *et al.* (2010) 'Association analyses of 249,796 individuals reveal 18 new loci associated with body mass index', *Nature Genetics*, 42(11), pp. 937–948. doi: 10.1038/ng.686.

Stainier, D. Y. *et al.* (1996) 'Mutations affecting the formation and function of the cardiovascular system in the zebrafish embryo.', *Development (Cambridge, England)*, 123, pp. 285–92. doi: 10.1038/nature18614.

Stainier, D. Y. R. *et al.* (2002) 'Endocardial cushion formation in zebrafish', *Cold Spring Harbor Symposia on Quantitative Biology*, 67(February), pp. 49–56. doi: 10.1101/sqb.2002.67.49.

Stainier, D. Y. R. *et al.* (2017) 'Guidelines for morpholino use in zebrafish', *PLOS Genetics*, 13(10), p. e1007000. doi: 10.1371/journal.pgen.1007000.

Staudt, D. W. *et al.* (2014) 'High-resolution imaging of cardiomyocyte behavior reveals two distinct steps in ventricular trabeculation', *Development (Cambridge)*, 141(3), pp. 585–593. doi: 10.1242/dev.098632.

Sturany, S. *et al.* (2001) 'Molecular cloning and characterization of the human protein kinase D2: A novel member of the protein kinase D family of serine threonine kinases', *Journal of Biological Chemistry*, 276(5), pp. 3310–3318. doi: 10.1074/jbc.M008719200.

Sudlow, C. *et al.* (2015) 'UK Biobank: An Open Access Resource for Identifying the Causes of a Wide Range of Complex Diseases of Middle and Old Age', *PLoS Medicine*, 12(3), pp. 1–10. doi: 10.1371/journal.pmed.1001779.

Sun, L. and Luk, E. (2017) 'Dual function of Swc5 in SWR remodeling ATPase activation and histone H2A eviction', *Nucleic Acids Research*, 45(17), pp. 9931–9946. doi: 10.1093/nar/gkx589.

Sung, Y. H. *et al.* (2014) 'Highly efficient gene knockout in mice and zebrafish with RNA-guided endonucleases', *Genome Research*, 24(1), pp. 125–131. doi: 10.1101/gr.163394.113.

Sung, Y. J. *et al.* (2018) 'A Large-Scale Multi-ancestry Genome-wide Study Accounting for Smoking Behavior Identifies Multiple Significant Loci for Blood Pressure', *American Journal of Human Genetics*, 102(3), pp. 375–400. doi: 10.1016/j.ajhg.2018.01.015.

Tabei, S. M. B. *et al.* (2014) 'Non-modifiable Factors of Coronary Artery Stenosis in Late Onset Patients with Coronary Artery Disease in Southern Iranian Population.', *Journal of Cardiovascular and Thoracic Research*, 6(1), pp. 51–55. doi: 10.5681/jcvtr.2014.010.

Tanaka, Y.; Hayashi, K.; Fujino, N.; Konno, T.; Tada, H.; Nakanishi, C. Functional Analysis of KCNH2 Gene Mutations of Type 2 Long QT Syndrome in Larval Zebrafish Using Microscopy and Electrocardiography. *Heart Vessels* **2018**, No. 0123456789. https://doi.org/10.1007/s00380-018-1231-4.

Tani, S. *et al.* (2017) 'Relation between low-density lipoprotein cholesterol/apolipoprotein B ratio and triglyceride-rich lipoproteins in patients with coronary artery disease and type 2 diabetes mellitus: A cross-sectional study', *Cardiovascular Diabetology*, 16(1), pp. 1–13. doi: 10.1186/s12933-017-0606-7.

Teslovich, T. M. *et al.* (2010) 'Biological, clinical and population relevance of 95 loci for blood lipids', *Nature*, 466(7307), pp. 707–713. doi: 10.1038/nature09270.

Tessadori, F. *et al.* (2012) 'Identification and Functional Characterization of Cardiac Pacemaker Cells in Zebrafish', *PLoS ONE*, 7(10), pp. 1–9. doi: 10.1371/journal.pone.0047644.

Thun, M. J. *et al.* (2013) '50-Year Trends in Smoking-Related Mortality in the United States', *New England Journal of Medicine*, 368(4), pp. 351–364. doi: 10.1056/nejmsa1211127.

Timmerman, L. A. *et al.* (2004) 'Notch promotes epithelial-mesenchymal transition during cardiac development and oncogenic transformation', *Genes and Development*, 18(1), pp. 99–

115. doi: 10.1101/gad.276304.

Trégouët, D. A. *et al.* (2009) 'Genome-wide haplotype association study identifies the SLC22A3-LPAL2-LPA gene cluster as a risk locus for coronary artery disease', *Nature Genetics*, 41(3), pp. 283–285. doi: 10.1038/ng.314.

Truebestein, L. and Leonard, T. A. (2016) 'Coiled-coils: The long and short of it', *BioEssays*, 38(9), pp. 903–916. doi: 10.1002/bies.201600062.

Tsai, C. T.; Hsieh, C. S.; Chang, S. N.; Chuang, E. Y.; Ueng, K. C.; Tsai, C. F.; Lin, T. H.; Wu, C. K.; Lee, J. K.; Lin, L. Y.; et al. Genome-Wide Screening Identifies a KCNIP1 Copy Number Variant as a Genetic Predictor for Atrial Fibrillation. *Nat. Commun.* **2016**, *7* (110), 1–9. doi.org/10.1038/ncomms10190.

Tsata, V. and Beis, D. (2020) 'In full force. Mechanotransduction and morphogenesis during homeostasis and tissue regeneration', *Journal of Cardiovascular Development and Disease*, 7(4), pp. 1–18. doi: 10.3390/jcdd7040040.

Tsybouleva, N. *et al.* (2004) 'Aldosterone, through novel signaling proteins, is a fundamental molecular bridge between the genetic defect and the cardiac phenotype of hypertrophic cardiomyopathy.', *Circulation*, 109(10), pp. 1284–91. doi: 10.1161/01.CIR.0000121426.43044.2B.

Tucker, N. R.; Dolmatova, E. V.; Lin, H.; Cooper, R. R.; Ye, J.; Hucker, W. J.; Jameson, H. S.; Parsons, V. A.; Weng, L. C.; Mills, R. W.; et al. Diminished PRRX1 Expression Is Associated with Increased Risk of Atrial Fibrillation and Shortening of the Cardiac Action Potential. *Circ. Cardiovasc. Genet.* **2017**, *10* (5). https://doi.org/10.1161/CIRCGENETICS.117.001902.

Uribe, V. *et al.* (2018) '*In vivo* analysis of cardiomyocyte proliferation during trabeculation', *Development*, 145(14), p. dev164194. doi: 10.1242/dev.164194.

Valverde, A. M. *et al.* (1994) 'Molecular cloning and characterization of protein kinase D: a target for diacylglycerol and phorbol esters with a distinctive catalytic domain.', *Proceedings of the National Academy of Sciences of the United States of America*, 91(18), pp. 8572–6. doi: 10.1073/pnas.91.18.8572.

Varshney GK, Pei W, LaFave MC, Idol J, Xu L, Gallardo V, Carrington B, B., K, Jones M, Li M, Harper U, Huang SC, Prakash A, Chen W, Sood R, Ledin J, B. and SM. (2015) 'High-throughput gene targeting and phenotyping in zebrafish using CRISPR/Cas9', *Genome Res.*, 25(7), pp. 1030–42. doi: 10.1101/gr.186379.114.

Vedula, V. *et al.* (2017) 'A method to quantify mechanobiologic forces during zebrafish cardiac development using 4-D light sheet imaging and computational modeling', *PLoS Computational Biology*, 13(10), pp. 1–24. doi: 10.1371/journal.pcbi.1005828.

Veljkovic, N. *et al.* (2018) 'Genetic markers for coronary artery disease', *Medicina (Lithuania)*, 54(3), pp. 1–13. doi: 10.3390/medicina54030036.

Voight, B. F. *et al.* (2012) 'Plasma HDL cholesterol and risk of myocardial infarction: A mendelian

randomisation study', *The Lancet*, 380(9841), pp. 572–580. doi: 10.1016/S0140-6736(12)60312-2.

Volgman, A. S. *et al.* (2018) *Atherosclerotic Cardiovascular Disease in South Asians in the United States: Epidemiology, Risk Factors, and Treatments: A Scientific Statement From the American Heart Association*, *Circulation*. doi: 10.1161/CIR.0000000000000580.

Vornanen, M. and Hassinen, M. (2016) 'Zebrafish heart as a model for human cardiac electrophysiology', *Channels*, 10(2), pp. 101–110. doi: 10.1080/19336950.2015.1121335.

Waldron, R. T., Iglesias, T. and Rozengurt, E. (1999) 'The pleckstrin homology domain of protein kinase D interacts preferentially with the η isoform of protein kinase C', *Journal of Biological Chemistry*, 274(14), pp. 9224–9230. doi: 10.1074/jbc.274.14.9224.

Walsh, E. C. and Stainier, D. Y. R. (2001) 'UDP-Glucose Dehydrogenase Required for Cardiac Valve Formation in Zebrafish', *Science*, 293(5535), pp. 1670–1673. doi: 10.1126/SCIENCE.293.5535.1670.

Wang, H. *et al.* (2016) 'Global, regional, and national life expectancy, all-cause mortality, and cause-specific mortality for 249 causes of death, 1980–2015: a systematic analysis for the Global Burden of Disease Study 2015', *The Lancet*, 388(10053), pp. 1459–1544. doi: 10.1016/S0140-6736(16)31012-1.

Webb, T. R. *et al.* (2017) 'Systematic Evaluation of Pleiotropy Identifies 6 Further Loci Associated With Coronary Artery Disease', *Journal of the American College of Cardiology*, 69(7), pp. 823–836. doi: 10.1016/j.jacc.2016.11.056.

Wei, N. *et al.* (2015) 'The cytotoxic effects of regorafenib in combination with protein kinase D inhibition in human colorectal cancer cells', *Oncotarget*, 6(7), pp. 4745–4756. doi: 10.18632/oncotarget.2938.

Wild, P. S. *et al.* (2017) 'Large-scale genome-wide analysis identifies genetic variants associated with cardiac structure and function', *Journal of Clinical Investigation*, 127(5), pp. 1798–1812. doi: 10.1172/JCI84840.

Windler, E., Eidenmüller, B. and Zyriax, B. C. (2004) 'Hormone replacement therapy and cardiovascular disease', *International Congress Series*, 1262(C), pp. 523–526. doi: 10.1016/j.ics.2004.01.089.

Wu, C. C. *et al.* (2016) 'Spatially Resolved Genome-wide Transcriptional Profiling Identifies BMP Signaling as Essential Regulator of Zebrafish Cardiomyocyte Regeneration', *Developmental Cell*, 36(1), pp. 36–49. doi: 10.1016/j.devcel.2015.12.010.

Wu, W. H. *et al.* (2005) 'Swc2 is a widely conserved H2AZ-binding module essential for ATP-dependent histone exchange', *Nature Structural and Molecular Biology*, 12(12), pp. 1064–1071. doi: 10.1038/nsmb1023.

Wu, W. H. *et al.* (2009) 'N terminus of Swr1 binds to histone H2AZ and provides a platform for subunit assembly in the chromatin remodeling complex', *Journal of Biological Chemistry*,

284(10), pp. 6200–6207. doi: 10.1074/jbc.M808830200.

Wu, Y. *et al.* (2021) 'Diagnostic and Prognostic Biomarkers for Myocardial Infarction', *Frontiers in Cardiovascular Medicine*, 7(February), pp. 1–13. doi: 10.3389/fcvm.2020.617277.

Xiao, L. *et al.* (2018) 'Association between single nucleotide polymorphism rs11057401 of CCDC92 gene and the risk of coronary heart disease (CHD)', *Lipids in Health and Disease*, 17(1), pp. 1–5. doi: 10.1186/s12944-018-0672-1.

Yalcin, H. C. *et al.* (2017) 'Heart function and hemodynamic analysis for zebrafish embryos', *Developmental Dynamics*, 246(11), pp. 868–880. doi: 10.1002/dvdy.24497.

Yang, H. *et al.* (2020) 'Methods favoring homology-directed repair choice in response to crispr/cas9 induced-double strand breaks', *International Journal of Molecular Sciences*, 21(18), pp. 1–20. doi: 10.3390/ijms21186461.

Yang, Y. *et al.* (2016) 'Alcohol consumption and risk of coronary artery disease: a dose–response meta- analysis of prospective studies', *Nutrition*, 32(6), p. 63644. doi: 10.1016/j.nut.2015.11.013.

Yu, F. *et al.* (2012) 'Flexible microelectrode arrays to interface epicardial electrical signals with intracardial calcium transients in zebrafish hearts', *Biomedical Microdevices*, 14(2), pp. 357–366. doi: 10.1007/s10544-011-9612-9.

Yuan, J. and Pandol, S. J. (2016) 'PKD signaling and pancreatitis', *Journal of Gastroenterology*, 51(7), pp. 651–659. doi: 10.1007/s00535-016-1175-3.

Yue, M. S., Peterson, R. E. and Heideman, W. (2015) 'Dioxin inhibition of swim bladder development in zebrafish: Is it secondary to heart failure?', *Aquatic Toxicology*, 162, pp. 10–17. doi: 10.1016/j.aquatox.2015.02.016.

Zdravkovic, S. *et al.* (2002) 'Heritability of death from coronary heart disease: A 36-year follow-up of 20 966 Swedish twins', *Journal of Internal Medicine*, 252(3), pp. 247–254. doi: 10.1046/j.1365-2796.2002.01029.x.

Zhao, W. *et al.* (2017) 'Identification of new susceptibility loci for type 2 diabetes and shared etiological pathways with coronary heart disease', *Nature Genetics*, 344(6188), pp. 1173–1178. doi: 10.1038/ng.3943.Identification.

Zheng, P. F. *et al.* (2020) 'Genes associated with inflammation may serve as biomarkers for the diagnosis of coronary artery disease and ischaemic stroke', *Lipids in Health and Disease*, 19(1), pp. 1–10. doi: 10.1186/s12944-020-01217-7.